Regenerative and Fibrotic Pathways in Canine Liver Disease

Bart Spee

Cover en druk: Atalanta Drukwerkbemiddeling, Houten.
Illustrations: Immunohistochemical staining of Collagen III in a dog with Chronic Hepatitis, chapter 4.

Spee, B. – **Regenerative and Fibrotic pathways in Canine Liver Disease**.
PhD thesis, Faculty of Veterinary Medicine, Utrecht University, 2006

ISBN-10: 90-393-4205-9
ISBN-13: 978-90-393-4205-3

Copyright© 2006 by Bart Spee. All rights reserved. No part of this publication may be reproduced or transmitted in any form or by any means, without permission in writing of the author.

Regenerative and Fibrotic Pathways in Canine Liver Disease

Biochemische analyse van regeneratie en fibrose bij leverziekten van de hond

Proefschrift

ter verkrijging van de graad van doctor aan de Universiteit Utrecht op gezag van de Rector Magnificus, Prof. Dr. W.H. Gispen, ingevolge het besluit van het College voor Promoties in het openbaar te verdedigen op
6 april 2006
des middags te 2.30 uur

door

Bart Spee

geboren op 4 mei 1978 te Gouda

promotor: Prof. Dr. J. Rothuizen

copromotoren: Dr. L.C. Penning
Dr. T.S.G.A.M. van den Ingh

Department of Clinical Sciences of Companion Animals
Faculty of veterinary medicine
Utrecht University
Utrecht, The Netherlands

The studies described in this thesis were conducted at the Department of Clinical Sciences of Companion Animals, Faculty of Veterinary Medicine, Utrecht University, Utrecht, The Netherlands; and were fully funded by Intervet international bv.

Universiteit Utrecht

Publication of this thesis was made possible by the generous support of: the Department of Clinical Sciences of Companion Animals, Faculty of Veterinary Medicine, Utrecht University; Intervet international bv.

Universiteit Utrecht

Contents

Aims and Scope

Theoretical background

Liver diseases occur quite frequently in dogs; the overall incidence in dogs has been estimated around 1-2% of the clinical cases [1,2]. Most liver diseases are, like in humans, chronic and occur through chronic inflammation due to different causes [3]. In all cases the on-going liver cell damage leads to a reduction of the functional liver cell mass and progressive deposition of fibrous tissue in the liver. These two phenomena, atrophy and fibrosis, are two sides of one medal and go hand in hand to cause fatal liver dysfunction in the end-stage. The large regenerative capacity of the liver is lost in the course of chronic disease.

There is convincing evidence that the two main counteracting factors, Hepatocyte Growth Factor (HGF) and Transforming Growth Factor-β1 (TGF-β1), determine the outcome of liver disease [4]. HGF is the principal factor stimulating the liver to grow and regenerate and suppresses fibrosis and apoptosis [5-7]. In contrast, TGF-β1 induces formation of excessive fibrous tissue and a reduction of the regenerative capacity together with stimulation of cell death [4,7-10]. The findings with respect to the crucial counteracting effects of HGF and TGF-β1 in liver growth, regeneration and fibrosis, have stimulated researchers to investigate the potential of administering HGF to experimental animals given hepatotoxic or fibrogenic drugs. Administration of HGF completely prevented or, when given afterwards, reversed toxic effects [11-17]. Even in cases of chronic damage with already formed disruption of the normal micro-architecture of the liver, fibrosis and atrophy (cirrhosis), this phenomenon could largely be reversed. Furthermore, the normal fatal course of peracute fulminant hepatitis (severe acute hepatic sepsis or toxicity) could be prevented in experimental animals [15-18]. The few studies in dogs indicate that the above findings also apply to this species [19]. Interestingly, one of the first reports of a very potent liver regeneration stimulating factor (now known as HGF) was found in dogs [20].

Extrapolation for the above mentioned rodent models to human medicine has not been achieved. The use of novel therapeutic approaches in dogs presented at the veterinary clinic could be seen as a much more relevant animal model for the translation to human clinical medicine. For instance, HGF treatment during normally life-threatening hepatic diseases could cause a revolution in the treatment of liver diseases (in both man and dog). Therapeutic intervention could be achieved by the addition of the HGF-glycoprotein itself [7,13-17]. Alternatively, and in line with the concept that the clinical outcome is determined by the balance between HGF and TGF-β1, gene therapy approaches resulting in blocking the effects of TGF-β1 have been similarly effective, at least in chronic disease models [21,22].

Taken together, the central theme of this thesis involves several aims. The first aim is to describe the regulatory roles of Hepatocyte Growth Factor (HGF) and Transforming Growth Factor-β1 (TGF-β1), via the respective receptors c-MET and TGF-β receptors type II and I in growth, regeneration, and formation of fibrosis in a variety of liver diseases. Second, development of therapeutic tools based on the above insights to treat liver diseases characterized by inadequate growth or atrophy with fibrosis and/or cirrhosis, especially by influencing the balance between HGF and TGF-β1 in the liver. Finally, initial evaluation of the effects of such therapeutic tools.

References

[1] Rothuizen J, Meyer HP. History, physical examination, and clinical signs of liver disease. In: Ettinger J, Feldman EC (eds) Textbook of veterinary internal medicine, 5th ed, Saunders, Philadelphia, 2000:1272-1277.

[2] Rothuizen J. Diseases of the liver and biliary tract. In: Dunn J (ed) Textbook of small animal medicine. Saunders, London, 1999:498-525.

[3] Boomkens SY, Penning LC, Egberink HF, et al. Hepatitis with special reference to dogs. A review on the pathogenesis and infectious etiologies, including unpublished results of recent own studies. Vet Q 2004, 26:107-114.

[4] Mori Y, Kawano K, Aramaki M, et al. Augmentive effect of cyclosporin A on rat liver regeneration: influence on hepatocyte growth factor and transforming growth factor beta-1. Eur Surg Res 1999, 31:399-405.

[5] Matsumoto K, Nakamura T. Emerging multipotent aspects of hepatocyte growth factor. J Biochem 1996, 119:591-600.

[6] Bardeli A, Longati P, Albero D, et al. HGF receptor associates with the anti-apoptotic protein BAG-1 and prevents cell death. EMBO J 1996, 15:6205-6212.

[7] Yasuda H, Imai E, Shiota A, et al. Antifibrogenic effect of a deletion variant of hepatocyte growth factor on liver fibrosis in rats. Hepatology 1996, 24:636-642.

[8] Michalopoulos GK, DeFrancis MC. Liver regeneration. Science 1997, 276:60-66.

[9] Masuhara M, Yasunaga M, Taigawa K, et al. Expression of hepatocyte growth factor, transforming growth factor alpha, and transforming growth factor beta-1 messenger RNA in various human liver diseases and correlation with hepatocyte proliferation. Hepatology 1996, 24:323-329.

[10] Napoli J, Prentice D, Niimami C, et al. Sequential increases in the intrahepatic expression of epidermal growth factor, basic fibroblast growth factor, and transforming growth factor β in a bile duct ligated rat model of cirrhosis. Hepatology 1997, 26:624-633.

[11] Shiota G, Kawasaki H. Hepatocyte growth factor in transgenic mice. Int J Exp Pathol 1998, 79:267-277.

[12] Shima N, Tsuda E, Goto M, et al. Hepatocyte growth factor and its variant with a deletion of five amino acids are distinguishable in their biological activity and tertiary structure. Biochem Biophys Res Commun 1994, 200:808-815.

[13] Kobayashi Y, Hamanoue M, Ueno S, et al. Induction of hepatocyte growth by intraportal infusion of HGF into beagle dogs. Biochem Biophys Res Comm 1996, 220:7-12.

[14] Kosai K-I, Matsumoto K, Funasoshi H, et al. Hepatocyte growth factor prevents endotoxin-induced lethal hepatic failure in mice. Hepatology 1999, 30:151-159.

[15] Gupta S, Rajvanshi P, Aragona E, et al. Transplanted hepatocytes proliferate differently after CCl_4 treatment and hepatocyte growth factor infusion. Am J Physiol 1999, 276:G629-638.

[16] Kaibori M, Kwon AH, Nakagawa M, et al. Stimulation of liver regeneration and function after partial hepatectomy in cirrhotic rats by continuous infusion of recombinant human hepatocyte growth factor. J Hepatol 1997, 27:381-390.

[17] Matsuda Y, Matsumoto K, Yamada A, et al. Preventive and therapeutic effects in rats of hepatocyte growth factor infusion on liver fibrosis/cirrhosis. Hepatology 1997, 26:81-89.

[18] Ueki T, Kaneda Y, Nakanishi K, et al. Hepatocyte growth factor gene therapy of liver cirrhosis in rats. Nature medicine 1999, 5:226-230.

[19] Ueno S, Aikou T, Tanabe G, et al. Exogenous hepatocyte growth factor markedly stimulates liver regeneration following portal branch ligation in dogs. Cancer Chemother Pharmacol 1996, 38:233-237.

[20] Starzl TE, Jones AF, Terblanche J, et al. Growth-stimulating factor in regenerating canine liver. Lancet 1979, I:127-130.

[21] Qi Z, Atsuchi N, Ooshima A, et al. Blockade of type β transforming growth factor signaling prevents liver fibrosis and dysfunction in the rat. Proc Natl Acad Sci USA 1999, 96:2345-2349.

[22] Nakamura T, Sakata R, Ueno T, et al. Inhibition of transforming growth factor β prevents progression of liver fibrosis and enhances hepatocyte regeneration in dimethylnitrosamine-treated rats. Hepatology 2000; 32:247-255.

Chapter 1

General Introduction

Canine liver diseases

Hepatitis is not as well defined in the dog as in its human counterparts. The etiology of canine hepatitis in most cases is unknown. Therefore diagnosis and treatment usually rely on histological descriptions. The various forms of canine hepatitis in the dog vary from acute to chronic hepatitis and cirrhosis. Acute hepatitis (AH) is characterized by hepatocellular necrosis or apoptosis with mononuclear or mixed inflammatory infiltrate, and in some instances regeneration [1]. Causes of acute hepatitis are unknown in most cases although in some cases canine adenovirus-1 (CAV-1) or bacterial infections were found. In other cases intoxications were found due to acetaminophen (paracetamol), poisonous mushrooms, or algae [2]. Chronic hepatitis (CH) is characterized by hepatocellular apoptosis or necrosis and variable mononuclear or mixed inflammatory infiltrate, regeneration, and fibrosis. The stages of chronic hepatitis can be determined by the amount of fibrosis and possible architectural fibrosis (cirrhosis). Several causes of chronic hepatitis have been described such as canine adenovirus-1 (CAV-1), canine acidophil cell hepatitis, and leptospirosis [3]. A common cause of chronic hepatitis in different breeds is associated with hepatic copper toxicosis (CT). This disease is commonly found in Bedlington terriers, Doberman pinschers, Sky terriers, West-Highland white terriers, Dalmatians, Anatolian shepherds, American and English Cocker spaniels, and Labrador retrievers. The increased incidence of CT in these breeds suggests some form of inherited disease. However, only in Bedlington terriers the genetic defect has been found with a deletion of the entire exon two of the *MURR1* (*COMMD1*) gene associated with copper excretion into bile [4]. When chronic hepatitis persists it will ultimately lead to cirrhosis (CIRR). Cirrhosis can be seen as an end-stage of chronic hepatitis with fibrosis and disruption of the lobular architecture into structurally abnormal parenchymal nodules and the presence of portocentral vascular anastomoses. Lobular Dissecting Hepatitis (LDH) is a special form of cirrhosis with a rapid clinical course seen in juvenile dogs with a typical dissection of the lobular architecture [5]. Causes have not been found although an infectious agent has been suggested [6]. For a more detailed description of these liver diseases see the World Small Animal Veterinary Association (WSAVA) Standards for histological and clinical diagnosis of canine and feline liver disease (ISBN 070202791X).

There are several other hepatic diseases which are common in dogs and associated with hepatic underdevelopment (hypoplasia), two examples are Congenital Portosystemic Shunt (CPSS) and Primary Portal Vein Hypoplasia (PPVH). The first disease, CPSS, was proven to be a hereditary disease in Irish Wolfhounds, Yorkshire terriers, and Cairn terriers. However an increased presence of CPSS was also found in Silky terriers, Australian Cattle Dogs, Bichon Frise's, Shih Tzu's, Miniature

Schnauzers, Border Collies, and Jack Russell terriers [7]. CPSS is characterized by an abnormal single large communication between the portal vein and a major systemic vein (caval vein or azygos vein). This results in the hypoperfusion of the portal vein and insufficient perfusion of the liver from birth on. Subsequently liver growth is reduced or remains nearly absent; however there is essentially no additional liver pathology. The second disease, PPVH is a developmental abnormality in which the portal vein and particularly its terminal branches are diminished in size or absent. In about half of the cases, the disease is associated with fibrosis of the portal areas without inflammation [8]. Due to the underdeveloped portal vein, PPVH is associated with portal hypertension and, subsequent to the associated portal venous hypoperfusion, reduced liver growth.

Biochemical molecular analysis

Understanding of the regulatory roles of Hepatocyte Growth Factor (HGF), and Transforming Growth Factor-β1 (TGF-β1), via the respective receptors c-MET and TGF-β receptors type I and II, is crucial for defining the diseases and stages of disease in which HGF-related therapies may be beneficial. Continued sampling of sera and liver tissues of dogs with spontaneous liver diseases and healthy dogs have resulted in a large collection of samples. In order to analyze responsible pathways we have set up quantitative real-time PCR (Q-PCR) using a separate reverse polymerase step followed by the SYBR Green I Real-Time PCR (two-step Real-Time PCR). Western blot analysis was used to confirm mRNA levels and show activated (phosphorylated) proteins. Another novel technique used in chapters 3, 9, and 10 is RNA inhibition (RNAi). The inhibition of RNA describes a recently found mechanism of post-transcriptional gene-silencing. It was first discovered in 1990 by botanical researchers in petunias where dsRNA showed to specifically inhibit mRNA translation [9]. In the year 2001 small interfering RNA (siRNA) molecules were shown to specifically cleave mRNA molecules in cultured mammalian cells and *Drosophila* leading to a suppression of the translation of specific mRNAs [10,11]. Since this discovery the use of small synthetic dsRNA molecules has been used frequently in *in vitro* and *in vivo* experiments to investigate the function of specific genes.

Regenerative pathways of the liver

Regeneration of the liver is a widely excepted phenomenon already described by the ancient Greek in the legend of Prometheus. The legend describes Prometheus, a titan punished by Zeus for giving fire to man, being chained to a rock for 30,000 years and having his liver eaten by an eagle each day only to regenerate during the night (Figure 1). Although the recuperative power of the liver in this myth was somewhat exaggerated, regeneration of liver is studied extensively and holds great potential for possible therapies.

Figure 1. *The legend of Prometheus.*

Normal liver consists of two major epithelial cell types, hepatocytes and biliary epithelial cells. Other cell types include mesenchymal cells such as stellate cells (Ito-cells or fat-storing cells) and Kupffer cells (macrophages) as well as endothelial cells. After damage to the liver restoration of the liver parenchyma is due to rapid hyperplasia of all cell-types, until the liver mass is restored. The ability of a certain tissue to regenerate is dependent on the type of cells the tissue holds. To fully understand the mechanism of regeneration we must understand that there are three types of cells: 1) *active cells* which are constantly proliferating, such as intestinal epithelia, bone marrow or epidermal cells. 2) *Latent cells* are normally found in a resting phase in adult tissues but can start dividing after specific signals. Hepatocytes are such an

example; although dormant in adult tissue after (for instance) a partial hepatectomy (PHx), cells are stimulated to proliferate until the liver is completely restored [12]. 3) *Innate cells* are believed never to divide such as nerve cells or cardiomyocytes. However axon (nerve) cells have been shown to have the ability to divide under specific conditions [13,14].

Although there are many reports on regenerative pathways in the liver as possible targets of therapy, in canine medicine there is little information. One of the regenerative pathways studied was stimulated by Hepatocyte Growth Factor (HGF), one of the first described growth factors of hepatocytes [15,16]. HGF is a potent growth factor, not only for the liver but also for all epithelial and endothelial cell types [17], and is involved in the growth and development of many tissues such as the liver, kidney [18-21], heart [22], neural tissue [23], and other tissues such as cartilage and bone [24-26]. HGF is a large, 90 kD glycosylated protein consisting of a 56 kD α-chain and a 34 kD β-chain. The β-chain contains a hairpin structure and four kringles, whereas the α-chain is a serine protease [27,28]. The hairpin and the adjacent two kringles are the essential structures for the typical functions of the HGF molecule [27-29]. HGF has not only been shown to stimulate normal growth but also to progress tumor cell growth [30,31], especially of carcinoma cells. In the liver HGF is predominantly produced by the hepatic stroma cells (stellate or fat storing cells). In hepatocytes and other tissues HGF functions through binding to the membrane receptor called c-MET [32]. Adequate concentrations of both HGF and its receptor are required for the proper effectiveness of HGF. The three main signaling pathways activated by the HGF/c-MET complex are; 1) PI-3-Kinase→ PKB/Akt→ inhibition of FOXO's; 2) MEK1/2→ERK1/2; 3) JAK→STAT3. It is not the aim of this thesis to dissect these different pathways in molecular detail; we only concentrated on the basic components. When bound to its receptor c-MET, PI-3-Kinase indirectly phosphorylates the protein kinase B (PKB) also known as Akt [33]. This multifunctional protein inhibits a variety of transcription factors such as FOXO's (forkhead box, subgroup "O" transcription factors) also known as forkhead receptors [34], which in turn activate important proteins in cell-maintenance and viability (Figure 2).

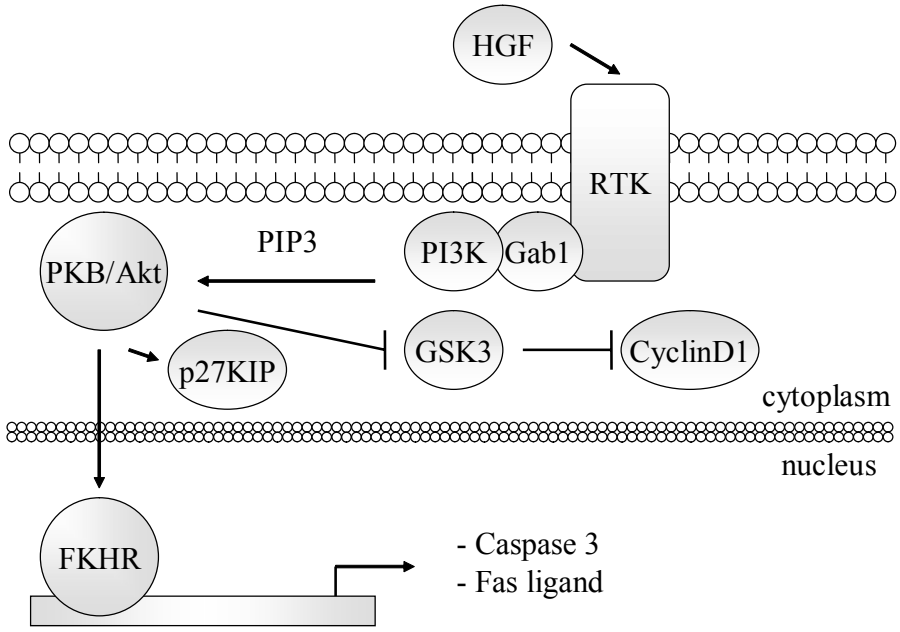

Figure 2. *PKB/Akt pathway.*
Growth factors, such as HGF, phosphorylate receptor tyrosine kinases (e.g. c-MET) and activate multiple intra-cellular pathways.

Other major regenerative pathways include Mitogen-Activated Protein Kinases (MAPKs) and the Jak-STAT pathway. MAP kinases signaling regulates cell proliferation, cell differentiation, and apoptosis [35]. MAPK signaling can be divided into three groups (Figure 3), the first ERK1/2 is predominantly activated by growth factors and is the best characterized member of the MAPK family [36]. After stimulation ERK1/2 translocates from the cytoplasm to the nucleus by passing through the nuclear pore by several independent mechanisms activating multiple targets involved in regeneration/growth and apoptosis. Second, the p38MAPK has been shown to be involved in cellular proliferation [37]. The third subgroup involves the c-jun N-terminal kinase or stress-activated protein kinases (JNK or SAPK). As suggested by the name these proteins are activated by many types of cellular stresses and extracellular signals [38]. Due to the involvement of SAPK/JNK in immune responses and organogenesis the pathway was not investigated in this thesis [39].

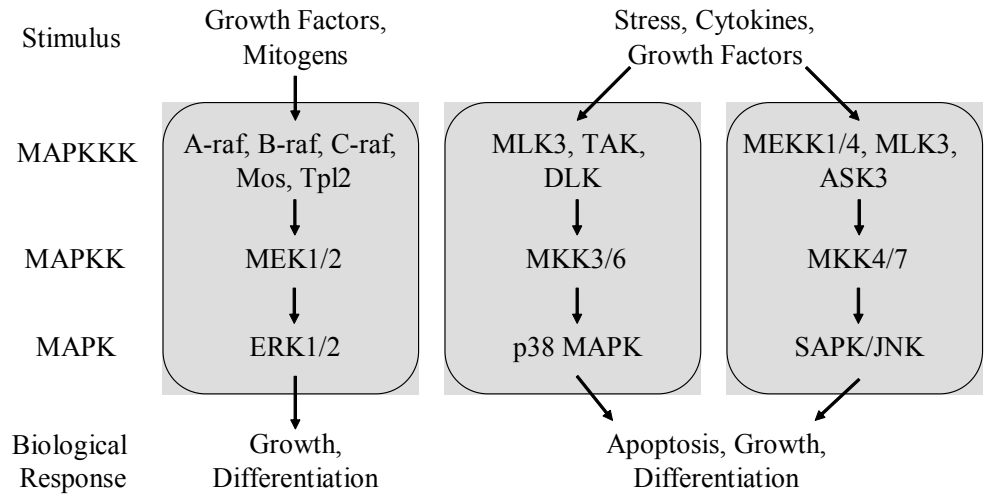

Figure 3. *Mitogen-Activated Protein Kinase (MAPK) pathways.*

Another pathway involved in regeneration is the STAT pathway and in particular STAT3. Although not as well characterized as the MAPKs the STAT3 pathway has been shown to be involved in mitogenic signals during liver regeneration [40]. One of the main stimulating factors is the inflammatory cytokine IL-6. After binding to the receptor the gp130 binding protein and Jak proteins will phosphorylate STAT3 on the tyrosine amino residue (Figure 4). STAT3 can also be phosphorylated on a serine amino residue by, for instance, HGF [41]. Furthermore, STAT3 has been shown to be phosphorylated (activated) by activated ERK1/2 [42].

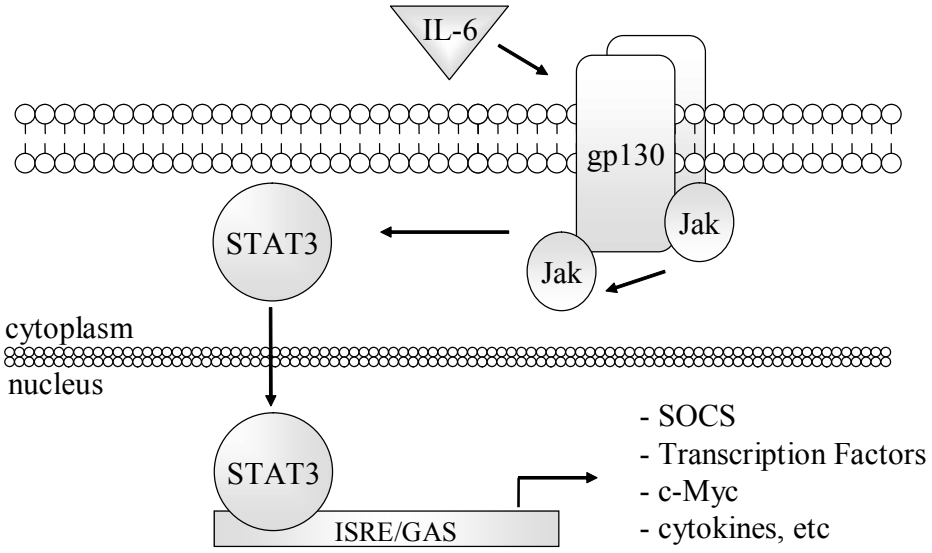

Figure 4. *Jak-STAT signaling: IL-6 receptor pathway.*
After transport into the nucleus STAT3 binds to interferon-stimulated responsive element and gamma-interferon-activated sequence (ISRE/GAS) transcribing various targets.

Fibrosis of the liver

The formation and breakdown of extra-cellular matrix (ECM) is a highly regulated process involving several signaling proteins and enzymes [43]. Fibrosis describes a pathological process where normal ECM stimulation is over-activated or ECM breakdown is disrupted. The current paradigm of fibrosis in man describes the increase of transforming growth factor-β1 (TGF-β1) which activates hepatic stellate cells (Ito-cells) to convert into myofibroblasts [44]. These myofibroblasts are the ECM producing cells of the liver (Figure 5). The myofibroblasts are motile cells that activate molecular programs capable of simultaneous degradation and *de novo* synthesis of ECM. This ECM production is regulated by binding of an active TGF-β1 to TGF-β receptor II (TGF-β RII). This activates TGF-β receptor I (TGF-β RI) which phosphorylates Smad proteins (Figure 5) [45]. Smad proteins are a family of related intracellular signal transducing complexes. After activation Smad complexes translocate into the nucleus, where they cooperate with sequence-specific transcription factors to regulate gene expression. One of the main targets of TGF-β1 receptor I is Smad2/3 transcribing TGF-β1 directed transcription factors which will ultimately lead to an increase in fibrosis [46-48].

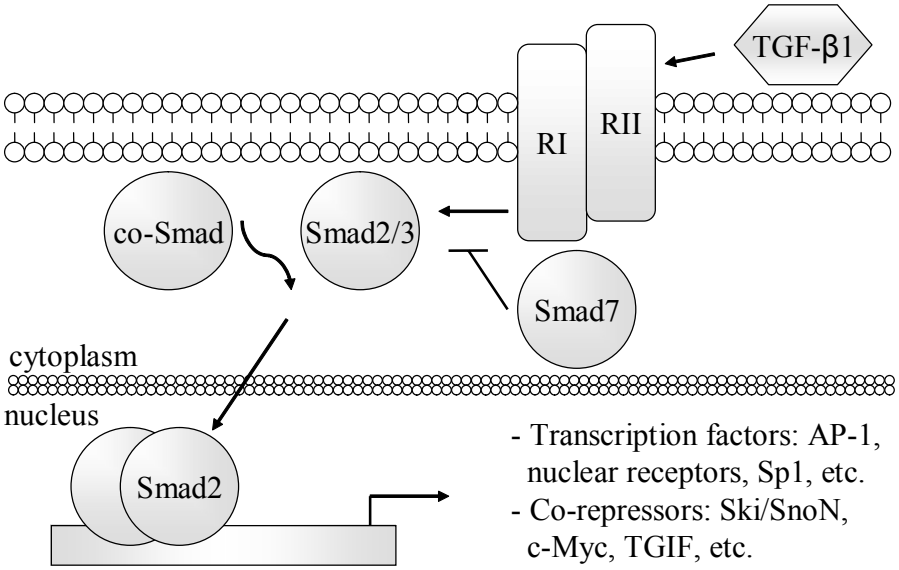

Figure 5. *TGF-β1 regulated Extra-Cellular Matrix (ECM) production.*

Apoptosis

Apoptosis is a regulated form of cell-death. Apoptosis can initiate through the intrinsic or the extrinsic pathway [49]. The intrinsic pathway is activated by intra-cellular stress caused by growth factor withdrawal, hypoxia, and DNA damage, and is triggered by cytochrome c release from the mitochondria. The extrinsic apoptotic pathway is triggered by death receptors such as Fas/CD95, TNF receptor, or the TRAIL receptor. The activation of these two pathways is not distinct as activation of one usually involves the other [50,51]. In this thesis we describe regulated cell-death in hepatic hypoplastic diseases and use the described processes as possible means for therapy in tumors. Other hepatic diseases are still under study, preliminary results indicate the importance of apoptosis during hepatic diseases. These processes are crucial to understand before any therapeutic approach can be developed.

Therapies developed for interfering with regenerative and fibrotic pathways

In this thesis, we investigated the possibility for growth factors, and in more detail HGF, as a possible treatment for acute or chronic hepatitis and cirrhosis as well as hypoplastic liver diseases. To asses the possible therapeutic use of HGF in these hepatic illnesses, regenerative- and fibrotic pathways were analyzed. Chronic hepatic diseases are highly complex, therefore we started analyzing regenerative and fibrotic pathways in hypoplastic diseases were complicating factors such as cholestasis and inflammation do not occur. These hypoplastic diseases with 'simple' pathogenesis were congenital portosystemic shunt (CPSS) and primary portal vein hypoplasia (PPVH), of which the latter is often associated with fibrosis (chapter 2). The second step was to extrapolate the results in the hypoplastic diseases to complex liver diseases. The same regenerative and fibrotic pathways were analyzed in acute hepatitis (AH), non-copper associated chronic hepatitis (CH), cirrhosis (CIRR), and a rapid form of cirrhosis, lobular dissecting hepatitis (LDH) (chapter 3 and 4). An important step in devising therapeutics is the production, purification, and application of the product. Therefore, in parallel to analyzing biochemical pathways, HGF was produced and tested for its biological activity (chapter 5).

Copper metabolism

As mentioned before many dog breeds are predisposed to hepatic copper toxicosis (CT) where a massive increase in hepatic copper leads to chronic hepatitis and ultimately cirrhosis. Although a vital component of several proteins, copper excess can very quickly become toxic inducing oxidative stress through the Haber-Weiss reaction [52]. Copper is taken up by the cell by an ATP dependent process through copper transporting receptor 1 (CTR1). From here several copper chelating proteins denoted copper chaperones are involved in the transport of copper to several intracellular compartments (Figure 6) [53]. The copper chaperone ATOX1 is involved in the transport of copper to the Golgi compartment. ATP7A and ATP7B, both present in the Golgi compartment under physiological conditions can excrete copper extracellularly (ATP7A), or transport copper to other copper chelating proteins (ATP7B) [54]. COMMD1, previously known as MURR1, has been shown to bind to the ATP7B N-terminal copper binding region [55]. As this protein was mutated in Bedlington terriers with hepatic copper toxicosis, COMMD1 was believed to play a critical role in copper excretion [11]. Other copper chelating proteins are ceruloplasmin (CP) and metallothionein (MT1A). CP is a known target of ATP7B transporting copper to the blood. MT1A is a copper storage protein highly regulated on a transcriptional level by copper availability [56,57].

Inherited defects of copper metabolism resulting in hepatic copper accumulation and oxidative-stress may cause different breed-associated forms of hepatitis [76]. It is currently hard to decide whether copper accumulation is the primary event causing these forms of hepatitis, or secondary due to impaired excretion into bile. The question that is raised in the literature with respect to hepatic copper accumulation has always been; does cholestasis as an inevitable component of hepatitis cause copper accumulation? This question has been addressed in this thesis (chapter 6), in order to develop solid criteria to answer this hen or egg dilemma.

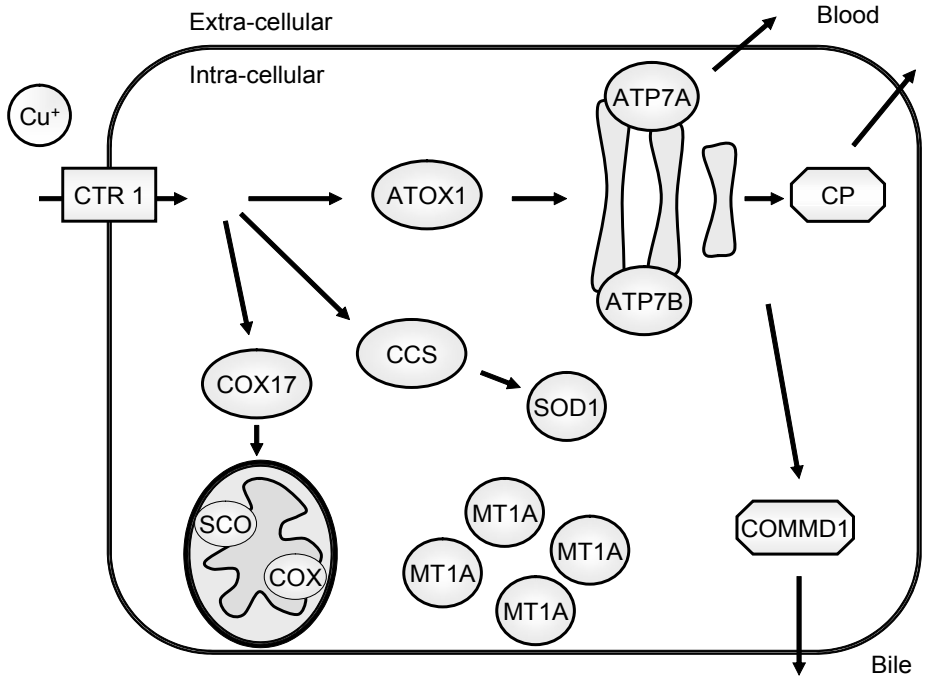

Figure 6. *Proteins involved in uptake, intracellular transport, and excretion of copper.*

As mentioned before a deletion in the COMMD1 protein showed to be responsible for increased hepatic copper concentrations in Bedlington terriers. As the homozygous deletion (39.7 kb) encompasses the entire exon two of the *COMMD1* gene the detection was based on positional cloning of the C04107 marker [59]. A simple and robust test for this deletion especially focusing on detecting heterozygous carriers would greatly enhance positive detections. Therefore in chapter 8 we describe the use of quantitative PCR on genomic DNA isolated from blood or buccal swabs detecting carriers and affected animals with great specificity. Furthermore the COMMD1 protein has shown to have several functions such as the regulation of NF-kappaB and sodium transport

[60,61]. However the role of COMMD1 in copper metabolism remains unclear. The establishment of a *COMMD1* knock-out (*COMMD1* $^{-/-}$) in mice would greatly enhance our current understanding of this gene; however *COMMD1* $^{-/-}$ mice were not viable. In fact an in-house dog line with a homozygous *COMMD1* deletion is the only viable mammalian *COMMD1* $^{-/-}$ species described thus far. These dogs allow us to study the progression of copper-induced chronic hepatitis longitudinally with biopsies taken every 6 months (R. Favier). As progression of the disease usually takes several years [62,63], we specifically knocked-down *COMMD1* gene-expression in order to evaluate gene-functions of COMMD1 in a hepatic epithelial cell-line. Results are described in chapter 9.

Inhibiting excessive growth

Cancers can be characterized by abnormal growth due to increased proliferation and/or increased cell survival. Because we have already analyzed growth signaling pathways in hepatic diseases we used the same techniques analyzing tumor growth. In a recently established cell-line from a hepatocellular carcinoma (HCC) we have shown the close resemblance to human HCC [64]. Potential treatment of cancers by inhibiting these pathways is not new, all therapies devised against tumors try to diminish the anti-apoptotic characteristic of tumors or reverse the increased growth. Potential targets of novel therapies are osteosarcoma and mammary tumors which are frequently found in dogs [65]. Osteosarcoma is predisposed to several (large) breeds and accounts for 5 to 6 percent of all canine malignancies [66,67]. Mammary tumors in dogs also occur frequently; in a recent study 13 percent of all female dogs older than 10 years old had at least one claim of mammary tumors with an overall mortality of 6 percent [68]. Furthermore patterns of biochemical changes in proteins of human and canine mammary tumors are highly similar validating the use of canine models to understand the molecular mechanisms of mammary carcinogenesis [69].

Questions

Based on the central themes of this thesis (concerning signal transduction pathways involved in regeneration, fibrosis, cellular homeostasis, copper handling, and oxidative stress), several questions are raised:

- Is the HGF/c-MET signaling pathway functional in congenital diseases (CPPS and PPVH) that are devoid of inflammation and cholestasis?
- Can the difference in these hypoplastic diseases, with regard to ECM-deposition, be explained by disturbed balance HGF-TGF-β1?
- Is the HGF/c-MET signaling pathway functional in more complex liver diseases like acute and chronic hepatitis, cirrhosis, and lobular dissecting hepatitis?
- If the HGF/c-MET signal transduction pathway is functional does this hold any promises for HGF treatment?
- Is the TGF-β1 signaling pathway activated in liver diseases associated with excessive amount of ECM-deposition? Can the difference with regard to fibrosis be explained by disturbed balance HGF-TGF-β1?
- Anticipating HGF as a possible treatment, recombinant canine HGF was produced in a Baculovirus expression system. Is this recombinant product biologically active, and does it activate cellular signal transduction pathways leading to heptocyte proliferation, anti-apoptosis, and anti-fibrosis?
- Is copper accumulation a consequence of cholestasis or a direct effect of affected intracellular copper transport? Do high intracellular copper levels reduce the cellular protection against (copper-induced) oxidative stress?
- Is the copper homeostasis disturbed in Doberman hepatitis, and to what extent is oxidative stress induced in livers of these animals?
- The genetic analysis of the COMMD1 mutation in Bedlington terriers with copper toxicosis is laborious due to large size of the deletion. Is it possible to develop a Q-PCR based rapid sensitive and reliable method for genetic screening for this deletion?
- Does siRNA-mediated knock-down of the COMMD1 gene product lead to increased copper retention in hepatic cells and what are the functional consequences of increased copper accumulation on cellular homeostasis?
- Does siRNA-mediated knock-down of the XIAP gene-product, which is associated with COMMD1 and is involved in protection against apoptosis, lead to increased sensitivity to different chemotherapeutics in cell-lines?

References

[1] Rothuizen J, van den Ingh TS. Hepatitis in dogs; a review. Tijdschr Diergeneeskd 1998 123:246-252.

[2] Cullen JM, MacLachlan NJ: Liver, biliary system, and exocrine pancreas. In: McGavin MD, Carlton WW, Zachary JF (eds) Thompson's Special Veterinary Pathology, 3rd ed, Mosby, St. Louis, 2001:81-124.

[3] Jarrett WF, O'Neil BW, Lindholm I. Persistent hepatitis and chronic fibrosis induced by canine acidophil cell hepatitis virus. Vet Rec 1987, 120:234-235.

[4] Klomp AE, van de Sluis B, Klomp LW, et al. The ubiquitously expressed MURR1 protein is absent in canine copper toxicosis. J Hepatol 2003, 39:703-709.

[5] Bennett AM, Davies JD, Gaskell CJ, et al. Lobular dissecting hepatitis in the dog. Vet Pathol 1983, 20:179-188.

[6] Hunt GB. Effect of breed on anatomy of portosystemic shunts resulting from congenital diseases in dogs and cats: a review of 242 cases. Aust Vet J 2004, 82:746-749.

[7] Van den Ingh TS, Rothuizen J, Meyer HP. Portal hypertension associated with primary hypoplasia of the hepatic portal vein in dogs. Vet Rec 1995, 137:424-427.

[8] Metzlaff M, O'Dell M, Cluster PD, et al. RNA-mediated RNA degradation and chalcone synthase A silencing in petunia. Cell 1997, 88:845-854.

[9] Elbashir SM, Harborth J, Lendeckel W, et al. Duplexes of 21-nucleotide RNAs mediate RNA interference in cultured mammalian cells. Nature 2001, 411:494-498.

[10] Elbashir SM, Lendeckel W, Tuschl T. RNA interference is mediated by 21- and 22-nucleotide RNAs. Genes Dev 2001, 15:188-200.

[11] Taub R. Liver regeneration: from myth to mechanism. Nat Rev Mol Cell Biol 2004, 5:836-847.

[12] Zhang M, Yannas IV. Peripheral nerve regeneration. Adv Biochem Eng Biotechnol 2005, 94:67-89.

[13] Mandemakers WJ, Barres BA. Axon regeneration: it's getting crowded at the gates of TROY. Curr Biol 2005, 15:R302-305.

[14] Russell WE, McGowan JA, Bucher NL. Partial characterization of a hepatocyte growth factor from rat platelets. J Cell Physiol 1984, 119:183-192.

[15] Michalopoulos G, Houck KA, Dolan ML, et al. Control of hepatocyte replication by two serum factors. Cancer Res 1984, 44:4414-4419.

[16] Brinkmann V, Foroutan H, Sachs M, et al. Heptocyte growth factor/scatter factor induces a variety of tissue-specific morphogenic programs in epithelial cells. J Cell Biol 1995, 131:1573-1586.

[17] Azuma H, Takahara S, Kitamura M, et al. Effect of hepatocyte growth factor on chronic rejection in rat renal allografts. Transplant Proc 1999, 31:854-855.

[18] Liu Y, Tolbert EM, Lin L, et al. Up-regulation of hepatocyte growth factor receptor: amplification and targeting mechanism for hepatocyte growth factor action in acute renal failure. Kidney Int 1999, 55:442-453.

[19] Takada, S, Takahara S, Nishimura K, et al. Effect of hepatocyte growth factor on tacrolimus-induced nephrotoxicity in spontaneously hypertensive rats. Transplant Int 1999;12:27-32.

[20] Matsumoto K, Morishita R, Morguchi A, et al. Prevention of renal damage by angiotensin II blockade, accompanied by increased renal hepatocyte growth factor in experimental hypertensive rats. Hypertension 1999, 34:279-284.

[21] Ueda H, Sawa Y, Kitagawa-Sakakida S, et al. Gene transfection of hepatocyte growth factor attenuates reperfusion injury in the heart. Ann Thorac Surg 1999, 76:1726-1731.

[22] Marina F, Klein R. Hepatocyte growth factor, a versatile signal for developing neurons. Nature Neuroscience 1999, 2:213-217.

[23] Kamalati T, Niranjan B, Yant J, et al. HGF/SF in mammary epithelial growth and morphogenesis: in vitro and vivo models. J Mammary Gland Biol Neoplasia 1999, 4:69-77.

[24] Nagahori T, Dohi M, Matsumoto K, et al. Interferon-gamma upregulates the c-Met/hepatocyte growth factor receptor expression in alveolar epithelial cells. Am J Respir Cell Mol Biol 1999, 21:490-497.

[25] Kermorgant S, Walker F, Hormi K, et al. Developmental expression and functionality of hepatocyte growth factor and c-Met in human fetal digestive tissues. Gastroenterology 1997, 112:1635-1647.

[26] Nakamura T. Stucture and function of hepatocyte growth factor. Progress in Growth Factor Research 1991, 3:67-85.

[27] Tamagnone L, Comoglio PM. Control of invasive growth by hepatocyte growth factor (HGF) and related scatter factors. Cytokine and Growth Factor Reviews 1997, 8:129-142.

[28] Sanuti-Ruiu E, Preisegger KH, Kiss A, et al. Inhibition of neoplastic development in the liver by hepatocyte growth factor in a transgenic mouse model. Proc Nat Acad Sci USA 1996, 93:9577-9582.

[29] Bardeli A, Longati P, Albero D, et al. HGF receptor associates with the anti-apoptotic protein BAG-1 and prevents cell death. EMBO J 1996, 15:6205-6212.

[30] Matsumoto K, Nakamura T. Emerging multipotent aspects of hepatocyte growth factor. J Biochem 1996, 119:591-600.

[31] Masuhara M, Yasunaga M, Taigawa K, et al. Expression of hepatocyte growth factor, transforming growth factor alpha, and transforming growth factor beta-1 messenger RNA in various human liver diseases and correlation with hepatocyte proliferation. Hepatology 1996, 24:323-329.

[32] Shiota G, Kawasaki H. Hepatocyte growth factor in transgenic mice. Int J Exp Pathol 1998, 79:267-277.

[33] Okano J, Shiota G, Matsumoto K, et al. Hepatocyte growth factor exerts a proliferative effect on oval cells through the PI3K/AKT signaling pathway. Biochem Biophys Res Commun 2003, 309:298-304.
[34] Tang ED, Nunez G, Barr FG, et al. Negative regulation of the forkhead transcription factor FKHR by Akt. J Biol Chem 1999, 274:16741-16746.
[35] Thomas G. MAP kinase by any other name smells just as sweet. Cell 1992, 68:3-6.
[36] Seger R, Krebs EG. The MAPK signaling cascade. FASEB J 1995, 9:726-735.
[37] Bulavin DV, Higashimoto Y, Popoff I, et al. Initiation of a G2/M checkpoint after ultraviolet radiation requires p38 kinase. Nature 2001, 411:102-107.
[38] Kyriakis JM, Banerjee P, Nikolakaki E, et al. The stress-activated protein kinase subfamily of c-Jun kinases. Nature 1994, 369:156-160.
[39] Nishina H, Wada T, Katada T. Physiological roles of SAPK/JNK signaling pathway. J Biochem 2004, 136:123-126.
[40] Terui K, Ozaki M. The role of STAT3 in liver regeneration. Drugs Today 2005, 41:461-469.
[41] Borowiak M, Garratt AN, Wustefeld T, et al. Met provides essential signals for liver regeneration. Proc Natl Acad Sci U S A 2004, 101:10608-10613.
[42] Nakagami H, Morishita R, Yamamoto K, et al. Mitogenic and antiapoptotic actions of hepatocyte growth factor through ERK, STAT3, and AKT in endothelial cells. Hypertension 2001, 37:581-586.
[43] Tsukada S, Parsons CJ, Rippe RA. Mechanisms of liver fibrosis. Clin Chim Acta 2005, 31: [Epub ahead of print] doi:10.1016/j.cca.2005.06.014.
[44] Zavadil J, Bottinger EP. TGF-beta and epithelial-to-mesenchymal transitions. Oncogene 2005, 24:5764-5774.
[45] Feng XH, Derynck R. Specificity and Versatility in TGF-β Signaling Through Smads. Annu Rev Cell Dev Biol. 2005, 21:659-693.
[46] Wrana JL. Crossing Smads. Sci STKE 2000, 2000:RE1.
[47] Attisano L, Wrana JL. Signal transduction by the TGF-beta superfamily. Science 2002, 296:1646-1647.
[48] Moustakas A, Souchelnytskyi S, Heldin CH. Smad regulation in TGF-beta signal transduction. J Cell Sci 2001, 114:4359-4369.
[49] Kim R. Recent advances in understanding the cell death pathways activated by anticancer therapy. Cancer 2005, 103:1551-1560.
[50] Bergman PJ. Mechanisms of anticancer drug resistance. Vet Clin North Am Small Anim Pract 2003, 33:651-667.
[51] Boatright KM, Salvesen GS. Mechanisms of caspase activation. Curr Opin Cell Biol 2003, 15:725-731.
[52] Klotz LO, Kroncke KD, Buchczyk DP, et al. Role of copper, zinc, selenium and tellurium in the cellular defense against oxidative and nitrosative stress. J Nutr 2003, 133:1448-1451.

[53] Dijkstra M, Vonk RJ, Kuipers F. How does copper get into bile? New insights into the mechanism(s) of hepatobiliary copper transport. J Hepatol 1996, 24:109-120.

[54] Vulpe C, Levinson B, Whitney S, et al. Isolation of a candidate gene for Menkes disease and evidence that it encodes a copper-transporting ATPase. Nat Genet 1993, 3:7-13.

[55] Tao TY, Liu F, Klomp L, et al. The copper toxicosis gene product Murr1 directly interacts with the Wilson disease protein. J Biol Chem 2003, 278:41593-41596.

[56] Daffada AA, Young AP. Coordinated regulation of ceruloplasmin and metallothionein MRNA by interleukin-1 and copper in HepG2 cells. Febs Lett 1999, 457:214-218.

[57] Mattie MD, Freedman JH. Copper-inducible transcription: regulation by metal- and oxidative stress-responsive pathways. Am J Physiol Cell Physiol 2004, 286:293-301.

[58] Thornburg LP. A perspective on copper and liver disease in the dog. J Vet Diagn Invest 2000, 12:101-110.

[59] van de Sluis B, Peter AT, Wijmenga C. Indirect molecular diagnosis of copper toxicosis in Bedlington terriers is complicated by haplotype diversity. J Hered. 2003, 94:256-259.

[60] Burstein E, Hoberg JE, Wilkinson AS, et al. COMMD proteins, a novel family of structural and functional homologs of MURR1. J Biol Chem 2005, 280:22222-22232.

[61] Biasio W, Chang T, McIntosh CJ, et al. Identification of Murr1 as a regulator of the human delta epithelial sodium channel. J Biol Chem 2003, 279:5429-5434.

[62] Sternlieb I. Copper toxicosis of the Bedlington terrier. J Rheumatol Suppl 1981, 7:94-95.

[63] Stockman MJ. Copper toxicosis in the Bedlington terrier. Vet Rec 1988, 123:355.

[64] Boomkens SY, Spee B, IJzer J, et al. The establishment and characterization of the first canine hepatocellular carcinoma cell line, which resembles human oncogenic expression patterns. Comp Hepatol 2004, 3:9.

[65] Vail DM, MacEwen EG. Spontaneously occurring tumors of companion animals as models for human cancer. Cancer Invest 2000, 18:781-792.

[66] Chun R, de Lorimier LP. Update on the biology and management of canine osteosarcoma. Vet Clin North Am Small Anim Pract 2003, 33:491-516.

[67] Endicott M. Principles of treatment for osteosarcoma. Clin Tech Small Anim Pract 2003, 18:110-114.

[68] Egenvall A, Bonnett BN, Ohagen P, et al. Incidence of and survival after mammary tumors in a population of over 80,000 insured female dogs in Sweden from 1995 to 2002. Prev Vet Med 2005, 69:109-127.

[69] Kumaraguruparan R, Karunagaran D, Balachandran C, et al. Of humans and canines: A comparative evaluation of heat shock and apoptosis-associated proteins in mammary tumors. Clin Chim Acta 2005, [Epub ahead of print] doi:10.1016/j.cca.2005.08.018.

Chapter 2

Regenerative and fibrotic pathways in canine hepatic portosystemic shunt and portal vein hypoplasia, new models for clinical hepatocyte growth factor (HGF) treatment

Bart Spee[1], Louis C. Penning[1], Ted S.G.A.M. van den Ingh[2], Brigitte Arends[1], Jooske IJzer[2], Frederik J. van Sluijs[1], and Jan Rothuizen[1]

From the Departments of [1]Clinical Sciences of Companion Animals and [2]Pathobiology, Faculty of Veterinary Medicine, Utrecht University, The Netherlands.

Adapted from *Comparative Hepatology* 2005, 4:7.

Abstract

We analyzed two spontaneous dog diseases characterized by subnormal portal perfusion and reduced liver growth: (i) congenital portosystemic shunts (CPSS) without fibrosis and (ii) primary portal vein hypoplasia (PPVH), a disease associated with fibrosis. These pathologies, that lack inflammation or cholestasis, may represent simplified models to study liver growth and fibrosis. To investigate the possible use of these models for Hepatocyte Growth Factor (HGF) treatment, we studied the functionality of HGF signaling in CPSS and PPVH dogs and compared this to aged-matched healthy controls. We used quantitative real-time polymerase chain reaction (Q-PCR) to analyze the mRNA expression of Hepatocyte Growth Factor (HGF), Transforming Growth Factor-β1 (TGF-β1), and relevant mediators in liver biopsies from cases with CPSS or PPVH, in comparison with healthy control dogs. CPSS and PPVH were associated with a decrease in mRNA expression of HGF and c-MET. Western blot analysis confirmed the Q-PCR results and showed that intracellular signaling components (PKB/Akt, ERK1/2, and STAT3) were functional. The TGF-β1 mRNA levels were unchanged in CPSS but t-fold increased in PPVH indicating an active TGF-β1 pathway, consistent with the observation of fibrosis seen in PPVH. Western blots on TGF-β1 and phosphorylated Smad2 confirmed an activated pro-fibrotic pathway in PPVH. Furthermore, Q-PCR showed an increase in the amount of Collagen I present in PPVH compared to CPSS and control, which was confirmed by Western blot analysis. The pathophysiological differences between CPSS and PPVH can adequately be explained by the Q-PCR measurements and Western blots. Although c-MET levels were reduced, downstream signaling seemed to be functional and provides a rational for HGF-supplementation in controlled studies with CPSS and PPVH. Furthermore both diseases may serve as simplified models for comparison with more complex chronic inflammatory diseases and cirrhosis.

Introduction

Chronic liver disease is characterized by decreased regeneration of hepatocytes and increased formation of fibrous tissue. These characteristics may be the sequel of various chronic processes such as cholestasis, viral infections, toxin exposure, and metabolic disorders. Dogs have complex liver diseases such as hepatitis and cirrhosis which are highly comparable with the human counterparts. Moreover, coding sequences of dogs proved highly homologous to the human sequences [1], especially compared to the rodent genome. Thus, dogs may fulfill a role as a spontaneous animal model in between toxin-induced or surgical models in rodents, and spontaneous diseases in man. The complex interplay of many factors active in chronic liver disease makes it difficult to unravel the roles of different individual pathogenetic pathways. Dogs display liver diseases, which are potentially valuable models to compare complex with simple pathologic entities.

We have chosen these two congenital dog diseases for comparative analysis of liver growth/regeneration, fibrosis, and hepatic homeostasis: congenital portosystemic shunt (CPSS) and primary portal vein hypoplasia (PPVH). CPSS is characterized by an abnormal single large communication between the portal vein and a major systemic vein (cava or azygos). This results in the virtual absence of portal vein perfusion to the liver from birth onwards. Liver growth remains nearly absent but there is essentially no liver pathology [2,3]. PPVH is a developmental abnormality in which the terminal vein branches are not or only partially present and, in most cases, in combination with congenital portal fibrosis, but without inflammation [4]. PPVH is associated with portal hypertension and reduced liver growth. Thus, these two congenital diseases represent relatively simple models for reduced liver growth associated with fibrosis (PPVH) or without fibrosis (CPSS). Both diseases have a decrease in liver growth due to markedly insufficient portal perfusion which results in a massive reduction of liver size.

Because hepatocyte growth factor (HGF) is one of the most important genes involved in liver growth/regeneration [5-7], abnormal expression of HGF could play a major role in the decreased liver size in CPSS or PPVH. Therefore, treatment of dogs with HGF could be a possible therapeutic approach. A pre-requisite for treatment is that HGF signaling components are unaffected in those dogs. Consequently, we focused on measuring gene products involved in signaling of HGF and counteracting transforming growth factor β1 (TGF-β1). All biological responses induced by HGF are elicited by binding to its receptor, a transmembrane tyrosine kinase encoded by the MET proto-oncogene (c-MET). The signaling cascade triggered by HGF begins with phosphorylation of the receptor and is mediated by concomitant activation of

different cytoplasmic effectors that bind to the same multifunctional binding site. The c-MET mediated response includes two key pathways involved in cell survival and mitogenesis [8]. The first; protein kinase B (PKB/Akt) is activated by phosphoinositide 3-kinase (PI3K) and elicits cell survival [9,10]. The second; ERK1/2 (also known as p42/44 MAPK), a member of the mitogen-activated protein (MAP) kinase family, is activated by the RAS-RAF-MEK pathway and is responsible for mitogenesis [11]. A third response of HGF is the branching morphogenesis which next to the PKB and ERK pathways requires involvement of the signal transducer and activator of transcription (STAT) 3 pathway [12].

It is well established that an increase of TGF-β1 in liver promotes the formation of extracellular matrix (ECM) components and suppresses hepatocyte proliferation [13,14]. Prolonged overexpression of TGF-β1 in non-parenchymal cells causes hepatic fibrosis in humans and experimental animals. In several fibrosis models, fibrotic lesions are associated with an increase in collagens and TGF-β1 mRNAs [15]. The intracellular pathway that is activated by TGF-β1 receptors is mediated by Smads. Smad2 is activated via carboxy-terminal phosphorylation by TGF-β1 type I receptor kinases. When bound with co-Smads, they act as TGF-β1-induced transcriptional activators of target genes [16].

Cell homeostasis is the result of balance between cell death, cell proliferation, and growth-arrest. Therefore we investigated expression levels of pro-apoptotic Fas-ligand and caspase-3, anti-apoptotic Bcl-2 [17], cell-cycle stimulating TGFα, and cell-cycle inhibitor p27kip. All of these gene-products are regulated directly or indirectly by PKB [9].

The present study was designed to describe the differential gene-expression of the above indicated crucial pathways involved in growth/regeneration, fibrosis, and cellular homeostasis in liver tissues of dogs with CPSS (reduced growth/regeneration without fibrosis) and PPVH (reduced growth/regeneration and fibrosis) in comparison with healthy animals. These simple congenital dog models may be used to unravel the roles of different gene products in those pathways. These well-defined large animal models are intended to serve as the first spontaneous liver diseases to investigate novel regenerative/anti-fibrotic therapies, such as HGF treatment. This study may also serve as a basis for future comparison with more complex diseases like chronic hepatitis and cirrhosis.

Materials and methods

Animals

All samples are obtained from different dog breeds appearing in the clinic with spontaneous diseases. Samples were randomly chosen and aimed to encompass different dog-breeds and both sexes in each group. The procedures were approved by the Ethical Committee as required under Dutch legislation.

Groups

The congenital portosystemic shunt (n = 11 dogs) and primary portal vein hypoplasia group (n = 8 dogs) were compared with a group of healthy dogs (n = 11 dogs). The inclusion criteria for CPSS were increased fasting plasma ammonia concentration, abnormal ammonia tolerance test (peak ammonia ≥ 150 μmol/L plasma) and ultrasonographic visualization of a small liver and a congenital portosystemic shunt with a diameter as wide as the portal vein trunk. The presence of the shunt was further confirmed with surgery. During surgery a wedge liver biopsy was taken and immediately put in liquid nitrogen and stored at -70^{o}C until analysis. In CPSS there is no portal hypertension. The inclusion criteria for PPVH were the visualization of a small liver with ultrasonography, presence of multiple small acquired portosystemic collaterals due to portal hypertension, and an abnormal ammonia tolerance test (peak ammonia ≥150 μmol/L plasma). Liver tissue of dogs with PPVH was obtained under local anaesthesia by ultrasound-guided biopsy with a true cut 16G biopsy needle. Two biopsies were immediately immersed in liquid nitrogen, and stored at –70^{o}C until analysis. The healthy control dogs were age-matched, and had AP, ALT, and fasting bile acids in plasma within the reference range. Ultrasonographically the control dog livers had a normal size, shape, and structure, and there were no histological abnormalities in stained histological sections.

Histological grading of fibrosis

All liver samples were fixed in 10% buffered formalin and routinely embedded in paraffin. Sections (4μm) were stained with haematoxylin eosin, the Van Gieson stain, and the reticulin stain according to Gordon and Sweet. Histologically the presence of fibrosis was evaluated semi-quantitatively (absent, slight, moderate, or marked) as well as with respect to its localization. Fibrosis scoring was performed according to Scheuer, a defined scoring method for fibrosis in hepatitis. The slides were independently examined by one certified veterinary pathologist.

RNA isolation and reverse-transcription polymerase chain reaction

Total cellular RNA was isolated from each frozen canine liver tissue in duplicate, using the RNeasy Mini Kit (Qiagen, Leusden, The Netherlands) according to the manufacturer's instructions. The RNA samples were treated with Dnase-I (Qiagen Rnase-free DNase kit). In total 3 µg of RNA was incubated with poly(dT) primers at 42°C for 45 min, in a 60 µl reaction volume, using the Reverse Transcription System from Promega (Promega Benelux, Leiden, The Netherlands).

Quantitative measurements of the mRNA levels of HGF, TGF-β1, and other related signaling molecules

Real-Time PCR based on the high affinity double-stranded DNA-binding dye SYBR® green I (BMA, Rockland, ME) was performed in triplicate in a spectro-fluoremetric thermal iCycler® (BioRad, Veenendaal, The Netherlands). Data were collected and analyzed with the provided application software. For each Q-PCR, 2 µl (of the 2 times diluted stock) of cDNA was used in a reaction volume of 50 µl containing 1x manufacturer's buffer, 2 mM $MgCl_2$, 0.5 × SYBR® green I, 200 µM dNTP's, 20 pmol of both primers, 1.25 units of AmpliTaq Gold (Applied Biosystems, Nieuwerkerk a/d IJssel, The Netherlands), on 96-well iCycler iQ plates (Bio-Rad). Primer pairs, depicted in Table 1, were designed using PrimerSelect software (DNASTAR Inc., Madison, WI). All PCR protocols included a 5-minute polymerase activation step and continued for 40 cycles at 95°C denaturation for 20 sec, annealing for 30 sec and elongation at 72°C for 30 sec with a final extension for 5 min at 72°C. Annealing temperatures were optimized at various levels ranging from 56°C till 67°C (Table 1). Melt curves (iCycler, BioRad), agarose gel electrophoresis, and standard sequencing procedures were used to examine each sample for purity and specificity (ABI PRISM 3100 Genetic Analyser, Applied Biosystems). Standard curves constructed by plotting the relative starting amount versus threshold cycles were generated using serial 4-fold dilutions of pooled cDNA fractions from both healthy and diseased liver tissues. The amplification efficiency,
$E\ (\%) = (10^{(1/-s)}-1)\ ^{*}\ 100$ (s = slope), of each standard curve was determined and appeared to be > 95 %, and < 105 %, over a wide dynamic range. For each experimental sample the amount of the gene of interest, and of the endogenous references glyceraldehyde-3-phosphate dehydrogenase (GAPDH) and hypoxanthine phosphoribosyl transferase (HPRT) were determined from the appropriate standard curve in autonomous experiments. If relative amounts of GAPDH and HPRT were constant for a sample, data were considered valid and the average amount was included in the study (data not shown). Results were normalized according to the average amount of

the endogenous references. The normalized values were divided by the normalized values of the calibrator (healthy group) to generate relative expression levels [18].

Statistical analysis

A Kolmogorov-Smirnov test was performed to establish a normal distribution and a Levene's test for the homogeneity of variances. All samples included in this study were normally distributed. The statistical significance of differences between diseased and control animals was determined by using the Student's *t*-test. A p-value < 0.05 was considered statistically significant. Analysis was performed using SPSS software (SPSS Benelux BV, Gorinchem, the Netherlands).

Western blot analysis

Used antibodies are described in Table 2. For Western blot analysis 30 mg of liver tissue from at least six samples of each group (n = 6 dogs per group, randomly chosen from original group) were pooled and analyzed. Liver tissues were homogenized in RIPA buffer containing 1 % Igepal, 0.6 mM Phenylmethylsulfonylfluoride, 17 µg/ml aprotinine, and 1 mM sodium-orthovanadate (Sigma chemical Co., Zwijndrecht, The Netherlands). Protein concentrations were obtained using a Lowry-based assay (DC Protein Assay, BioRad). Twenty µg of protein of the supernatant was denatured for 3 min at 95^{o}C and electroferesed on 7.5 % Tris-HCl polyacrylamide gels (BioRad) and the proteins were transferred onto Hybond-C Extra Nitrocellulose membranes (Amersham Biosciences Europe, Roosendaal, The Netherlands) using a Mini Trans-Blot® Cell blot-apparatus (BioRad). Immunodetection was based on an ECL Western blot analysis system, performed according to the manufacturer's instructions (Amersham Biosciences Europe). The membranes were incubated with 4 % ECL blocking solution in TBS for 1 hour under gentle shaking. The incubation of the primary antibody was performed at 4^{o}C over-night for all antibodies (see Table 2) in TBS with 0.1 % Tween-20 (Boom B.V., Meppel, The Netherlands). After washing, the membranes were incubated with their respective horseradish peroxidase-conjugated secondary antibody (R&D systems, Europe Ltd., Abingdon, UK) at room temperature for 1 h and exposed to Kodak BioMax Light-1 films (Sigma chemical Co.). Densitometric analysis of immunoreactive bands was performed with a Gel Doc 2000 system with Quantity One 4.3.0 Software (BioRad).

Table 1. *Nucleotide Sequences of Dog-Specific Primers for Real-Time Q-PCR*

Gene	F/R	Sequence (5'-3')	Tm (°C)	Product size (bp)	Accession number
GAPDH	F	TGT CCC CAC CCC CAA TGT ATC	58	100	AB038240
	R	CTC CGA TGC CTG CTT CAC TAC CTT			
HPRT	F	AGC TTG CTG GTG AAA AGG AC	56	100	L77488 / L77489
	R	TTA TAG TCA AGG GCA TAT CC			
HGF	F	AAA GGA GAT GAG AAA CGC AAA CAG	58	92	BD105535
	R	GGC CTA GCA AGC TTC AGT AAT ACC			
c-MET	F	TGT GCT GTG AAA TCC CTG AAT AGA AATC	59	112	AB118945
	R	CCA AGA GTG AGA GTA CGT TTG GAT GAC			
TGFα	F	CCG CCT TGG TGG TGG TCT CC	63	136	AY458143
	R	AGG GCG CTG GGC TTC TCG T			
HGF	F	ACA CAG ACG TTT GGC ATC GAG AAG TAT	60	128	AY458142
	R	AAA CTG GAG CGG ATG GCA CAG			
p27kip	F	CGG AGG GAC GCC AAA CAG G	60	90	AY455798
	R	GTC CCG GGT CAA CTC TTC GTG			
TGF-β1	F	CAA GGA TCT GGG CTG GAA GTG GA	66	113	L34956
	R	CCA GGA CCT TGC TGT ACT GCG TGT			
TGF-β1 R I	F	CAG TCA CCG AGA CCA CAG ACA AAG T	59	101	AY455799
	R	TGA AGA TGG TGC ACA AAC AAA TGG			
TGF-β1 R II	F	GAC CTG CTG CCT GTG TGA CTT TG	61	116	AY455800
	R	GGA CTT CGG GAG CCA TGT ATC TTG			
UPA	F	CTG GGG AGA TGA AGT TTG AGG TGG	64.5	105	AY455801
	R	TGG AAC GGA TCT TCA GCA AGG C			
Bcl-2	F	TGG AGA GCG TCA ACC GGG AGA TGT	61	87	AB116145
	R	AGG TGT GCA GAT GCC GGT TCA GGT			
Fas Ligand	F	GGG GTC AGT CCT GCA ACA ACA A	54	94	AY603042
	R	ATC TTC CCC TCC ATC AGC ATC AG			
Caspase-3	F	ATC ACT GAA GAT GGA TGG GTT GGT	58	140	AB085580
	R	GAA AGG AGC ATG TTC TGA AGT AGC ACT			
HIF1α	F	TTA CGT TCC TTC GAT CAG TTG TCA	61	106	AY455802
	R	GAG GAG GTT CTT GCA TTG GAG TC			
Collagen I	F	GTG TGT ACA GAA CGG CCT CA	61	111	AF056303
	R	TCG CAA ATC ACG TCA TCG			
Collagen III	F	ATA GAG GCT TTG ATG GAC GAA	65	134	AB042266
	R	CCT CGC TCA CCA GGA GC			
Collagen IV	F	CAC AGC CAG ACA ACA GAT GC	67	151	U07888
	R	GCA TGG TAC TGA AGC GAC G			
Fibronectin	F	AGG TTG TTA CCA TGG GCA	61	91	U52106
	R	GCA TAA TGG GAA ACC GTG TAG			

F: Forward primer; R: reversed primer

Table 2. *Used antibodies in Western blot experiments*

Antigen	Product size (kDa)	Dilution	Manufacturer	Secondary antibody	Dilution
HGF	82	1:100	Neomarkers	Anti-mouse HRP	1:20,000
p-c-MET	169	1:750	Abcam	Anti-rabbit HRP	1:20,000
c-MET	145	1:750	Sigma	Anti-goat HRP	1:20,000
p-PKB	60	1:1,000	Cell-Signaling	Anti-mouse HRP	1:20,000
PKB	60	1:250	BD Biosciences	Anti-mouse HRP	1:20,000
p-STAT3	86	1:1,000	Cell Signaling	Anti-rabbit HRP	1:20,000
STAT3	86	1:2,500	BD Biosciences	Anti-mouse HRP	1:20,000
p-Erk1/2	42/44	1:1,500	Cell Signaling	Anti-rabbit HRP	1:20,000
ERK1/2	42/44	1:1,000	Cell Signaling	Anti-rabbit HRP	1:20,000
TGF-β1	25	1:1,000	Abcam	Anti-rabbit HRP	1:20,000
p-Smad2	58	1:2,000	Cell-Signaling	Anti-rabbit HRP	1:20,000
Smad2	58	1:500	BD Biosciences	Anti-mouse HRP	1:20,000
Collagen I	95/210	1:500	Calbiochem	Anti-mouse HRP	1:20,000
Caspase-3	34/20/18	1:1,000	Calbiochem	Anti-rabbit HRP	1:20,000
Beta-actin	42	1:2,000	Neomarkers	Anti-mouse HRP	1:20,000

Results

Histological grading of fibrosis

No fibrosis was seen in liver biopsies of CPSS dogs. In the PPVH dogs histological examination revealed slight portal fibrosis in one dog, slight to moderate portal fibrosis associated with slight to moderate centrolobular fibrosis in four dogs, and marked portal fibrosis with biliary proliferation in three dogs. The control dogs showed a normal liver without fibrosis. Examples of histological examination of CPSS and PPVH are included as Figures 1A and 1B, respectively.

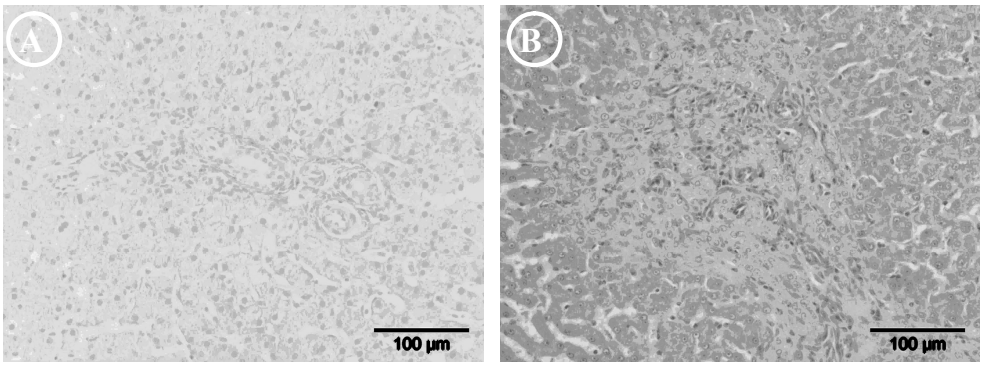

Figure 1. *Histological grading of fibrosis.*
(A) CPSS, Portal area without recognizable portal vein and arteriolar proliferation. Van Gieson stain. (B) PPVH, Markedly enlarged portal area with fibrosis and extensive arteriolar and ductular proliferation. Van Gieson stain. Color-figure see Appendix 1, page 218.

HGF/c-MET signaling pathway involved in regeneration and growth

One of the main *in vivo* events during regeneration and growth is the signaling via phosphorylation of the HGF receptor c-MET. Q-PCR analysis revealed that HGF mRNA levels in both CPSS and PPVH were decreased three-fold in comparison with healthy dogs (Figure 2). Moreover, the c-MET levels in CPSS and PPVH were significantly decreased (two- and three-fold, respectively). The levels of the mRNAs for TGFα (proliferation) were decreased six-fold in both CPSS and PPVH. The serine-protease HGF activator mRNA was doubled in dogs with CPSS. In contrast, it was halved in dogs with PPVH. The cell-cycle inhibitor p27kip mRNA was decreased in both conditions, although not significantly in dogs with CPSS.

TGF-β1 cascade signaling pathway involved in fibrosis

The fibrosis signaling pathway is activated through bindings of the active TGF-β1 dimer to the heteromeric type-I and type-II serine/threonine receptor kinases. As shown in Figure 3, TGF-β1 mRNA levels were increased two-fold in dogs with PPVH, whereas the levels in dogs with CPSS were not changed significantly. The receptor type-I, was induced in both liver diseases but only significantly in PPVH. Receptor type-II was increased in both CPSS and PPVH (4- and 5-fold, respectively), indicating an increased binding capacity. One of the proteolytic enzymes involved in activation of TGF-β1 is urokinase plasminogen activator (uPA). The uPA mRNA level was decreased two-fold in dogs with CPSS, and in contrast doubled in dogs with PPVH.

Gene-expression of apoptosis-related signaling proteins and hypoxia induced factor

We measured three well-known basic apoptotic components of which two are pro-apoptotic (Caspase-3 and Fas ligand) and one is anti-apoptotic (Bcl-2). Figure 4, shows that pro-apoptotic mediator Fas ligand was severely inhibited in both dogs with CPSS and in dogs with PPVH, (14- and 8-fold, respectively). Moreover, Caspase-3 was halved in both CPSS and PPVH. On the other hand, no induction of the anti-apoptotic Bcl-2 was seen in dogs with CPSS, whereas Bcl-2 in dogs with PPVH was doubled. The mechanisms underlying progressive fibrosis are unknown, but fibrosis and hypoxia could have been a fibrogenic stimulus. Hypoxia coordinately up-regulates matrix production and hypoxia induced factor 1 alpha (HIF1α) [19]. These direct hypoxic effects on the expression of genes involved in fibrogenesis was shown in our dogs with PPVH which indeed had elevated levels of HIF1α.

Gene-expression of extracellular matrix gene products

The analysis of ECM expression was performed on three collagens (I, III and IV) and one glycoprotein (fibronectin). Interstitial collagens types I and III are the most commonly found collagens, collagen type IV is a basal membrane collagen. In Figure 5, Collagen I was shown to be significantly increased in PPVH (two-fold), whereas CPSS was unchanged. Collagen III and IV were not significantly changed in both groups. Fibronectin showed to be halved in the PPVH group where CPSS remained normal.

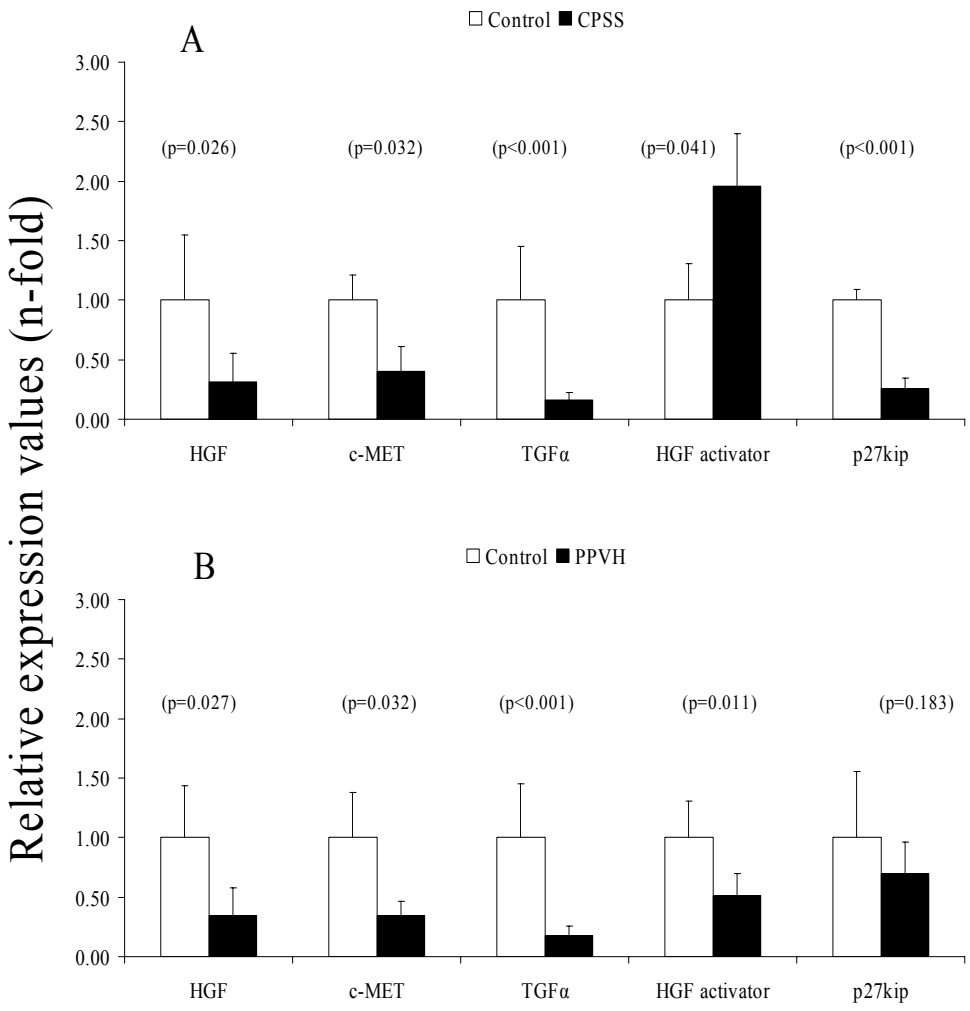

Figure 2. Quantitative Real-Time PCR of genes involved in regeneration and growth.
Representative data of mRNA levels of congenital portosystemic shunt (CPSS, n = 11 dogs) is shown in (A). Representative data of mRNA levels of primary portal vein hypoplasia (PPVH, n = 8 dogs) is shown in (B). Data represent mean + SD.

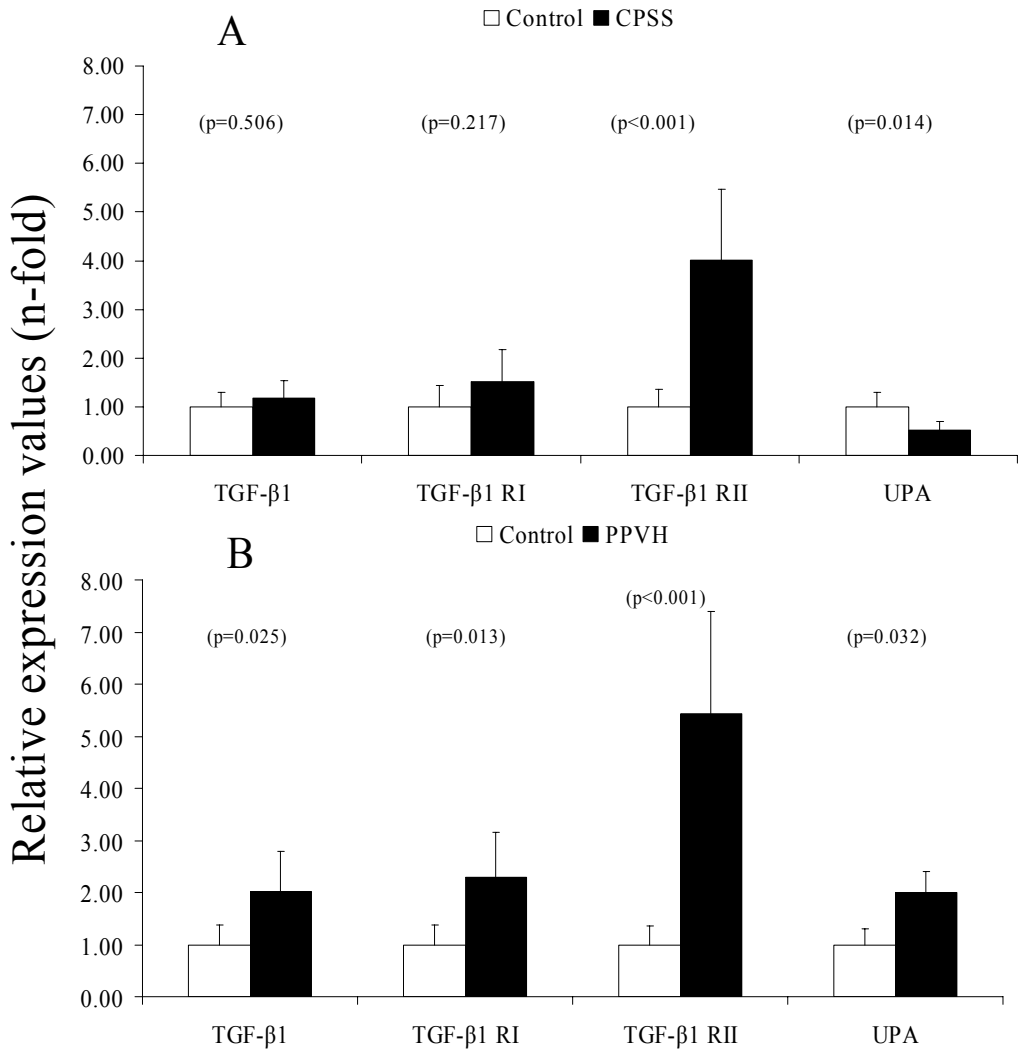

Figure 3. *Quantitative Real-Time PCR of genes involved in fibrosis. Representative data of mRNA levels of congenital portosystemic shunt (CPSS, n = 11 dogs) is shown in (A). Representative data of mRNA levels of primary portal vein hypoplasia (PPVH, n = 8 dogs) is shown in (B). Data represent mean + SD.*

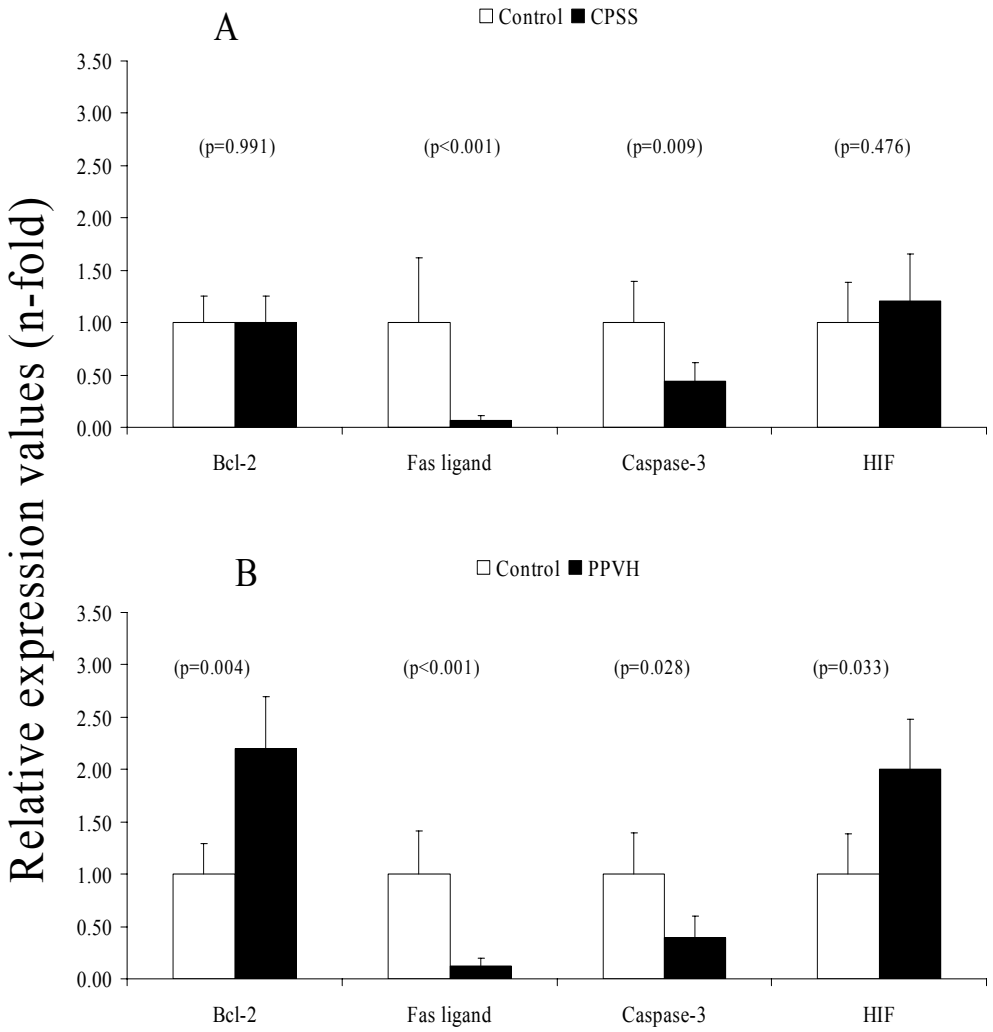

Figure 4. *Quantitative Real-Time PCR of apoptosis genes and a hypoxia related gene. Representative data of mRNA levels of congenital portosystemic shunt (CPSS, n = 11 dogs) is shown in (A). Representative data of mRNA levels of primary portal vein hypoplasia (PPVH, n = 8 dogs) is shown in (B). Data represent mean + SD.*

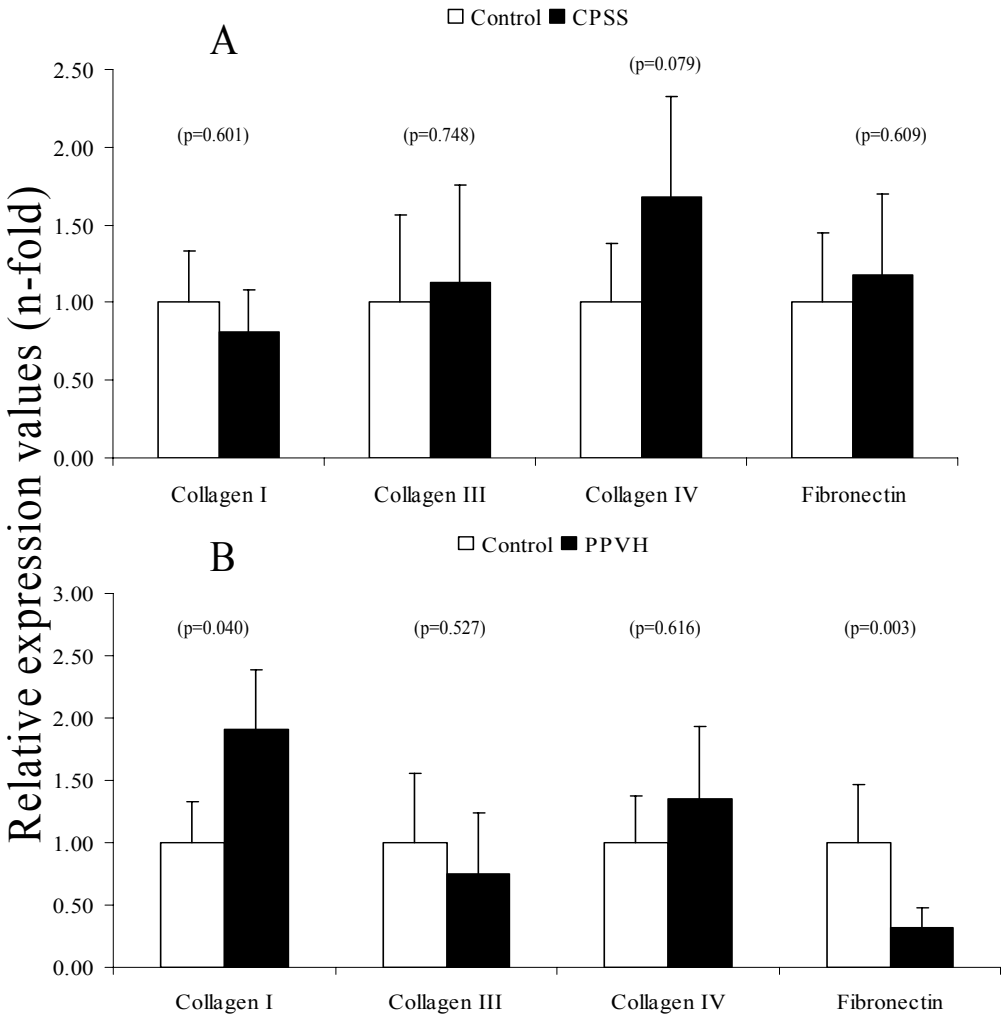

Figure 5. *Quantitative Real-Time PCR of extracellular matrix gene products. Representative data of mRNA levels of congenital portosystemic shunt (CPSS, n = 11 dogs) is shown in (A). Representative data of mRNA levels of primary portal vein hypoplasia (PPVH, n = 8 dogs) is shown in (B). Data represent mean + SD.*

Western blot analysis of HGF, c-MET, PKB, STAT, ERK, TGF-β1, Smad2, Collagen I, and Caspase-3

PKB plays a pivotal role in liver regeneration and growth upon activation of the c-MET-HGF signaling pathway [10]. Western blot analysis of HGF showed an immunoreactive band at 82 kDa with no apparent quantitative differences (Figure 6A). Total c-MET was detected in all samples, where it was present as an immuno-reactive band of 145 kDa. Results showed a decrease in the amount of c-MET in both diseases. On the other hand, the anti-phosphorylated c-MET antibody showed an immunoreactive band in all samples with no apparent quantitative differences. Total PKB was detected in all samples, where it was present as a single band of 60 kDa. The anti-phosphorylated PKB antibody showed an immunoreactive band in all samples. Two immunoreactive bands at 42 and 44 kDa representing the MAP kinase ERK1/2 showed to be equally present at the protein level between the diseased groups and healthy controls. Interestingly this also applied for the phosphorylated form where no apparent quantitative differences were found. The 80 kDa STAT3 protein showed a similar result with no apparent quantitative differences in the total form; however the STAT3 protein seemed to be somewhat less phosphorylated at the serine 727 residue in the PPVH group. TGF-β1 exerts its actions through complex intracellular signaling pathways. All downstream signaling routes following binding of an active TGF-β1 to its receptors type-I and II elicit phosphorylation of Smad2. TGF-β1 was seen in all diseases as a single band of 25 kDa under non-denaturing conditions (Figure 6B). Interestingly, the amount of TGF-β1 was induced in PPVH compared to CPSS and controls. Total Smad2 was detected in all samples, where it was present as a single band of 58 kDa, with no apparent changes in quantity. Interestingly, the anti-phosphorylated Smad2 antibody showed a slight band in CPSS whereas in PPVH a phosphorylated Smad2 is clearly present. Moreover, anti-Collagen I showed an increase in the amount of protein in PPVH compared to CPSS and healthy controls, all together emphasizing the differences in fibrosis between CPSS and PPVH. Inactive or uncleaved Caspase-3 was detected in all samples (Figure 6C), where it was present as a single band of 34 kDa, although reduced in the CPSS and PPVH group. Interestingly, the processed forms of 20 and 13 kDa showed to be increased in CPSS and PPVH towards healthy controls.

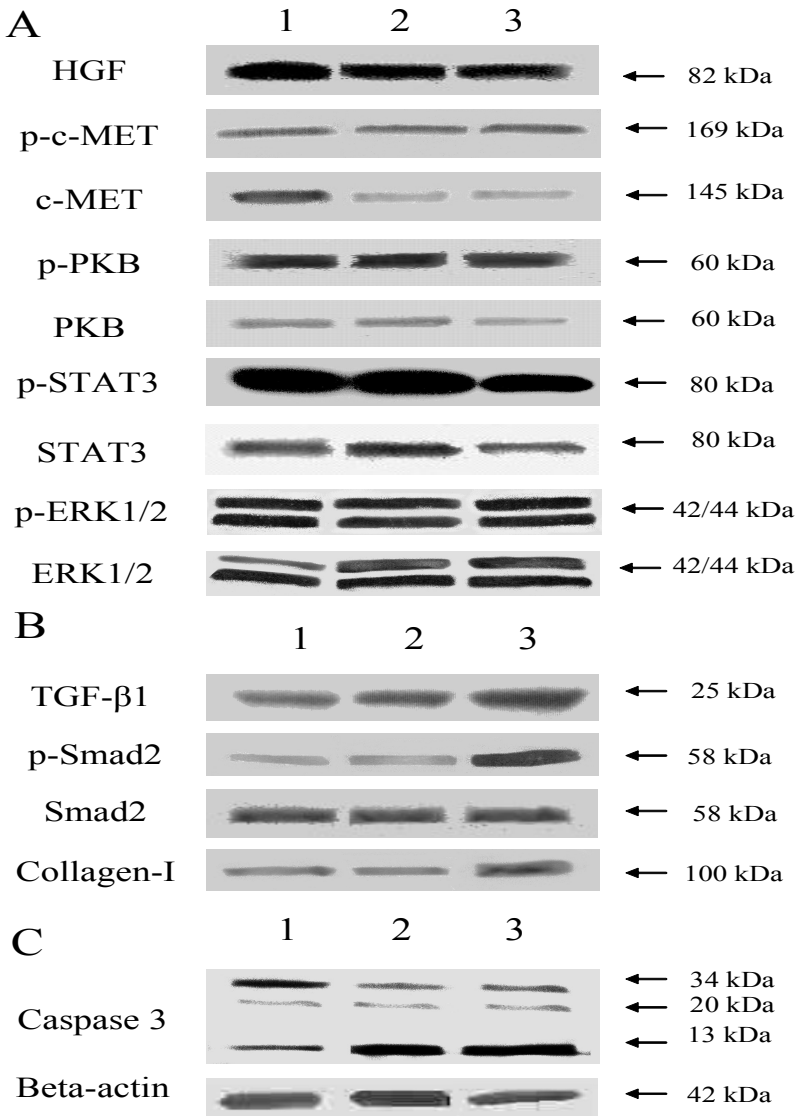

Figure 6. *Western blot analysis of liver homogenates of controls, CPSS, and PPVH. Detection of HGF, c-MET, PKB, STAT, and ERK shown in (A), detection of the TGF-β1, Smad2, and Collagen I in (B), and detection of the Caspase-3 protein, uncleaved/inactive 34 kDa, and cleaved/active products of 20 kDa and 13 kDa in (C). Western blot analysis of liver homogenates (n = 6 dogs, randomly chosen from original group). Lane 1: Control; Lane 2: Congenital portosystemic shunts; Lane 3: Primary portal vein hypoplasia.*

Discussion

Two congenital canine liver diseases were molecularly dissected in order to analyze the possibility of growth factor therapy. The expression of a total of 17 gene products involved in liver growth/regeneration, fibrosis, ECM, and cellular homeostasis was measured and normalized to the average amount of two reference genes (Q-PCR). Western blot analysis confirmed the quantitative mRNA results and furthermore showed activated pathways. These two independent techniques provided insight into the effects of portal venous hypoperfusion in two canine hepatic diseases; congenital portosystemic shunt (CPSS) without fibrosis and primary portal vein hypoplasia (PPVH) with fibrosis. Taken together, the obtained data provided insights in the feasibility for HGF-treatment.

The normalization performed in this study is obtained by averaging the amount of two different reference genes (GAPDH and HPRT). No samples were more than 5 percent apart from the individual measured reference genes levels (data not shown). This normalization strategy, using the average amount of two reference genes, is a prerequisite for accurate RT-PCR expression profiling which enables us to measure small expression differences and allows the study of their biological relevance [20].

It is well known that HGF plays an essential role in development [21] and regeneration of the liver, and increases hepatocyte viability. The found decrease in gene-expression of both HGF and its receptor agrees with the reduced liver size in these canine disorders. However, in contrast to the c-MET levels which correlate nicely with the found protein levels, the amount of HGF mRNA does not seem to reflect protein levels. This can be contributed to HGF which can be a paracrine but also an endocrine factor. Extra hepatic HGF could have been present in the pancreas or intestinal tract [22].

Although HGF and c-MET mRNA levels were decreased, downstream targets of this tyrosine cascade signaling pathway were still active. Downstream targets, such as Fas ligand and p27kip, were chosen as direct or indirect targets of the HGF-cMET-PI3K-PKB axis. Fas ligand transcription is regulated by FOXO's. The decrease in Fas ligand can therefore be explained by an active PKB which directly phosphorylates FOXO's [23]. A similar result can be seen in the reduced levels of p27kip mRNA, as this is down-regulated at the gene-transcription level by active PKB [24]. Combined, this indicates that PKB is active in both diseases, which was confirmed by Western blot analysis. It remains to be seen if other receptor tyrosine kinases (e.g. EGF receptor or insulin receptor) activate this pathway in these dogs [25]. Next to the activated PKB pathway, we have analyzed other c-MET mediated responses in

CPSS and PPVH. ERK1/2 showed to be activated in both diseases to a similar level as the healthy controls. The significance of the slightly reduced phosphorylated STAT3 in PPVH, which is phosphorylated by HGF on serine 727 [26], needs to be further investigated. Taken together, the pathways which elicit all major biological functions of c-MET showed to be active in CPSS and PPVH.

Prolonged or overexpression of TGF-β1 acts to suppress cell proliferation, and induces a deposition of ECM proteins, resulting in fibrosis in major organs such as liver [27,28]. We showed that in PPVH the TGF-β1 pathway through Smad2 is activated, consistent with the fibrosis seen in PPVH. Measurements on fibrosis related gene products revealed no elevated activity of the TGF-β1 pathway in CPSS. Gene expression levels related to the TGF-β1 pathway, including its receptors, and the proteolytic activator of TGF-β1 (uPA) were elevated in PPVH, thus indicating an active Smad pathway that could subsequently lead to fibrosis. Western blot analysis confirmed found TGF-β1 levels. Measurements on collagen gene-expression, especially collagen I, confirmed the current paradigm of TGF-β1 signaling in fibrous tissues like PPVH [29]. Contrary, non-fibrotic CPSS did not show any alterations in collagen expression. The observation of phosphorylated Smad2 in healthy liver tissue showed that the phosphorylation of Smad2 is a dynamic process and has already been described in other publications [30,31].

The expressions of the pro-apoptotic genes Fas ligand and Caspase-3 were clearly decreased. Bcl-2 gene-expression was elevated two times in PPVH, but not in CPSS (Figure 2). Western blot analysis showed that the unprocessed form of Caspase-3 was present in lesser amount in CPSS and PPVH, however the amount of processed or active bands compared to healthy control was higher in the diseases compared to healthy controls. This indicates that although the total amount of Caspase-3 is lower, there is more cleavage of the Caspase-3 to its active forms in the diseases, possibly leading to an increase in apoptosis.

Both HGF and TGF-β1 need extracellular processing to become biologically active. The serine protease HGF activator is responsible for activation of proHGF [32]. Our studies revealed that HGF activator gene-expression was doubled in dogs with CPSS and halved in case of PPVH. This indicated an increased HGF activation in CPSS. Although levels of HGF activator were reduced in PPVH, this does not necessarily indicate a lack of extracellular processing of HGF. Interestingly uPA, the activator of TGF-β1, was expressed at an increased level in dogs with PPVH. This may, via active TGF-β1-receptor interaction, indicate an activation of Smads and thus the formation of collagens.

Differential gene expression measurements on hepatic diseases have been performed in the past, nevertheless little is known about levels of genes that play an important role in fibrosis. There have been measurements on cirrhosis in man and rat that indicate an up or down-regulated expression of several proteins [33]. Although these results might be significant in severe forms of fibrosis, these data depict an end-point of the disease whereas earlier stages may be more informative.

Regeneration with recombinant HGF has been achieved in rodent models of liver failure [34,35]. Moreover, besides its regenerative capacity, HGF is known to have an antifibrogenic effect [36,37] and thus reduces or prevent fibrosis in PPVH. TGF-β1 intervention to halt the progression of liver fibrosis and positively effect regeneration, has been applied successfully [38] even in cirrhosis [39]. The measured gene products involved in fibrosis in PPVH make it a good spontaneous animal model to investigate new therapeutic strategies to influence the HGF and/or TGF-β1 pathways *in vivo*. Furthermore, most fibrogenic models are induced by toxins such as dimethylnitrosamine (DMN), CCl_4, or thioacetamide [40]. The canine PPVH model is not drug-induced and therefore may be better to compare with human diseases and thus fill the gap between induced rodent models and human diseases.

This study is the first to measure expression profiles of crucial pathways of liver growth/regeneration, fibrosis, and hepatic homeostasis in spontaneous canine liver diseases. The present findings in two diseases with relatively simple pathogenesis may also serve as basis for evaluation of more complex diseases like hepatitis and cirrhosis. Evaluation of such complex diseases in dogs is highly suitable for comparative studies on the roles of different pathways in the pathogenesis of liver diseases in man. Two further conclusions can be deduced from the data presented here. *First*, the pathophysiological differences between CPSS and PPVH can nicely be explained by the Q-PCR measurements and Western blots. *Second,* although c-MET levels were reduced, downstream signaling seemed to be functional and provides a rational background to design controlled studies for HGF-supplementation in CPSS and PPVH.

References

[1] Guyon R, Lorentzen TD, Hitte C, et al. A 1-Mb resolution radiation hybrid map of the canine genome. Proc Natl Acad Sci U S A 2003, 100:5296-5301.

[2] Murray CP, Yoo SJ, Babyn PS. Congenital extrahepatic portosystemic shunts. Pediatr Radio 2003, 33:614-620.

[3] van den Ingh TS, Rothuizen J, Meyer HP. Circulatory disorder of the liver in dogs and cats. Vet Q 1995, 17:70-76.

[4] van den Ingh TS, Rothuizen J, Meyer HP. Portal Hypertension associated with primary hypoplasia of the hepatic portal vein in dogs. Vet Rec 1995, 137:424-427.

[5] Michalopoulos KM, DeFrances MC. Liver regeneration. Science 1997, 276:60-66.

[6] Trusolino L, Comoglio PM. Scatter-factor and semaphorin receptors: cell signalling for invasive growth. Nat Rev Cancer 2002, 2:289-300.

[7] Fausto N. Liver regeneration. J Hepatol 2000, Suppl 1:19-31.

[8] Funakoshi H, Nakamura T. Hepatocyte growth factor: from diagnosis to clinical applications. Clin Chim Acta 2003, 327:1-23.

[9] Scheid MP, Woodgett JR. Unravelling the activation mechanisms of protein kinase B/Akt. FEBS Lett 2003, 546:108-112.

[10] Coffer PJ, Jin J, Woodgett JR. Protein kinase B (c-Akt): a multifunctional mediator of phosphatidylinositol 3-kinase activation. Biochem J 1998, 335:1-13.

[11] Paumelle R, Tulasne D, Kherrouche Z, et al. Hepatocyte growth factor/scatter factor activates the ETS1 transcription factor by a RAS-RAF-MEK-ERK signaling pathway. Oncogene 2002, 21:2309-2319.

[12] Boccaccio C, Ando M, Tamagnone L, et al. Induction of epithelial tubules by growth factor HGF depends on the STAT pathway. Nature 1998, 391:285-288.

[13] Derynck R, Akhurst R J, Balmain A. TGF-β signaling in tumor suppression and cancer progression. Nature Genet 2001, 29:117-129.

[14] Piek E, Heldin CA, ten Dijke P. Specificity, diversity, and regulation in TGF-β superfamily signalling. FASEB J 1999, 13:2105-2124.

[15] Aihara Y, Kasuya H, Onda H, et al. Quantitative analysis of gene expressions related to inflammation in canine spastic artery after subarachnoid hemorrhage. Stroke. 2001, 32:212-217.

[16] Massague J. How cells read TGF-beta signals. Nat Rev Mol Cell Biol 2000, 1:169-178.

[17] Hengartner MO. The biochemistry of apoptosis. Nature 2000, 407:770-776.

[18] Kimura Y, Leung PS, Kenny TP, et al. Differential expression of intestinal trefoil factor in biliary epithelial cells of primary biliary cirrhosis. Hepatology 2002, 36:1227-1235.

[19] Norman JT, Clark IM, Garcia PL. Hypoxia promotes fibrogenesis in human renal fibroblasts. Kidney Int 2000, 58:2351-2366.

[20] Vandesompele J, De Preter K, Pattyn F, et al. Accurate normalization of real-time quantitative RT-PCR data by geometric averaging of multiple internal control genes. Genome Biol 2002, 3:research0034.1-research0034.11.

[21] Schmidt C, Bladt F, Goedecke S, et al. Scatter factor/hepatocyte growth factor is essential for liver development. Nature 1995, 373:699-702.

[22] La Rosa S, Uccella S, Capella C, et al. Localization of Hepatocyte Growth Factor and Its Receptor met in Endocrine Cells and Related Tumors of the Gut and Pancreas: An Immunohistochemical Study. Endocr Pathol 2000, 11:315-329.

[23] Barthelemy C, Henderson CE, Pettmann B. Foxo3a induces motoneuron death through the Fas pathway in cooperation with JNK. BMC Neurosci 2004, 5:48.

[24] Chandramohan V, Jeay S, Pianetti S, et al. Reciprocal control of Forkhead box O 3a and c-Myc via the phosphatidylinositol 3-kinase pathway coordinately regulates p27Kip1 levels. J Immunol 2004, 172:5522-5527.

[25] Hanada M, Feng J, Hemmings BA. Structure, regulation and function of PKB/AKT--a major therapeutic target. Biochim Biophys Acta 2004, 1697:3-16.

[26] Nakagami H, Morishita R, Yamamoto K, et al. Mitogenic and antiapoptotic actions of hepatocyte growth factor through ERK, STAT3, and AKT in endothelial cells. Hypertension 2001, 37:581-586.

[27] Diez-Marques L, Ortega-Velazquez R, Langa C, et al. Expression of endoglin in human mesangial cells: modulation of extracellular matrix synthesis. Biochim Biophys Acta 2002, 1587:36-44.

[28] Zhu HJ, Burgess AW. Regulation of transforming growth factor-beta signaling. Mol Cell Biol Res Commun 2001, 4:321-330.

[29] Tsukada S, Parsons CJ, Rippe RA. Mechanisms of liver fibrosis. Clin Chim Act, in press

[30] Liu C, Gaca MD, Swenson ES, et al. Smads 2 and 3 are differentially activated by transforming growth factor-beta (TGF-beta) in quiescent and activated hepatic stellate cells. Constitutive nuclear localization of Smads in activated cells is TGF-beta-independent. J Biol Chem 2003, 278:11721-11728.

[31] Kondou H, Mushiake S, Etani Y, et al. A blocking peptide for transforming growth factor-beta1 activation prevents hepatic fibrosis in vivo. J Hepatol 2003, 39:742-748.

[32] Kataoka H, Miyata S, Uchinokura S, et al. Roles of hepatocyte growth factor (HGF) activator and HGF activator inhibitor in the pericellular activation of HGF/scatter factor. Cancer Metastasis Rev 2003, 22:223-236.

[33] Wang HT, Chen S, Wang J, et al. Expression of growth hormone receptor and its mRNA in hepatic cirrhosis. World J Gastroenterol 2003, 9:765-770.

[34] Kosai K, Matsumoto K, Funakoshi H, et al. Hepatocyte growth factor prevents endotoxin-induced lethal hepatic failure in mice. Hepatology 1999, 30:151-159.

[35] Yasuda H, Imai E, Shiota A, et al. Antifibrogenic effect of a deletion variant of hepatocyte growth factor on liver fibrosis in rats. Hepatology 1996, 24:636-642.

[36] Ueki T, Kaneda Y, Tsutsui H, et al. Hepatocyte growth factor gene therapy of liver cirrhosis in rats. Nat Med 1999, 5:226-230.

[37] Matsuda Y, Matsumoto K, Yamada A, et al. Preventive and therapeutic effects in rats of hepatocyte growth factor infusion on liver fibrosis/cirrhosis. Hepatology 1997, 26:81-89.

[38] Ohara K, Kusano M. Anti-transforming growth factor-beta1 antibody improves survival rate following partial hepatectomy in cirrhotic rats. Hepatol Res 2002, 24:174.

[39] Nakamura T, Sakata R, Ueno T, et al. Inhibition of transforming growth factor β prevents progression of liver fibrosis and enhanced hepatocyte regeneration in dimethylnitrosamine-treated rats. Hepatology 2000, 32:247-255.

[40] Sato M, Kakubari M, Kawamura M, et al. The decrease in total collagen fibers in the liver by hepatocyte growth factor after formation of cirrhosis induced by thioacetamide. Biochem Pharmacol 2000, 59:681-690.

Chapter 3

Major regenerative pathways in dog models of hepatitis and cirrhosis, in comparison with man

Bart Spee[1], Brigitte Arends[1], Ted S.G.A.M. van den Ingh[2], Tania Roskams[3], Jan Rothuizen[1], and Louis C. Penning[1]

From the Departments of [1]Clinical Sciences of Companion Animals and [2]Pathobiology, Faculty of Veterinary Medicine, Faculty of Veterinary Medicine, Utrecht University, The Netherlands, and Department of Pathology, University Hospitals of Leuven, Belgium.

Submitted

Abstract

Acute and chronic hepatitis affect hepatic regeneration. We have analyzed canine clinical liver samples from four different forms of hepatitis; Acute Hepatitis (AH), Chronic Hepatitis (CH), Cirrhosis (CIRR), and Lobular Dissecting Hepatitis (LDH) in comparison with human liver samples from cirrhotic stages of alcoholic liver disease (hALC) and chronic hepatitis C infection (hHC). We used Q-PCR to analyze the canine specific mRNA expression of Hepatocyte Growth Factor (HGF) and relevant down-stream mediators. Furthermore, we analyzed activation of STAT3, PKB, ERK1/2, and p38-MAPK by Western blotting in both dog and man. In all canine groups, c-MET (HGF receptor) mRNA levels were significantly decreased ($P < 0.05$) up to four-fold compared to control. Western blotting on canine samples showed an increased activation of STAT3 (Serine), PKB, ERK1/2, and p38-MAPK in CH and LDH. Similar activations were found in human samples (hHC and hALC). Partial loss of c-MET (siRNA) in a canine hepatic cell-line, does not lead to severe loss in HGF-sensitivity. In conclusion, despite the reduced c-MET levels in canine hepatitis and cirrhosis major regenerative downstream pathways are still activated, and considered highly comparable to man. Furthermore, canine hepatitis and cirrhosis could be an important clinical model to evaluate novel interventions such as HGF treatment.

Introduction

Hepatitis is a very complex interplay of many factors, all of which compose the pathogenesis of liver disease. This makes it difficult to dissect the roles of different individual pathogenetic pathways. Dogs have liver diseases highly comparable with the human counterparts and have a high resemblance at the genetic level [1,2]. Furthermore dogs are within the same body weight range and share many years in close proximity of humans exposing them to the same environmental and biological stresses. Therefore, privately owned dogs may fulfill an important translational role between toxin induced- or surgical-models in rodents, and clinical cases in man.

We have chosen four different forms of hepatitis and cirrhosis in dogs for comparative analysis of major regenerative pathways. Although the etiology of canine hepatitis is largely unknown, several known etiologies of hepatitis in other species have been excluded [3]. In contrast to rodent models, hepatitis in these dogs is not deliberately induced. Hepatitis ranged from Acute Hepatitis (AH) without fibrosis to Chronic Hepatitis (CH), and cirrhosis (CIRR), including Lobular Dissecting Hepatitis (LDH). The last disease is a specific form of cirrhosis with severe fibrosis and complete disruption of the lobular architecture, mainly seen in young dogs [4,5]. As in humans, chronic hepatitis in dogs is associated with progressive fibrosis, reduction in liver size and regeneration, and finally disruption of the liver architecture (cirrhosis), which may cause portal hypertension, ascites, and portosystemic encephalopathy [6].

Liver regeneration is a complex interplay of different factors [7]. Many of these vital regenerative factors have been investigated after partial hepatectomy (PH) and in toxin-induced rodent models. However, little is known how regeneration is affected in the process of hepatic diseases. One of the main growth factors identified in liver regeneration is the Hepatocyte Growth Factor (HGF). HGF activates the proto-oncogenic receptor tyrosine kinase c-MET [8], and subsequent down-stream pathways, including PI-3-Kinase, protein kinase-B (PKB/Akt), MAP-kinases such as ERK1/2 (p42/44 MAPK), and Signal Transducers and Activators of Transcription (STATs) [9].

The present study was undertaken to investigate these crucial pathways involved in regeneration in liver tissues obtained from dogs with different forms of hepatitis. The results from canine samples were compared to the activity of the same regenerative proteins derived from human liver explant samples with alcoholic cirrhosis (hALC) respectively cirrhosis due to hepatitis C virus (hHC) in order to validate the dog as a model for man. The great similarities between man and dogs are already described at

the genetic [2], the pathophysiological, and at the pathology level. The present data indicate that the regenerative signal transduction level the pathways are also highly comparable. This emphasizes the potential of dogs to bridge between toxin-induced rodent models and human clinical situation. Furthermore, results might give a rational to initiate growth factor therapy in dogs and man.

Materials and Methods

Animals

All samples were obtained from privately owned dogs of different breeds referred to our veterinary clinic. All procedures were approved by Utrecht University's Ethical Committee, as required under Dutch legislation. Each disease group (n = 11 dogs) was compared age-matched healthy control dogs (n = 12 dogs), without clinical signs of hepatitis or other disease (histopathology did not reveal any abnormalities). Liver tissue was obtained from all dogs under local anesthesia by ultrasound-guided biopsy with a true cut 14G biopsy needle, preceded by ultrasonographic evaluation of the liver to exclude biopsy artifacts in case of non-homogeneous hepatic changes. Two formalin-fixed biopsies were embedded in paraffin, sliced, and stained with hematoxylin and eosin, Van Gieson stain, and reticulin stain according to Gordon and Sweet. All histological examinations were performed by one experienced, certified veterinary pathologist. Two other biopsies were snap-frozen, and stored at $-70^{o}C$ until molecular analysis.

Human patients

All samples were obtained from surgical patients who were transplanted at the Department of Abdominal Transplantation in the University Hospital Leuven, Leuven, Belgium. The procedures were approved by Leuven University's Ethical Committee, as required under Belgian legislation. Human explant samples were collected directly after surgery and immediately snap-frozen. All patients, predominantly male, were presented with micronodular cirrhosis. The Alcoholic Cirrhosis (hALC) group contained five patients (n = 5) characterized by cirrhosis with neutrophil infiltrations, alcohol related morphological changes (hepatocyte ballooning, Mallory bodies, necrosis), and in some cases steatosis and increased iron deposition. The Hepatitis C (hHC) group contained four patients (n = 4) characterized by cirrhosis with neutrophil infiltrations, lymphoid follicles and aggregates. All cases were presented with hepatocyte decay, apoptosis/necrosis, regeneration, and fibrosis.

Quantitative PCR

Quantitative real-time PCR (Q-PCR) was performed on a total of six gene products; HGF, c-MET, TGFα, HGF activator, p27kip, and PTEN. The abundance of mRNA was determined by Reverse Transcription (RT) followed by real-time quantitative PCR using appropriate primers (Table 1), as previously described [10]. For each experimental sample, two references genes (GAPDH and HPRT) were included. Results were normalized according to the average amount of the endogenous references and were divided by the normalized values of the control group to generate relative expression levels [11].

Silencing c-MET levels by RNA interference

For silencing experiments, Stealth™ dsRNA molecules were obtained from Invitrogen (Invitrogen, Breda, The Netherlands). Specific sequence (Genbank AB118945) for canine c-MET silencing (5'-GCAUCCUUGUGCUUCUGUUUACCUU-3') was selected after general recommendations (Invitrogen). A random non-sense sequence was used as a negative control (5'-GCAGGUGCUAGUACAAGUCCGACAA-3'). Transfection was performed on canine bile duct epithelial (BDE) cells [12], characterized by serum albumin and ceruloplasmin expression (data not shown). Cells were acquired from the Experimental Liver Cell Bank (Prof. Oude-Elferink, AMC-Amsterdam, The Netherlands). BDE cells were grown in glutamine- and gentamycin-supplemented DMEM with 10% FCS (Life Technologies, Inc., Invitrogen) at 37°C in a humidified atmosphere of 5% CO_2 in air. Cells were seeded into 96-wells plates in a concentration of $3x10^4$ cells/well. Transfection was performed with the Magnet-Assisted-Transfection (MATra) technique (IBA BioTAGnology/Westburg b.v., Leusden, The Netherlands), in combination with Lipofectamine2000™ (Invitrogen), according to the manufacturers instructions. In short, siRNA molecules were transfected into BDE cells, with the optimized concentration Lipofectamin2000™ (1.2 µl/ml) for 20 minutes on the plate magnet. After transfection normal growth media including gentamycin was added.

Viability assay

48 Hours after transfection the cells were treated with recombinant human HGF (R&D Systems, Abingdon, United Kingdom; end-concentration HGF 100 ng/ml) in glutamine- and gentamycin-supplemented DMEM with 10% FCS. After 24 hours, the viability was measured with a MTT assay (5 mg/ml).

Table 1. *Nucleotide Sequences of Dog-Specific Primers for Real-Time Quantitative PCR*

Gene	F/R	Sequence (5'-3')	Tm (^{o}C)	Product size (bp)	Accession number
GAPD	F	TGT CCC CAC CCC CAA TGT ATC	58	100	AB038240
	R	CTC CGA TGC CTG CTT CAC TAC CTT			
HPRT	F	AGC TTG CTG GTG AAA AGG AC	56	100	L77488 /
	R	TTA TAG TCA AGG GCA TAT CC			L77489
HGF	F	AAA GGA GAT GAG AAA CGC AAA CAG	58	92	BD105535
	R	GGC CTA GCA AGC TTC AGT AAT ACC			
c-MET	F	TGT GCT GTG AAA TCC CTG AAT AGA AATC	59	112	AB118945
	R	CCA AGA GTG AGA GTA CGT TTG GAT GAC			
TGFα	F	CCG CCT TGG TGG TGG TCT CC	63	122	AY458143
	R	AGG GCG CTG GGC TTC TCG T			
HGFA	F	AAA CTG GAG CGG ATG GCA CAG	60	127	AY458142
	R	ACA CAG ACG TTT GGC ATC GAG AAG TAT			
p27kip	F	CGG AGG GAC GCC AAA CAG G	60	90	AY455798
	R	GTC CCG GGT CAA CTC TTC GTG			
PTEN	F	AGA TGT TAG TGA CAA TGA ACC T	64.5	110	U92435
	R	GTG ATT TGT GTG TGC TGA TC			

F: Forward primer; R: reversed primer

Immunoblot analysis

Twenty micrograms of pooled protein extracts (n=6 dogs per group, randomly chosen) was electrophoresed on SDS-PAGE, and transferred to a Hybond ECL nitro-cellulose membrane (Amersham-Biosciences, Cleveland, OH). The procedure for immunodetection was based on an ECL-Western blot analysis system, as previously described [13]. Primary antibodies are depicted in Table 2. Densitometric analysis was performed with a Geldoc2000 system with QuantityOne 4.3.0 software (Biorad).

Table 2. Primary Antibodies used in Western blot experiments

Antibody	Product size (kDa)	Dilution	Supplier
Goat anti-human HGF	80	1:1,000	Santa Cruz
Goat anti-human c-MET	145	1:1,000	Santa Cruz
Rabbit anti-human c-MET (Tyr1230/1234/1235)	169	1:1,000	Abcam
Rabbit anti-human/dog STAT3	86	1:2,500	BDBioscience
Rabbit anti-human phospho-STAT3 (Ser727)	86	1:1,000	Cell Signalling
Mouse anti-human phospho-STAT3 (Tyr705)	86	1:1,000	Cell Signalling
Mouse anti-human/dog PKB	60	1:250	BDBioscience
Rabbit anti-human phospho-PKB (Thr308)	60	1:1,000	Cell Signalling
Rabbit anti-human Erk1/2	42/44	1:1,000	Cell Signalling
Rabbit anti-human phospho-ERK1/2 (Thr202/Tyr204)	42/44	1:1,500	Cell Signalling
Rabbit anti-human p38-MAPK	38	1:500	Abcam
Rabbit anti-human phospho-p38-MAPK (Thr180/Tyr182)	38	1:1,000	Abcam
Mouse anti-human/dog Beta-actin (pan Ab-5)	42	1:2,000	Neomarkers

Results

Q-PCR on the HGF/c-MET signaling pathways involved in canine regeneration and growth in AH, CH, CIRR, and LDH

HGF mRNA levels were induced in CH, LDH, and CIRR, three-, five-, and five-fold, respectively (Figure 1). In AH, HGF mRNA levels remained unchanged. The c-MET mRNA levels in all groups were significantly decreased, with a maximum four-fold reduction in AH. The mRNA levels for TGFα were not aberrant in CH, but were decreased in LDH and AH (two- and 15-fold, respectively). In CIRR, however, the mRNA levels of TGFα were doubled. The serine protease HGF-activator (HGFA) mRNA levels were inhibited in LDH. In contrast HGFA was doubled in dogs with AH and not significantly changed in CH and CIRR. A cell cycle inhibitor, p27KIP, was halved in CH and LDH. Interestingly, in AH p27KIP mRNA levels were inhibited 19-fold, unchanged in CIRR. The mRNA levels of PTEN, a tumor-suppressor gene inhibiting PI-3-K activity, was unchanged in CH, but doubled in LDH and CIRR. In AH, however, the PTEN mRNA levels were halved.

Western blot analysis on HGF, c-MET, STAT3, PKB/Akt, ERK1/2, and p38-MAPK

In Figure 2, Western blot analysis showed the presence of a single HGF band (80 kDa) in all samples. Interestingly, there is a clear correlation between HGF protein and mRNA levels, as the protein (and mRNA) levels of HGF is increased in CH, LDH, and CIRR. The same correlation was seen with the c-MET protein and mRNA; all diseases have decreased c-MET protein levels similar to reduced mRNA levels (Figure 2C). Analysis on phosphorylated c-MET showed an immuno-reactive band in CH, LDH, and CIRR, which was almost absent in AH (Figure 2C). Important downstream signaling proteins of HGF/c-MET, e.g. STAT3, PKB/Akt, ERK1/2, and p38-MAPK, were measured (Figure 3). The total STAT3 was detected as an immuno-reactive 86 kDa band in all hepatic diseases, with slightly lower expression in CH, LDH, and CIRR. Tyrosine (Tyr705)-phosphorylated STAT3 was strongly reduced in AH and seemed to be increased in LDH. Healthy controls, CH, and CIRR groups had comparable levels of Tyr-phosphorylated STAT3. Interestingly Serine (Ser727)-phosphorylated STAT3 was slightly increased in LDH, conversely slightly reduced in CIRR. PKB/Akt plays a pivotal role during regeneration and growth [14]. Total PKB/Akt was detected in all hepatic diseases as a single 60 kDa protein. Threonine (Thr308)-phosphorylated PKB/Akt was less present in AH and CIRR, whereas CH and LDH showed no apparent quantitative differences toward healthy controls. Analysis of total ERK1/2 (42/44 kDa), a principle kinase in growth factor signaling, showed a slight reduction in AH, and moderate increases in CH, LDH, and CIRR. The phosphorylated form threonine/tyrosine (Thr202/Tyr204)-phosphorylated ERK1/2 was strongly increased in CH and LDH. A similar effect can be seen in p38-MAPK (represents a point of convergence for multiple signalling processes that are activated during inflammation, a key potential target for the modulation of cytokine production); an increased expression of total p38-MAPK in CH, LDH, and CIRR and decreased levels in AH. The threonine/tyrosine (Thr180/Tyr182)-phosphorylated p38-MAPK form is increased in CH and LDH.

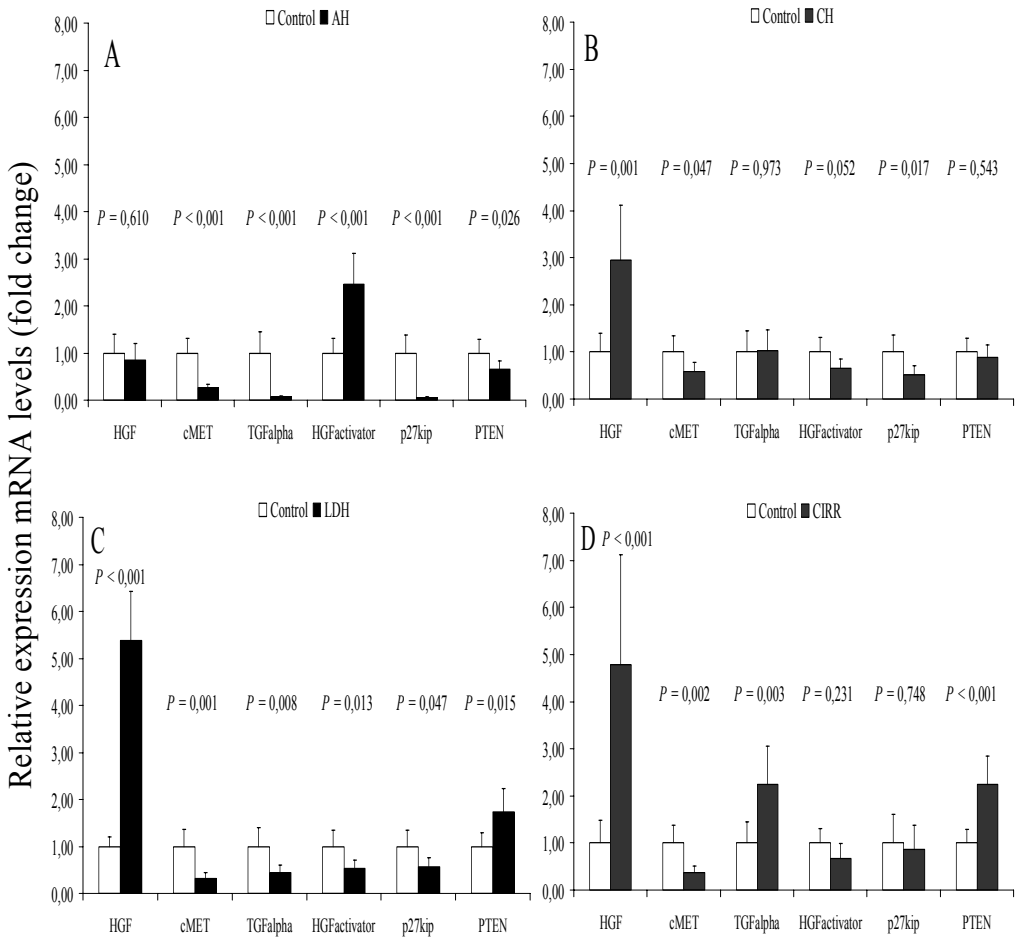

Figure 1. *Quantitative Real-Time PCR of gene products involved in regeneration and growth. Representative data of mRNA levels of acute hepatitis (AH) shunt is shown in (A). Representative data of mRNA levels of chronic hepatitis (CH) is shown in (B). Representative data of mRNA levels of lobular dissecting hepatitis (LDH) is shown in (C). Representative data of mRNA levels of cirrhotic samples (CIRR) is shown in (D). Data represent mean + SD. A Kolmogorov-Smirnov test was performed to establish a normal distribution and a Levene's test for the homogeneity of variances. All samples included in this study were normally distributed. The statistical significance of differences between diseased and control animals was determined by using the Student's t-test. A p-value < 0.05 was considered statistically significant. Analysis was performed using SPSS software (SPSS Benelux BV, Gorinchem, the Netherlands).*

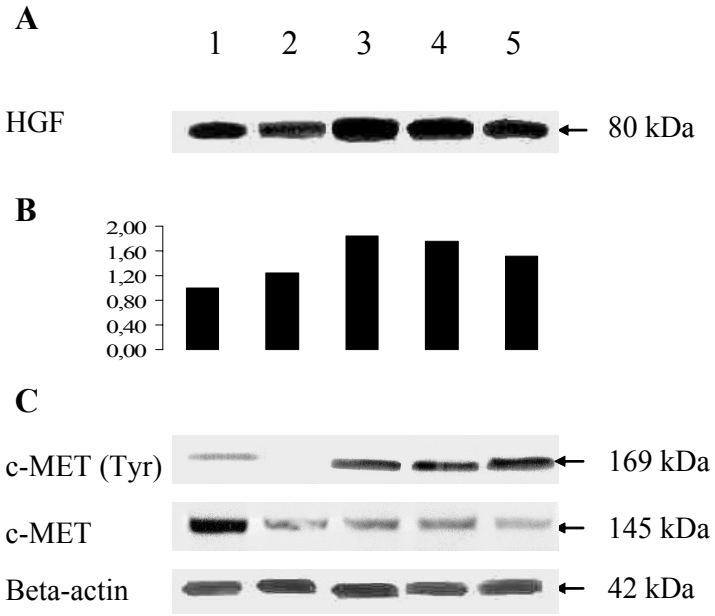

***Figure 2**. Western blot analysis of canine liver homogenates of several diseases (n = 6). Detection of the 80 kDa HGF protein shown in (A). Analysis of HGF immunoreactive bands by means of Optical Density (OD) measurement corrected for the amount of loading control beta-actin as shown in (B). Detection of the HGF receptor c-MET including phosphorylated (Tyr) form shown in (C). Lane 1: Control; Lane 2: Acute Hepatitis; Lane 3: Chronic Hepatitis; Lane 4: Lobular Dissecting Hepatitis; Lane 5: Cirrhosis*

Western blot analysis on human cirrhotic explant samples after alcohol abuse (hALC) and after hepatitis C virus infection (hHC)

Western blot analysis on hALC and hHC samples showed a detectable 80 kDa HGF in all samples with minor quantitative differences (Figure 4). The 145 kDa c-MET was also detected in all samples. In contrast, the phosphorylated form was detected in all samples although three patients had increased c-MET (Tyr) in the ALC-group as well as two patients in the hHC-group. Total STAT3 was detectable in all individual samples. Tyr-phosphorylated STAT3 was easier detectable than Ser-phosphorylated STAT3 in hALC samples. In contrast, in the hHC-group both phosphorylated STAT3 proteins were relatively equally detectable. Comparing hALC versus hHC, Tyr-phosphorylated STAT3 was about equally expressed, whereas Ser-phosphorylated STAT3 was in most samples stronger expressed in hHC compared to hALC. Total PKB/Akt was detected in all samples. Interestingly, the phosphorylated PKB (Thr)

was induced in three hALC-samples and two hHC-samples. Overall PKB was active in all samples under study. Total ERK1/2 was detected in all samples. Phosphorylated ERK1/2 showed a similar pattern although two samples in the hALC-group generally were less phosphorylated. In the 38 kDa p38-MAPK samples no quantitative differences were found in total p38-MAPK or the phosphorylated form, which both were detected in all samples.

c-MET siRNA experiments

We partially knocked-down c-MET in BDE cells in order to see if HGF treatment still provided a cellular proliferation signal. Both mRNA and protein of c-MET are partially knocked-down by using a serial dilution of c-MET directed siRNA's ranging from 100 pM to 50 nM (Figure 5). An 85 percent knock-down was obtained with 10 and 50 nM siRNA's. Non-sense siRNA did not affect c-MET mRNA and protein levels. Interestingly, even with 80 percent reduced c-MET mRNA levels (2 nM siRNA), the cells were still sensitive for a proliferative HGF treatment as these cells significantly proliferated almost 28 percent compared to control (Figure 5C).

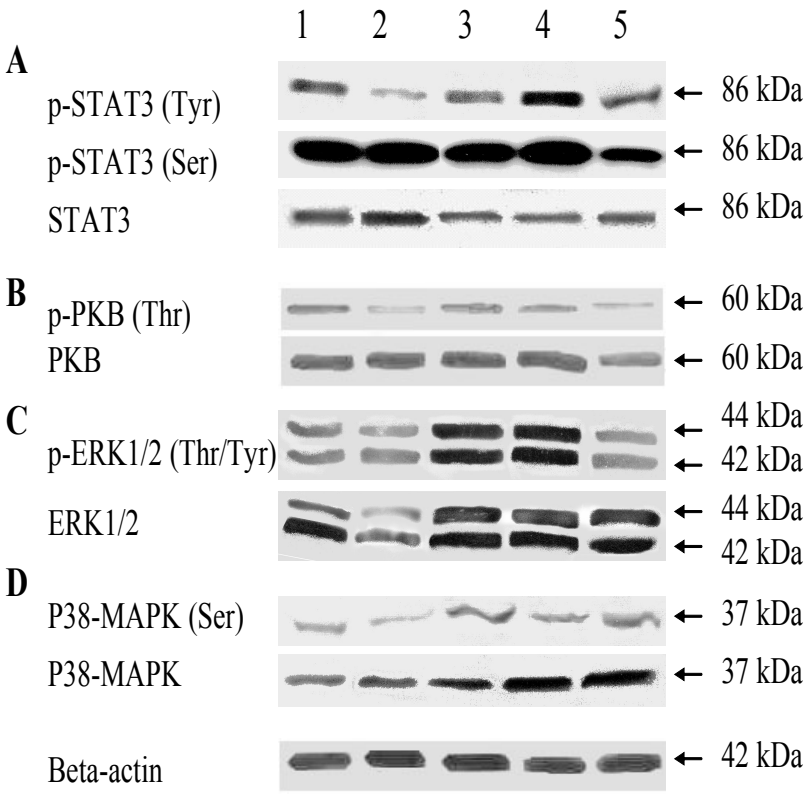

Figure 3. *Western blot analysis of pooled canine liver homogenates of several diseases (n = 6). Detection of the 86 kDa STAT3 protein (A), detection of the 60 kDa PKB protein (B), detection of the 44/42 kDa ERK 1/2 protein shown in (C), and detection of the p38-MAPK protein shown in (D). Lane 1: Control; Lane 2: Acute Hepatitis; Lane 3: Chronic Hepatitis; Lane 4: Lobular Dissecting Hepatitis; Lane 5: Cirrhosis. Beta-actin was used as a loading control.*

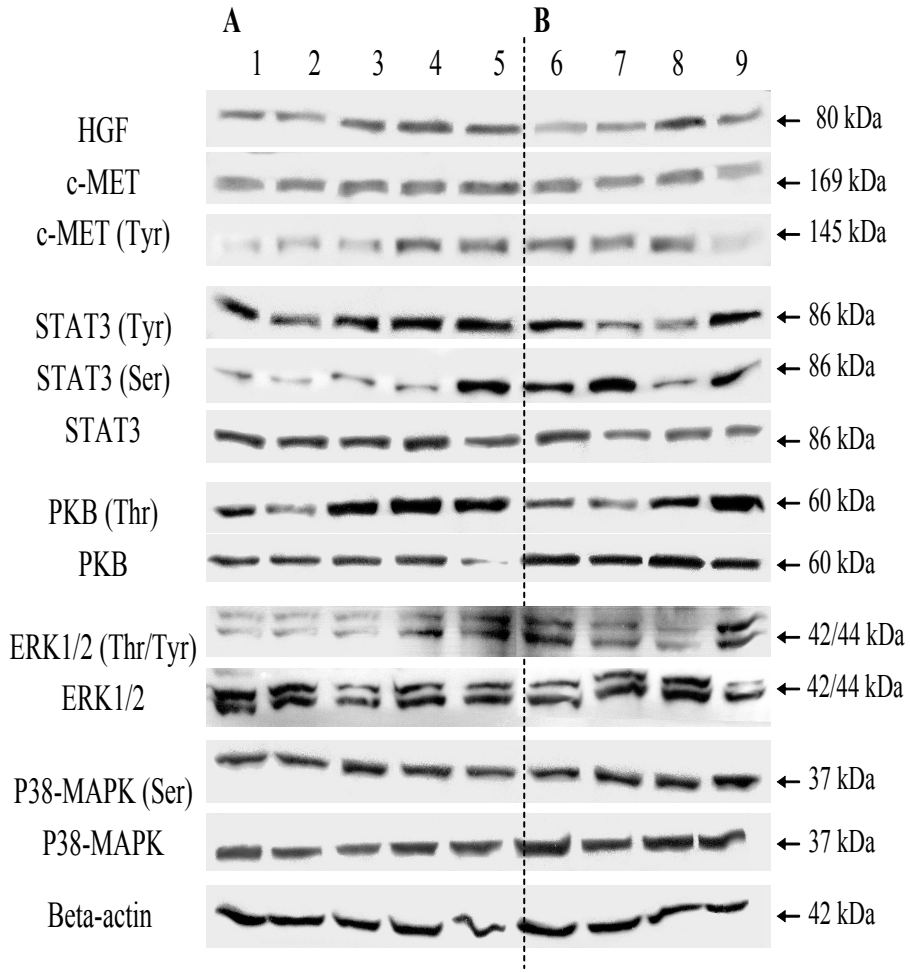

***Figure 4**. Western blot analysis of human liver homogenates of several diseases (n = 6). Samples 1 to 5 represent individual alcoholic cirrhosis (hALC) shown in (A), samples 6 to 9 represent individual HC cirrhotic samples (hHC) shown in (B). Beta-actin was used as a loading control.*

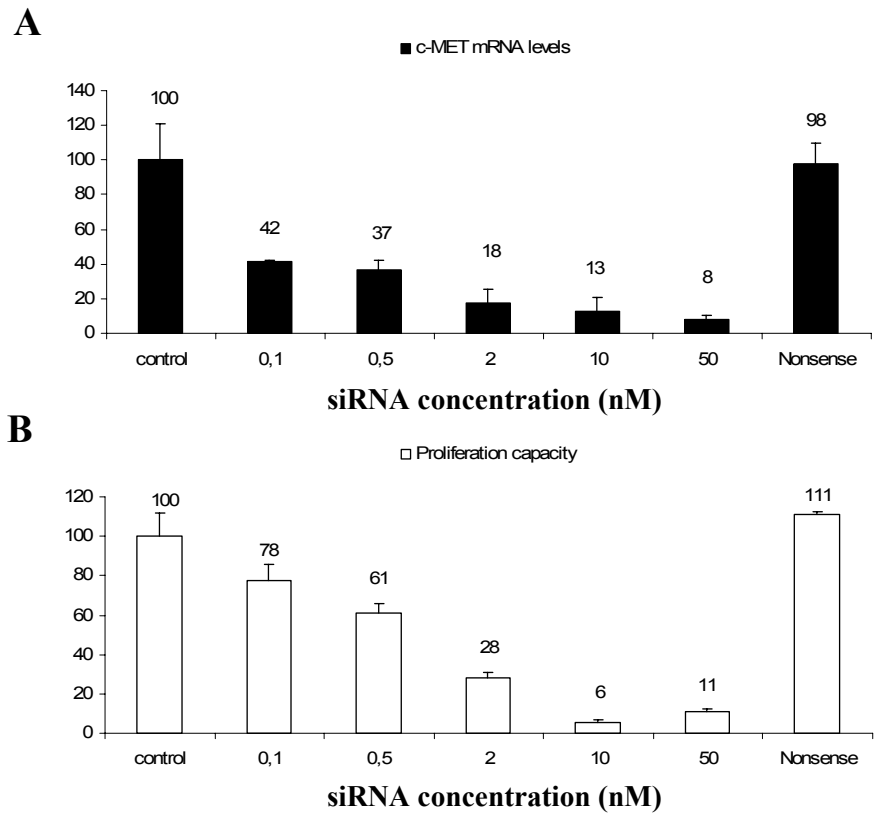

Figure 5. *c-MET gene silencing experiments.*
Data is expressed as mean percentage mRNA levels shown in (A), mean + SE. Western blot analysis showing quantitative presence of the 145 kDa c-MET protein is shown in (B). Proliferation capacity is expressed as mean percentage toward untreated controls shown in (C), mean + SE.

Discussion

In the present study the expression of a total of six gene products involved in liver regeneration was measured. Furthermore, Western blot experiments were used to show the de/activation of important signaling pathways of liver regeneration. This provided insight into major regeneration pathways of four canine hepatic diseases; acute hepatitis (AH), chronic hepatitis (CH), lobular dissecting hepatitis (LDH), and cirrhosis (CIRR). Human explant samples were used for comparison to assess the possible use of dogs with spontaneous liver diseases as a model for growth factor therapy.

The two major pathways involved in regeneration of the liver are the Jak/STAT and the MAPK pathway [15]. From the MAPK pathway two major members are often coupled with regeneration, viz. ERK1/2 and p38MAPK [16]. Both MAPK and the STAT3 pathway can be activated by a variety of cytokines and growth factors. HGF can indirectly activate STAT3 on the serine residue through activation of ERK1/2 [17]. Indeed, the phosphorylated serine STAT3 was observed in all diseases and controls indicating an active STAT3 pathway (Figure 3). Although STAT3 serine phosphorylation negatively modulates the tyrosine phosphorylation *in vitro* [18], both forms were observed in all diseases. Serine phosphorylation of STAT3 results in a significant up-regulation of the transcriptional activity [19]. Furthermore, the *in vivo* serine phosphorylation of STAT3 appears essential for postnatal survival as the knock-in S727A STAT3 mice failed to compensate the noted phenotype [20]. Taken together the presence of a serine phosphorylated STAT3 could contribute to the chronic nature of all hepatic diseases under study. The lowered tyrosine phosphorylated STAT3 in CIRR could be contributed to inactive cirrhosis with slight or no cytokine activity. The reduction tyrosine phosphorylation of STAT3 in CH however is not expected and could be contributed to activate Suppressors of Cytokine Signaling (SOCS) which negatively regulate STAT3 activity after liver injury [21], which remains to be proven.

HGF plays an essential part in the development and regeneration of the liver, and has anti-apoptotic activity in hepatocytes [22]. The levels of HGF (mRNA and protein) seemed to be induced in our disease models were chronic inflammation is present. These finding of increased expression of HGF in these canine disorders with reduced hepatocyte regeneration could indicate an active c-MET pathway. This idea was strengthened by the measurements on the PKB pathway, both phosphorylated PKB itself and downstream targets clearly showed an active PKB pathway in CH and LDH. However, PKB can be phosphorylated by several other receptor tyrosine kinases such as epidermal growth factor receptor or the insulin receptor [23]. Moreover,

previous measurements on PKB in congenital canine liver hypoplasia where HGF and c-MET levels were significantly lower [13], an active, thus phosphorylated PKB was also found. This indicates that although the phosphorylated PKB as is shown to be active, this effect can not be solely regarded as a c-MET mediated response. In order to see if the lowered c-MET mRNA levels reduced the hepatocytes ability to proliferate we partially knocked down c-MET in epithelial liver cells. Results showed that even though the c-MET mRNA levels are over five times reduced the cells are still sensitive for recombinant HGF treatment.

The liver is comprised of several cell-types of both mesenchymal and parenchymal origin. Therefore, the observed differences in gene-expression in our measurements could be due to changes in the amount of cell-types and the relative ratios between cell-types present. For instance the observed increase in HGF both at mRNA as protein level could be due to an increase in (myo)fibroblasts (activated stellate cells) which express HGF [24]. Immunohistochemistry and laser micro-dissection can answer which specific cell-types are involved in the pathogenesis of these hepatic diseases.

HGF needs extracellular processing to become biologically active. The serine protease HGF activator (HGFA) is responsible for activation of proHGF [25]. Our studies revealed that HGFA was doubled in dogs with AH and halved in case of LDH, but unchanged in CH and CIRR. This may indicate increased HGF activation in AH. Although levels of HGFA were reduced in LDH, this does not necessarily indicate a lack of extracellular processing of HGF as HGF can be activated by other proteases [26].

Surgical animal models for liver regeneration, such as partial hepatectomy (PHx), represent an over-simplification by the absence of inflammation or overperfusion; furthermore, all hepatocytes are stimulated by PHx to enter the G1 phase simultaneously. Toxic models induced by dimethylnitrosamine (DMN), CCl_4, acetominophen, or thioacetamide can represent chronic as well as acute/fulminant hepatitis [27-29]. Toxic models are better clinical models as hepatotoxins can be used to selectively induce centrolobular and periportal necrotic lesions and thus mimic spontaneous liver diseases. However toxin-induced models do not represent the full range of changes seen in spontaneous human liver disease [30]. Comparison between dog and human diseases were obtained by using samples derived from cirrhotic human samples derived from alcohol abuse or hepatitis C infection, two of the most common causes of hepatitis in the Western world [31,32]. Overall, differences between individual human samples and between groups showed to be minor and highly comparable to canine cirrhosis. The homogenous groups emphasize the validity to use

pooled canine livers samples in stead of individual measurements. A few differences in the individual human cirrhotic samples were found. As mentioned before, three patients in the hALC-group (3-5, Figure 5A), and two in the hHC-group (8-9, Figure 5B) showed an increase in phosphorylated c-MET and the downstream PKB towards the other samples. The same samples showed slight increases in HGF protein. This indicated that these patients probably had active cirrhosis, in combination with regenerative pockets.

This study is the first to measure expression profiles of crucial pathways of liver regeneration and apoptosis in complex spontaneous canine liver diseases in comparison with man. Our canine liver diseases are spontaneous models representing the entire complexity of spontaneous human liver diseases so that they represent natural models to compare with human diseases. Moreover, dogs are large animals permitting procedures which would also be relevant for human medicine. Therefore, privately owned dogs may help to fill in the gap between induced rodent models and human diseases. More specifically, these results indicated that AH, CH, LDH, and CIRR are good spontaneous large animal models to evaluate the clinical application of therapies such as cell transplantation or administration of growth factors.

Acknowledgements

The authors thank Prof. Oude-Elferink for the BDE cells, and Dr. Libbrecht for the (description of) the human samples.

References

[1] Sutter NB, Ostrander EA. Dog star rising: the canine genetic system. Nat Rev Genet 2004, 5:900-910.

[2] Ostrander EA, Wayne RK. The canine genome. Genome Res 2005, 15:1706-1716.

[3] Boomkens SY, Penning LC, Egberink HF, et al. Hepatitis with special reference to dogs. A review on the pathogenesis and infectious etiologies, including unpublished results of recent own studies. Vet Q 2004, 26:107-114.

[4] Bennett AM, Davies JD, Gaskell CJ, et al. Lobular dissecting hepatitis in the dog. Vet Pathol 1983, 20:179-188.

[5] van den Ingh TS, Rothuizen J. Lobular dissecting hepatitis in juvenile and young adult dogs. J Vet Intern Med 1994, 8:217-220.

[6] Jalan R, Hayes PC. Sodium handling in patients with well compensated cirrhosis is dependent on the severity of liver disease and portal pressure. Gut 2000, 46:527-533.

[7] Koniaris LG, McKillop IH, Schwartz SI, et al. Liver regeneration. J Am Coll Surg 2003, 197:634-659.

[8] Birchmeier C, Birchmeier W, Gherardi E, et al. Met, metastasis, motility and more. Nat Rev Mol Cell Biol 2003, 4:915-925.

[9] Okano J, Shiota G, Matsumoto K, et al. Hepatocyte growth factor exerts a proliferative effect on oval cells through the PI3K/AKT signaling pathway. Biochem Biophys Res Commun 2003, 309:298-304.

[10] Spee B, Mandigers PJ, Arends B, et al. Differential expression of copper-associated and oxidative stress related proteins in a new variant of copper toxicosis in Doberman pinschers. Comp Hepatol 2005, 4:3.

[11] Vandesompele J, De Preter K, Pattyn F, et al. Accurate normalization of real-time quantitative RT-PCR data by geometric averaging of multiple internal control genes. Genome Biol 2002, 3:RESEARCH0034.

[12] Oda D, Savard CE, Nguyen TD, et al. Dog pancreatic duct epithelial cells: long-term culture and characterization. Am J Pathol 1996, 148:977-985.

[13] Spee B, Penning LC, van den Ingh TS, et al. Regenerative and fibrotic pathways in canine hepatic portosystemic shunt and portal vein hypoplasia, new models for clinical hepatocyte growth factor treatment. Comp Hepatol 2005, 4:7.

[14] Hanada M, Feng J, Hemmings BA. Structure, regulation and function of PKB/AKT--a major therapeutic target. Biochim Biophys Acta. 2004, 1697:3-16.

[15] Taub R. Liver regeneration: from myth to mechanism. Nat Rev Mol Cell Biol 2004, 5:836-847.

[16] Roux PP, Blenis J. ERK and p38 MAPK-activated protein kinases: a family of protein kinases with diverse biological functions. Microbiol Mol Biol Rev 2004, 68:320-344.

[17] Seger R, Krebs EG. The MAPK signaling cascade. FASEB J 1995, 9:726-735.

[18] Chung J, Uchida E, Grammer TC, et al. STAT3 serine phosphorylation by ERK-dependent and -independent pathways negatively modulates its tyrosine phosphorylation. Mol Cell Biol 1997, 17:6508-6516.

[19] Decker T, Kovarik P. Serine phosphorylation of STATs. Oncogene 2000, 19:2628-2637.

[20] Shen Y, Schlessinger K, Zhu X, et al. Essential role of STAT3 in postnatal survival and growth revealed by mice lacking STAT3 serine 727 phosphorylation. Mol Cell Biol 2004, 1:407-419.

[21] Sakuda S, Tamura S, Yamada A, et al. Activation of signal transducer and activator transcription 3 and expression of suppressor of cytokine signal 1 during liver regeneration in rats. J Hepatol 2002, 36:378-384.

[22] Okano J, Shiota G, Matsumoto K, et al. Hepatocyte growth factor exerts a proliferative effect on oval cells through the PI3K/AKT signaling pathway. Biochem Biophys Res Commun 2003, 309:298-304.

[23] Meier R, Hemmings BA. Regulation of protein kinase B. J Recept Signal Transduct Res 1999, 19:121-128.

[24] Schirmacher P, Geerts A, Jung W, et al. The role of Ito cells in the biosynthesis of HGF-SF in the liver. EXS 1993, 65:285-299.

[25] Kataoka H, Miyata S, Uchinokura S, et al. Roles of hepatocyte growth factor (HGF) activator and HGF activator inhibitor in the pericellular activation of HGF/scatter factor.
Cancer Metastasis Rev 2003, 22:223-236.

[26] Naldini L, Tamagnone L, Vigna E, et al. Extracellular proteolytic cleavage by urokinase is required for activation of hepatocyte growth factor/scatter factor. EMBO J 1992, 13:4825-4833.

[27] Kosai K-I, Matsumoto K, Funakoshi H, et al. Hepatocyte growth factor prevents endotoxin-induced lethal hepatic failure in mice. Hepatology 1999, 30:151-159.

[28] Gupta S, Rajvanshi P, Aragona E, et al. Transplanted hepatocytes proliferate differently after CCl_4 treatment and hepatocyte growth factor infusion. Am J Physiol 1999, 276:G629-G638.

[29] Matsuda Y, Matsumoto K, Yamada A, et al. Preventive and therapeutic effects in rats of hepatocyte growth factor infusion on liver fibrosis/cirrhosis. Hepatology 1997, 26:81-89.

[30] Palmes D, Spiegel HU. Animal models of liver regeneration. Biomaterials 2004, 25:1601-1611.

[31] Morgan G. Beneficial effects of NSAIDs in the gastrointestinal tract. Eur J Gastroenterol Hepatol 1999, 11:393-400.

[32] Corrao G, Zambon A, Torchio P, et al. Attributable risk for symptomatic liver cirrhosis in Italy. Collaborative Groups for the Study of Liver Diseases in Italy. J Hepatol 1998, 28:608-614.

Chapter 4

TGFβ-1 signalling in canine hepatic diseases, new models for human fibrotic liver pathologies

Bart Spee[1], Brigitte Arends[1], Ted S.G.A.M. van den Ingh[2], Bas Brinkhof[1], Hubertus Nederbragt[2], Jooske IJzer[2], Tania Roskams[3], Louis C. Penning[1], and Jan Rothuizen[1]

From the Departments of [1]Clinical Sciences of Companion Animals and [2]Pathobiology, Faculty of Veterinary Medicine, Faculty of Veterinary Medicine, Utrecht University, The Netherlands, and [3]Department of Pathology, University Hospitals of Leuven, Belgium.

Submitted

Abstract

The purpose of this study was to validate spontaneous chronic hepatitis and cirrhosis in dogs as a potential large animal model for fibrotic liver disease in man by evaluating their molecular pathophysiology. Transforming growth factor-β1 (TGF-β1) signalling was analysed in liver samples of dogs with Acute Hepatitis (AH), Chronic Hepatitis (CH), Cirrhosis (CIRR), and a specific form of cirrhosis, Lobular Dissecting Hepatitis (LDH) in comparison with human cirrhotic samples from alcohol abuse (ALC) and hepatitis C (HC). Canine samples were investigated with quantitative real-time PCR (Q-PCR) and Western blotting on TGF-β1 signalling including Smad2/3 phosphorylation. Immunohistochemistry on collagen-I and –III was performed. Q-PCR showed an increase in TGF-β1 levels and downstream effector gene products in CH, LDH, and CIRR. The same fibrotic diseases also showed an increase in phosphorylated Smad2/3 and a higher deposition of collagen-I and collagen-III. In contrast, in AH neither active TGF-β1 signalling nor collagen deposition was observed. Western blot analysis on human ALC and HC indicated a high similarity with canine samples in TGF-β1 expression and Smad2/3 phosphorylation. In conclusion, our results demonstrate that fibrosis in spontaneous dog liver diseases is highly comparable to their human counterparts and might serve as models for anti-fibrotic strategies.

Introduction

Chronic hepatitis is characterized by hepatocellular apoptosis or necrosis, inflammation, and fibrosis. Fibrosis is the major factor causing morbidity and mortality due to the development of cirrhosis [1,2]. Chronic hepatitis may be the sequel of various causes such as (viral) infections, exposure to toxins and drugs, or immunological and metabolic disorders [3]. Dogs have chronic liver diseases which are clinically and pathologically highly comparable to their human liver disease counterparts; they may thus fulfil a role as spontaneous (non-experimental) animal model, in between induced toxic or surgical models in rodents, and diseases in man [4]. To become fully accepted as a model for human diseases molecular pathways must be similarly affected.

We chose four different spontaneous forms of hepatitis and cirrhosis in dogs for comparative analysis of fibrosis. They ranged from Acute Hepatitis (AH) without fibrosis to Chronic Hepatitis (CH), and cirrhosis (CIRR), including Lobular Dissecting Hepatitis (LDH). The last disease is a specific form of cirrhosis with severe fibrosis and complete disruption of the lobular architecture and is comparable to neonatal hepatitis in humans [5,6]. Although the aetiology of canine hepatitis is largely unknown, the reaction patterns (clinical and pathological) of the liver to injury are uniform and therefore mimic their human counterparts [7]. Like in man, cirrhosis is the end stage of chronic hepatitis which typically needs 1-5 years to be reached. Dogs with cirrhosis develop portal hypertension, and in the decompensated stage this may be complicated by formation of ascites and development of hepatic encephalopathy and coagulopathies [5-7].

It has already been established that a transient increase of transforming growth factor β1 (TGF-β1) in the liver promotes fibrosis with the formation of extracellular matrix (ECM) components and suppresses hepatocyte proliferation [8,9]. The major components of the ECM are interstitial collagens (types I and III), membrane collagen (type IV), and non-collagenous glycoproteins, such as laminin and fibronectin [10]. In several toxin-induced liver fibrosis models, fibrotic lesions are associated with an increase in procollagens type I, III, IV and TGF-β1 mRNAs [11,12]. Intracellular TGF-β1 signalling involves interaction of Smad proteins [13]. Smad-2 and -3 are phosphorylated at the carboxy-terminus by activated TGF-β receptor kinases. When bound with co-Smads, the Smad-complex translocates into the nucleus and acts as TGF-β1-induced transcriptional activator of target genes [14].

The present study was undertaken to investigate molecular pathophysiology of canine liver disease and compare it to the current paradigm of liver fibrosis in man

[15-17]. Therefore our emphasis was on the TGF-β1 signalling routes which are involved in the crucial pathways of fibrosis. We analysed TGF-β1 signalling in liver tissues obtained from dogs with different forms of hepatitis, encompassing acute to chronic hepatitis and cirrhosis. In contrast with chemically induced rodent models, these spontaneous dog diseases are expected to be very well comparable with chronic human liver disease. If TGF-β1 signalling is similarly affected in canine and human diseases these spontaneous dogs could form a good model for evaluating clinical effects of new therapies, such as anti-fibrotic factors, prior to their application in man. Then, these animals can bridge the gap between basic physiology and clinical patient care.

Materials and methods

Animals

All samples were obtained from dogs of different breeds examined at our faculty of veterinary medicine. The procedures were approved by Utrecht University's Ethical Committee, as required under Dutch legislation.
Each disease group contained eleven dogs (n = 11 dogs), and was compared to a group of twelve age-matched healthy control dogs (n = 12 dogs), without clinical signs of hepatitis or other disease. Liver tissue was obtained from all dogs under local anaesthesia by ultrasound-guided biopsy with a true cut 14G biopsy needle, preceded by ultrasonographic evaluation of the liver to exclude biopsy artefacts in case of non-homogeneous hepatic changes. Two formalin-fixed biopsies were embedded in paraffin, sliced, and stained with hematoxylin and eosin, Van Gieson stain, and reticulin stain according to Gordon and Sweet. Fibrosis scoring was performed according to Scheuer, a defined scoring method for fibrosis in hepatitis [18]. The slides were examined by one certified veterinary pathologist. Two other biopsies were snap-frozen in liquid nitrogen, and stored at $-70^{o}C$ until molecular analysis. Dogs with hepatitis presented with apathy, anorexia, vomiting and/or jaundice, and in cases of CIRR and LDH often with signs of liver decompensation with ascites and hepatic encephalopathy. The presence of a liver disease was confirmed by finding high plasma levels of AP, ALT, and/or BA. The AH, CH, CIRR, and LDH diseases were diagnosed according to the criteria of the World Small Animal Veterinary Association (WSAVA) Liver Diseases and Pathology Standardization Research Group [19]. Acute hepatitis (AH) was clinically characterized by acute onset of the disease and histologically by inflammation, hepatocellular apoptosis and necrosis. Chronic hepatitis (CH) was characterized histologically by mononuclear or mixed

inflammation, apoptosis and necrosis of hepatocytes, fibrosis, and regeneration. Cirrhosis (CIRR), the end stage of chronic hepatitis, was characterized by bridging fibrosis, shunting of afferent and efferent vessels, and conversion of the normal liver architecture into abnormally structured parenchymal nodules. Lobular dissecting hepatitis (LDH), a rapidly progressive form of cirrhosis was characterized by fibrosis surrounding individual hepatocytes with complete disruption of the lobular architecture. Although the aetiology of canine hepatitis is largely unknown, several known aetiological agents associated with hepatitis in other species have been excluded [20]. Furthermore, two known causes of hepatitis in the dog, CAV-1 and copper toxicosis, have been excluded by PCR and (immuno)histochemistry.

Human patients

All samples were obtained from surgical patients who were transplanted at the department of Abdominal Transplantation in the University Hospital Leuven, Leuven, Belgium. The procedures were approved by Leuven University's Ethical Committee, as required under Belgian legislation. Human explant samples were collected directly after surgery and immediately snap frozen. All patients were presented with micronodular cirrhosis and were predominantly male. The Alcoholic Cirrhosis (hALC) group contained five patients (n = 5) characterized by cirrhosis with neutronphil infiltrations, alcohol related morphological changes (hepatocyte ballooning, Mallory bodies, necrosis), and in some cases steatosis and increased iron deposition. The Hepatitis C (hHC) group contained four patients (n = 4) characterized by cirrhosis with neutrophil infiltrations, lymphoid follicles and aggregates, and in one case in combination with hepatocellular carcinoma (HCC, sample 6, Figure 4). All cases were presented with hepatocyte decay, apoptosis/necrosis, regeneration, and fibrosis.

Quantitative PCR and statistical methods

Quantitative real-time PCR (Q-PCR) was performed on a total of 9 gene products involved in fibrosis; e.g. TGF-β1, TGF-β receptor type I (TGF-β RI), TGF-β receptor type II (TGF-β RII), uPA, collagen-I, collagen-III, collagen-IV, fibronectin, and HIF-1α. The abundance of mRNA was determined by Reverse Transcription (RT) followed by real-time quantitative PCR using appropriate primers (Table 1), as previously described [21]. In short, total cellular RNA was isolated from each frozen canine liver tissue in duplicate, using Qiagen RNeasy Mini Kit (Qiagen, Leusden, the Netherlands) according to the manufacturer's instructions. The RNA samples were treated with DNase-I (Qiagen Rnase-free DNase kit). In total, 3 µg of RNA was incubated with poly(dT) primers at 42°C for 45 min, in a 60 µl reaction volume, using the RT System from Promega (Promega Benelux, Leiden, the Netherlands). Q-PCR was

based on the high affinity double-stranded DNA-binding dye SYBR® green I (BMA, Rockland, ME). For each experimental sample, the amount of the gene of interest and of the two independent endogenous references (glyceraldehyde-3-phosphate dehydrogenase (GAPDH) and hypoxanthine phosphoribosyl transferase (HPRT)) was determined from the appropriate standard curve in autonomous experiments. If relative amounts of GAPDH and HPRT were constant for a sample, data were considered valid and the average amount was used as a normalization factor in the study (data not shown). Results were normalized according to the average amount of the endogenous references. The normalized values were divided by the normalized values of the calibrator (healthy group) to generate relative expression levels [22].

A Kolmogorov-Smirnov test was performed to establish a normal distribution and a Levene's test for the homogeneity of variances. All samples included in this study were normally distributed. The statistical significance of differences between diseased and control animals was determined by using the Student's *t*-test. A p-value < 0.05 was considered statistically significant. Analysis was performed using SPSS software (SPSS Benelux BV, Gorinchem, the Netherlands).

Immunoblot analysis

Pooled liver tissues (n = 6 dogs per group, randomly chosen from original group) were homogenized in RIPA buffer containing 1% Igepal, 0.6 mM Phenylmethylsulfonyl fluoride, 17 μg/ml aprotinine and 1 mM sodium orthovanadate (Sigma chemical Co., Zwijndrecht, the Netherlands). Protein concentrations were obtained using a Lowry-based assay (DC Protein Assay, BioRad). Detection of TGF-β1 was performed under non-denaturing conditions with twenty μg of protein on 15% Tris-HCl polyacrylamide gels (BioRad). For the detection of Smad's twenty μg of protein of the supernatant was denatured for 3 min at 95°C and separated on 7.5% Tris-HCl polyacrylamide gels (BioRad). The procedure for immunodetection was based on an ECL Western blot analysis system, performed according to the manufacturer's instructions (Amersham-Biosciences). The membranes were incubated with 4% ECL blocking solution in TBS for 1 hour under gentle shaking. The incubation of the primary antibody was performed at 4°C overnight in TBST with 4% BSA (Table 2). After washing, the membranes were incubated with the appropriate horseradish peroxidase-conjugated secondary antibody at room temperature for 1 h in TBST with 4% BSA. Exposures were made with Kodak BioMax Light-1 films (Sigma-Aldrich, Zwijndrecht, the Netherlands). Densitometric analysis of immunoreactive bands was performed with a Gel Doc 2000 system using Quantity One 4.3.0 Software (BioRad).

Table 1. *Nucleotide Sequences of Dog-Specific Primers for Real-Time Quantitative PCR*

Gene	F/R	Sequence (5'-3')	Tm (°C)	Product size (bp)	Accession number
GAPDH	F	TGT CCC CAC CCC CAA TGT ATC	58	100	AB038240
	R	CTC CGA TGC CTG CTT CAC TAC CTT			
HPRT	F	AGC TTG CTG GTG AAA AGG AC	56	100	L77488 / L77489
	R	TTA TAG TCA AGG GCA TAT CC			
TGF-β1	F	CAA GGA TCT GGG CTG GAA GTG GA	66	113	L34956
	R	CCA GGA CCT TGC TGT ACT GCG TGT			
TGF-β R I	F	CAG TCA CCG AGA CCA CAG ACA AAG T	59	101	AY455799
	R	TGA AGA TGG TGC ACA AAC AAA TGG			
TGF-β R II	F	GAC CTG CTG CCT GTG TGA CTT TG	61	116	AY455800
	R	GGA CTT CGG GAG CCA TGT ATC TTG			
uPA	F	CTG GGG AGA TGA AGT TTG AGG TGG	64.5	105	AY455801
	R	TGG AAC GGA TCT TCA GCA AGG C			
Collagen-I	F	GTG TGT ACA GAA CGG CCT CA	61	111	AF056303
	R	TCG CAA ATC ACG TCA TCG			
Collagen-III	F	ATA GAG GCT TTG ATG GAC GAA	65	134	AB042266
	R	CCT CGC TCA CCA GGA GC			
Collagen-IV	F	CAC AGC CAG ACA ACA GAT GC	67	151	U07888
	R	GCA TGG TAC TGA AGC GAC G			
Fibronectin	F	AGG TTG TTA CCA TGG GCA	61	91	U52106
	R	GCA TAA TGG GAA ACC GTG TAG			
HIF-1α	F	TTA CGT TCC TTC GAT CAG TTG TCA	61	106	AY455802
	R	GAG GAG GTT CTT GCA TTG GAG TC			

F: Forward primer; R: reversed primer

Immunohistochemistry

Collagens-I and -III were evaluated from at least 4 sections per group (n = 4 dogs, randomly chosen) and compared to sections from normal control dogs (n = 4 dogs, randomly chosen). For antigen retrieval the sections (3 μm) were heated in 10 mM citrate buffer (pH 6.0) in a microwave-oven (850 W) at full power until boiling-point, after which the sections were heated for 15 minutes at half-power. Sections were incubated in 0.3% hydrogen peroxide in PBS for 30 min at RT to quench endogenous peroxidase activity. After washing with PBS buffer containing 0.1% Tween-20, background staining was blocked in 10% normal horse serum in PBS for 30 min at RT. Sections were incubated overnight at 4°C with the primary antibody mouse anti-collagen-I (Abcam, Cambridge, UK) diluted 1:100 in PBS with 2% bovine serum albumin (BSA). The primary antibody mouse anti-collagen-III (Chemicon, Victoria, Australia) was diluted 1:50 in PBS. After washing in PBS-Tween, slides

Table 2. *Used antibodies in Western blot experiments*

Antigen	Product size (kDa)	Dilution	Manufacturer	Secondary antibody	Dilution
TGF-β1	25	1:1,000	Abcam	Anti-rabbit HRP	1:20,000
p-Smad2/3 (Ser 465/467)	58	1:500	Cell-Signaling	Anti-rabbit HRP	1:20,000
Smad2/3	58	1:500	BD Biosciences	Anti-mouse HRP	1:20,000
Beta-actin	42	1:2,000	Neomarkers	Anti-mouse HRP	1:20,000

were incubated with the biotinylated secondary antibody horse anti-mouse IgG (Vector Laboratories, Peterborough, UK) diluted 1:125 in PBS for 1 hour at RT. After washing in PBS buffer, slides were treated with the ABC peroxidase complex (Vectastain from Brunschwig, Amsterdam, the Netherlands) for 1 hour at RT. The peroxidase activity was visualized by applying 0.5 mg/ml diaminobenzidine chromogen containing 0.035% hydrogen peroxide in PBS for 10 min at RT. The DAB solution contained 0.3% (w/v) di-ammonium nickel (II) 6-hydrate (Brunschwig) to improve contrast. The sections were counterstained with hematoxylin, dehydrated, and mounted. They were examined and photographed using an Olympus BX41 light microscope equipped with an Olympus DP50 digital camera (Olympus, Zoeterwoude, the Netherlands). The amount of positive staining was semi-quantitatively assessed by one certified veterinary pathologist examining the sections (original magnification of 450x) and the sections were also evaluated with respect to localization of the staining. Negative controls were performed as described above, yet without incubation of the primary antibody; these sections showed no positive staining in any of the diseases under study (data not shown).

Results

To gain insight into the activity of the TGF-β1 pathway in spontaneous canine liver diseases we first measured mRNA levels by means of Q-PCR. Second, Western blotting was performed to confirm mRNA quantities and to show activation at the protein level. Third, Western blots were used to compare canine samples to human cirrhotic samples from alcohol abuse (hALC) and hepatitis C (hHC). Finally, immunohistochemistry was used to determine ECM deposition.

TGF-β1 cascade signalling pathway involved in fibrosis

In AH (Figure 1A) none of the mRNA levels analysed were significantly changed. In contrast, in CH (Figure 1B) we found that all analysed mRNA levels were significantly induced. An induction was seen in the TGF-β1 mRNA levels (2-fold), whe-

reas the receptors type I (signalling) and type II (binding) were induced 3- and 2-fold, respectively. The proteolytic enzyme involved in activation of TGF-β1, urokinase type plasminogen activator (uPA), was induced 2-fold in the CH group. In the LDH group (Figure 1C), TGF-β1 mRNA levels were induced 4-fold, type I receptor 3-fold and type II receptor 4-fold. The uPA mRNA levels were highly induced (6-fold). In the CIRR group (Figure 1D), an increase in TGF-β1 mRNA levels was also seen (2-fold). The highest induction of TGF-β receptor type I mRNA levels was seen (12-fold) in this group, but type II mRNA levels were not significantly changed. The uPA mRNA level was induced 5-fold.

Gene expression of extra-cellular matrix (ECM) gene products and HIF-1α

Collagen-I levels are commonly associated with severe forms of hepatic fibrosis [23]. The mRNA levels of collagens-I, -III, and -IV were decreased 3-, 6-, and 4-fold, respectively, in AH, although fibronectin and HIF-1α mRNA levels did not change significantly (Figure 2A). In the CH group, the only significant change was seen in the collagen-III mRNA level, which was elevated 2-fold (Figure 2B). All mRNA levels were significantly elevated in the LDH group (9-, 4-, 4-, 3-, and 3-fold, for collagens I, III, and IV, fibronectin, and HIF-1α, respectively) (Figure 2C). In the cirrhosis group (Figure 2D), the mRNA levels of collagen-I were induced 3-fold, but the mRNA levels of collagen-IV and fibronectin were significantly decreased (2- and 4-fold, respectively). The highest increase in HIF-1α mRNA levels was found in this group, with a 7-fold induction compared to the healthy group.

Western blot analysis on canine AH, CH, CIRR, and LDH

TGF-β1 was detected in all diseases as a peptide of 25 kDa (Fig. 3). TGF-β1 seemed to be induced in all fibrotic diseases compared to the healthy group, with the highest increase in CIRR. The non-phosphorylated Smad2/3 (58 kDa) was detected in fibrotic disease types, with a slight quantitative increase in CH. The activated thus phosphorylated Smad2/3 was detected in CH, LDH, and CIRR, where it was present as a single band of 58 kDa. Interestingly, the quantity of phosphorylated Smad2/3 was very low in healthy samples and AH, the latter emphasizing the absence of fibrogenesis in this type of disease. Furthermore, the phosphorylated Smad2/3 protein showed the highest increase in LDH.

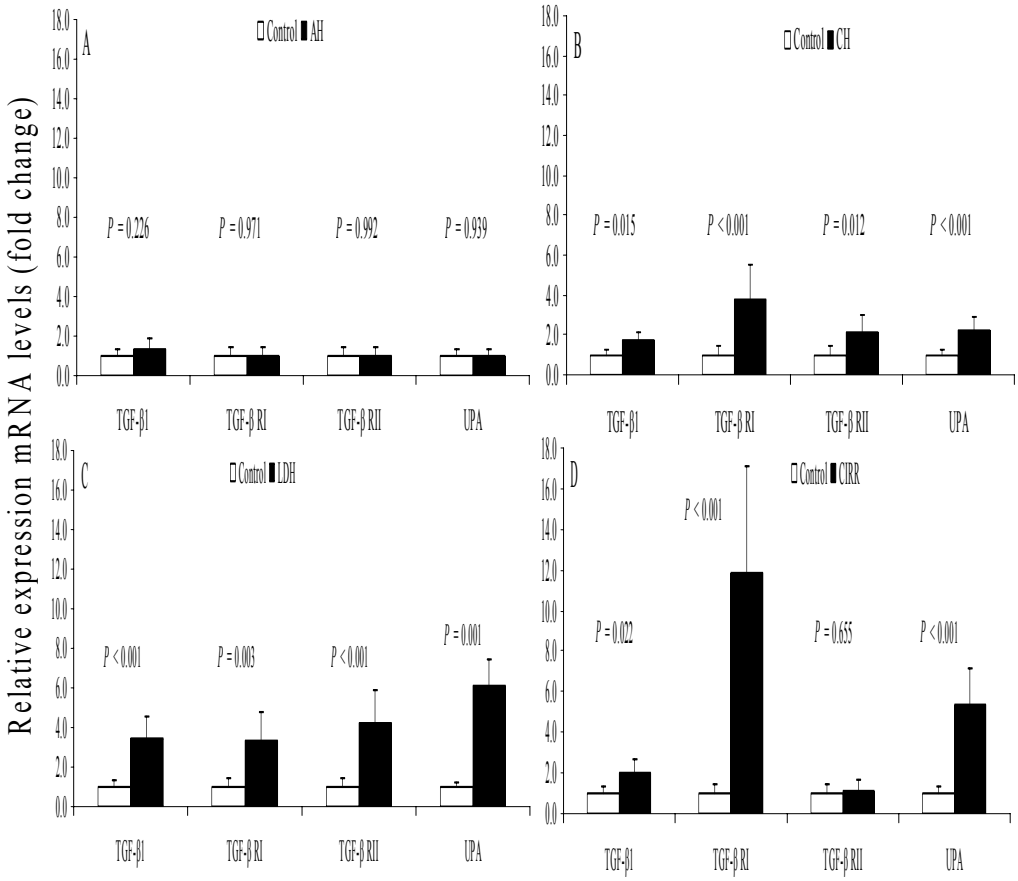

Figure 1. *Quantitative Real-Time PCR of gene-products involved in fibrosis.*
Relative expression of mRNA levels in acute hepatitis (AH) shunt is shown in (A), in chronic hepatitis (CH) in (B), in lobular dissecting hepatitis (LDH) in (C), and in cirrhotic samples (CIRR) in (D). Data represent mean + SD.

Western blot analysis on human cirrhotic explant samples after alcohol abuse (hALC) and after hepatitis C virus infection (hHC)

Western blot analysis on human hALC and hHC samples showed a detectable 25 kDa TGF-β1 in all samples with minor quantitative differences (Figure 4). The 58 kDa Smad2/3 was also detected in all samples although two samples in the hHC-group (Figure 4B, lane 7 and 8) were present to a lesser extent. The phosphorylated

form of Smad2/3 (58 kDa) was detected in all samples; however two samples in the hHC-group had a diminished phosphorylation of the Smad2/3 protein (Figure 4B, lane 7 and 8).

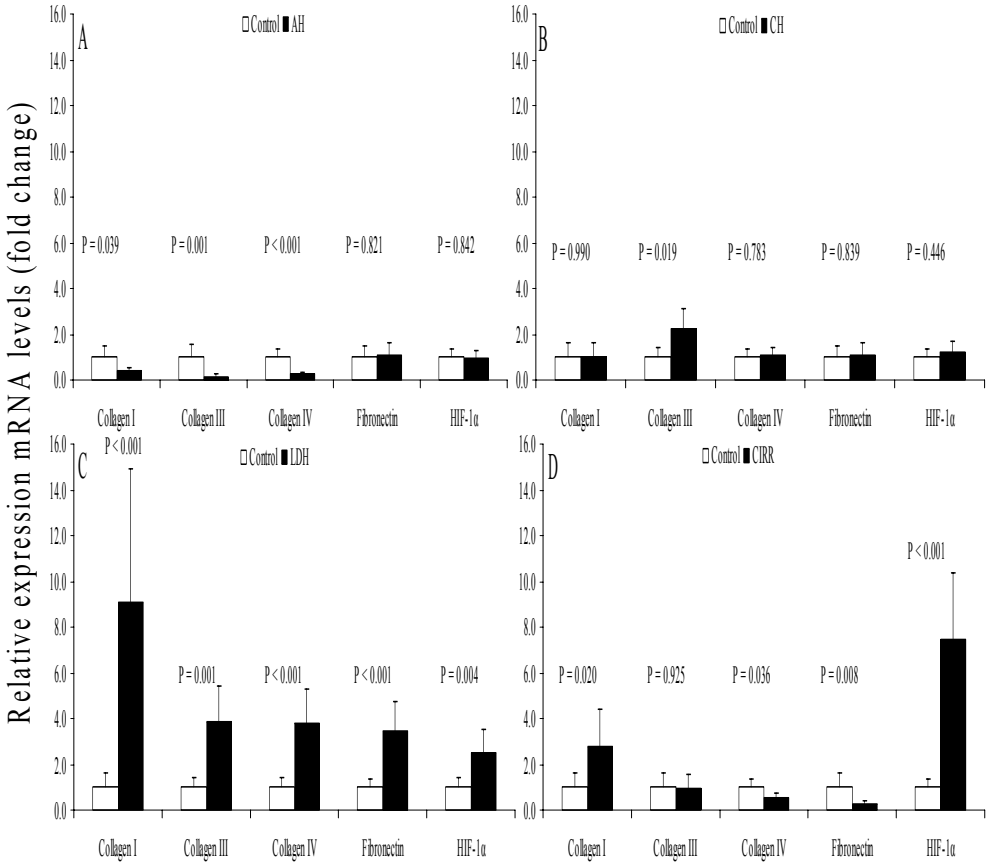

Figure 2. *Quantitative Real-Time PCR of collagens, fibronectin, and HIF-1α.*
Relative expression of mRNA levels in acute hepatitis (AH) shunt is shown in (A), in chronic hepatitis (CH) in (B), in lobular dissecting hepatitis (LDH) in (C), and in cirrhotic samples (CIRR) in (D). Data represent mean + SD.

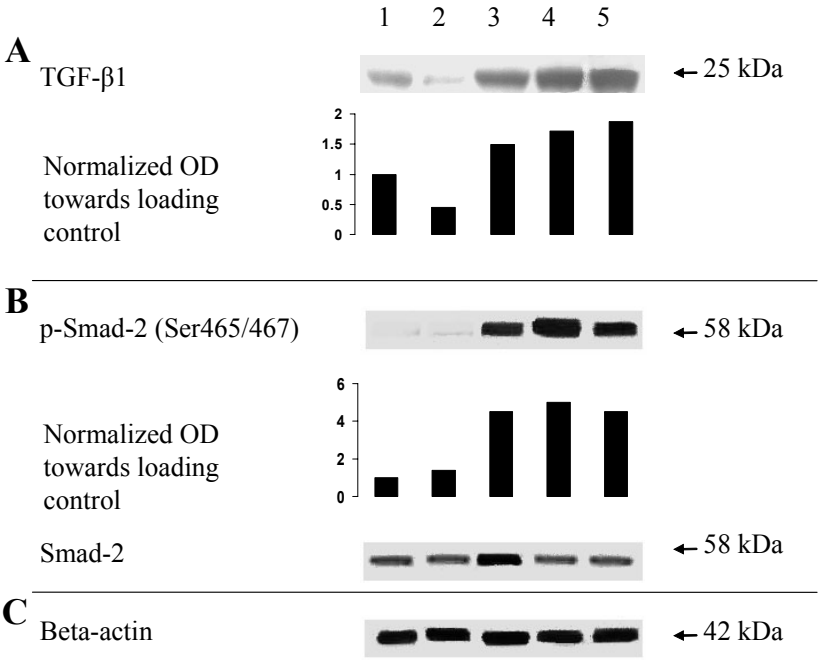

Figure 3. *Western blot analysis of diseased and control canine liver homogenates.* *Detection of the 25 kDa TGF-β1 protein is shown in (A). Detection of the 58 kDa Smad-2 protein is shown in (B). Beta-actin served as a loading control is shown in (C). Quantitative analysis of immunoreactive bands by means of Optical Density (OD) measurements corrected for the amount of beta-actin (loading control, shown in (C)). Lane 1: Control; Lane 2: Acute Hepatitis; Lane 3: Chronic Hepatitis; Lane 4: Lobular Dissecting Hepatitis; Lane 5: Cirrhosis*

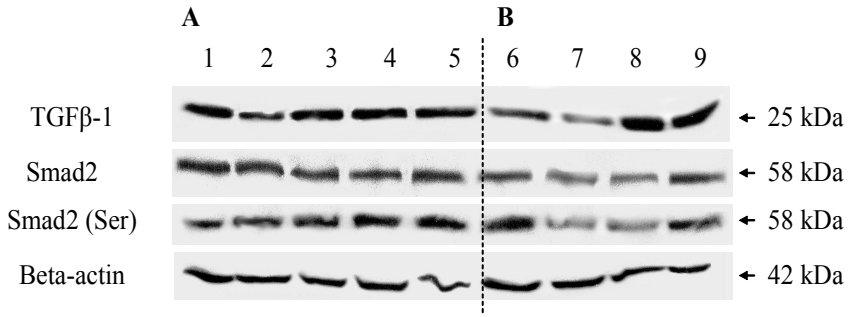

Figure 4. *Western blot analysis of human liver homogenates. Analysis of the (25 kDa) TGF-β1, (58 kDa) Smad-2 protein, and (42 kDa) Beta-actin (loading control). Human cirrhotic samples from alcohol abuse (hALC, lane 1-5) is shown in (A), cirrhotic samples after hepatitis C infection (hHC, lane 6-9) is shown in (B).*

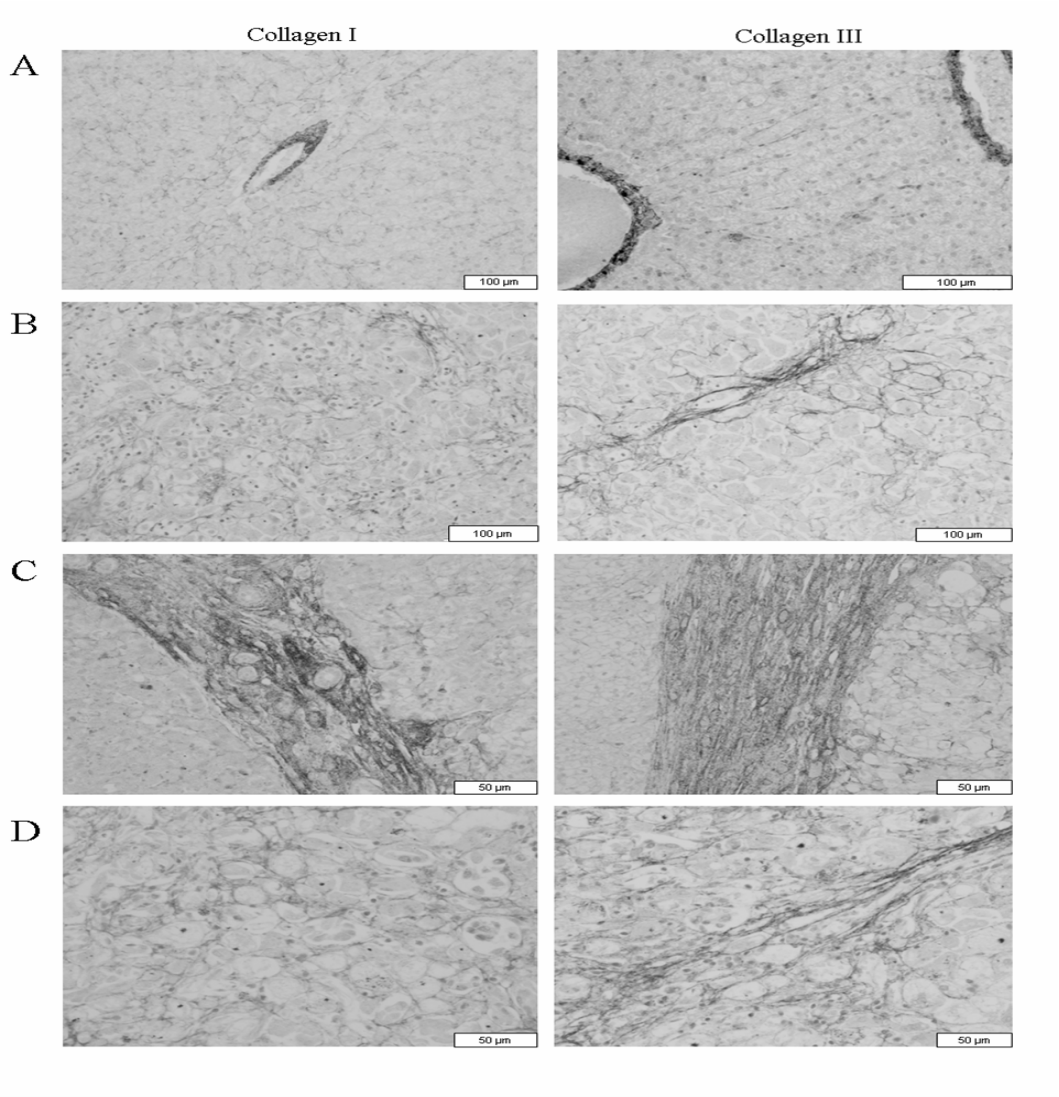

Figure 5. *Immunohistochemistry on collagen-I and -III in liver samples.*
Collagen-I and-III in healthy liver tissue is shown in (A). Collagen-I and -III in Chronic Hepatitis is shown in (B). Collagen-I and -III in cirrhotic liver tissue is shown in (C). Collagen-I and -III in Lobular Dissecting Hepatitis is shown in (D). Size bar indicated in figures. Color-figure see Appendix 2, page 219.

Immunohistochemical observation of collagen levels

Collagens-I and -III showed a similar pattern in the normal canine liver. Marked positive staining was seen in the stroma of the larger portal areas and around the larger hepatic veins, whereas mild staining was seen in the smaller portal and perivenous areas. Moreover, a fine fibrillar staining was often observed in the perisinusoidal space in the centrolobular areas (Figure 5A). In the AH group, the collagen-I and -III staining showed a pattern comparable to that of the control dogs although the fibers in the centrolobular areas were less recognizable. In the CH group (Figure 5B), the stroma of the portal areas and around the hepatic veins stained as in the normal dogs. The parenchyma showed an increased presence of both collagens-I and -III in the periportal and centrolobular parenchyma, regularly surrounding individual liver cells or groups of them, and associated with inflammation. In the CIRR group (Figure 5C), there was marked staining for both collagens-I and -III in the fibrous septa separating large parenchymal hyperplastic nodules. Staining within these nodules varied depending of the activity of the disease as evidenced by the degree of inflammation and necrosis. In nodules without inflammation only the pre-existent stroma of the portal areas and around the hepatic veins stained positive, whereas in nodules with inflammation and necrosis an increased staining was often seen encircling single liver cells or small groups of them. An increased staining for collagen-I and -III surrounding individual and small groups of hepatocytes was also observed in larger areas between nodules with a mixture of hepatocytes, inflammation and fibrosis. In the LDH group (Figure 5D), a marked increase of collagen-I and -III was seen throughout the parenchyma encircling individual liver cells and small groups of hepatocytes. In some dogs small hyperplastic parenchymal nodules were seen surrounded by thin fibrous septa containing both collagen-I and -III; in these nodules only slight staining for collagen-I and -III was present.

Discussion

The results of this study showed that the molecular pathophysiology of canine fibrotic liver diseases is highly comparable to the pathophysiology of their human counterparts. This emphasizes the potential of spontaneous dog diseases as models for human clinical investigation. We have analyzed liver fibrosis using several molecular and biochemical techniques (Q-PCR, Western blotting, and immunohistochemistry on ECM proteins). This provided insight into the TGF-β1 pathway in four spontaneous canine hepatic diseases; acute hepatitis (AH), chronic hepatitis (CH), lobular dissecting hepatitis (LDH) and cirrhosis (CIRR).

Prolonged overexpression of TGF-β1 suppresses cell proliferation, is pro-apoptotic, and induces a deposition of ECM proteins, resulting in fibrosis in major organs such as the liver [15]. By independent techniques we showed that in fibrotic diseases (CH, LDH, and CIRR) the TGF-β1 pathway was activated. First, we found an increase in mRNA levels of the TGF-β1 ligand and the two receptors. Second, uPA (Figure 1), the activator of TGF-β1, was expressed at a higher level [24]. Third, Western blotting confirmed increased TGF-β1 (Figure 3A) in these diseases. Taken together, increased levels of TGF-β1 signalling may very well explain the activation of Smad2/3 and subsequently the formation of collagens. Comparing Western blot analysis with cirrhotic samples derived from human explant samples indicated a high similarity in protein quantity and activity of TGF-β1 signalling components. In both analysed human cirrhotic groups (alcohol induced (ALC) or due to hepatitis C infection (HC)) TGF-β1 was detected (Figure 4). More importantly, phosphorylated Smad2/3 was detected in all samples, although somewhat reduced in lane 7 and 8 as shown in Figure 4B. This observation probably is due to a decrease in total amount of Smad2/3 whereas beta-actin indicated an equal amount of protein loading.

Immunostaining against collagen-I and -III on normal liver tissues showed slight staining of the collagens in portal tracts, around the hepatic veins, as well as in the perisinoidal space (particularly centrolobular). Our observations of an increase in collagen-III mRNA levels in dogs with CH and the increased presence of collagen-I mRNA levels in CIRR were surprising. These data indicate that the chronic accumulation of collagens could begin with collagen-III and gradually form broad septal tracts composed of collagen-I and -III in CIRR. However, immunostaining against collagen-I and -III in CH and CIRR showed increased presence of both collagens. This indicates that the mRNA levels for collagen do not always reflect the presence of the protein product. This observation can be ascribed to the chronic stage of our cirrhotic samples and most likely is due to the long half-life of these ECM-proteins. The corresponding results of mRNA levels and immunostaining in LDH can be explained by the rapid clinical course of the disease in LDH. The different inflammatory activities of our cirrhotic samples, which varied from very active to almost inactive, are associated with rather small standard deviations at the mRNA level. Thus it seems that the number of patients in each group, combined with different biopsies per individual, greatly averages the differences between active and non-active CIRR. In CCl_4-induced rodent models of liver fibrosis, TGF-β1 and procollagen mRNAs were increased, including procollagen-I, -III, and -IV [25,26]. The fact that in our spontaneous dog liver diseases not all the collagens were induced stresses the importance of studying spontaneous chronic models in comparison with toxin-induced models [27].

The liver is comprised of several cell-types of both mesenchymal and parenchymal origin. Therefore, the observed differences in gene-expression in our measurements could be due to changes in the amount of cell-types and the relative ratios between cell-types present. For instance the observed increase in TGF-β1 mRNA and protein level could be due to an increase in (myo)fibroblasts (activated stellate cells) which express TGF-β1 in the perpetuation phase of fibrosis [28]. Immunohistochemistry and micro-dissection can answer which specific cell-types are involved in the pathogenesis of these hepatic diseases. Furthermore the discrepancy between TGF-β1 mRNA and protein level as seen in AH, could be contributed to the lack of activation of TGF-β1 in this group, which could be still be noncovalently bound to the Latency Associated Peptide (LAP), which occurs after expression [15].

The mechanisms underlying progressive fibrosis are unknown, but hypoxia is a known fibrogenic stimulus [29]. On the other hand, it is conceivable that increased collagen deposition leads to reduced oxygen levels in the surrounding tissue and consequently up-regulates HIF-1α. Indeed, the two major fibrotic diseases, LDH and CIRR, clearly showed an induction of HIF-1α mRNA levels of 3- and 7-fold respectively, indicating the correlation between extensive fibrosis and presence of HIF-1α.

The use of TGF-β1 intervention to halt the progression of liver fibrosis and aid regeneration has been applied successfully in animal models [30-33]. Although many of these techniques are based on rodent models [34], they could be further evaluated in these spontaneous canine liver diseases.

In conclusion, our canine liver diseases are spontaneous models representing the entire complexity of human liver diseases so that they provide natural models for comparison with human diseases. The variations with in age, body weight, feeding- and drinking behaviour and sex, as presented by the dogs visiting our clinic, nicely resemble the variations in a human population. Moreover, dogs are large animals permitting procedures which would also be relevant for human medicine. Finally, the use of canine patients can lead to a reduction in the amount of experimental animals. Proven effects in dogs may predict potential effects in human medicine with much greater power than effects in artificial rodent models. Our spontaneous dog models may therefore help to bridge the gap between basic physiology in rodent models and patient care in human diseases.

References

[1] Bataller R, Brenner DA. Liver fibrosis. J Clin Invest 2005; 115: 209-18.

[2] Desmet VJ, Roskams T. Cirrhosis reversal: a duel between dogma and myth. J Hepatol 2004, 40:860-867.

[3] Koniaris LG, McKillop IH, Schwartz S I, et al. Liver regeneration. J Am Coll Surg 2003, 197:634-659.

[4] Sterczer A, Gaal T, Perge E, et al. Chronic hepatitis in the dog--a review. Vet Q 2001, 23:148-52.

[5] Bennett AM, Davies JD, Gaskell CJ, et al. Lobular dissecting hepatitis in the dog. Vet Pathol 1983, 20:179-188.

[6] van den Ingh TSGAM, Rothuizen J. Lobular dissecting hepatitis in juvenile and young adult dogs. J Vet Intern Med 1994, 8:217-20.

[7] Boomkens SY, Penning LC, Egberink HF, et al. Hepatitis with special reference to dogs. A review on the pathogenesis and infectious etiologies, including unpublished results of recent own studies. Vet Q 2004; 26: 107-14.

[8] Mulder KM. Role of Ras and Mapks in TGFbeta signaling. Cytokine Growth Factor Rev 2000; 11: 23-35.

[9] Piek E, Heldin CH, ten Dijke P. Specificity, diversity, and regulation in TGF-beta superfamily signaling. FASEB J 1999; 13: 2105-24.

[10] Schuppan D, Ruehl M, Somasundaram R, et al. Matrix as a modulator of hepatic fibrogenesis. Semin Liver Dis 2001; 21: 351-72.

[11] Hsu YC, Chiu YT, Lee CY, et al. Increases in fibrosis-related gene transcripts in livers of dimethylnitrosamine-intoxicated rats. J Biomed Sci 2004; 3: 408-17.

[12] Shiba M, Shimizu I, Yasuda M, et al. Expression of type I and type III collagens during the course of dimethylnitrosamine-induced hepatic fibrosis in rats. Liver 1998; 3: 196-204.

[13] Liu C, Gaca M D, Swenson E S, et al. Smads 2 and 3 are differentially activated by transforming growth factor-beta (TGF-beta) in quiescent and activated hepatic stellate cells. Constitutive nuclear localization of Smads in activated cells is TGF-beta-independent. J Biol Chem 2003; 278: 11721-8.

[14] Leask A, Abraham DJ. TGF-beta signaling and the fibrotic response. FASEB J 2004; 18: 816-27.

[15] Gressner AM, Weiskirchen R, Breitkopf K, et al. Roles of TGF-beta in hepatic fibrosis. Front Biosci 2002; 7: d793-d807.Q

[16] Sanderson N, Factor V, Nagy P, et al. Hepatic expression of mature transforming growth factor beta 1 in transgenic mice results in multiple tissue lesions. Proc Natl Acad Sci U S A 1995; 92: 2572-6.

[17] Kanzler S, Lohse AW, Keil A, et al. TGF-beta1 in liver fibrosis: an inducible transgenic mouse model to study liver fibrogenesis. Am J Physiol 1999; 276: G1059-68.
[18] Scheuer PJ, Maggi G. Hepatic fibrosis and collapse: histological distinction by orecin staining. Histopathology 1980; 4: 487-90.
[19] Rothuizen J. Seeking global standardisation on liver disease. J Small Anim Pract 2001; 42: 424-5.
[20] Boomkens SY, Slump E, Egberink HF, et al. PCR screening for candidate etiological agents of canine hepatitis. Vet Microbiol 2005; 108: 49-55.
[21] Spee B, Mandigers PJ, Arends B, et al. Differential expression of copper-associated and oxidative stress related proteins in a new variant of copper toxicosis in Doberman pinschers. Comp Hepatol 2005; 4: 3.
[22] Vandesompele J, De Preter K, Pattyn F, et al. Accurate normalization of real-time quantitative RT-PCR data by geometric averaging of multiple internal control genes. Genome Biol 2002; 3: RESEARCH0034
[23] Aycock RS, Seyer JM. Collagens of normal and cirrhotic human liver. Connect Tissue Res 1989; 23: 19-31.
[24] Lin Y, Xie WF, Chen YX, et al. Treatment of experimental hepatic fibrosis by combinational delivery of urokinase-type plasminogen activator and hepatocyte growth factor genes. Liver Int 2005; 25: 796-807.
[25] Milani S, Herbst H, Schuppan D, et al. In situ hybridization for procollagen types I, III and IV mRNA in normal and fibrotic rat liver: evidence for predominant expression in nonparenchymal liver cells. Hepatology 1989; 10: 84-92.
[26] Nakatsukasa H, Nagy P, Evarts RP, et al. Cellular distribution of transforming growth factor-beta 1 and procollagen types I, III, and IV transcripts in carbon tetrachloride-induced rat liver fibrosis. J Clin Invest 1990; 85: 1833-43.
[27] Palmes D, Spiegel HU. Animal models of liver regeneration. Biomaterials 2004; 25: 1601-11.
[28] Bedossa P, Paradis V. Liver extracellular matrix in health and disease. J Pathol 2003; 200: 504-15.
[29] Norman JT, Clark IM, Garcia PL. Hypoxia promotes fibrogenesis in human renal fibroblasts. Kidney Int 2000; 58: 2351-66.
[30] Inagaki Y, Kushida M, Higashi K, et al. Cell type-specific intervention of transforming growth factor beta/Smad signaling suppresses collagen gene expression and hepatic fibrosis in mice. Gastroenterology 2005; 129: 259-68.
[31] Nakamura T, Sakata R, Ueno T, et al. Inhibition of transforming growth factor beta prevents progression of liver fibrosis and enhances hepatocyte regeneration in dimethylnitrosamine-treated rats. Hepatology 2000; 32: 247-55.
[32] Ueki T, Kaneda Y, Tsutsui H, et al. Hepatocyte growth factor gene therapy of liver cirrhosis in rats. Nat Med 1999; 5: 226-30.
[33] Yasuda H, Imai E, Shiota A, et al. Antifibrogenic effect of a deletion variant of hepatocyte growth factor on liver fibrosis in rats. Hepatology 1996; 24: 636-42.
[34] Nakamura H, Siddiqui S S, Shen X, et al. RNA interference targeting transforming growth factor-beta type II receptor suppresses ocular inflammation and fibrosis. Mol Vis 2004; 10: 703-11.

Chapter 5

Functional *in vitro* studies on purified recombinant canine Hepatocyte Growth Factor

Brigitte Arends[1], Bart Spee[1], Estel Slump[1], Ted S.G.A.M. van den Ingh[2], Karin H.A. van der Heijden-Liefkens[3], Paul J.A. Sondermeijer[3], Louis C. Penning[1] and Jan Rothuizen[1]

From the Departments of [1]Clinical Sciences of Companion Animals and [2]Pathobiology, Faculty of Veterinary Medicine, Utrecht University, The Netherlands, and [3]Intervet International, Boxmeer, The Netherlands.

Manuscript in preparation

Abstract

Hepatocyte Growth Factor (HGF), the most important factor for the development and regeneration of the liver, may potentially be useful for the treatment of several liver diseases. In the present study, we report on the successful expression, purification, and *in vitro* activity of recombinant canine HGF (rcHGF) produced by means of a baculoviral expression system in High-5 cells. Biological activity of rcHGF was equal to the activity of recombinant human HGF (rhHGF), as determined in a MTT proliferation assay using a canine hepatic epithelial cell-line. Furthermore, Western blot analysis showed that rcHGF induces three different signaling pathways that are important for liver regeneration; e.g. ERK1/2, STAT3, and PKB/Akt. We conclude that rcHGF is bioactive and permits future *in vivo* evaluation of its therapeutic potentials.

Introduction

Hepatocyte growth factor (HGF) is a multifunctional growth factor, originally identified in the plasma of partially hepatectomized rats as a potent mitogen for hepatocytes in primary culture [1]. This kringle-containing heterodimeric glycoprotein is synthesized and secreted by cells of mesenchymal origin and targets a variety of epithelial and endothelial cells in an endocrine and/or paracrine fashion [2]. HGF triggers a wide variety of cellular responses through its receptor, the proto-oncogene c-MET, including mitogenic, motogenic, morphogenic, and anti-apoptotic activities [3]. Activation of the c-MET signaling pathway has been shown to play an important role in many physiological processes, including embryological development and tissue regeneration. In a variety of liver diseases, especially in patients with fulminant hepatitis, serum levels of hepatocyte growth factor (HGF) are increased [4]. Furthermore, exogenous administration of recombinant HGF or the HGF gene was found to be protective against toxin-induced acute and chronic liver failure in animal models [5-8]. To examine its relevance as a therapeutic agent, the ability of HGF to promote tissue repair and organ regeneration after injury in animal models should be extrapolated for application in human medicine. The evaluation of HGF treatment in naturally occurring canine liver diseases, presented at the veterinary clinic, may provide a tool to form a bridge between rodent animal models and spontaneous diseases in man.

Liver diseases occur frequently in dogs; the overall incidence in dogs has been estimated around 1-2% of the clinical cases [9,10]. Recently, we showed that HGF mRNA levels were also induced in canine liver diseases with chronic inflammation and cirrhosis. Furthermore, we showed an increased activation of components of three major pathways involved in regeneration of the liver; e.g. the mitogen activated protein (MAP) kinase ERK1/2, the Signal Transducers and Activators of Transcription 3 (STAT3), and the protein kinase B (PKB, also known as Akt). The results were highly comparable to the results from samples derived from cirrhotic human samples after alcohol abuse or hepatitis C infection. Therefore, chronic liver diseases in dogs are highly comparable with the human counterparts [11]. These canine liver diseases can be used as models for evaluation of novel treatment options which may also become available for human liver diseases.

In this study, we showed the *in vitro* activity of functionally active recombinant canine HGF (rcHGF). To examine its biological activity, the proliferative activity of rcHGF was compared to the activity of recombinant human HGF in a canine hepatic epithelial cell line. Furthermore, we showed that rcHGF is able to induce the main downstream signaling transduction pathways that are known to play an important

role in tissue regeneration in a canine hepatic epithelial cell-line and the frequently used Madin-Darby Canine Kidney (MDCK) cell line.

Materials and methods

HGF production

Plasmid was constructed by inserting the complete coding region of canine HGF [12] including a 6xHis tag into pFastBac1. Recombinant baculovirus expressing canine HGF was obtained with the Bac-to-Bac expression system (Invitrogen, Breda, The Netherlands). RcHGF was produced by infection of High-5 (BTI-TN-5B1-4) cells in SF900 medium (Invitrogen) containing 3 % FCS with a multiplicity of infection (m.o.i.) of 0.1. The rcHGF containing supernatant was harvested 3 days after infection and was concentrated by ultra microfiltration (NORIT Membrane Technology B.V., Enschede, The Netherlands). The concentrate was centrifuged at 100.000xg for 1 hour and the supernatant was gamma irradiated (25kGray) to inactivate residual baculovirus.

Partial purification and determination of rcHGF concentration

RcHGF was purified on a heparine-sepharose CL-6B column (Amersham Biosciences Europe, Roosendaal, The Netherlands) [13], according to the manufacturer's instructions. In short, rcHGF containing supernatant was applied to the column equilibrated with 25 mM Tris-HCl and 400 mM NaCl (pH 7.4) with a rate of 1 ml/min and a sample pressure of 0.03 Mpa. RcHGF was eluted with a continuous increasing gradient of 0.4–1.5 mM NaCl in 25 mM Tris-HCl at a flow rate of 1 ml/min. Fractions of 0,5 ml were collected for further protein determination by coomassie gel staining and Western blot analysis. Western blotting was performed under denaturing conditions. Concentration of rcHGF was determined by ELISA, based on capture with a mouse monoclonal antibody against human HGF (Lab Vision Corporation, USA) and detection was performed with a biotin labeled, polyclonal goat-anti-human HGF (Sanbio/Monosan, Uden, The Netherlands).

Cell lines and cultures

The canine bile-duct epithelial (BDE) cell line was acquired from the Amsterdam Medical Centre, Experimental Liver cell bank (Amsterdam, The Netherlands) [14]. This liver cell line is characterized by albumin and ceruloplasmin expression, data not shown. The Madin-Darby Canine Kidney (MDCK) cell line was purchased from

the American Type Culture Collection (ATCC, Cat.no. CCL-34). All cultures were maintained in DMEM (Life technologies, Inc., Invitrogen) supplemented with 10% FCS (Fetal Calf Serum Gold, PAA Laboratories GmBH, Pasching, Austria) and standard antibiotics at 37ºC with 5% CO_2 and 95% air under a humidified atmosphere.

MTT proliferation assay

The *in vitro* activity of purified rcHGF on the proliferation activity of BDE and MDCK cells was evaluated by a colormetric 3-[4,5-dimethylthiazol-2-yl]-2,5-diphenyltetrazolium bromide (MTT) assay [15]. The proliferating activity was compared to the proliferative activity of the commercially available recombinant human HGF (rhHGF) (R&D systems, Abingdon, UK). In short, cells were seeded in 96-well culture plates at a density of $1.5x10^4$ cells/100µl well in DMEM medium containing 1% FCS. After an overnight culture starvation period, rcHGF (or rhHGF) was added to the first column of the plate in triplicate to a final concentration of 300 ng/ml. The rcHGF containing medium was serially diluted three times, except for the last column (non-treated cells). After 24 hours under culture conditions, 10µl MTT (0.5 mg/ml) was added in each well and incubated at 37°C for 1.5 hours. Culture medium was decanted and the formed dark blue formazan crystals dissolved by adding 100 µl DMSO. Absorbances were measured after 15 minutes by means of a micro plate reader (BioRad, Veenendaal, The Netherlands) at 595 nm with a reference of 650 nm. The increase in absorbance is directly proportional to the number of viable cells. Proliferation activity was calculated as percentage increase in absorbance of treated cells compared to non-treated cells.

Cell treatment and Western blot analysis of c-MET, ERK1/2, STAT3, and PKB

For Western blot analysis, BDE and MDCK cells were seeded in 6-well tissue culture dishes at a density of $1.5x10^5$ cells/well. After an overnight starvation period, cells were treated with 0, 1.5, 15, or 150 ng/ml rcHGF for 5 minutes. Cells were lysed in RIPA buffer containing 1 % Igepal, 0.6 mM PhenylMethylSulfonyl-Fluoride, 17 µg/ml aprotinine, and 1 mM sodium-orthovanadate (Sigma chemical Co., Zwijndrecht, The Netherlands). Protein concentrations were obtained using a Lowry-based assay (DC Protein Assay, BioRad). Twenty µg of protein of the supernatant was denatured for 3 min at 95ºC and electroferesed on Tris-HCl polyacrylamide gels (BioRad) and the proteins were transferred onto Hybond-C Extra Nitrocellulose membranes (Amersham Biosciences Europe, Roosendaal, The Netherlands) using a Mini Trans-Blot® Cell blot-apparatus (BioRad). The used antibodies are listed in Table 1. In general, the incubation of the primary antibody was performed at

4°C over-night for all antibodies in TBS with 0.1 % Tween-20 (Boom B.V., Meppel, The Netherlands). After washing, the membranes were incubated with horseradish peroxidase-conjugated secondary antibody at room temperature for 1 h. The procedure for immunodetection was based on an ECL Western blot analysis system, performed according to the manufacturer's instructions (Amersham Biosciences Europe). Exposures were made with Kodak BioMax Light-1 films (Sigma chemical Co.). Densitometric analysis was performed with a GelDoc 2000 system using Quantity One 4.3.0 Software (BioRad).

Table 1. *Used antibodies in Western blot experiments*

Antigen	Product size (kDa)	Dilution	Manufacturer	Secondary antibody	Dilution
HGF	78	1:200	Labvision	Anti-mouse HRP	1:20,000
c-MET	145	1:750	Sigma	Anti-goat HRP	1:20,000
c-MET (Tyr)	169	1:750	Abcam	Anti-rabbit HRP	1:20,000
Stat 3	86	1:2,500	BD Biosciences	Anti-mouse HRP	1:20,000
Stat 3 (Ser727)	86	1:1,000	Cell-Signaling	Anti-rabbit HRP	1:20,000
Stat 3 (Tyr705)	86	1:1,000	Cell-Signaling	Anti-mouse HRP	1:20,000
Erk1/2	44/42	1:1,000	Cell-Signaling	Anti-rabbit HRP	1:20,000
Erk1/2 (Thr/Tyr)	44/42	1:1,500	Cell-Signaling	Anti-rabbit HRP	1:20,000
Beta-actin	40	1:2,000	Labvision	Anti-mouse HRP	1:20,000
PKB	58	1:250	BD Biosciences	Anti-mouse HRP	1:20,000
PKB (Thr 308)	58	1:1,000	Cell-Signaling	Anti-mouse HRP	1:20,000
Beta-actin	40	1:2,000	Labvision	Anti-mouse HRP	1:20,000

Results

Production and purification of rcHGF

RcHGF was produced by means of a baculoviral expression system in High-5 cells. The supernatant harvested 3 days after infection contained between 10 and 20 mg/l of rcHGF as determined by ELISA. After purification using a heparine-sepharose column, concentration was around 5 mg/l. Western-blotting showed specific rcHGF bands in collected fractions eluted at 0,8-1,2 M NaCl and a conduction of 50 - 70 mS/cm. Coomassie gel staining showed a purification of around 80% (see Figure 1).

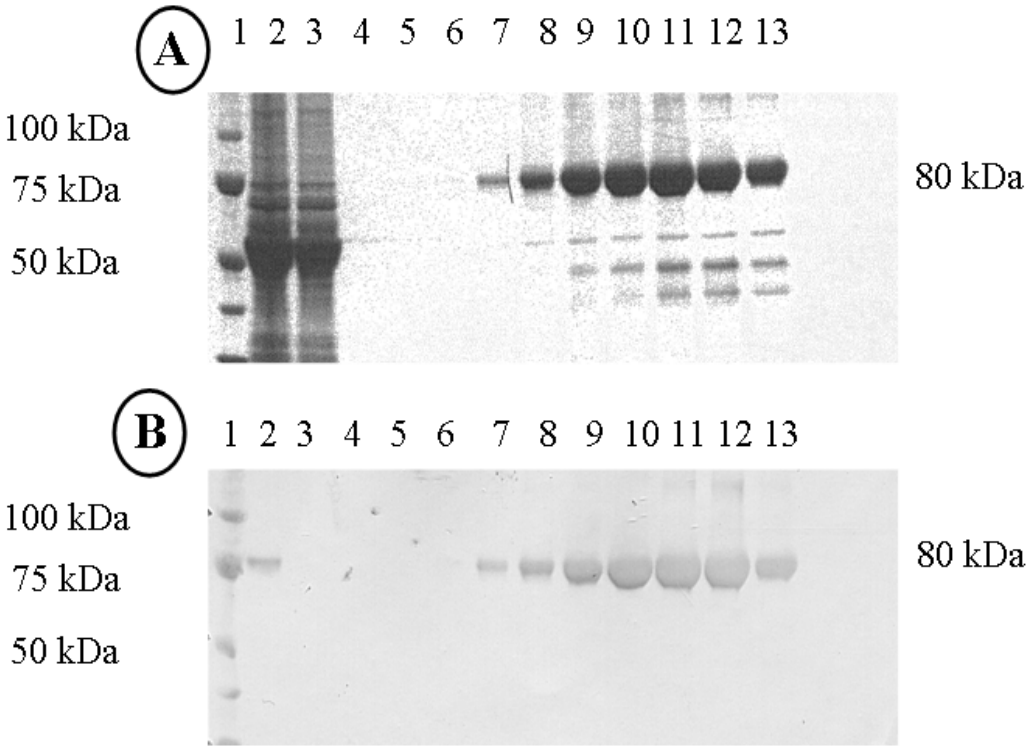

Figure 1. *Detection of the rcHGF protein on Coomassie stained gels and Western blot analysis.*
Coomasie stained gel is shown in (A); Lane 1: Biorad prestained precision marker, lane 2: RcHGFafter gamma irradiation, lane 3: RcHGF flow through, lane 4-13: RcHGF elution fractions (nr 10 to 19 of the heparine-sepharose column). Western blot analysis with HGF specific antibody is shown in (B); Lane 1: Biorad prestained precision marker, lane 2: RcHGF after gamma irradiation, lane 3: RcHGF flow through, lane 4-13: RcHGF elution fraction nr 10 to 19.

Proliferation assay (MTT)

To investigate the *in vitro* proliferation activity of the purified rcHGF, we measured cell growth of BDE cells in a MTT proliferation assay after rcHGF treatment. Results were compared with the same concentration recombinant human HGF (hHGF). As shown in Figure 2, rcHGF and hHGF stimulated cell growth in BDE cells in a dose-dependent manner. Maximum proliferation activity, for both rcHGF and hHGF, was seen at 100 ng/ml.

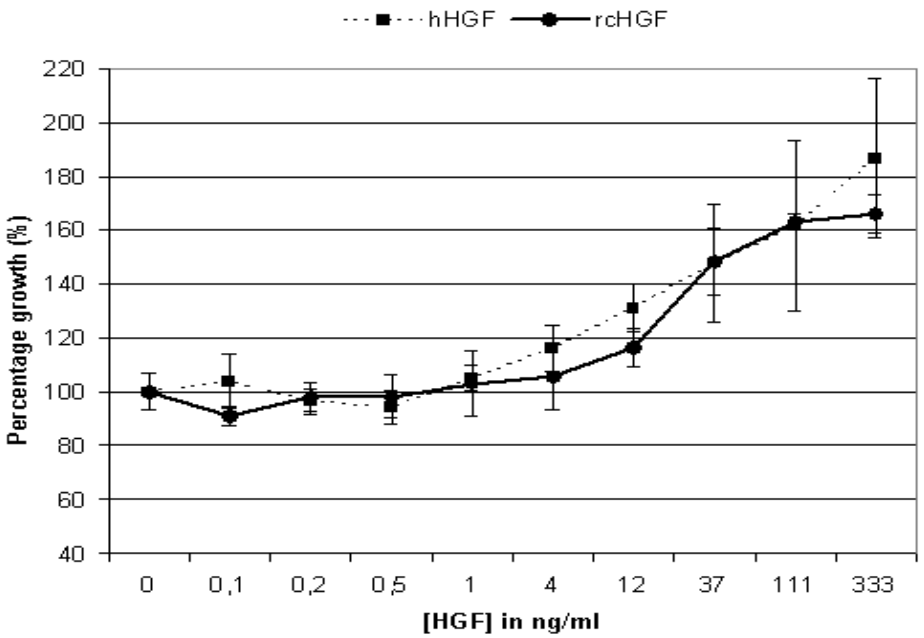

Figure 2. *MTT proliferation assay of HGF treated BDE-cells.*
Cell viability of BDE-cells after canine recombinant HGF (rcHGF) and commercially available human recombinant HGF (hHGF). Cells were treated for 24 hours with HGF after an overnight starvation period.Experiment performed in triplicate, data expressed as average ± SD.

Western blot analysis of c-MET, ERK2, STAT3, and PKB.

To further analyze the biological activity of rcHGF, Western blot analysis was performed on MDCK and BDE cells (Figure 3). We investigated rcHGF-induced activation of important transduction pathway signals that are involved in tissue regeneration; e.g. c-MET, ERK1/2, STAT3, and PKB. Results showed that the phosphorylation of the HGF receptor c-MET (169 kDa) occurred in a dose-dependent fashion in both cell lines, whereas the total c-MET (145 kDa) showed no increase after 5 minutes. From the MAP kinase pathway, ERK1/2 (particular important for c-MET elicited proliferation) was measured after rcHGF treatment. Both cell-lines showed a maximal increase in phosphorylation of ERK1/2 (42/44 kDa) at a concentration of 15 ng/ml HGF, while total ERK1/2 showed no changes in expression. From the STAT pathway, STAT3 (86 kDa) and the two phosphorylated forms (Ser727 and Tyr705) were analyzed by Western blot. Total STAT3 did not change in MDCK and BDE cells after rcHGF treatment, whereas the serine phosphorylation

was induced in both cell lines. In contrast, tyrosine phosphorylation did not show any activation upon rcHGF treatment. Finally, Western blot results showed a dose dependent activation of PKB (Thr308) in MDCK and BDE cells, whereas no changes were seen in the non-phosphorylated PKB protein (60 kDa).

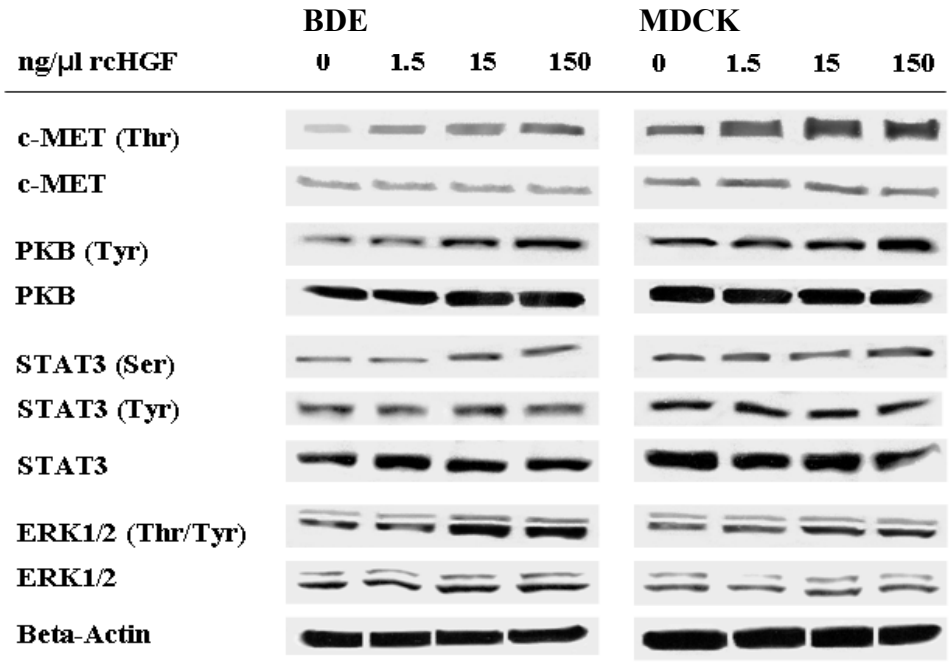

Figure 3. *Western blot analysis of c-MET, ERK2, STAT3, and PKB.*
Protein analysis of major regenerative pathways in BDE- and MDCK-cells treated with a serial dilution of rcHGF for 5 minutes.

Discussion

In the present study, we report the successful expression, purification, and *in vitro* bioactivity of recombinant canine HGF (rcHGF) produced by means of a baculoviral expression system in High-5 cells. Biological activity of rcHGF was equal to the activity of recombinant human HGF (rhHGF), as determined in a MTT proliferation assay using a canine hepatic epithelial cell-line. Furthermore, Western blot analysis showed rcHGF/c-MET induced effects on three different signaling pathways that are important for liver regeneration; e.g. ERK1/2, STAT3, and PKB/Akt.

HGF is synthesized and secreted as an inactive single-chain precursor protein that must be proteolytically cleaved between Arg494 and Val495 to form a biologically active disulfide-linked heterodimer. The proteases that are responsible for this conversion are HGF activator (HGFA) and, with a 1,000-fold lower activity, urokinase type plasminogen activator (uPA) [16,17]. Mature HGF consists of a α-chain, important for the high affinity binding to the receptor, and a β-chain that seems to play an important role in the optimal activation of the receptor for the transduction of multiple biological activities [18]. In this study, we showed that the biological activity of rcHGF, produced by High-5 cells, is similar to human rcHGF, indicating a complete conversion to the active heterodimeric form of HGF.

Biological activities of HGF are triggered by the phosphorylation of the tyrosine residue of a heterodimeric membrane-spanning tyrosine kinase receptor encoded by c-MET [19]. After binding to its receptor, c-MET binds and activates the PI-3-kinase /PKB signal transduction pathway and the Ras-mitogen-activated protein (MAP) kinase cascade [20]. These signal transduction pathways are important in tissue regeneration as they coordinately regulate cell proliferation, differentiation, motility, and survival in a wide variety of cells.

Mitogen activated protein (MAP) kinase pathways play important roles in the regulation of cell growth and differentiation in response to extracellular signals. The most extensively studied groups of MAP kinases are the ERK1/2, JNKs, and p38 kinases [21]. MAP kinases can be activated by a wide variety of different stimuli, but in general, growth factors and other mitogenic stimuli usually activate ERK1/2, while the JNK and p38 kinases are more responsive to cytokines and factors that promote growth inhibition and apoptosis [22].

STAT3 is a cytoplasmatic transcription factor that is frequently activated by cytokines through JAK-mediated tyrosine phosphorylation. After activation, STAT3 dimerizes and translocates to the nucleus, where it activates immediate early genes

that are important for liver regeneration [23]. In addition to cytokines, growth factors can also indirectly activate STAT3 by ERK, which specifically activates STAT3 at Serine727 [24,25]. Indeed, in the present study we observed a phosphorylation of ERK1/2 and STAT3 (Ser727), whereas STAT3 (Tyr727) remained equally phosphorylated in both cell lines.

The therapeutic potential of HGF has been demonstrated in various toxin-induced acute and chronic liver failure in rodent models [26]. The next step is to study these therapeutic effects by *in vivo* studies followed by evaluation in clinical cases. As shown in several rodent models, the immediate availability of the HGF protein for a relative short period may be life saving in fulminate or severe acute hepatitis [5,27-28]. The use of HGF as a therapy in dogs with spontaneously occurring liver diseases may be regarded as an important translational step to explore the clinical applicability in human medicine. It is feasible to start the first clinical studies in veterinary medicine in the near future after successful efficacy- and safety-studies of rcHGF in dogs.

In conclusion, we showed that the purified recombinant canine HGF is a biologically active recombinant protein, able to activate different signal transduction pathways that are important in tissue regeneration; e.g. ERK1/2, STAT3, and PKB/Akt. The practical use of recombinant rcHGF holds great potential in the therapeutic use of canine liver diseases and provides a rationale for translational research in man.

References

[1] Nakamura T, Nawa K, Ichihara A, et al. Purification and subunit structure of hepatocyte growth factor from rat platelets. FEBS Lett 1987, 224:311-316.

[2] Matsumoto K, Nakamura T. Hepatocyte growth factor (HGF) as a tissue organizer for organogenesis and regeneration. Biochem Biophys Res Commun 1997, 239:639-644.

[3] Bottaro DP, Rubin JS, Faletto DL, et al. Identification of the hepatocyte growth factor receptor as the c-met proto-oncogene product. Science 1991, 251:802-804.

[4] Shiota G, Okano J, Kawasaki H, et al. Serum hepatocyte growth factor levels in liver diseases: clinical implications. Hepatology 1995, 21:106-112.

[5] Yasuda H, Imai E, Shiota A, et al. Antifibrogenic effect of a deletion variant of hepatocyte growth factor on liver fibrosis in rats. Hepatology 1996, 24:636-642.

[6] Ueki T, Kaneda Y, Tsutsui H, et al. Hepatocyte growth factor gene therapy of liver cirrhosis in rats. Nat Med 1999, 5:226-230.

[7] Matsuda Y, Matsumoto K, Yamada A, et al. Preventive and therapeutic effects in rats of hepatocyte growth factor infusion on liver fibrosis/cirrhosis. Hepatology 1997, 26:81-89.

[8] Kosai K, Matsumoto K, Funakoshi H, et al. Hepatocyte growth factor prevents endotoxin-induced lethal hepatic failure in mice. Hepatology 1999, 30:151-159.

[9] Rothuizen J, Meyer HP. History, physical examination, and clinical signs of liver disease. In: Ettinger J, Feldman EC (eds) Textbook of veterinary internal medicine, 5th ed, Saunders, Philadelphia, 2000:1272-1277.

[10] Rothuizen J. Diseases of the liver and biliary tract. In: Dunn J (ed) Textbook of small animal medicine. Saunders, London, 1999:498-525.

[11] Spee B, Penning LC, van den Ingh TS, et al. Regenerative and fibrotic pathways in canine hepatic portosystemic shunt and portal vein hypoplasia, new models for clinical hepatocyte growth factor treatment. Comp Hepatol 2005, 4:7.

[12] Nakamura T, Nishizawa T, Hagiya M, et al. Molecular cloning and expression of human hepatocyte growth factor. Nature 1989, 342:440-443.

[13] Depuydt CE, Zalata A, Falmagne JB, et al. Purification and characterization of hepatocyte growth factor (HGF) from human seminal plasma. Int J Androl 1997, 20:306-314.

[14] Oda D, Savard CE, Nguyen TD, et al. Dog pancreatic duct epithelial cells: long-term culture and characterization. Am J Pathol 1996, 148:977-985.

[15] Carmichael J, DeGraff WG, Gazdar AF, et al. Evaluation of a tetrazolium-based semiautomated colorimetric assay: assessment of radiosensitivity. Cancer Res 1987, 47:943-946.

[16] Shimomura T, Miyazawa K, Komiyama Y, et al. Activation of hepatocyte growth factor by two homologous proteases, blood-coagulation factor XIIa and hepatocyte growth factor activator. Eur J Biochem 1995, 229:257-261.

[17] Naldini L, Tamagnone L, Vigna E, et al. Extracellular proteolytic cleavage by urokinase is required for activation of hepatocyte growth factor/scatter factor. EMBO J 1992, 11:4825-4833.

[18] Matsumoto K, Kataoka H, Date K, et al. Cooperative interaction between alpha- and beta-chains of hepatocyte growth factor on c-Met receptor confers ligand-induced receptor tyrosine phosphorylation and multiple biological responses. J Biol Chem 1998, 273:22913-22920.

[19] Borowiak M, Garratt AN, Wustefeld T, et al. Met provides essential signals for liver regeneration. Proc Natl Acad Sci U S A 2004, 101:10608-10613.

[20] Okano J, Shiota G, Matsumoto K, et al. Hepatocyte growth factor exerts a proliferative effect on oval cells through the PI3K/AKT signaling pathway. Biochem Biophys Res Commun 2003, 309:298-304.

[21] Seger R, Krebs EG. The MAPK signaling cascade. FASEB J 1995, 9:726-735.

[22] Taub R. Adenovirus-mediated overexpression of activin beta(C) subunit accelerates liver regeneration in partially hepatectomized rats. J Hepatol 2005, 43:751-753.

[23] Terui K, Ozaki M. The role of STAT3 in liver regeneration. Drugs Today (Barc) 2005, 41:461-469.

[24] Gao B. Cytokines, STATs and liver disease. Cell Mol Immunol 2005, 2:92-100.

[25] Nakagami H, Morishita R, Yamamoto K, et al. Anti-apoptotic action of hepatocyte growth factor through mitogen-activated protein kinase on human aortic endothelial cells. J Hypertens 2000, 18:1411-1420.

[26] Ueki T, Kaneda Y, Nakanishi K, et al. Hepatocyte growth factor gene therapy of liver cirrhosis in rats. Nat Med 1999, 5:226-230.

[27] Matsuda Y, Matsumoto K, Yamada A, et al. Preventive and therapeutic effects in rats of hepatocyte growth factor infusion on liver fibrosis/cirrhosis. Hepatology 1997, 26:81-89.

[28] Kosai K-I, Matsumoto K, Funasoshi H, et al. Hepatocyte growth factor prevents endotoxin-induced lethal hepatic failure in mice. Hepatology 1999, 30:151-159.

Chapter 6

Copper Metabolism and Oxidative Stress in Chronic Inflammatory and Cholestatic Liver Diseases in the Dog

Bart Spee[1], Brigitte Arends[1], Ted S.G.A.M. van den Ingh[2],
Louis C. Penning[1], and Jan Rothuizen[1]

From the Departments of [1]Clinical Sciences of Companion Animals and
[2]Pathobiology, Faculty of Veterinary Medicine, Utrecht University, the Netherlands.

Submitted

Abstract

Inherited defects of copper metabolism resulting in hepatic copper accumulation and oxidative-stress may cause different breed-associated forms of hepatitis. Biliary excretion is the major elimination route of copper, therefore increased hepatic copper levels could also be caused by cholestasis. The aim of this study was to find criteria to determine whether copper-accumulation is primary or secondary to hepatitis. Liver samples of Bedlington terriers with copper toxicosis (CT) and non-copper associated breeds with chronic extrahepatic cholestasis (EC) or chronic hepatitis (CH) in comparison with healthy dogs were used. Copper metabolism was analyzed using histochemical staining (copper levels) and quantitative RT-PCR (Q-PCR) on copper excretion/-storage (ATOX1, COX17, ATP7A, ATP7B, CP, MT1A, MURR1, XIAP). Oxidative stress was measured by determining GSH/GSSG ratios and gene-expression (SOD1, CAT, GSHS, GPX1, CCS, p27KIP, Bcl-2). Results showed 5+ copper in CT, but no or 1-2+ copper in EC and CH. Most gene-products for copper metabolism remained at control levels. Three clear exceptions were observed in CT; 3-fold mRNA increase of ATP7A and XIAP and complete absence of MURR1. The only quantitative differences between the diseases and the control group were observed regarding oxidative stress, confirmed by reductions in all GSH/GSSG ratios. We conclude that 3+ or higher histochemical detection of copper indicates a primary copper storage disease. The expression profile of copper-associated genes can be used as a reference for future studies on copper-associated diseases. All three diseases have reduced protection against oxidative stress, opening a rationale to use anti-oxidants as possible therapy.

Introduction

Copper is an integral part of many important enzymes involved in several vital biological processes [1]. In humans the only copper storage disease of which the molecular background is resolved is Wilson's disease; unresolved hepatic copper storage diseases are Indian Childhood Cirrhosis and Endemic Infantile Tyrolean Cirrhosis [2,3]. A major pathogenetic pathway is the formation of highly reactive oxygen species (ROS) such as hydroxyl radicals, by accumulated copper [4]. As in man, in dogs hepatic copper accumulation may cause hepatitis which ultimately causes cirrhosis. Copper associated hepatitis has been described in dog breeds such as Bedlington terriers, Doberman pinschers, Sky terriers, West-Highland white terriers, Dalmatians, Anatolian shepherds, and Labrador retrievers [5-7]. Copper Toxicosis (CT) in Bedlington terriers is an autosomal recessive disorder causing impaired biliary copper excretion [8]. The resulting progressive lysosomal accumulation of copper becomes histologically evident at one year of age [9,10]. Recently the genetic defect in Bedlington terriers has been ascribed to a deletion of exon 2 of the *MURR1* (*COMMD1*) gene [9]. In all other dog breeds the molecular background of the disease is unknown. Therefore it is uncertain whether increased hepatic copper is the cause or consequence of the disease. Cholestasis, which is a sequel of most parenchymal liver diseases, could cause a reduced biliary copper excretion and consequently copper accumulation.

Copper is intracellularly bound to specific proteins [10]. Small copper-binding proteins, denoted copper chaperones, distribute copper to specific intracellular destinations. ATOX1 for instance, delivers copper to ATPases, CCS distributes copper to Cu/Zn superoxide dismutase (SOD1), COX17 delivers copper to cytochrome c oxidase in the mitochondria. MURR1 is implicated in the lysosomal copper storage and excretion into bile [11]. The ATPases ATP7A and ATP7B transport copper to the cuproenzymes and ameliorate excretion of excess copper. Ceruloplasmin (CP) is a metalloprotein which binds copper during synthesis after which the complex is secreted into serum. Metallothionein 1A (MT1A) is a small intracellular protein capable of chelating several metal ions, including copper [12]. XIAP is an X-linked inhibitor of apoptosis recently associated with MURR1 [13].

Excess copper can induce oxidative stress which could lead to chronic inflammation [15,16]. Oxidative stress occurs when cells are exposed to increased ROS due to enhancement of reactive oxygen production or inhibition of its removal. Most of the anti-oxidants can be grouped into either enzymatic or non-enzymatic defenses [16]. The enzymatic defense against oxidative stress consists of several tightly regulated proteins such as Cu/Zn superoxide dismutase (SOD1) and Catalase (CAT). Non-

enzymatic defenses are exerted by molecules such as alpha-tocopherol, beta-carotene, ascorbate, and a ubiquitous low molecular thiol component, Glutathione [17]. The synthesis of Glutathione from glutamate, cysteine, and glycine is catalyzed by two cytosolic enzymes, γ-glutamilcysteine synthetase (GCS) and GSH synthetase (GSHS). Glutathione is mainly present in its reduced form (GSH); during oxidative stress glutathione is converted to the oxidized form GSSG. GPX1 another main antioxidant, converts GSH into its oxidized form GSSG [18]. The redox status of GSH depends on the relative amounts of the reduced and oxidized forms of glutathione (GSH/GSSG) and appears to be a critical determinant in the cell [19].

In this study we investigated the presence of copper and its possible role in inflammatory and cholestatic chronic liver diseases. To study the effect of cholestasis, we examined dogs with the most pronounced form caused by chronic extrahepatic cholestasis (EC) due to bile duct obstruction. In comparison we have studied idiopathic chronic hepatitis (CH) in dogs of breeds not associated with copper accumulation, and the only proven inherited form of copper toxicosis in dogs, CT in Bedlington terriers. We have previously shown that copper accumulation causes a decrease in enzymatic and non-enzymatic ROS defenses and affects several copper associated gene products [20]. Therefore, we analyzed copper metabolism pathways and ROS defenses including glutathione metabolism in these chronic liver diseases.

Materials and Methods

Dogs

Dogs were kept privately as companion animals. The dogs were presented to the Department of Clinical Sciences of Companion Animals, Utrecht University for spontaneously occurring liver disease. All samples were obtained after fully informed consent of the owner. The procedures were approved by the Utrecht University Ethical Committee as required under Dutch legislation.

Groups

The presence of a liver disease was confirmed by finding increased plasma activities of the liver enzymes AP and/or ALT, and increased plasma bile acid (BA) concentration. Liver tissue of all dogs was obtained using the Menghini (14-gauge) aspiration technique under local anesthesia. Two biopsies were used for histopathological examination and directly fixed in 10% neutral buffered formalin. Two other biopsies were collected in a cryo vial, snap-frozen in liquid nitrogen, and stored at -

70^0C for future measurements. Sections (4μm) of the fixed and paraffin-embedded biopsies were stained with haematoxylin eosin, the Van Gieson's stain, the reticulin stain according to Gordon and Sweet, and rubeanic acid staining for copper. The diagnoses of CT, EC, and CH were made according to the criteria of the World Small Animal Veterinary Association (WSAVA) Liver Diseases and Pathology Standardization Research Group [21]. All histological examinations were performed by one experienced board certified veterinary pathologist. The dogs were also evaluated with abdominal ultrasonography, using a high-definition Ultrasound system with a 4–7 MHz broad-band Faced-array transducer (HDI 3000 ATL, Philips Medical Systems, Eindhoven, The Netherlands).

Four groups were included in this study:

1) *Healthy group* (n = 12 dogs). Age-matched clinically healthy dogs with normal liver enzymes and bile acids. Histopathology of the liver revealed no abnormalities.
2) *Copper toxicosis group* (CT, n = 12 dogs). Plasma liver enzymes AP and ALT as well as BA were at least three times elevated above normal reference values. Abdominal ultrasound revealed a normally sized or somewhat small liver with a slightly or moderately irregular structure. Histopathology showed chronic hepatitis often with histological evidence of cirrhosis associated with marked copper accumulation. All dogs were Bedlington terriers carrying a deletion of exon-2 of the *MURR1 (COMMD1)* gene and were detected as previously described [22].
3) *Extrahepatic cholestasis group* (EC, n = 6 dogs). The presence of chronic extrahepatic cholestasis was diagnosed by the presence of dilated and often tortuous extrahepatic bile ducts at ultrasonography, in combination with the characteristic histopathological lesions. There was hepatocanalicular cholestasis in the parenchyma. The portal areas showed fibrosis with bile duct proliferation and periductal concentric fibrosis, and inflammation limited to the portal areas with pigment-laden macrophages, lymphocytes, plasma cells and neutrophils. The plasma AP, ALT and BA levels were increased at least three times elevated above the upper reference values. All dogs had clinical icterus.
4) *Chronic Hepatitis group* (CH, n = 12 dogs). Chronic hepatitis was characterized histologically by mononuclear or mixed inflammation, apoptosis and necrosis of hepatocytes, fibrosis and in some cases evidence of cirrhosis with regenerative nodules of hepatic parenchyma. The disease was chronic in all cases as judged by the presence of fibrosis. Plasma AP, ALT, and BA were at least three times elevated above upper normal reference values. Abdominal ultrasound revealed a small liver with an irregular structure. All cases of hepatitis were idiopathic. With PCR or RT-PCR performed on DNA, respectively cDNA isolated from liver tissue, potential infectious agents were excluded (CAV-1, hepadna-, adeno-, or

parvoviridae, *Helicobacter* spp, *Leptospira* spp, *Borrelia* spp) [23]. None of the dogs was of a breed known for copper associated hepatitis.

Histological grading of copper accumulation

The presence of copper was evaluated semi-quantitatively scored in a scale from 0 to 5+ as previously described, as well as with respect to its localization in the liver lobules [24]. The slides were examined by one board-certified veterinary pathologist.

Quantitative PCR and statistical methods

Quantitative real-time PCR (Q-PCR) was performed on a total of 15 gene products involved in copper metabolism (ATOX1, COX17, ATP7A, ATP7B, CP, MT1A, MURR1, and XIAP), oxidative stress defences (SOD1, CAT, GSHS, GPX1 and CCS), and cell homeostasis (p27KIP and Bcl-2). The concentration of mRNA was determined after a Reverse Transcription (RT) step, by real-time quantitative PCR using appropriate primers (Table 1) as previously described [20]. In short, Q-PCR was based on the high affinity double-stranded DNA-binding dye SYBR® green I (BMA, Rockland, MA). For each experimental sample, the amount of the gene of interest and of the two independent endogenous references (glyceraldehyde-3-phosphate dehydrogenase (GAPDH) and hypoxanthine phosphoribosyl transferase (HPRT)) was determined from the appropriate standard curve in autonomous experiments. If relative amounts of GAPDH and HPRT were constant for a sample, data were considered valid and the average amount was used in the study. Results were normalized according to the average amount of the endogenous references. The normalized values were divided by the normalized values of the healthy group to generate relative expression levels.

The relative gene-expression of each gene-product was used as the basis for all comparisons. The results were assessed for normality using the Kolmogorov Smirnoff and the Levene's test. The data were not normally distributed; therefore the non-parametric (Kruskal-Wallis) analysis of variance was used for all comparisons. Post-test analysis was performed with a Mann-Whitney test ($P < .05$). Analysis was performed using SPSS software (SPSS Benelux BV, Gorinchem, the Netherlands).

GSH/GSSG-assay

The total amount of GSH was determined by a modified version of a total Glutathione Determination Colorimetric Microplate assay according to Allen et al. [25], based on the original Tietze macro assay [26]. In short, 25 µl of the cell-lysate (1 mg/ml) was added in triplicate in a 96-wells plate. The lysates were incubated for 5 minutes with 50 µl of 1,5 mM DTNB, and 50 µl GSH reductase (7.5 U/ml) (Sigma). To start the reaction 50 µl of NADPH was added to the wells (Sigma). Absorbance at 450 nm was measured immediately after the NADPH addition and after 4 minutes. The rate of TNB production was measured in delta absorbance per minute and was directly proportionate with the amount of GSH in the samples. To determine the amount of GSSG, GSH was first trapped with 3 mM 1-methyl-2-vinylpyridine triflate (Sigma-Aldrich Chemie B.V., Zwijndrecht, The Netherlands). A standard curve of GSH (0-20 µM) was used to determine the GSH and GSSG concentrations in the samples. Samples were normalized to the amount of total protein as determined by a Lowry-based assay (DC Protein Assay, BioRad, Veenendaal, The Netherlands).

Table 1. *Nucleotide Sequences of Dog-Specific Primers for Quantitative Real-Time PCR*

Gene	F/R	Sequence (5'-3')	Tm (°C)	Product size (bp)	Accession number
	F	TGT CCC CAC CCC CAA TGT ATC	58	100	AB038240
	R	CTC CGA TGC CTG CTT CAC TAC CTT			
HPRT	F	AGC TTG CTG GTG AAA AGG AC	56	100	L77488 /
	R	TTA TAG TCA AGG GCA TAT CC			L77489
SOD1	F	TGG TGG TCC ACG AGA AAC GAG ATG	64	99	AF346417
	R	CAA TGA CAC CAC AAG CCA AAC GAC T			
CAT	F	TGA GCC CAG CCC TGA CAA AAT G	62	119	AB012918
	R	CTC GAG CCC GGA AAG GAC AGT T			
GSHS	F	CTG GAG CGG CTG AAG GAC A	62	131	AY572226
	R	AGC TCT GAG ATG CAC TGG ACA			
GPX1	F	GCA ACC AGT TCG GGC ATC AG	62	123	AY572225
	R	CGT TCA CCT CGC ACT TCT CAA AA			
CCS	F	TGT GGC ATC ATC GCA CGC TCT G	64	96	AY572228
	R	GGG CCG GCC TCG CTC CTC			
p27KIP	F	CGG AGG GAC GCC AAA CAG G	60	90	AY455798
	R	GTC CCG GGT CAA CTC TTC GTG			
Bcl-2	F	TGG AGA GCG TCA ACC GGG AGA TGT	61	87	AB116145
	R	AGG TGT GCA GAT GCC GGT TCA GGT			
ATOX1	F	ACG CGG TCA GTC GGG TGC TC	67	137	AF179715
	R	AAC GGC CTT TCC TGT TTT CTC CAG			
COX17	F	ATC ATT GAG AAA GGA GAG GAG CAC	60	127	AY603041
	R	TTC ATT CTT CAA GGA TTA TTC ATT TAC			
ATP7A	F	ĈTA CTG TCT GAT AAA CGG TCC CTA AA	50	99	AY603040
	R	TGT GGT GTC ATC ATC TTC CCT GTA			
ATP7B	F	GGT GGC CAT CGA CGG TGT GC	56	136	AY603039
	R	CGT CTT GCG GTT GTC TCC TGT GAT			
CP	F	AAT TCT CCC TTC TGT TTT TGG TT	62	97	AY572227
	R	TTG TTT ACT TTC TCA GGG TGG TTA			
MT1A	F	AGC TGC TGT GCC TGA TGT G	64	130	D84397
	R	TAT ACA AAC GGG AAT GTA GAA AAC			
MURR1	F	GAC CAA GCT GCT GTC ATT TCC AA	58	122	AY047597
	R	TTG CCG TCA ACT CTC CAA CTC A			
XIAP	F	ACT ATG TAT CAC TTG AGG CTC TGG TTT	54	80	AY603038
	R	ÂGT CTG GCT TGA TTC ATC TTG TGT ATG			

F: Forward primer; R: reversed primer

Results

Copper-staining

No copper accumulation was detected in the healthy control group and were therefore deemed copper negative (0). In the copper toxicosis (CT) group all samples showed a marked copper-staining (5+) with massive copper accumulation in the hepatocytes diffusely throughout the liver parenchyma and macrophages in inflammatory foci (see example Figure 1A). In the chronic extrahepatic cholestasis (EC) group no copper was found in two out of six dogs. In the other dogs a slight to moderate degree of copper staining (1-2+) was seen centrolobularly (see example Figure 1B), and in one case there was also a slight stain in the periportal hepatocytes (see Figure 1C). In the chronic hepatitis (CH) group no positive copper staining was found in six out of twelve dogs. In the other samples a slight to moderate degree of copper staining (1-2+) was seen in the hepatocytes and in one case within some macrophages (see example Figure 1D).

Gene-expression of copper metabolism related gene-products

The relative amount of mRNA coding for proteins involved in copper metabolism was measured to gain insight into the pathogenesis of copper accumulation in the liver. Statistically significant differences (Kruskal-Wallis test) was identified in the expression of mRNA encoding COX17 ($P = .017$), ATP7A ($P = .008$), ATP7B ($P = .016$), CP ($P = .047$), MT1A ($P < .001$), MURR1 ($P = .040$), and XIAP ($P = .007$). No significant differences (Kruskal-Wallis test) was identified in the expression of mRNA encoding ATOX1 ($P = .959$). COX17, a copper chaperone, was halved in gene-expression in the CT-group (Figure 2). The mRNA levels of ATP7A were unchanged in the CH and EC-group; interestingly ATP7A was significantly increased in the CT-group. On the other hand ATP7B was inhibited in all groups, with halved mRNA levels in the CT and EC-group, and a 3-fold decrease in the CH-group. Ceruloplasmin was equal at the gene-expression level in the EC and CH-group towards control, and halved in the CT-group. Metallothionein (MT1A), was inhibited two-fold at the gene-expression level in the CH-group, and halved in the CT-group towards control. MURR1 was equally expressed in the CH and EC-group towards control. The absence of MURR1 as seen in the CT-group was expected as these primers were designed on the exon which is deleted in these Bedlington terriers. XIAP was halved at gene-expression level in the EC-group, but was doubled in the CT-group towards control. Overall, the reductions as seen in MURR1 mRNA and increases in ATP7A and XIAP mRNA seem to be exclusive for the CT-group com-

pared to the other diseases. The mRNA levels of the copper chaperone ATOX1 remained equal in all groups.

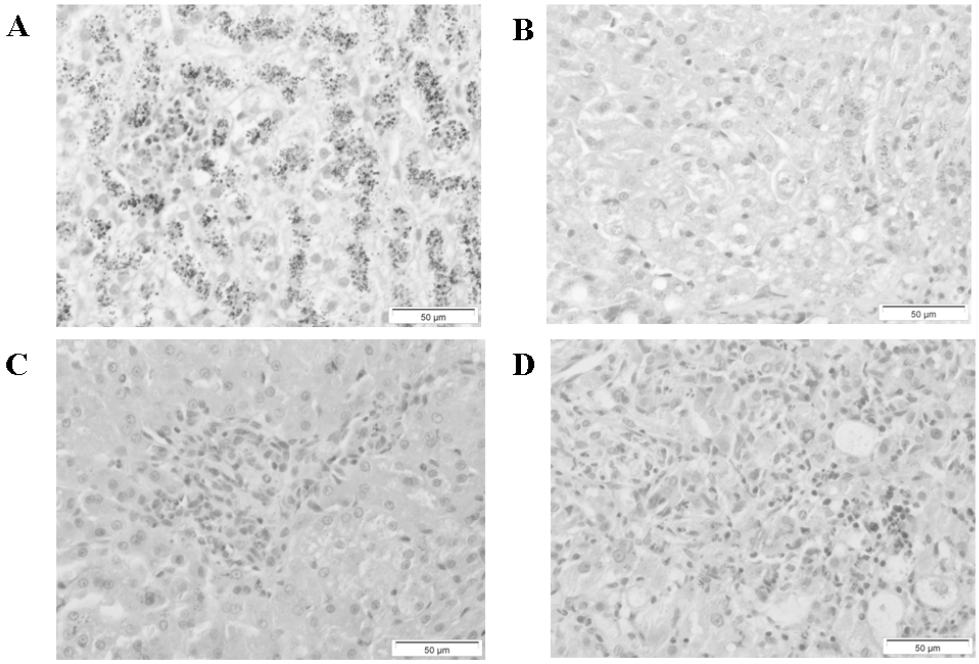

Figure 1. *Copper staining.*
Examples of Rubeanic acid staining on Copper Toxicosis with 5+ copper shown in (A), Extrahepatic cholestasis with 1-2+ centrolobular staining (B), Extrahepatic cholestasis with staining in periportal hepatocytes in (C), and Chronic hepatitis with 1-2+ copper shown in (D). Color-figure see Appendix 3, page 222.

Gene-expression measurements on oxidative stress markers, apoptosis, and cell-proliferation

To gain insight into oxidative stress during copper toxicosis, chronic extrahepatic cholestasis, and chronic hepatitis we first measured mRNA levels on several important gene products by means of Q-PCR. Statistically significant differences (Kruskal-Wallis test) was identified in the expression of mRNA encoding SOD1 ($P = .004$), CAT ($P = .003$), GSHS ($P = .002$), GPX1 ($P < .001$), CCS ($P = .002$), and p27KIP ($P = .014$). No significant differences (Kruskal-Wallis test) was identified in the expression of mRNA encoding Bcl-2 ($P = .227$). SOD1 and CAT were inhibited 3-fold in the CT-group compared to healthy controls (Figure 3). A two-fold reduction in mRNA levels of both genes was also seen in the EC and CH-groups. GSHS mRNA levels were equal to control in CH but halved in EC and CT-groups. GPX1 was induced in the CT and CH-group, and remained equal in the EC-group towards control. The mRNA levels of CCS were inhibited 3-fold in the CT and CH-group, and halved in the EC-group. Measurements on the cell-cycle inhibitor p27kip showed a large decrease in mRNA levels in the CH-group (5-fold), and remained equal to control in the EC and CT-group. Overall, the reductions as seen with CAT and GSHS seem to be exclusive for the CT-group compared to the other diseases. One anti-apoptotic marker Bcl-2 showed no change at the gene-expression level in any of the groups.

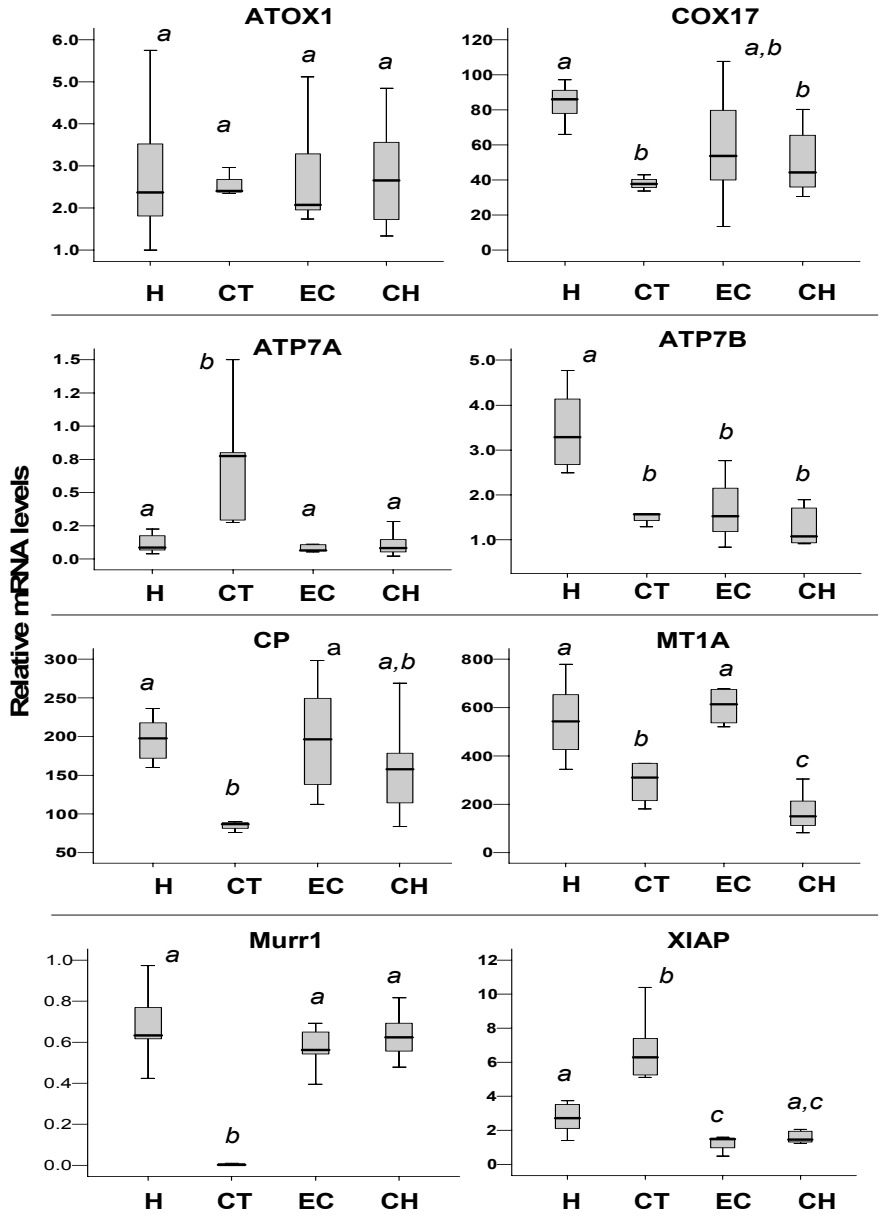

Figure 2. *Box plots of quantitative Real-Time PCR for copper metabolism related gene products. Relative expression of mRNA levels in copper toxicosis (CT), extrahepatic cholestasis (EC), and chronic hepatitis (CH). After initial analysis of variance with the Kruskal-Wallis test (see results), post-test was performed with a Mann-Whitney test for analysis between groups. Different letters above bars indicate when the median differed significantly (P < .05).*

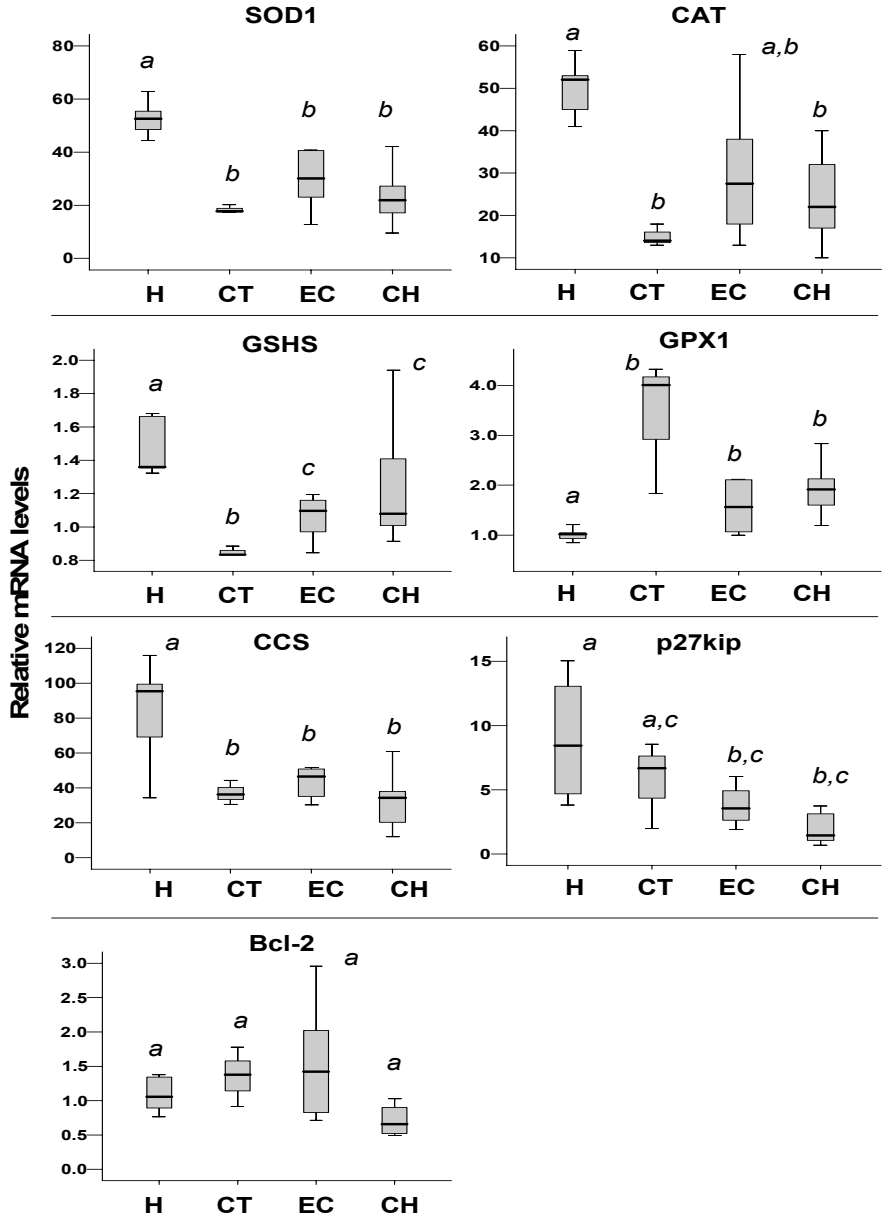

Figure 3. *Box plots of quantitative Real-Time PCR for oxidative stress and cell homeostasis related gene products. Relative expression of mRNA levels in copper toxicosis (CT), extrahepatic cholestasis (EC), and chronic hepatitis (CH). After initial analysis of variance with the Kruskal-Wallis test (see results), post-test was performed with a Mann-Whitney test for analysis between groups. Different letters above bars indicate when the median differed significantly (P < .05).*

GSH/GSSG measurements

To indicate the levels of oxidative stress, we measured the reduced glutathione (GSH) and its oxidized form GSSG. In Figure 4A, all disease groups showed a significant decrease, up to three-fold, of GSH in the liver. In contrast, the GSSG levels (Figure 4B) were significantly increased in all groups, with the highest values in the dogs with EC, which had on average a three-fold increase of GSSG. Consequently the GSH/GSSG ratios were decreased in all groups; seven-fold in the CT-group, six-fold in the EC-group, and four-fold in the CH-group (Figure 4C).

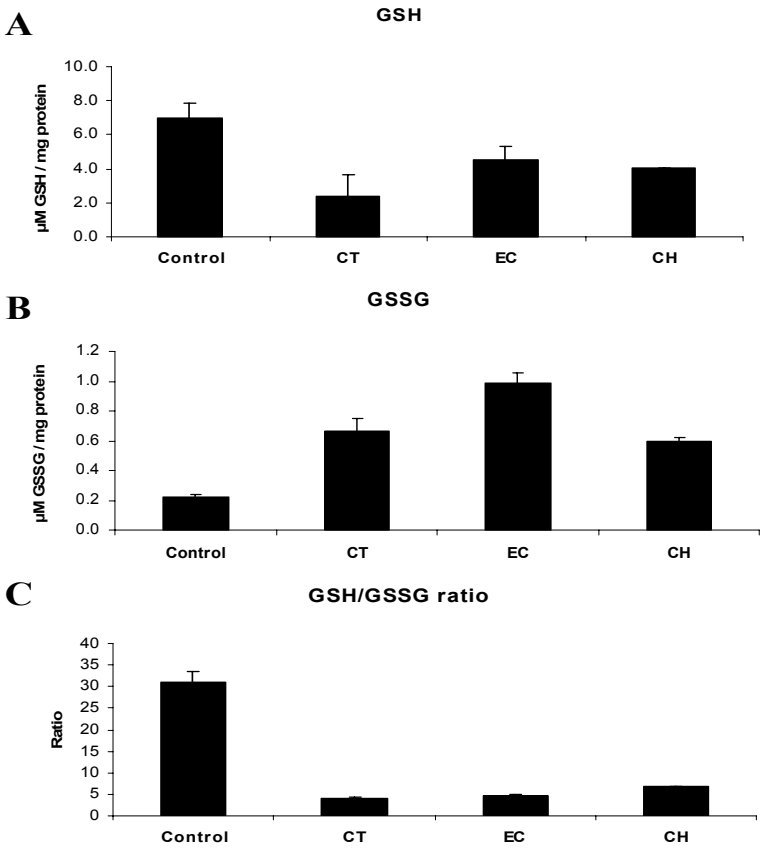

Figure 4. *Glutathione measurements.*
GSH levels normalized against the amount of protein are shown in (A), GSSG levels normalized against the amount of protein are shown in (B), and GSH/GSSG ratios are shown in (C).

Discussion

In the present study we analyzed copper metabolism and oxidative stress in three forms of chronic liver disease in the dog. Although copper is an essential component of different vital proteins, most of the ingested copper is in excess and has to be eliminated by the liver in order not to become toxic. To date, different intracellular routes of copper are known in detail [11], which are essential in defending the cell against damage and in eliminating copper by biliary excretion. The central role of the liver in copper homeostasis makes it also the most important target organ if any of the above processes fails. Besides copper-toxicosis in Bedlington terriers, there are a number of dog breeds with an increased prevalence of hepatitis associated with copper accumulation [27]. Examples are Dalmatians, Labrador retrievers, West-Highland white terriers, Skye terriers, and Anatolian shepherds. It is currently hard to decide whether copper accumulation is the primary event causing these forms of hepatitis, or secondary due to impaired copper handling. Because biliary excretion is the principal route of copper elimination, cholestasis could cause copper accumulation. The present study was undertaken to differentiate between primary and secondary copper accumulation. To this end, we have not only included two forms of hepatitis (copper- and non copper-associated) but also the most pronounced form of cholestasis, chronic extrahepatic bile duct obstruction (EC). EC may reflect the effect of cholestasis on copper accumulation, and helps interpret copper effects in more modest forms of intrahepatic cholestasis in hepatitis.

Observations on the histological grading of copper in CT showed a marked diffuse copper accumulation in the hepatocytes and focally in macrophages, in agreement with earlier reports [6,22]. On the other hand, in EC and CH there were no copper granules detectable in respectively 33 and 50 percent of the cases. The rest showed only a slight to moderate degree of copper staining. This implies that copper accumulation is not a consistent feature and never exceeds moderately increased copper levels. Copper may thus be of minor importance in prolonged idiopathic inflammation (CH) or cholestasis (EC).

Comparing the differential expression profiles of diseases with varying levels of copper accumulation and severity of inflammation allowed us to discriminate between direct copper-induced damage and damage inflicted by the infiltrating inflammatory cells. The large differences between the three diseases, with respect mRNAs for the copper handling proteins, were limited to ATP7A and XIAP. The large increase in XIAP and ATP7A in Bedlington terriers lacking functional MURR1 is most likely a compensatory effect to overcome complete absence of MURR1 [28]. In the EC and CH-group no significant changes in mRNA levels were found in the

excretory copper proteins, ATP7A, CP, and MURR1. Perhaps only the decrease in ATP7B mRNA has had an effect to produce slight accumulation of copper in the EC and CH-group. MT1A mRNA as well as protein levels are known to increase after acute copper administration [29]. Surprisingly the mRNA level in the CT and CH-group showed significant decreases in metallothionein transcription. The majority of copper is intracellularly bound to metallothionein and stored in lysozomes as copper-metallothionein complexes. Therefore, it is highly probable that, despite lowered mRNA levels, metallothionein protein levels are increasingly present in the hepatocytes during CT.

With respect to the defense against oxidative stress, the expression profiles for EC and CH were similar. Apparently cholestasis and/or inflammation reduced mRNA expression of SOD1 and CAT. However, these reductions were greater in the CT-group. We conclude that, although copper is a major trigger for oxidative stress, diseases with primary copper accumulation cannot be distinguished from primary cholestatic or inflammatory diseases based on their reaction profile when exposed to ROS.

Non-enzymatic defenses against oxidative stress showed marked reductions in glutathione synthesis (GSHS) in the CT and EC-group although lowest in CT. GSH measurements corroborated these measurements where the lowest GSH level was seen in the CT-group. A similar reduction of GSH was seen in the EC- and CH-groups. Interestingly, the amount of GSSG, the oxidized form of glutathione, showed inductions in all diseases with the highest amount in the EC-group. Consequently, GSH/GSSG ratios were decreased in all diseases with the highest reduction in the CT-group. A similar induction of the GSSG and a reduced GSH/GSSG ratio has been reported in rats with bile-duct ligation [30]. Hepatic depletion of GSH occurs also in human Wilson's disease and acetaminophen-induced liver toxicity [16,31]. Recently, a reduction in GSH levels was also shown in copper toxicosis of Doberman pinchers [20]. Overall, the GSH depletion in all copper toxicosis related diseases (Wilson's, LEC-rats, and Bedlington Terrier Copper Toxicosis), but also in EC and idiopathic hepatitis seems to be a critical factor in the hepatocellular damage.

The use of anti-oxidants or GSH esters may be effective in treating these liver pathologies. However, oral administration of GSH in healthy and GSH depleted subjects was not clinically beneficial [32]. Alternative medications could be ascorbic acid, D-penicillamine, and zinc. The GSH precursor S-adenosylmethionine (SAM-e or AdoMet) has already been shown to reduce oxidative stress levels in cultured primary hepatocytes [33]. Furthermore, in cirrhotic rat models SAM-e inhibited collagen-I production which could ameliorate liver fibrosis [34]. Because of the de-

crease in oxidative stress defenses (enzymatic and non-enzymatic), the use of SAM-e could be considered in dogs with CT, but also in other inflammatory and/or cholestatic liver diseases.

To our knowledge this is the first study to show the effects of copper toxicosis, chronic hepatitis and extrahepatic cholestasis on copper metabolism and oxidative stress. Results clearly showed that cholestasis and inflammation cause no or only limited copper accumulation. Results clearly showed that even in severe cases such as chronic extrahepatic cholestasis only limited copper accumulation was found, indicating that cholestasis does not increase copper levels. Similarly inflammation did not seem to induce these copper levels. ATP7B is the only gene-product in the copper metabolic pathway affected by both cholestasis and idiopathic hepatitis. This implies that high increases of copper in the liver (>3+) and/or changes in the expression of copper metabolic genes, other than ATP7B, indicate the presence of a primary disease of copper metabolism. These findings may help to determine the (inherited) nature of potential primary copper storage diseases in different dog breeds with hepatopathies. Finally, the reductions in defenses against oxidative stress in all chronic liver diseases studied may imply that therapeutic approaches against oxidative stress have a broad indication in canine liver diseases.

References

[1] Valko M, Morris H, Cronin MT. Metals, toxicity and oxidative stress. Curr Med Chem 2005, 12:1161-1208.

[2] Muller T, Feichtinger H, Berger H, et al. Endemic Tyrolean infantile cirrhosis: an ecogenetic disorder. Lancet 1996, 347:877-880.

[3] Klotz LO, Kroncke KD, Buchczyk DP, Sies H. Role of copper, zinc, selenium and tellurium in the cellular defense against oxidative and nitrosative stress. J Nutr 2003, 133:1448S-1451S.

[4] Haywood S, Rutgers HC, Christian MK. Hepatitis and copper accumulation in Skye terriers. Vet Pathol 1988, 25:408-414.

[5] Klomp AE, van De SB, Klomp LW, et al. The ubiquitously expressed MURR1 protein is absent in canine copper toxicosis. J Hepatol 2003, 39:703-709.

[6] Mandigers PJ, van den Ingh TSGAM, Spee B, et al. Chronic hepatitis in Doberman pinschers. A review. Vet Q 2004, 26:98-106.

[7] Ludwig J, Owen CA Jr., Barham SS, et al. The liver in the inherited copper disease of Bedlington terriers. Lab Invest 1980, 43:82-87.

[8] Sternlieb I. Copper toxicosis of the Bedlington terrier. J Rheumatol Suppl 1981; 7:94-95.

[9] Stockman MJ. Copper toxicosis in the Bedlington terrier. Vet Rec 1988, 123:355.

[10] Wijmenga C, Klomp LW. Molecular regulation of copper excretion in the liver. Proc Nutr Soc 2004, 63:31-39.

[11] Tao TY, Liu F, Klomp L, et al. The copper toxicosis gene product Murr1 directly interacts with the Wilson disease protein. J Biol Chem 2003, 278:41593-41596.

[12] Bertinato J, L'Abbe MR. Maintaining copper homeostasis: regulation of copper-trafficking proteins in response to copper deficiency or overload. J Nutr Biochem 2004, 15:316-322.

[13] Burstein E, Ganesh L, Dick RD, et al. A novel role for XIAP in copper homeostasis through regulation of MURR1. EMBO J 2004, 23:244-254.

[14] Dijkstra M, Vonk RJ, Kuipers F. How does copper get into bile? New insights into the mechanism(s) of hepatobiliary copper transport. J Hepatol 1996, 24 Suppl 1:109-120.

[15] Samuele A, Mangiagalli A, Armentero MT, et al. Oxidative stress and pro-apoptotic conditions in a rodent model of Wilson's disease. Biochim Biophys Acta 2005, 1741:325-330.

[16] Gaetke LM, Chow CK. Copper toxicity, oxidative stress, and antioxidant nutrients. Toxicology 2003, 189:147-163.

[17] Freedman JH, Ciriolo MR, Peisach J. The role of glutathione in copper metabolism and toxicity. J Biol Chem 1989, 264:5598-5605.

[18] Dickinson DA, Forman HJ. Glutathione in defense and signaling: lessons from a small thiol. Ann N Y Acad Sci 2002, 973:488-504.

[19] Ghezzi P. Regulation of protein function by glutathionylation. Free Radic Res 2005, 39:573-580.
[20] Spee B, Mandigers PJ, Arends B, et al. Differential expression of copper-associated and oxidative stress related proteins in a new variant of copper toxicosis in Doberman pinschers. Comp Hepatol 2005, 4:3.
[21] Rothuizen J. Seeking global standardisation on liver disease. J Small Anim Pract 2001, 42:424-425.
[22] Favier RP, Spee B, Penning LC, et al. Quantitative PCR method to detect a 13-kb deletion in the MURR1 gene associated with copper toxicosis and HIV-1 replication. Mamm Genome 2005, 16:460-463.
[23] Boomkens SY, Penning LC, Egberink HF, et al. Hepatitis with special reference to dogs. A review on the pathogenesis and infectious etiologies, including unpublished results of recent own studies. Vet Q 2004; 26:107-114.
[24] van den Ingh TSGAM, Rothuizen J, Cupery R. Chronic active hepatitis with cirrhosis in the Doberman pinscher. Vet Q 1988; 10:84-89.
[25] Allen S, Shea JM, Felmet T, et al. A kinetic microassay for glutathione in cells plated on 96-well microtiter plates. Methods Cell Sci 2000; 22:305-312.
[26] Tietze F. Enzymic method for quantitative determination of nanogram amounts of total and oxidized glutathione: applications to mammalian blood and other tissues. Anal Biochem 1969; 27:502-522.
[27] Fuentealba IC, Aburto EM. Animal models of copper-associated liver disease. Comp Hepatol 2003; 2:5
[28] Burstein E, Hoberg JE, Wilkinson AS, et al. COMMD proteins, a novel family of structural and functional homologs of MURR1. J Biol Chem 2005; 280:22222-22232.
[29] Packman S, Palmiter RD, Karin M, O'Toole C. Metallothionein messenger RNA regulation in the mottled mouse and Menkes kinky hair syndrome. J Clin Invest 1987; 79:1338-1342.
[30] Baron V, Muriel P. Role of glutathione, lipid peroxidation and antioxidants on acute bile-duct obstruction in the rat. Biochim Biophys Acta 1999; 1472:173-180.
[31] Summer KH, Eisenburg J. Low content of hepatic reduced glutathione in patients with Wilson's disease. Biochem Med 1985; 34:107-111.
[32] Witschi A, Reddy S, Stofer B, Lauterburg BH. The systemic availability of oral glutathione. Eur J Clin Pharmacol 1992; 43:667-669.
[33] Lotkova H, Cervinkova Z, Kucera O, et al. Protective effect of S-adenosylmethionine on cellular and mitochondrial membranes of rat hepatocytes against tert-butylhydroperoxide-induced injury in primary culture. Chem Biol Interact 2005; 156:13-23.
[34] Nieto N, Cederbaum AI. S-adenosylmethionine blocks collagen I production by preventing transforming growth factor-beta induction of the COL1A2 promoter. J Biol Chem 2005; 280:30963-30974.

Chapter 7

Differential expression of copper-associated and oxidative stress related proteins in a new variant of copper toxicosis in Doberman pinschers

Bart Spee[1], Paul J.J. Mandigers[1], Brigitte Arends[1], Peter Bode[2], Ted S.G.A.M. van den Ingh[3], Gaby Hoffmann[1], Jan Rothuizen[1], and Louis C. Penning[1]

[1]Department of Clinical Sciences of Companion Animals, Faculty of Veterinary Medicine, Utrecht University, The Netherlands, and [2]Interfacultary Reactor Institute, Delft University, The Netherlands, and [3]Department of Pathobiology, Faculty of Veterinary Medicine, Utrecht University, The Netherlands

Adapted from *Comparative Hepatology* 2005, 4:3

Abstract

The role of copper accumulation in the onset of hepatitis is still unclear. Therefore, we investigated a spontaneous disease model of primary copper-toxicosis in Doberman pinschers to gain insights into the pathophysiology of copper toxicosis, namely on genes involved in copper metabolism and reactive oxygen species (ROS) defences. We used quantitative real-time PCR to determine differentially expressed genes within a target panel, investigating different groups ranging from copper-associated subclinical hepatitis (CASH) to a clinical chronic hepatitis with high hepatic copper concentrations (Doberman hepatitis, DH). Furthermore, a non-copper associated subclinical hepatitis group (N-CASH) with normal hepatic copper concentrations was added as a control. Most mRNA levels of proteins involved in copper binding, transport, and excretion were around control values in the N-CASH and CASH group. In contrast, many of these (including ATP7A, ATP7B, ceruloplasmin, and metallothionein) were significantly reduced in the DH group. Measurements on defences against oxidative stress showed a decrease in gene-expression of superoxide dismutase 1 and catalase in both groups with high copper. Moreover, the anti-oxidative glutathione molecule was clearly reduced in the DH group. In the DH group the expression of gene products involved in copper efflux was significantly reduced, which might explain the high hepatic copper levels in this disease. ROS defences were most likely impaired in the CASH and DH group. Overall, this study describes a new variant of primary copper toxicosis and could provide a molecular basis for equating future treatments in dog and in man.

Introduction

Copper is an imperative molecule in life; in contradiction, however, it is highly toxic [1]. Like zinc, iron, and selenium, copper is an essential trace element in diets and is required for the activity of a number of physiologically important enzymes [2]. Cells have highly specialized and complex systems for maintaining intracellular copper concentrations [3]. If this balance is disturbed, excess copper can induce oxidative stress that could lead to chronic inflammation [4,5]. Copper induced hepatitis has been described both in humans (Wilson's disease) as well as in dogs. There are several non-human models of copper toxicosis models, such as the Long-Evans Cinnamon rats and Bedlington terriers. Although the gene underlying Wilson's disease (ATP7B) is deficient in Long-Evans Cinnamon rats [6-9], in Bedlington terriers it has been excluded as a candidate for copper toxicosis [10]. The recent discovery of mutations in gene MURR1, responsible for copper toxicosis in Bedlington terriers, has given rise to the discovery of a new copper pathway [11]. Here, we describe in Doberman pinschers a copper associated chronic hepatitis (also called Doberman hepatitis), characterized by micro-nodular cirrhosis with elevated hepatic copper concentrations [12-15]. Doberman hepatitis accounts for 4 % of all deaths in a Dutch population of 340 Dobermans [16]. Until recently, the role of copper in the development and progression of hepatitis in the Doberman pinscher had been unclear. Recent studies using intravenous ^{64}Cu clearly show an impaired copper excretion in dogs with hepatitis and elevated copper concentrations [17]. However, genes ATP7B and MURR1 have been excluded by us as possible candidates by genotyping (data not shown). Therefore, Doberman hepatitis can be seen as a separate form of copper toxicosis and a possible model for other types of copper toxicosis in humans, such as Indian childhood cirrhosis, non-Indian childhood cirrhosis, or idiopathic copper toxicosis.

Intracellular copper is always transiently associated with small copper-binding proteins (See Figure 6, Chapter 1), denoted copper chaperones, which distribute copper to specific intracellular destinations [18]. One of these copper chaperones is the antioxidant protein 1 (ATOX1) [19], which transports copper to the copper-transporting ATPases ATP7A and ATP7B [20], located in the trans-Golgi network. Copper can then be bound to liver specific ceruloplasmin (CP) [21] or MURR1 and transferred outside the cell to blood and bile, respectively [22]. The second chaperone – cytochrome c oxidase (COX17) is responsible for delivering copper to the mitochondria for incorporation into cytochrome c oxidase [23]. The third chaperone – copper chaperone for superoxide oxidase (CCS) is responsible for the incorporation of copper into Cu/Zn superoxide dismutase (SOD1) – one of the most important cytosolic enzymes in the defence against oxidative stress [24,25]. Also known as ferroxi-

dase or oxygen oxidoreductase, CP is a plasma metalloprotein which is involved in peroxidation of Fe(II)transferrin to Fe(III)transferrin and forms 90 to 95 % of plasma copper. CP is synthesized in hepatocytes and is secreted into the serum with copper incorporated during biosynthesis. Metallothionein 1A (MT1A) is a small intracellular protein capable of chelating several metal ions, including copper. It contains many cysteine residues, which allow binding and storage of copper. Furthermore, MT1A is inducible, at the transcriptional level, by metals and a variety of stressors such as reactive oxygen species (ROS), hypoxia, and UV radiation [26]. MT1A can donate copper to other proteins, either following degradation in lysosomes or by exchange via glutathione (GSH) complexation [27].

High hepatic levels of copper induce oxidative stress. There are several important proteins and molecules involved in the defence against oxidative stress. Most of the anti-oxidants can be grouped into either enzymatic defences or non-enzymatic defences [28]. The enzymatic defence against oxidative stress consists of several proteins that have tight regulations such as SOD1 and catalase (CAT). Non-enzymatic defences against oxidative stress consist of molecules such as α-tocopherol, β-carotene, ascorbate, and a ubiquitous low molecular thiol component – the GSH [29]. The present study was undertaken to investigate the effect of copper toxicosis on expression of gene-products involved in copper metabolism and oxidative stress in several gradations of hepatic copper toxicosis in Doberman pinschers.

Materials and methods

Dogs

Doberman pinschers were kept privately as companion animals. The dogs were presented to the Department of Clinical Sciences of Companion Animals, Utrecht University, either for a survey investigating the prevalence of Doberman (chronic) hepatitis, as described by Mandigers *et al.* [30] or were referred for spontaneously occurring liver disease. All samples were obtained after written consent of the owner. The procedures were approved by the Ethical Committee, as required under Dutch legislation.

Groups

Animals were divided in groups based on histopathological examination and quantitative copper analysis. Each group contained both sexes from four to seven years of age. (A possible gender effect was later excluded by looking at the individual data). Liver tissue of all Doberman pinschers was obtained using the Menghini aspiration technique [31]. Four biopsies, 2–3 cm in length, were taken with a 14-gauge Menghini needle for histopathological examination and quantitative copper analysis and stored for future quantitative PCR and protein investigations. The quantitative copper analysis was performed using instrumental neutron activation analysis via the determination of ^{64}Cu [32]. Histopathological biopsies were fixed in 10% neutral buffered formalin, routinely dehydrated and embedded in paraffin. Sections (4 μm thick) were stained with haematoxylin-eosin, van Gieson's stain, reticulin stain (according to Gordon and Sweet), and with rubeanic acid. One experienced board certified veterinary pathologist performed all histological examinations. All diseased groups contained at least six animals that were compared with a group of eight age-matched healthy dogs. Four groups were included in this study (Table 1):

1) Healthy group (n = 8 dogs), clinically healthy dogs with normal liver enzymes and bile acids. Histopathology of the liver did not reveal histomorphological lesions. Liver copper concentrations were below 200 mg/kg dry matter.

2) Non-copper associated subclinical hepatitis group (N-CASH, n = 6 dogs), dogs with liver enzymes and bile acids within reference values. Although histological examination showed evidence of a slight hepatitis, hepatic copper concentrations were within normal levels, *i.e.*, below 300 mg/kg dry matter. The dogs were classified as suffering from subclinical hepatitis, which most likely was the result of a different etiological factor, such as infections, deficiencies, other toxins, deficient immune status or immune-mediated mechanism [33].

3) Copper associated subclinical hepatitis group (CASH, n = 6 dogs), dogs with liver enzymes and bile acids within reference values. At histopathology these dogs showed centrolobular copper-laden hepatocytes, on occasions apoptotic hepatocytes associated with copper-laden Kupffer cells, lymphocytes, plasma cells and scattered neutrophils. These lesions were classified as subclinical copper-associated hepatitis [34,35]. Hepatic copper concentrations were in all dogs above 600 mg/kg dry matter.

4) Doberman hepatitis group (DH, n = 6 dogs), dogs with chronic hepatitis and elevated hepatic copper concentrations. All dogs were referred with a clinical presen-

tation of hepatic failure (apathy, anorexia, vomiting, jaundice, and in chronic cases sometimes ascites) and died within 2 months after diagnosis from this disease. Heparinized plasma liver enzymes (alkaline phosphatase and alanine aminotransferase) and fasting bile acids were, at least, three times elevated above normal reference values. Abdominal ultrasound revealed small irregular shaped echo dense liver, as performed with a high definition Ultrasound system – HDI 3000 ATL (Philips) – with a 4–7 MHz broad band Faced-array transducer. Histopathology showed chronic hepatitis (Figure 1A) with histological features of fibrosis / micronodular cirrhosis, etc. These lesions are comparable to chronic hepatitis in man [33]. Rubeanic acid staining revealed copper accumulation in hepatocytes and Kupffer cells / macrophages (Figure 1B). Hepatic copper concentrations were in all cases above 1500 mg/kg dry matter.

Table 1. *Doberman pinscher group description*

Group	n	Hepatic copper	Copper concentrations mg/kg dry matter	Clinical observation
Healthy	8	Normal	100 – 200	No abnormalities
N-CASH	6	Normal	< 300	Sub-clinical hepatitis
CASH	6	Elevated copper levels	> 600	Sub-clinical hepatitis
DH	6	Highly elevated copper levels	> 1500	Chronic hepatitis

RNA isolation and reverse-transcription polymerase chain reaction

Total cellular RNA was isolated from each frozen Doberman liver tissue in duplicate, using Qiagen RNeasy Mini Kit (Qiagen, Leusden, The Netherlands) according to the manufacturer's instructions. The RNA samples were treated with Dnase-I (Qiagen Rnase-free DNase kit). In total 3 μg of RNA was incubated with poly(dT) primers at 42°C for 45 min, in a 60 μl reaction volume, using the Reverse Transcription System from Promega (Promega Benelux, Leiden, The Netherlands).

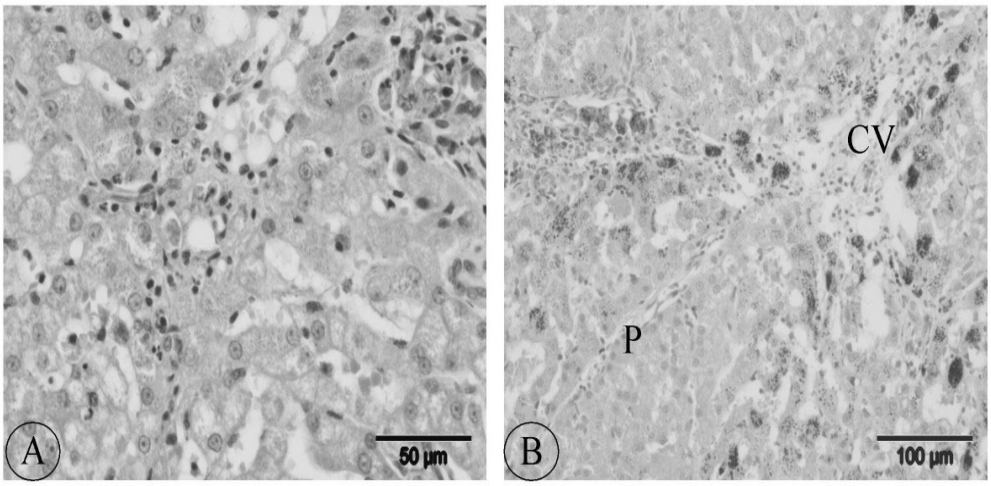

Figure 1. *Histological evaluation of Doberman hepatitis.*
(A) Hepatitis characterised by accumulation of pigmented granules (probably Cu) in hepatocytes, and inflammation with lymphocytes and pigmented (probably Cu) macrophages. HE staining. (B) Centrolobular accumulation of copper in hepatocytes and band of fibrous tissue with inflammatory cells and Cu-laden macrophages. Rubeanic acid staining. P = Portal area, CV = Central Vein area. Color-figure see appendix 4, page 223.

Q-PCR of oxidative-stress gene-products, copper metabolism and other related signalling molecules

Q-PCR was performed on a total of 17 genes involved in oxidative stress and copper metabolism. Real-time PCR was based on the high affinity double-stranded DNA-binding dye SYBR green I (SYBR® green I, BMA, Rockland, ME) and was performed in triplicate in a spectrofluorometric thermal cycler (iCycler®, BioRad, Veenendaal, The Netherlands). For each PCR reaction, 1.67 µl (of the 2× diluted stock) of cDNA was used in a reaction volume of 50 µl containing 1× manufacturer's buffer, 2 mM $MgCl_2$, 0.5 × SYBR® green I, 200 µM dNTP's, 20 pmol of both primers, 1.25 units of AmpliTaq Gold (Applied Biosystems, Nieuwerkerk a/d IJssel, the Netherlands), on 96-well iCycler iQ plates (BioRad). Primer pairs, depicted in Table 2, were designed using PrimerSelect software (DNASTAR Inc., Madison, WI). All PCR protocols included a 5-minute polymerase activation step and continued with for 40 cycles (denaturation) at 95°C for 20 sec, annealing for 30 sec, and elongation at 72°C for 30 sec with a final extension for 5 min at 72°C. Annealing temperatures were optimized at various levels ranging from 50°C till 67°C (Table 2). Melt curves (iCycler, BioRad), agarose gel electrophoresis, and standard sequencing procedures were used to examine each sample for purity and specificity (ABI PRISM 3100

Genetic Analyser, Applied Biosystems). Standard curves constructed by plotting the relative starting amount *versus* threshold cycles were generated using serial 4-fold dilutions of pooled cDNA fractions from both healthy and diseased liver tissues. The amplification efficiency, E (%) = $(10^{(1/-s)}-1)\cdot 100$ (s = slope), of each standard curve was determined and appeared to be > 95 %, and < 105 %, over a wide dynamic range. For each experimental sample the amount of the gene of interest, and of the endogenous references glyceraldehyde-3-phosphate dehydrogenase (GAPDH) and hypoxanthine phosphoribosyl transferase (HPRT) were determined from the appropriate standard curve in autonomous experiments. If relative amounts of GAPDH and HPRT were constant for a sample, data were considered valid and the average amount was included in the study (data not shown). Results were normalized according to the average amount of the endogenous references. The normalized values were divided by the normalized values of the calibrator (healthy group) to generate relative expression levels.

Western blot analysis

Pooled liver tissues (n = 6 dogs) were homogenized in RIPA buffer containing 1 % Igepal, 0.6 mM Phenylmethylsulfonyl fluoride, 17 µg/ml aprotinine and 1 mM sodium orthovanadate (Sigma chemical Co., Zwijndrecht, The Netherlands). Protein concentrations were obtained using a Lowry-based assay (DC Protein Assay, Bio-Rad). Thirty five µg of protein of the supernatant was denatured in Leammli-buffer supplemented with Dithiothreitol (Sigma Chemical Co.) for 3 min at 95°C and electrophoresed on 10 % Tris-HCl SDS PAGE polyacrylamide gels (BioRad). Proteins were transferred onto Hybond-C Extra Nitrocellulose membranes (Amersham Biosciences Europe, Roosendaal, The Netherlands) using a Mini Trans-Blot® Cell blot-apparatus (BioRad). The procedure for immunodetection was based on an ECL western blot analysis system, performed according to the manufacturer's instructions (Amersham Biosciences Europe). The membranes were incubated with 4 % ECL blocking solution and 0.1 % Tween 20 (Boom B.V., Meppel, The Netherlands) in TBS for 1 hour under gentle shaking. The incubation of the primary antibody was performed at room temperature for one hour, with a 1:2000 dilution of mouse anti-horse metallothionein (DakoCytomation B.V., Heverlee, Belgium). After washing, the membranes were incubated with horseradish peroxidase-conjugated chicken anti-mouse (Westburg B.V., Leusden, The Netherlands) at room temperature for one hour. Exposures were made with Kodak BioMax Light-1 films (Sigma chemical Co.).

Total GSH assay

The total amount of GSH was determined by a modified version of a total GSH Determination Colorimetric Microplate Assay according to Allen *et al.* [36], based on the original Tietze macro assay [37]. Protein samples from Doberman hepatitis (n = 6 dogs) and healthy controls (n = 8 dogs) were isolated as described in Western blot analysis and subsequently pooled. Total protein concentration was measured using a Lowry-based assay (DC Protein Assay, BioRad). In short, 50 µl of the cell-lysate (1 mg/ml) was used in triplicate in a 96-wells plate. The lysates were incubated for 5 minutes with 50 µl of 1.3 mM 5,5'dithiobis-2-nitrobenzoic acid (DTNB), and 50 µl GSH reductase (1.5 U/ml). To start the reaction 50 µl of NADPH (0.7 mM) was added to the wells. Absorbance at 450 nm was measured at start and after 5 minutes. The rate of 2-nitro-5-thiobenzoic acid production (yellow product) was measured in delta absorbance per minute and is directly proportionate with the amount of GSH in the samples. A standard curve was added with known concentrations GSH (0 to 20 µM) in order to determine the GSH concentrations in the samples.

Statistical analysis

A Kolmogorov-Smirnov test was performed to confirm normal distribution of every group, and a Levene's test checked the homogeneity of variances across groups. After both verifications, the statistical significance of the difference between the control group and each particular non-healthy group was determined by using the Student's *t*-Test. The significance level (α) was set at 0.05.

Table 2. Nucleotide Sequences of Dog-Specific Primers for Quantitative Real-Time PCR

Gene	F/R	Sequence (5'-3')	Tm (°C)	Product size (bp)	Accession number
GAPDH	F	TGT CCC CAC CCC CAA TGT ATC	58	100	AB038240
	R	CTC CGA TGC CTG CTT CAC TAC CTT			
HPRT	F	AGC TTG CTG GTG AAA AGG AC	56	100	L77488 / L77489
	R	TTA TAG TCA AGG GCA TAT CC			
SOD1	F	TGG TGG TCC ACG AGA AAC GAG ATG	64	99	AF346417
	R	CAA TGA CAC CAC AAG CCA AAC GAC T			
CAT	F	TGA GCC CAG CCC TGA CAA AAT G	62	119	AB012918
	R	CTC GAG CCC GGA AAG GAC AGT T			
GSS	F	CTG GAG CGG CTG AAG GAC A	62	131	AY572226
	R	AGC TCT GAG ATG CAC TGG ACA			
GPX1	F	GCA ACC AGT TCG GGC ATC AG	62	123	AY572225
	R	CGT TCA CCT CGC ACT TCT CAA AA			
CCS	F	TGT GGC ATC ATC GCA CGC TCT G	64	96	AY572228
	R	GGG CCG GCC TCG CTC CTC			
p27KIP	F	CGG AGG GAC GCC AAA CAG G	60	90	AY455798
	R	GTC CCG GGT CAA CTC TTC GTG			
Bcl-2	F	TGG AGA GCG TCA ACC GGG AGA TGT	61	87	AB116145
	R	AGG TGT GCA GAT GCC GGT TCA GGT			
ATOX1	F	ACG CGG TCA GTC GGG TGC TC	67	137	AF179715
	R	AAC GGC CTT TCC TGT TTT CTC CAG			
COX17	F	ATC ATT GAG AAA GGA GAG GAG CAC	60	127	AY603041
	R	TTC ATT CTT CAA GGA TTA TTC ATT TAC A			
ATP7A	F	CTA CTG TCT GAT AAA CGG TCC CTA AA	50	99	AY603040
	R	TGT GGT GTC ATC ATC TTC CCT GTA			
ATP7B	F	GGT GGC CAT CGA CGG TGT GC	56	136	AY603039
	R	CGT CTT GCG GTT GTC TCC TGT GAT			
CP	F	AAT TCT CCC TTC TGT TTT TGG TT	62	97	AY572227
	R	TTG TTT ACT TTC TCA GGG TGG TTA			
MT1A	F	AGC TGC TGT GCC TGA TGT G	64	130	D84397
	R	TAT ACA AAC GGG AAT GTA GAA AAC			
MURR1	F	GAC CAA GCT GCT GTC ATT TCC AA	58	122	AY047597
	R	TTG CCG TCA ACT CTC CAA CTC A			
XIAP	F	ACT ATG TAT CAC TTG AGG CTC TGG TTT C	54	80	AY603038
	R	AGT CTG GCT TGA TTC ATC TTG TGT ATG			

F: Forward primer; R: reversed primer

Results

To gain insight into the pathogenesis of copper toxicosis, we first measured mRNA levels on several important copper binding gene-products by means of quantitative real-time PCR (Q-PCR). Because copper toxicity is often associated with oxidative stress, we also measured several oxidative stress related gene-products. To determine a possible damaging effect of the oxidative stress, we investigated proteins involved in apoptosis and cell-proliferation.

Gene-expression measurements on copper metabolism related gene products

Several proteins in the Doberman hepatitis (DH) group are reduced compared to healthy controls (Figure 2C). In all groups the copper chaperone ATOX1 is not affected, whereas COX17 is decreased three-fold in the DH group and remains unchanged in the non-copper associated subclinical hepatitis group (N-CASH, Figure 3A) and copper associated subclinical hepatitis group (CASH, Figure 2B). In the DH group, the mRNA levels of both trans-Golgi copper transporting proteins ATP7A and ATP7B are decreased, three- and two-fold respectively. Interestingly, mRNA levels of ATP7A are decreased in the CASH group as well (Figure 2B). In contrast, ATP7B is not affected in the CASH group but is induced two-fold in the N-CASH group. CP mRNA levels are normal except for the DH group where it is decreased two-fold. The same observation was made with measurements on MT1A mRNA, although this protein is decreased four-fold in the DH group. The protein MURR1 (that transports copper from hepatocytes into bile) is unaffected in the N-CASH group but halved in the CASH and DH groups.

Gene expression measurements on oxidative stress markers

SOD1 and CAT are reduced 7- and 4-fold (respectively) in the DH group when compared to healthy controls (Figure 3C). This reduction in mRNA levels can be seen in the CASH group (Figure 3B), where SOD1 and CAT are halved, but are not lowered significantly in the N-CASH group (Figure 3A). One of the GSH synthesis enzymes – the glutathione synthetase (GSS) is unaffected in the N-CASH group but reduced 2 to 4-fold in the CASH and DH group, respectively. The glutathione peroxidase (GPX1) responsible for converting oxidized glutathione (GSSG) into its reduced form (GSH) is induced slightly in mRNA expression in the N-CASH group, and is doubled in the CASH and DH groups. The third copper chaperone CCS, responsible for the transport of copper to SOD1, is inhibited 8-fold in the DH group, 2-fold in the CASH group, and remained unchanged in the N-CASH group.

Gene expression measurements on apoptosis and cell proliferation

We measured two anti-apoptotic gene products, viz. Bcl-2, the frequently described anti-apoptotic protein, and a x-linked inhibitor of apoptosis (XIAP) recently associated with MURR1 [38]. Our apoptosis measurements on Bcl-2 showed no reduction in gene expression in the N-CASH group (Figure 4A), but is inhibited 4-fold in the CASH and DH groups (Figures 4B and 4C, respectively). XIAP is halved in all groups. The most dramatic changes were found in the mRNA levels of the cell-cycle inhibitor p27KIP which is inhibited 24-fold in the DH group, 12-fold in the CASH group, and 3-fold in the N-CASH group.

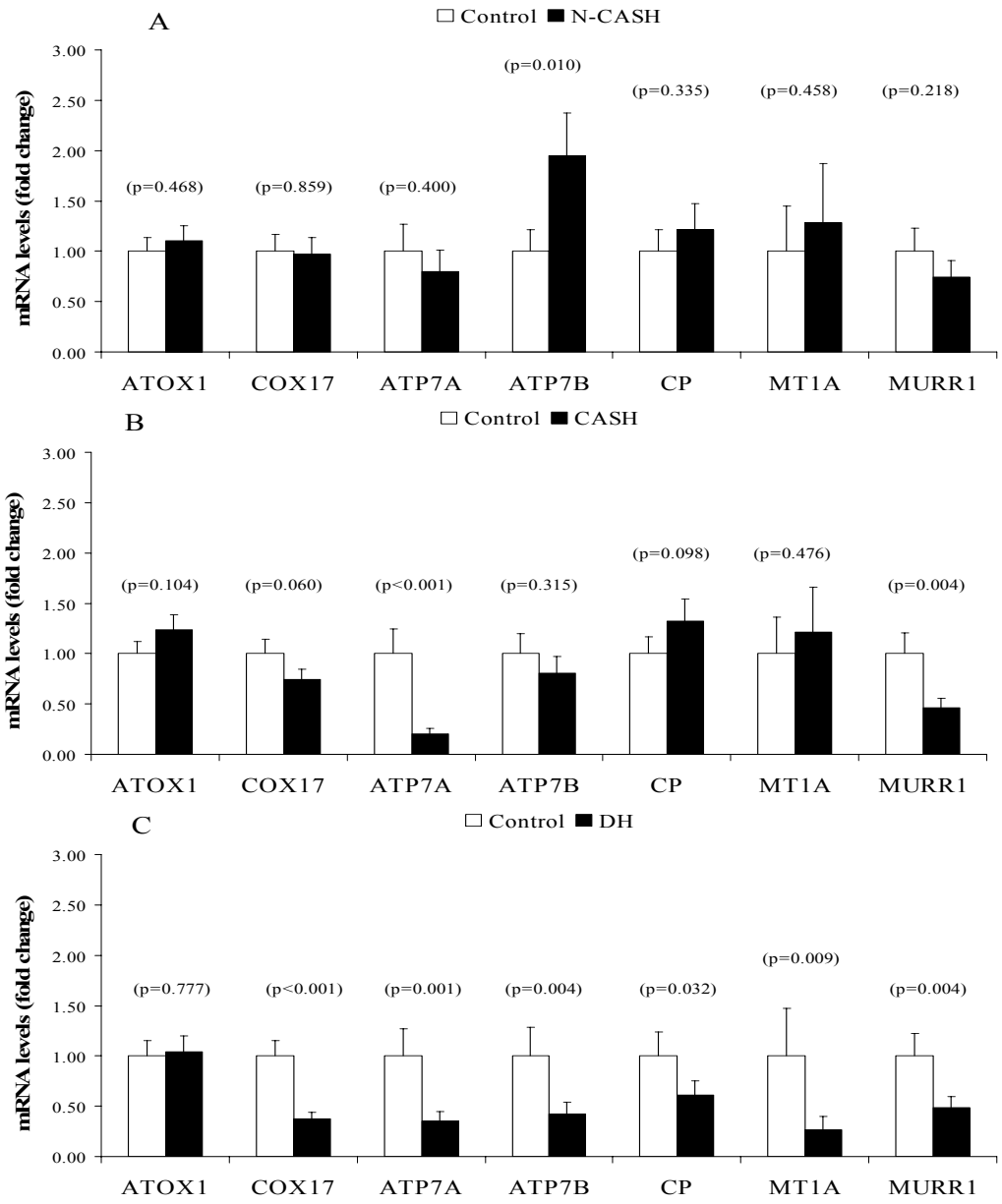

Figure 2. *Quantitative Real-Time PCR of copper metabolism related genes. mRNA levels of non-copper associated subclinical hepatitis (n = 6 dogs) is shown in (A). mRNA levels of copper associated subclinical hepatitis (n = 6 dogs) is shown in (B). mRNA levels of Doberman hepatitis (n = 6 dogs) is shown in (C). Data represent mean + SD.*

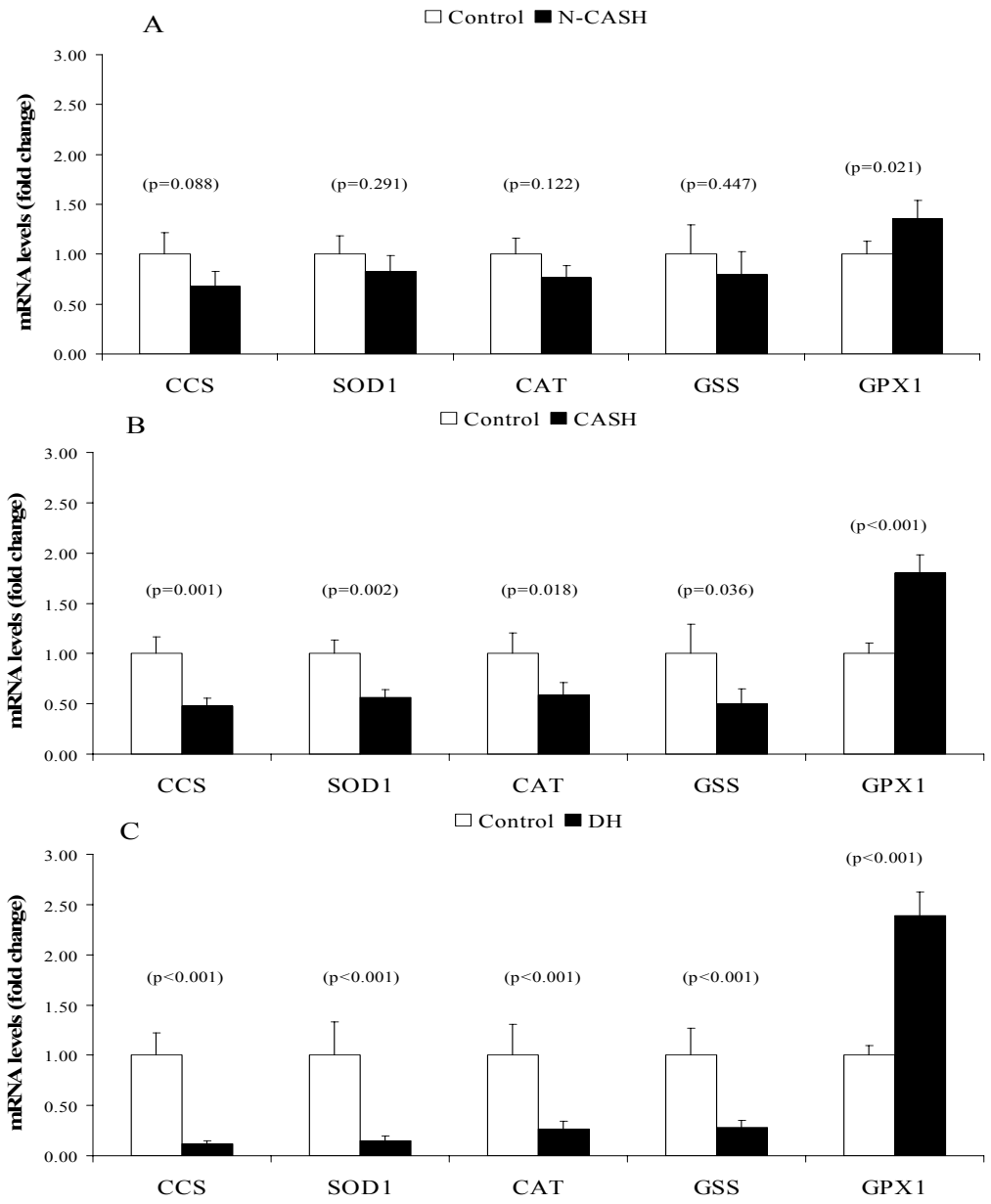

Figure 3. *Quantitative Real-Time PCR of oxidative stress markers. mRNA levels of non-copper associated subclinical hepatitis (n = 6 dogs) is shown in (A). mRNA levels of copper associated subclinical hepatitis (n = 6 dogs) is shown in (B). mRNA levels of Doberman hepatitis (n = 6 dogs) is shown in (C). Data represent mean + SD.*

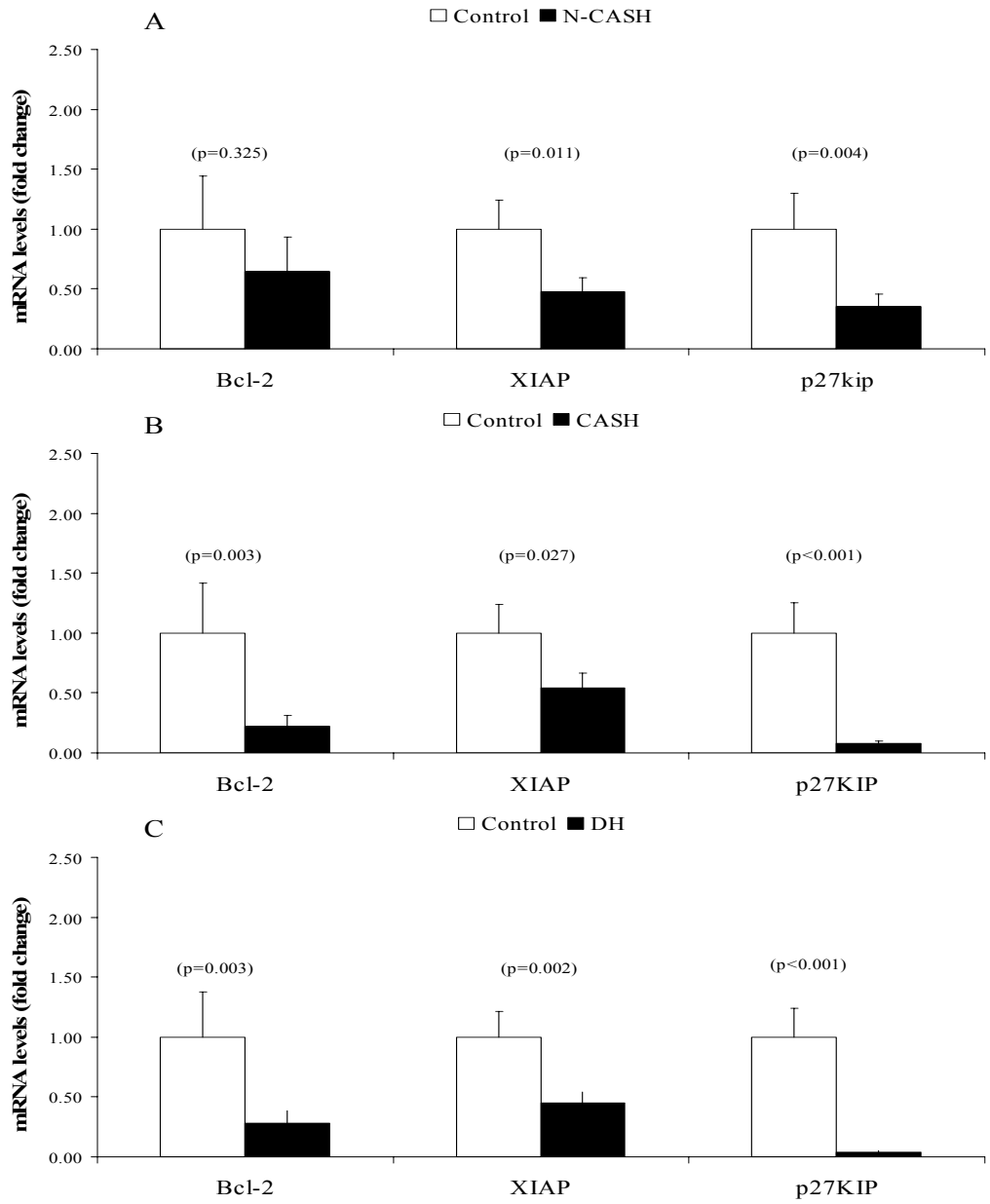

Figure 4. *Quantitative Real-Time PCR of apoptosis and cell proliferation related genes. mRNA levels of non-copper associated subclinical hepatitis (n = 6 dogs) is shown in (A). mRNA levels of copper associated subclinical hepatitis (n = 6 dogs) is shown in (B). mRNA levels of Doberman hepatitis (n = 6 dogs) is shown in (C). Data represent mean + SD.*

Western blots analysis on metallothionein proteins during copper toxicosis

Measurements on the mRNA levels of MT1A showed a marked decrease in gene expression in the DH group. In order to see whether this decrease was also occurring at the protein level, Western blots were performed in order to confirm decreased mRNA levels. Therefore, the total amount of metallothionein was determined from Doberman pinschers with chronic hepatitis and high copper (DH-group) levels compared to healthy Dobermans. Metallothionein was detected in both samples, where it was present as a single band of 6 kDa (Figure 5). Interestingly, the immuno-reactive band shows no difference in concentration between the two samples.

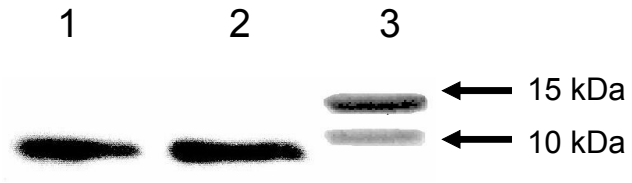

Figure 5. *Western blot analysis of the metallothionein proteins. Immunoreactive bands of total metallothionein of pooled fractions of the Doberman hepatitis (DH) group (n = 6 dogs) versus healthy controls (n = 8 dogs). Lane 1; Doberman hepatitis, Lane 2; Healthy control, Lane 3; protein precision marker.*

Total Glutathione measurements during copper toxicosis

In order to determine whether the decrease in mRNA levels of GSS decreases the GSH levels, we measured the total amount of GSH. Interestingly, in Figure 6, the total amount of GSH in the high copper group is halved when compared to healthy controls.

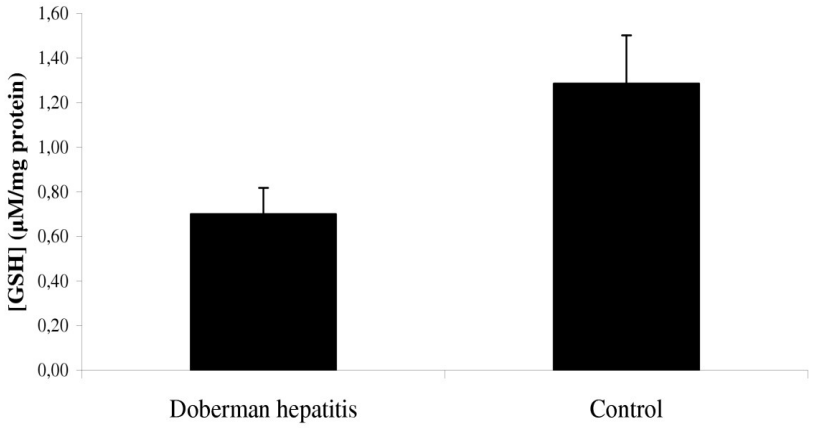

Figure 6. *Total glutathione (GSH) measurements during copper toxicosis in Doberman. Total GSH levels of pooled protein fractions of the Doberman hepatitis (DH) group (n = 6 dogs) versus healthy controls (n = 8 dogs). Data represent mean + SD.*

Discussion

In the present study, the expression of a total of 15 gene products involved in copper metabolism of Doberman pinschers was measured. This provided insight into the molecular pathways of a canine copper-associated hepatic disease model ranging from subclinical hepatitis with elevated copper levels (CASH) to severe chronic hepatitis with high hepatic copper levels (DH). Furthermore, these diseases were compared to non-copper associated subclinical hepatitis (N-CASH).

Because of the centrolobular accumulation of copper in the hepatocytes during copper toxicosis in the Doberman, a probable defect may be sought in the copper metabolism instead of a secondary effect due to, for instance, cholestasis. Recent findings by Mandigers *et al.* [17] indicated that Doberman pinschers with hepatitis and elevated copper concentrations suffer from impaired ^{64}Cu bile excretion which is, together with other studies, conclusive that copper toxicosis exists in the Doberman pinscher. Furthermore, a double blind placebo-controlled study with the copper chelating agent, D-penicillamine, on Doberman pinschers with CASH showed a marked improvement of liver pathology [39]; currently, that agent is the only treatment option.

If copper is sequestered, in time metallothioneins will store the copper in lysosomes, as described by Klein *et al*. [40]. They found that chronic copper toxicity in Long-Evans Cinnamon rats involved the uptake of copper-loaded metallothioneins into lysosomes, where it was incompletely degraded and polymerized into an insoluble material, which contained reactive copper. This copper initiated a lysosomal lipid peroxidation, which led to hepatocyte necrosis. Phagocytosis of this reactive copper by Kupffer cells amplified the liver damage. Histological examination of the DH (Figure 2) and CASH group samples revealed copper accumulation in hepatocytes and copper-laden Kupffer cells similar to that described by Klein *et al.* [40]; therefore, that can be denoted as benchmarks of chronic exposure to copper.

In our study, the gene expression levels of several gene products involved in copper metabolism seem to be reduced in the DH and CASH groups when compared to healthy controls. Short term studies on *in vitro* models all show an induction of MT1A or CP indicative of a higher storage respectively efflux of copper from hepatocytes [41,42]. The reductions that are seen in our results could therefore be ascribed to the prolonged or chronic nature of copper accumulation as dogs in the high copper or DH group present clinical signs after 2 years. Therefore, our observations are not directly comparable with the short-term induced copper effects *in vitro*, but are clinically more relevant, showing the effects of long-term copper accumulation in Doberman hepatitis. However, Western blot experiments on metallothionein, which stores the copper in lysosomes, did not show any reduction at the protein level. This observation could be ascribed to the antibody that binds all metallothioneins, including metallothionein 2 (MT2A), which also is present in the liver. It remains to be proven if this effect is a compensation for the decrease of MT1A.

In the earlier stages of copper accumulation, comparable to the CASH group, higher amounts of copper can still be excreted. Interestingly, in the N-CASH group, ATP7B is indeed induced compared to healthy controls, emphasizing a possible higher efflux of copper. Furthermore, from the two subclinical disease groups, the N-CASH group is the only one able to recuperate, whereas the CASH group will eventually turn into clinical hepatitis as seen in the DH group (data not shown). Taken together, our data suggest that in the Doberman pinchers copper accumulates in time and, finally, will have its negative effect on copper metabolism and induce oxidative stress.

Oxidative stress has been ascribed to copper toxicosis as one of the most important negative effects [43]. We can confirm this with four different observations: (i) our measurements showed a decrease in mRNA levels of SOD1 and CAT, indicative of a reduction in the enzymatic defence against oxidative stress in all groups with copper accumulation; (ii) a reduction of GSS mRNA levels (glutathione synthesis),

indicative for a reduced glutathione level in these groups which is one of the most important non-enzymatic molecules against oxidative stress; (iii) the mRNA levels of GPX1 were significantly increased, indicating an increase in GSH oxidation; (iv) the decrease in GSH was confirmed by measuring total glutathione levels in the DH group towards healthy Doberman pinschers. A similar decrease in expression of anti-oxidant enzymes was observed in ApoE-deficient mice in response to chronic inflammation [44], and inflammatory bowel disease (IBD) [45]. This indicates that chronic inflammation (copper toxicosis, atherosclerosis, IBD) is associated with reduced protection against enhanced exposure to ROS.

Other effects of high copper can also be seen in the measurements on apoptosis and cell-cycle. Measurements on Bcl-2 and XIAP indicate a decrease of protection against apoptosis; however, the most affected hepatocytes will go into necrosis due to the formation of hydroxyl radicals by the Haber-Weiss reaction, which is catalyzed by copper [46]. A striking observation was made measuring p27KIP which was shown to be reduced up to 24-fold in the DH group. This could indicate an induction of cell-cycle compared to healthy controls. This could be ascribed to the renewal of hepatocytes, thus managing the total amount of copper in time.

Whether differential gene expression is cause-or-consequence of hepatitis is unknown. However, it is conceivable that the reduction in copper processing gene products might explain copper accumulation and the subsequent oxidative stress. Furthermore, recent Q-PCR measurements on non-copper related hepatitis and extra hepatic cholestasis suggest that ATP7A and CP are not down-regulated by inflammation or cholestasis (data not shown). Therefore, we can conclude that the decreased expression of these gene products is a Doberman hepatitis specific effect. Other important copper associated gene products such as COX17, ATP7B, and MT1A are probably down-regulated due to inflammation.

This study is the first to show the effect of prolonged exposure to different copper levels on oxidative stress and copper metabolism in canine livers. Our data supports that: (i) Doberman hepatitis is a new variant of primary copper toxicosis; (ii) there is a clear indication of a reduced copper excretion in the Doberman hepatitis group; (iii) there is a clear correlation between high copper levels and reduced protection against ROS; (iv) this Doberman hepatitis could be a good model to study copper toxicosis and its effects for several human copper storage diseases such as Indian childhood cirrhosis, non-Indian childhood cirrhosis, and idiopathic copper toxicosis, and provide the basis for possible future treatments in dog and even in man.

References

[1] Hamza I, Faisst A, Prohaska J, et al. The metallochaperone Atox1 plays a critical role in perinatal copper homeostasis. Proc Natl Acad Sci U S A 2001, 98:6848-6852.

[2] Mertz M: The essential trace elements. Science 1981, 213:1332-1336.

[3] Dijkstra M, Vonk RJ, Kuipers F. How does copper get into bile? New insights into the mechanism(s) of hepatobiliary copper transport. J Hepatol 1996, 24:109-120.

[4] Sternlieb I. Copper and the liver. Gastroenterology 1980, 78:1615-1628.

[5] Thornburg LP. A perspective on copper and liver disease in the dog. J Vet Diagn Invest 2000, 12:101-110.

[6] Haywood S, Fuentealba IC, Kemp SJ, et al. Copper toxicosis in the Bedlington terrier: a diagnostic dilemma. J Small Anim Pract 2001, 42:181-185.

[7] Hultgren BD, Stevens JB, Hardy RM. Inherited, chronic, progressive hepatic degeneration in Bedlington terriers with increased liver copper concentrations: clinical and pathologic observations and comparison with other copper-associated liver diseases. Am J Vet Res 1986, 47:365-377.

[8] Owen CA Jr, Bowie EJ, McCall JT, et al. Hemostasis in the copper-laden Bedlington terrier: a possible model of Wilson's disease. Haemostasis 1980, 9:160-166.

[9] Twedt DC, Sternlieb I, Gilbertson SR. Clinical, morphologic, and chemical studies on copper toxicosis of Bedlington Terriers. J Am Vet Med Assoc 1979, 175:269-275.

[10] Sluis van de BJ, Breen M, Nanji M, et al. Genetic mapping of the copper toxicosis locus in Bedlington terriers to dog chromosome 10, in a region syntenic to human chromosome region 2p13-p16. Hum Mol Genet 1999, 8:501-507.

[11] Sluis van de BJ, Rothuizen J, Pearson PL, et al. Identification of a new copper metabolism gene by positional cloning in a purebred dog population. Hum Mol Genet 2002, 11:165-173.

[12] Crawford MA, Schall WD, Jensen RK, et al. Chronic active hepatitis in 26 Dobermann pinschers. J Am Vet Med Assoc 1985, 187:1343-1350.

[13] Ingh van den T, Rothuizen J, Cupery R. Chronic active hepatitis with cirrhosis in the Dobermann pinscher. Vet Q 1988, 10:84-89.

[14] Thornburg LP. Histomorphological and immunohistochemical studies of chronic active hepatitis in Dobermann Pinschers. Vet Pathol 1998, 35:380-385.

[15] Rolfe DS, Twedt DC. Copper-associated hepatopathies in dogs. Vet Clin North Am Small Anim Pract 1995, 25:399-417.

[16] Mandigers PJ, Senders T, Rothuizen J. Morbidity and mortality in a Dutch Dobermann population born between 1993 and 1999. Vet Rec 2005, in press.

[17] Mandigers PJ, Ingh van den T, Spee B, et al. Chronic hepatitis in Doberman pinschers. A review. Vet Q 2004, 26:98-106.

[18] Lippard SJ. Free copper ions in the cell? Science 1999, 284:748-749.

[19] Klomp LW, Lin SJ, Yuan DS, et al. Identification and functional expression of HAH1, a novel human gene involved in copper homeostasis. J Biol Chem 1997, 272:9221-9226.

[20] Vulpe C, Levinson B, Whitney S, et al. Isolation of a candidate gene for Menkes disease and evidence that it encodes a copper-transporting ATPase. Nat Genet 1993, 3:7-13.

[21] Bull PC, Thomas GR, Rommens JM, et al. The Wilson disease gene is a putative copper transporting P-type ATPase similar to the Menkes gene. Nat Genet 1993, 5:327-337.

[22] Wijmenga C, Klomp LW. Molecular regulation of copper excretion in the liver. Proc Nutr Soc 2004, 63:31-39.

[23] Cox DW. Genes of the copper pathway. Am J Hum Genet 1995, 56:828-834.

[24] Valentine JS, Gralla EB. Delivering copper inside yeast and human cells. Science 1997, 278:817-818.

[25] Harris ED. Cellular copper transport and metabolism. Annu Rev Nutr 2000, 20:291-310.

[26] Yagle MK, Palmiter RD. Coordinate regulation of mouse metallothionein I and II genes by heavy metals and glucocorticoids. Mol Cell Biol 1985, 5:291-294.

[27] Ferenci P, Zollner G, Trauner M. Hepatic transport systems. J Gastroenterol Hepatol 2002, (Suppl 17):105-112.

[28] Gaetke LM, Chow CK. Copper toxicity, oxidative stress, and antioxidant nutrients. Toxicology 2003, 189:147-163.

[29] Uhlig S, Wendel A. Glutathione enhancement in various mouse organs and protection by glutathione isopropyl ester against liver injury. Biochem Pharmacol 1990, 39:1877-1881.

[30] Mandigers PJ, Ingh van den T, Bode P, et al. Association between liver copper concentration and subclinical hepatitis in Doberman pinschers. J Vet Intern Med 2004, 18:647-650.

[31] Osborne CA, Hardy RM, Stevens JB, et al. Liver biopsy. Vet Clin North Am 1974, 4:333-350.

[32] Bode P. Automation and Quality Assurance in the Neutron Activation Facilities in Delft. J Radioanal Nucl Chem 2000, 245:127-132.

[33] Sterczer A, Gaal T, Perge E, et al. Chronic hepatitis in the dog – a review. Vet Q 2001, 23:148-152.

[34] Speeti M, Eriksson J, Saari S, et al. Lesions of subclinical Dobermann hepatitis. Vet Pathol 1998, 35:361-369.

[35] Fuentealba I, Haywood S, Trafford DJ. Variations in the intralobular distribution of copper in the livers of copper-loaded rats in relation to the pathogenesis of copper storage diseases. J Comp Pathol 1989, 100:1-11.

[36] Allen S, Shea JM, Felmet T, et al. A kinetic microassay for glutathione in cells plated on 96-well microtiter plates. Methods Cell Sci 2000, 22:305-312.

[37] Teitze F. Enzymatic method for quantitative determination of nanogram amounts of total oxidized glutathione: Applications to mammalian blood and other tissues. Anal Biochem 1969, 27:502-522.

[38] Burstein E, Ganesh L, Dick RD, et al. A novel role for XIAP in copper homeostasis through regulation of MURR1. EMBO J 2004, 14:244-254.

[39] Mandigers PJ, Ingh van den T, Bode P, et al. Improvement in liver pathology after 4 months of D-penicillamine in 5 Doberman pinschers with subclinical hepatitis. J Vet Intern Med 2005, 19:40-43.

[40] Klein D, Lichtmannegger J, Heinzman U, et al. Association of copper to metallothionein in hepatic lysosomes of Long-Evans cinnamon (LEC) rats during the development of hepatitis. Eur J Clin Invest 1998, 28:302-310.

[41] Daffada AA, Young AP. Coordinated regulation of ceruloplasmin and metallothionein MRNA by interleukin-1 and copper in HepG2 cells. Febs Lett 1999, 457:214-218.

[42] Mattie MD, Freedman JH. Copper-inducible transcription: regulation by metal- and oxidative stress-responsive pathways. Am J Physiol Cell Physiol 2004, 286:293-301.

[43] Ozcelik D, Ozaras R, Gurel Z, et al. Copper-mediated oxidative stress in rat liver. Biol Trace Elem Res 2003, 96:209-215.

[44] Hoen 't PA, Lans van der CA, Eck van M, et al. Aorta of ApoE-deficient mice responds to atherogenic stimuli by a prelesional increase and subsequent decrease in the expression of antioxidant enzymes. Circ Res 2003, 8:262-269.

[45] Kruidenier L, Kuiper I, Duijn van W, et al. Differential mucosal expression of three superoxide dismutase isoforms in inflammatory bowel disease. J Pathol 2003, 201:7-16.

[46] Klotz LO, Kroncke KD, Buchczyk DP, et al. Role of copper, zinc, selenium and tellurium in the cellular defense against oxidative and nitrosative stress. J Nutr 2003, 133:1448-1451.

Chapter 8

Quantitative PCR method to detect a 13-kb deletion in the *MURR1 (COMMD1)* gene associated with copper toxicosis and HIV-1 replication

Bart Spee*, Robert P. Favier*, Louis C. Penning, Bas Brinkhof, and Jan Rothuizen

Department of Clinical Sciences of Companion Animals, Faculty of Veterinary Medicine, Utrecht University, The Netherlands.

* Bart Spee and Robert P. Favier contributed equally to this work.

Adapted from *Mammalian Genome* 2005, 16:460-463.

Abstract

The recently discovered locus for copper toxicosis (CT) in Bedlington terriers (BT) has a 13-kb deletion enveloping the 187-bp exon-2 of the *MURR1 (COMMD1)* gene. This *MURR1* gene is not only involved with biliary copper excretion but also associated with HIV-1 replication. The microsatellite C04107 lying in an intron of the *MURR1* gene is highly associated with the disease but shows haplotype diversity. The only solid molecular test for the disease is by showing the deletion in exon-2 in cDNA in liver tissue; this test is not robust on RNA from peripheral leukocytes because of their low MURR1 expression level. Because of these drawbacks, we developed a new quantitative PCR (Q-PCR) protocol. Here we show that the *MURR1* exon-2/exon-3 ratio measured by Q-PCR on genomic DNA correlates perfectly with the microsattelite marker and with RT-PCR data from blood samples, buccal swabs, and liver biopsies. In view of the important role of *MURR1* in cells of many tissues, this new test has a wide range of applications in comparative biomedical research. Furthermore, Q-PCR on DNA may be a new tool in general to analyze mutations that cannot be approached by standard methods.

Introduction

Copper toxicosis (CT) affecting the liver was identified as an inherited disease in Bedlington terriers in 1975 by Hardy *et al*. [1]. CT is inherited as an autosomal recessive disorder [2] characterized by an inefficient excretion of copper via the bile [3]. The result is a progressive accumulation of copper in the hepatocellular lysosomes, becoming histologically distinguishable from the normal situation at one year of age and leading to progressive hepatitis and cirrhosis [1,4,5]. The disease appeared to be caused by a 13-kb deletion in a then unknown gene that plays a crucial role not only in copper metabolism but also in other cell functions. Recent research revealed that (i) *MURR1* (also known as *COMMD1*) restricts HIV-1 replication in resting $CD4^+$ lymphocytes by increasing NF-κB activity [6], (ii) *MURR1* is a regulator of the human δ epithelial sodium channel [7], and (iii) there is a novel role for XIAP, an anti-apoptotic protein, in copper homeostasis through regulating MURR1 [8]. Close linkage of the microsattelite marker C04107 to the disease was found by Yuzbasiyan-Gurkan *et al* [9]. C04107 lies in an intron of the causative gene *MURR1* [10]. Because of haplotype diversity, however, it is less reliable for diagnostic testing [11-13]. It proved impossible to develop a practical PCR reaction to show the absence or presence of the 13-kb deletion because only one side of the deletion could be identified [14]. Therefore, the only PCR-based molecular test possible today is by showing the deletion of exon-2 by RT-PCR on RNA from liver tissue. MURR1 expression level is very low in peripheral leukocytes, which makes a robust RT-PCR-based test less feasible (unpublished). Because of these drawbacks, we developed a new DNA-based method based on a variation of the Q-PCR protocol recently reported by Faugere *et al* [15], by measuring the ratio of exon-2 to exon-3. A clear correlation between this ratio and independent genotyping was found. We show that two-tube Q-PCR on small amounts of DNA from peripheral blood leukocytes or buccal swabs provides a reliable alternative for molecular diagnostics of this mutation, providing a new tool to evaluate mutations that cannot be approached with standard methods.

Materials and methods

DNA isolations from whole blood

Genomic DNA was isolated from 4 ml of blood collected in EDTA tubes by using the Qiagen QIAamp DNA Mini Kit (Hilden, Germany) and blood and body fluid spin protocol according to the manufacturer's instructions. The DNA samples were

digested with Qiagen Ribonuclease A (28 U) to remove RNA. The amount of DNA was quantified spectrophotometrically by the absorbance at λ = 260 nm.

DNA isolations from swabs

Genomic DNA obtained from buccal swabs (Omni Swabs, Fitzco Inc., Spring Park, MN) was isolated by using the Qiagen QIAamp DNA Mini Kit and buccal swab spin protocol according to the manufacturer's instructions. DNA samples were digested with Qiagen Ribonuclease A (28 U) to remove RNA from samples. The amount of DNA was quantified spectrophotometrically by absorbance at λ = 260 nm.

Quantitative PCR

Q-PCR involved amplification of two exons of the *MURR1* gene with primers in combination with high-affinity, double-stranded (ds), DNA-binding dye SYBR green I (SYBR® green I, BMA, Rockland, ME). Reactions were performed in triplicate in a spectrofluorometric thermal cycler (iCycler®, BioRad Laboratories, Hercules, CA). Data were collected and analyzed with the provided application software. For each real-time PCR reaction, 1.67 µl of genomic DNA (1–100 ng/ml) were used in a 50-µl reaction volume containing 1× manufacturer's buffer (Applied Biosystems, Roche, Brandenburg, NJ), 0.5× SYBR® green I, 200 µM dNTPs (PromegaBenelux, Leiden, The Netherlands), 20 pmol of both primers (Table 1) that were designed using PrimerSelect software (DNASTAR Inc., Madison, WI), and 1.25 units of AmpliTaq Gold (Roche, Brandenburg, NJ) on 96-well iCycler iQ plates (BioRad Laboratories). All PCR protocols included a 5-min polymerase activation step followed by 40 cycles consisting of a 95°C denaturation for 20 sec, annealing at 60°C for 30 sec, and an elongation step at 72°C for 30 sec with a final extension step for 5 min at 72°C. Melt curves (iCycler, BioRad), agarose gel electrophoresis, and standard sequencing procedures were used to examine each sample for purity and specificity (ABI PRISM 3100 Genetic Analyzer, Applied Biosystems, Foster City, CA). Standard curves constructed by plotting the relative starting amount versus threshold cycles were generated using serial fourfold dilutions of pooled DNA fractions containing DNA from healthy dogs. The amplification efficiency, E (%) = $(10^{(1/-s)} - 1)*100$ (s=slope), of each standard curve was determined and appeared to be greater than 95% and less than 105%, over a large dynamic range. For each experimental sample the amount of *MURR1* exon-2 and the amount of the endogenous reference *MURR1* exon-3 were determined from the appropriate standard curve in autonomous experiments. Results were normalized according to the average amount of the endogenous reference.

Table 1. *Primer sets*

Gene	Primer sequence (5′–3′)	Annealing	products
MURR1 exon-2	Forward: GACCAAGCTGCTGTCATTTCCAA	60(°C)	122 bp
	Reverse: TTGCCGTCAACTCTCCAACTCA		
MURR1 exon-3	Forward: GTTCATGATCCCTCCCCAGTG	60(°C)	118 bp
	Reverse: AAAGACAAAAGAAATCTCAGCAAGTG		

Animals

For the *MURR1* exon-2 vs. exon-3 expression experiment, nine dogs from our breeding colony were used. These dogs were offspring of Bedlington terriers with copper toxicosis (proven by liver histology) and beagles. Eight of these dogs were known heterozygous carriers; one was homozygous affected. One healthy dog, not Bedlington terrier associated, served as a control. The RT-PCR was performed on liver tissue as described by van de Sluis *et al*. [10]. For further validation 11 dogs from our in house breeding colony (seven from the first experiment and 4 new born affected) were used next to six healthy dogs, not Bedlington terrier associated. In addition, we used stored DNA samples isolated from peripheral blood leukocytes from 20 purebred Bedlington terriers of which the status was assessed with the microsattelite marker C04107.

Results

The results of Q-PCR of exon-2 were expressed as a fraction of the measured amount of exon-3 for which all animals are homozygous. For all eight dogs known to be heterozygous (RT-PCR) the ratio exon-2/exon-3 appeared very close to 0.5. In the single affected dog (RT-PCR) from our colony the ratio was close to zero (Table 2). Because taking buccal swabs is less invasive than blood sampling, we measured in four dogs (two carriers, one affected, and one healthy) the exon-2/exon-3 ratio in buccal swab–derived DNA. These ratios closely resembled the results from whole blood. To make sure that there was no confounding effect of the dogs' age with regard to the exon-2/exon-3 ratio; we measured this ratio repetitively over a wide age range.

As shown in Figure 1, the exon-2/exon-3 ratio was not influenced by age. To compare this new technique with the microsatellite marker C04107, we measured blindly the exon-2/exon-3 ratio in blood samples from 20 purebred Bedlington terriers (Table 3).

Table 2. *Q-PCR on MURR1 exon-2 vs. exon-3 expression in whole blood, in nine mixed-breed dogs and one healthy dog. Nos. 1 to 8-carrier (C) 9 and 10-affected (A) (one dog), 11-healthy (H). Values, measured in triplicate, are expressed as mean ± SE.*

Dog	Liver tissue	*MURR1* exon2/exon3ratio Whole blood
1	C	0.36 ± 0.08
2	C	0.37 ± 0.05
3	C	0.43 ± 0.0
4	C	0.42 ± 0.01
5	C	0.49 ± 0.01
6	C	0.52 ± 0.09
7	C	0.46 ± 0.02
8	C	0.48 ± 0.13
9	A	0.00 ± 0.0
10	A	0.00 ± 0.0
11	H	0.93 ± 0.10

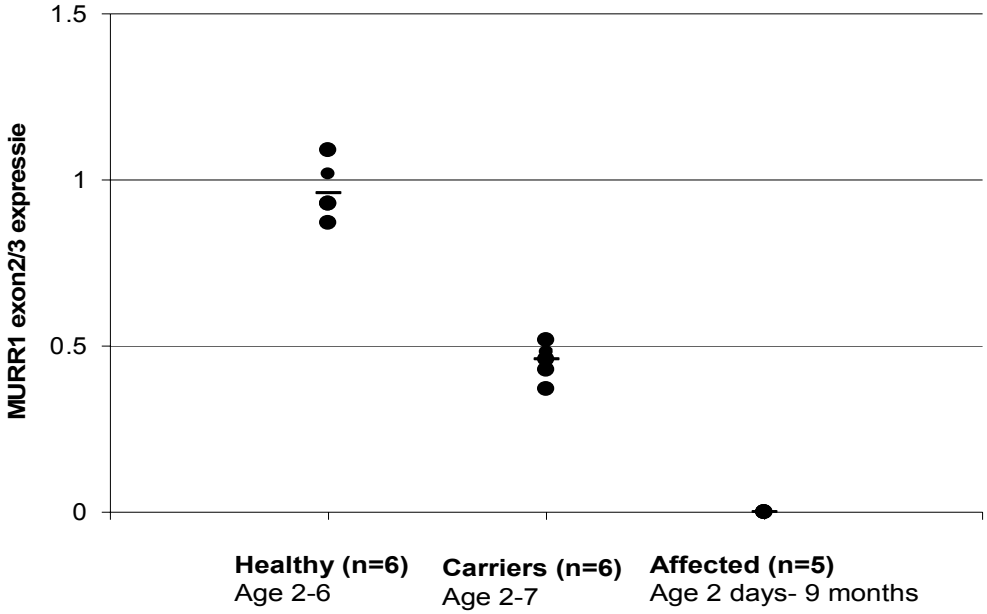

Figure 1. *Quantitative PCR on MURR1 exon-2/exon-3 ratio in healthy, carriers, and affected dogs; long-term reproducibility. In affected dog, ratio was close to zero at each time point. Heavy bar indicates mean within groups.*

Table 3. *MURR1 exon-2 vs. exon-3 expression in 20 pure-bed Bedlington terriers in whole blood, formerly diagnosed with the C04107 microsattelite marker*

Group	Range	Median
Affected (n = 3)	0.002–0.083	0.016
Carrier (n = 11)	0.39–0.60	0.44
Healthy (n = 6)	0.92–1.15	0.99

Discussion

We have found that Q-PCR on DNA isolated from blood samples and buccal swabs permits differentiation between affected, heterozygote, and healthy individuals. The accuracy is very high and it is valid, independent of age. The application of Q-PCR on genomic DNA is principally different from that in RT-PCR reaction. It should be noted that RT-PCR amplification is not a gold standard; it may be hard to read the difference between heterozygotes and healthy homozygotes for two reasons; first, organ-specific splice variants [10], second, low expression levels, as was the case in peripheral blood leukocytes. Quantitative evaluation of PCR products has been developed to analyze differential levels of expression of genes involved in pathways under study. Quantitative analysis at the level of DNA aims at measuring within a narrow variation; there may be zero, one, or two copies of an allele of interest. Therefore, it was critical to evaluate the sensitivity and reproducibility of the measurements performed in this study.

We have validated the method described in several ways. First, we used the non-affected adjacent exon-3 as an internal standard. While the possible forms of exon-2 were absent, present, or double present, the normal exon-3 could be present only twice. Exon-3 could therefore serve as a standardization factor for the outcome of amplification of exon-2, with both PCR reactions being carried out on the same narrow region of genomic DNA. We obtained similar results when the reference gene *GAPDH* was used as an internal standard (data not shown), emphasizing the validity of using exon-3 as an internal standard. Second, all reactions were done in triplicate to analyze the reproducibility, proving little variation in the outcomes of the measurements per sample (Tables 2 and 3, Figure 1). Third, final proof of validation was obtained by performing the quantitative genomic PCR reaction on DNA of animals of which the genetic status could be assessed independently. Our colony of cross-bred dogs was obtained by mating an affected Bedlington terrier sire to healthy beagle dams, producing offspring of obligatory heterozygote carriers. Samples of these dogs could serve as an independent gold standard. In freshly isolated whole-

blood samples, we could test the smallest possible variation 1× exon-2 compared with 2× exon-3 in nine of these dogs. There was 100% agreement between the outcome of the Q-PCR reaction and the genetic status of these nine dogs (Table 2), and also between the outcomes of this new test and those of microsattelite marker C04107 genotyping in 20 Bedlington terriers (Table 3).

This report emphasizes the value of successful application of quantitative genomic PCR for molecular diagnostics of a genetic mutation [15]. This method should therefore be more generally applicable, especially if large genomic deletions are involved, mRNA levels are very low, or there is the presence of splice variants. It should also be possible to develop a test for other mutations that cannot be evaluated with standard methods by variants of this quantitative genomic PCR reading.

The *MURR1* gene that underlies a newly discovered copper storage disease has to be analyzed with respect to its function in copper homeostasis. From its phenotypical impact in dogs with the disease, one may conclude that *MURR1* has a major role in the cellular handling of copper. In analogy to dogs, defects in this gene will also appear to relate to pathologies in humans and rodent models, as emphasized by recent publications. For instance, Tao *et al*. [16] demonstrated that the Wilson disease protein, a copper-transporting ATPase, directly interacts with the human homolog of *MURR1 in vitro* and *in* vivo. Ganesh *et al*. [6] found that MURR1 restricts HIV-1 replication in resting $CD4^+$ lymphocytes. Furthermore, Burstein *et al*. [8] discovered an association between the anti-apoptotic protein XIAP and MURR1. Biasio *et al*. [7] showed that the MURR1 protein functions as a regulator of the human δ epithelial sodium channel. Genetic screening for *MURR1* mutations is thus expected to become very important in comparative studies on the role of *MURR1* in different cellular processes in man and animals.

References

[1] Hardy RM, Stevens JB, Stowe CM. Chronic progressive hepatitis in Bedlington terriers associated with elevated liver copper concentrations. Minn Vet 1975, 15:13–24.

[2] Johnson GF, Sternlieb I, Twedt DC, et al. Inheritance of copper toxicosis in Bedlington Terriers. Am J Vet Res 1980, 41:1865–1866.

[3] Su LC, Ravanshad S, Owen CA Jr, et al. A comparison of copper-loading disease in Bedlington terriers and Wilson's disease in humans. Am J Physiol 1982, 243:G226–G230.

[4] Twedt DC, Sternlieb I, Gilbertson SR. Clinical, morphologic, and chemical studies on copper toxicosis of Bedlington terriers. J Am Vet Med Assoc 1979,175:269–275.

[5] Heritage ME, Seymour CA, White RAS, et al. Inherited copper toxicosis in the Bedlington terriers: prevalence in asymptomatic dogs. J Small Anim Pract 1987, 28:1141–1151.

[6] Ganesh L, Burstein E, Guha–Niyogi A, et al. The gene product Murr1 restricts HIV-1 replication in resting CD4+ lymphocytes. Nature 2003, 426:853–857.

[7] Biasio W, Chang T, McIntosh CJ, et al. Identification of Murr1 as a regulator of the human delta epithelial sodium channel. J Biol Chem 2003, 279:5429–5434.

[8] Burstein E, Ganesh L, Dick RD, et al. A novel role for XIAP in copper homeostasis through regulation of MURR1. EMBO J 2003, 23:244–254.

[9] Yuzbasiyan–Gurkan V, Blanton SH, Cao Y, et al. Linkage of a microsatellite marker to the canine copper toxicosis locus in Bedlington terriers. Am J Vet Res 1997, 58:23–27.

[10] Van de Sluis BJ, Rothuizen J, Pearson PL, van Cost BA, et al. Identification of a new copper metabolism gene by positional cloning in a purebred dog population. Hum Mol Genet 2002, 2:165–173.

[11] Haywood S, Fuentealba 1C, Kemp SJ, et al. Copper toxicosis in the Bedlington terrier: a diagnostic dilemma. J Small Anim Pract 2001, 42:181–185.

[12] Van de Sluis BJ, Peter AT, Wijmenga C. Indirect molecular diagnosis of copper toxicosis in Bedlington terriers is complicated by haplotype diversity. J Hered 2003, 94:256–259.

[13] Coronado VA, Damaraju D, Kohijoki R, et al. New haplotypes in the Bedlington terrier indicate complexity copper toxicosis. Mamm Genome 2003, 14:483–491.

[14] Klomp AE, van de Sluis BJ, Klomp LW, et al. The ubiquitously expressed MURR1 protein is absent in canine copper toxicosis. J Hepatol 2003, 39:703–709.

[15] Faugere V, Tuffery–Giraud S, Hamel C, et al. Identification of three novel OAI gene mutations identified in three families misdiagnosed with congenital nystagmus and carrier status determination by real-time quantitative PCR assay. BMC Genet 2003, 4:1.

[16] Tao TY, Liu F, Klomp L, et al. The copper toxicosis gene product Murr1 directly interacts with the Wilson disease protein. J Biol Chem 2003, 43:41593–41596.

Chapter 9

Impaired copper metabolism in hepatic epithelial cells after RNA interference targeting COMMD1

Bart Spee[1], Brigitte Arends[1], Ank M.T.C. van Wees[1], Peter Bode[2], Louis C. Penning[1], and Jan Rothuizen[1].

From the [1]Department of Clinical Sciences of Companion Animals, Faculty of Veterinary Medicine, Utrecht University, The Netherlands and the [2]Interfacultary Reactor Institute, Delft University, the Netherlands.

Submitted

Abstract

A deletion in the copper metabolism MURR1 domain-containing protein 1 (COMMD1) is associated with hepatic copper toxicosis in dogs. Although a role in copper metabolism of COMMD1 has been suggested, evidence of copper retention in COMMD1 depleted hepatic epithelial cells has not been shown. We used dog hepatic epithelial cells and analysed the copper metabolic function after siRNA mediated COMMD1 knock-down. An 80% reduction for both mRNA and protein was obtained with 50 nM siRNA. Exposure to ^{64}Cu resulted in a 1.5-fold increase in copper-retention in COMMD1 depleted cells. COMMD1 depleted cells were almost three times more sensitive to high extra-cellular copper concentrations. Copper-mediated regulation of MT1A gene expression was additively induced in COMMD1 depleted cells upon extra-cellular copper treatment. Q-PCR on most other copper excretory and storage gene-products did not indicate any compensatory effect after COMMD1 depletion. We conclude that COMMD1 has a major function in copper retention in hepatic epithelial cells.

Introduction

The COMMD family is characterized by the presence of a conserved and unique motif called COMM (Copper Metabolism MURR1 containing) domain [1]. COMMD1, previously known as MURR1, functions as an interface for protein-protein interactions [2]. Several functions of COMMD1 have been reported such as the regulation of sodium transport, and copper metabolism [3,4]. Recently COMMD1 has also been associated with other cells such as T-cells, where COMMD1 inhibits HIV-1 growth in unstimulated CD4+ T-cells [5]. This inhibition was mediated in part through its ability to inhibit basal and cytokine-stimulated nuclear factor NF-kappaB activity [2]. *In vivo* studies are hampered due to lack of *COMMD1*$^{-/-}$ mice. *COMMD1* was shown to be mutated in Bedlington terriers in association with massive accumulation of hepatic copper subsequently leading to increased oxidative stress, hepatitis, and finally cirrhosis [6]. The deletion of exon-2 in Bedlington terriers leads to the complete absence of the protein [7]. The phenotype of the affected Bedlington terriers does not indicate a role for COMMD1 in sodium transport or immune regulation.

The precise role of COMMD1 in copper metabolism has not yet been fully elucidated. In a human embryonic kidney epithelial cell line mRNA interference experiments showed an increased retention of copper in kidney cells (HEK293) during silencing of the gene [8]. *COMMD1*, which has the highest expression in the liver, was also found to be expressed in heart, kidney, muscle, and placenta [7]. However, in the Bedlington terriers copper accumulation is restricted to the liver only. For further elucidation of the role of COMMD1 in hepatic copper metabolism, studies in liver cells, preferably derived from dogs, are therefore required.

In order to clarify the role of COMMD1 in copper metabolism of dog liver epithelial cells we used a RNA interference (RNAi) strategy to target the COMMD1 gene product. Small interfering RNA's (siRNA's) have been shown to be of great value in knocking down specific gene-products in a variety of biological systems [9-12]. COMMD1 specific siRNA's were transfected into bile-ductular epithelial (BDE) cells which display all characteristics of hepatocytes, such as production of serum albumin and ceruloplasmin. Furthermore we investigated the differences in ^{64}Cu retention and cell-viability in BDE cells after COMMD1 gene silencing with siRNA's. Differential expression of genes involved in known pathways of copper metabolism was measured to evaluate effects of the loss of COMMD1 on these pathways. Our results (i) confirmed that COMMD1 has an essential role in copper accumulation in hepatic epithelial cells; (ii) gave no indications for general compensatory mechanisms; (iii) showed that COMMD1 depletion sensitizes canine hepatic cells to high

extracellular copper levels; (iv) copper-mediated up-regulation of metallothionein by excessive copper levels is increased in COMMD1 depleted cells.

Materials and methods

Hepatic epithelial cells

Canine bile-duct epithelial (BDE) cells were acquired from the Amsterdam Medical Center, Experimental Liver cell bank (Amsterdam, The Netherlands) [13]. BDE cells are characterized by ceruloplasmin and serum albumin expression (data not shown), exemplifying its hepatic stem cell origin. BDE cells were grown in DMEM (Life Technologies, Inc., Invitrogen, Breda, The Netherlands) supplemented with 580 mg/l glutamine, 10 μg/ml gentamicin, and 10% (v/v) heat-inactivated fetal calf serum (FCS; Harlan Sera-Lab, Loughborough, United Kingdom) at 37°C in a humidified atmosphere of 5% CO_2 in air. Cells were split once every week, all measurements were performed within 15 passages. Mycoplasma testing was performed once every two months, all measurements were deemed negative (data not shown).

Establishment of COMMD1 knock-down in canine BDE cells

For silencing experiments, Stealth™ dsRNA molecules were obtained from Invitrogen. A specific sequence for canine COMMD1 silencing (5'-CCCUGUUGC-CAUAAUGGAGCUGGAA-3') was selected after general recommendations (In-vitrogen) and was designed from the canine COMMD1 gene sequence (Genbank accession number NM_001003055). A nonsense sequence was used as a negative control (5'-GCAGGUGCUAGUACAAGUCCGACAA-3'). Transfection was perfor-med with the Magnet Assisted Transfection (MATra) technique (IBA BioTAGno-logy/Westburg b.v., Leusden, The Netherlands), in combination with Lipofect-amine2000™ (Invitrogen), according to the manufacturer's instructions. In short, 50 nM siRNA molecules were transfected into the cell-lines in the presence of an opti-mized concentration Lipofectamin2000™ (1.2 μl/ml), for 20 minutes on the plate magnet under cell-culture conditions. After transfection, cells were washed twice with HBBS and growth media including antibiotics replaced the transfection media. Control samples were mock transfected with Lipofectamine2000™ and magnetic beads from the MATra technique, a nonsense siRNA transfection was also used.

Copper treatment

BDE cells were plated into 96-well plates in a final concentration of $0.4*10^5$ cells/ml in supplemented DMEM media. Cells were transfected with media (control), COMMD1 siRNA's, or nonsense siRNA's 24 hours after seeding. For copper treatment, a copper wire was dissolved in 50 µl concentrated HNO_3 (10.3 M) and neutralized with 1.3 ml 0.5 M NaOH. DMEM media with additives was added to a final concentration of 4.7 mM copper. A serial dilution of 600 to 0 µM copper was used in DMEM media with additives. Treatment started 24 hours after transfection. 48 Hours after treatment, proliferation and viability was measured with a MTT assay (5 mg/ml). Statistical significance of differences in viability of the COMMD1 siRNA treated cell-lines at different copper concentrations compared to control cells was determined by a one-way ANOVA using the Dunnett multiple comparisons test. $P< 0.05$ was considered to indicate statistical significance. Analysis was performed using SPSS software (SPSS Benelux, Gorinchem, the Netherlands).

RNA isolation and Reverse-transcription polymerase chain reaction

For total cellular RNA isolation we used the Qiagen RNeasy Mini Kit (Qiagen, Leusden, The Netherlands) according to the manufacturer's instructions. In short, RNA was isolated from each sample by adding 350 µl lysis buffer (RLT containing 1 % (v/v) β-mercaptoethanol) directly after decanting the media. The RNA samples were treated with DNase-I (Qiagen RNase-free DNase kit). In total 3 µg of RNA were incubated with poly(dT) primers at 42°C for 45 min, in a 60 µl reaction volume, using the Reverse Transcription System from Promega (Promega Benelux, Leiden, The Netherlands).

Quantitative measurements of the mRNA levels

Quantitative real-time PCR (Q-PCR) was performed on a total of 9 gene products; GAPDH, HPRT, COMMD1, ATOX1, COX17, ATP7B, metallothionein (MT1A), ceruloplasmin (CP), and X-linked inhibitor of apoptosis (XIAP). The abundance of mRNA was measured by real-time quantitative PCR using appropriate primers (Table 1) as previously described [14]. In short, Q-PCR was based on the high affinity double-stranded DNA-binding dye SYBR® green I. For each experimental sample, the amount of the gene of interest and of the two independent endogenous references (glyceraldehyde-3-phosphate dehydrogenase (GAPDH) and hypoxanthine phosphoribosyl transferase (HPRT)) was determined from the appropriate standard curve in independent experiments. If relative amounts of GAPDH and HPRT were constant for a sample, data were considered valid and the average amount was in-

cluded in the study (data not shown). Results were normalized according to the average amount of the endogenous references. The normalized values were divided by the normalized values of the calibrator (healthy group) to generate relative expression levels [15]. Statistical significance of differences between treated and control samples were determined by using the Mann-Whitney U-test. A p-value < 0.05 was considered statistically significant. Analysis was performed using SPSS software (SPSS Benelux, Gorinchem, The Netherlands).

Western blot analysis

Samples were homogenized in 350 µl RIPA buffer containing 1 % Igepal, 0.6 mM PhenylMethylSulfonyl Fluoride (PMSF), 17 µg/ml aprotinine, and 1 mM sodium orthovanadate (Sigma chemical Co., Zwijndrecht, The Netherlands) for 30 minutes on ice. Protein concentrations were obtained using a Lowry-based assay (DC Protein Assay, BioRad, Veenendaal, The Netherlands). Fifteen µg of protein of the supernatant was denatured for 3 min at 95^{o}C, electrophoresis was performed on 15 % Tris-HCl polyacrylamide gels (BioRad). Proteins were transferred onto Hybond-C Extra Nitrocellulose membranes (Amersham Biosciences Europe, Roosendaal, The Netherlands) using a Mini Trans-Blot® Cell blot-apparatus (BioRad). The procedure for immunodetection was based on an ECL Western blot analysis system, performed according to the manufacturer's instructions (Amersham Biosciences Europe). The membranes were incubated with 4 % ECL blocking solution and 0.1 % Tween 20 (Boom B.V., Meppel, The Netherlands) in TBS for 1 hour under gentle shaking. Primary antibodies were incubated at 4^{o}C overnight. For COMMD1 a mouse anti-dog COMMD1 antibody (obtained from the department of metabolic diseases, Wilhelmina Children's Hospital, The Netherlands) was used in a dilution of 1:1,000 in TBST with 4% BSA. As a loading control a mouse anti-dog Beta-Actin antibody was used in a 1:2,000 dilution in TBST with 4% BSA. After washing, the membranes were incubated with a goat anti-mouse antibody (R&D Systems-/Westburg b.v.) in TBST with 4% BSA for 1 hour at room temperature. Exposures were made with Kodak BioMax Light-1 films (Sigma chemical Co.). Densitometric analysis of immunoreactive bands was performed with a Gel Doc 2000 system coupled to the Quantity One 4.3.0 software (BioRad).

Table 1. *Nucleotide Sequences of Dog-Specific Primers for Quantitative Real-Time PCR*

Gene	F/R	Sequence (5'-3')	Tm (°C)	Product size (bp)	Accession number
GAPDH	F	TGT CCC CAC CCC CAA TGT ATC	58	100	AB038240
	R	CTC CGA TGC CTG CTT CAC TAC CTT			
HPRT	F	AGC TTG CTG GTG AAA AGG AC	56	100	L77488 /
	R	TTA TAG TCA AGG GCA TAT CC			L77489
COMMD1	F	GAC CAA GCT GCT GTC ATT TCC AA	58	122	AY047597
	R	TTG CCG TCA ACT CTC CAA CTC A			
ATP7B	F	GGT GGC CAT CGA CGG TGT GC	56	136	AY603039
	R	CGT CTT GCG GTT GTC TCC TGT GAT			
MT1A	F	AGC TGC TGT GCC TGA TGT G	64	130	D84397
	R	TAT ACA AAC GGG AAT GTA GAA AAC			
COX17	F	ATC ATT GAG AAA GGA GAG GAG CAC	60	127	AY603041
	R	TTC ATT CTT CAA GGA TTA TTC ATT TAC A			
ATOX1	F	ACG CGG TCA GTC GGG TGC TC	67	137	AF179715
	R	AAC GGC CTT TCC TGT TTT CTC CAG			
CP	F	AAT TCT CCC TTC TGT TTT TGG TT	62	97	AY572227
	R	TTG TTT ACT TTC TCA GGG TGG TTA			
XIAP	F	ACT ATG TAT CAC TTG AGG CTC TGG TTT C	54	80	AY603038
	R	AGT CTG GCT TGA TTC ATC TTG TGT ATG			

F: Forward primer; R: reversed primer

Radioactive Copper Analysis

BDE cells were plated into 6-well plates in a final concentration of $0.4*10^5$ cells/ml in supplemented DMEM media. Cells were transfected with media (control), COMMD1 siRNA's, or nonsense siRNA's 24 hours before treatment as described above. Cells were treated with three different copper concentrations in independent experiments; 100, 50, and 25 μM copper. An MTT assay (5 mg/ml) was ran in parallel to measure the viability to correct for cell-death due to copper treatment. The ^{64}Cu isotope was made using metallic copper wire (1.5 mg) that was irradiated over-night in a reactor at a thermal neutron flux rate of $5*10^{16}$ $m^{-2}s^{-1}$, providing an induced activity of approximately 35 $MBq.mg^{-1}$. Upon arrival, approximately four hours after irradiation and 30 minutes prior to the start of the study, the copper wire was dissolved in 50 μl concentrated HNO_3 (10.3 M) and neutralized with 1.3 ml 0.5 M NaOH. DMEM media was added to a final concentration of 4.7 mM copper. Cells

were incubated in 100, 50, and 25 μM copper for 48 hours. After treatment media was removed and cells were washed three times with Hanks. After washing 2 ml of 0.2% (w/v) SDS in ETN buffer (10 nmol EDTA, 10 mmol Tris-HCl, and 100 mmol NaCl pH 7.0) was added to lyse the cells and cell-lysates were pipetted into counting tubes. Emission was measured in individual tubes containing media, washing steps, or lysate in a Packard B5003 gamma-counter (Packard BioScience Benelux, Groningen, The Netherlands) between 450 and 800 keV for 2 minutes. Statistical signifycance of differences in gamma-counts of the COMMD1 depleted cell-lines compared to control and mock treated cells were determined by a one-way ANOVA using the Dunnett multiple comparisons test. $P < 0.05$ was considered to indicate statistical significance. Analysis was performed using SPSS software (SPSS Benelux, Gorinchem, the Netherlands).

Results

COMMD1 Gene-silencing

Using the Lipofectamine reagent, we transfected canine hepatic epithelial cells with siRNA based on the canine COMMD1 gene sequence. The transfection-efficiency was optimized and proved to be greater than 95% of the total amount of cells (assayed with FITC-labeled siRNA). Staining was observed in the cytoplasm and partially surrounding the nucleus (data not shown). When treated with the optimal amount of siRNA (50 nM) for 72 hours, the COMMD1 expression was markedly reduced (Figure 1A). Cells treated with nonsense siRNA exhibited a similar expression pattern as the untreated control cells (Figure 1A). Western blotting (Figure 1B) yielded a 25 kDa band immunoreactive to COMMD1 in the untreated control and nonsense siRNA transfected samples. At 48 h after transfection a marked decrease was observed in signal intensity for COMMD1 compared to controls. Densitometric analysis indicated an 80% reduction of COMMD1 protein levels in the siRNA treated samples. Gene-expression measurements and protein analysis did not indicate any effect on COMMD1 levels treated with different concentrations of extracellular copper over a two-day period.

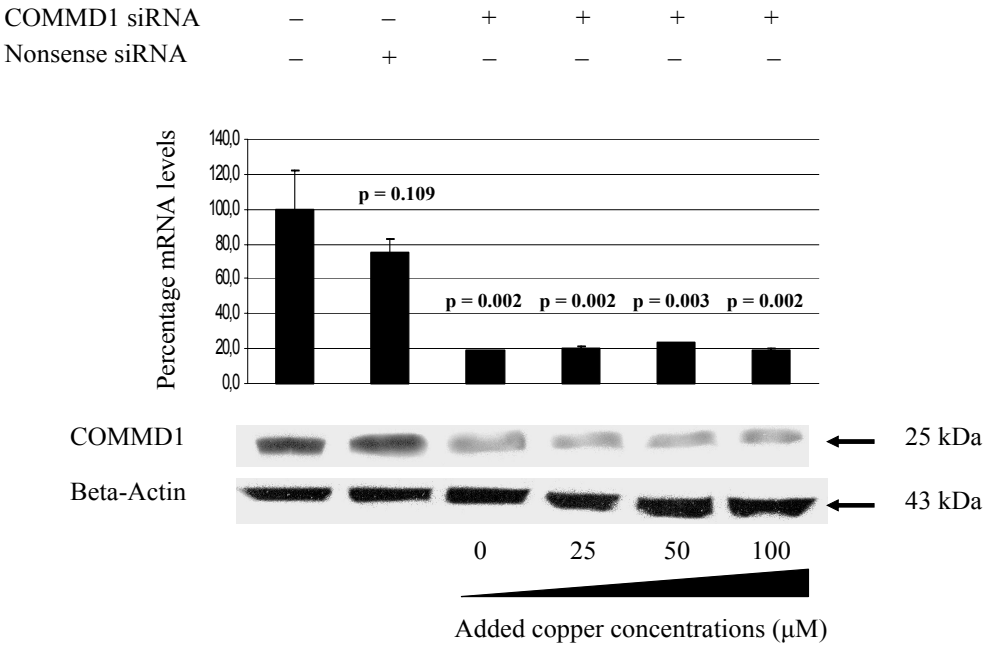

Figure 1. *Relative mRNA levels of BDE cells for COMDD1 is shown in (A). Western blot analysis for the 25 kDa COMDD1 and loading control beta-actin (43 kDa) is shown in (B), data expressed as mean + SD. Statistical significance of differences between treated and control samples were determined by using the Mann-Whitney U-test. A p-value < 0.05 was considered statistically significant.*

Gene-expression measurements on copper-metabolism proteins

Gene-expression of several products involved in copper metabolism were measured to gain insight into the effect of COMMD1 knockdown in BDE cells; e.g. ATOX1, COX17, ATP7B, MT1A, CP, and XIAP. In Figure 2, results showed no significant changes in gene-expression of the nonsense siRNA treated samples. In contrast, the COMMD1 siRNA treated samples did show a two-fold decrease in gene-expression of the copper chelating proteins COX17 and ATOX1. Ceruloplasmin (CP), an important excretory protein also showed a two-fold decrease in gene-expression in the COMMD1 depleted cells. ATP7B, an ATPase from the trans-Golgi network involved in copper metabolism showed a similar result in a two-fold decrease in gene-expression. The mRNA levels of XIAP, recently linked with COMMD1, was also reduced two-fold. In contrast metallothionein (MT1A), an important copper storage protein did not show any changes after treatment with siRNA's.

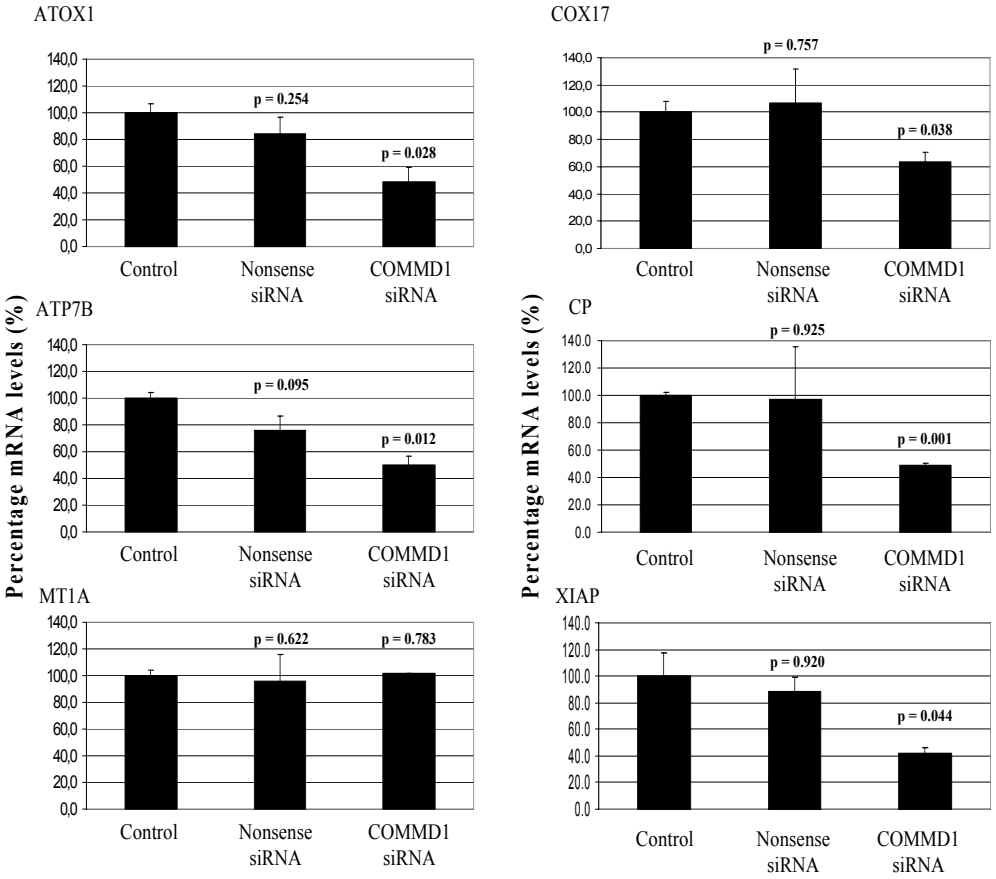

Figure 2. *Gene-expression analysis of copper metabolism related proteins. Gene-expression of copper associated proteins, e.g. ATOX1, COX17, ATP7B, MT1A, CP, and XIAP, was measured three days after transfection. Data depicts mean + SD. Statistical significance of differences between treated and control samples were determined by using the Mann-Whitney U-test. A p-value < 0.05 was considered statistically significant.*

Copper treatment on BDE cells

The sensitivity towards extracellular copper of COMDD1 depleted cells was determined by the frequently used MTT cell viability assay. Mock transfected cells and nonsense siRNAs were used as a control. Results in Figure 3 showed that the ED_{50} of the COMMD1 depleted cells was reduced almost three-fold from approximately 70 to 27 µg/ml.

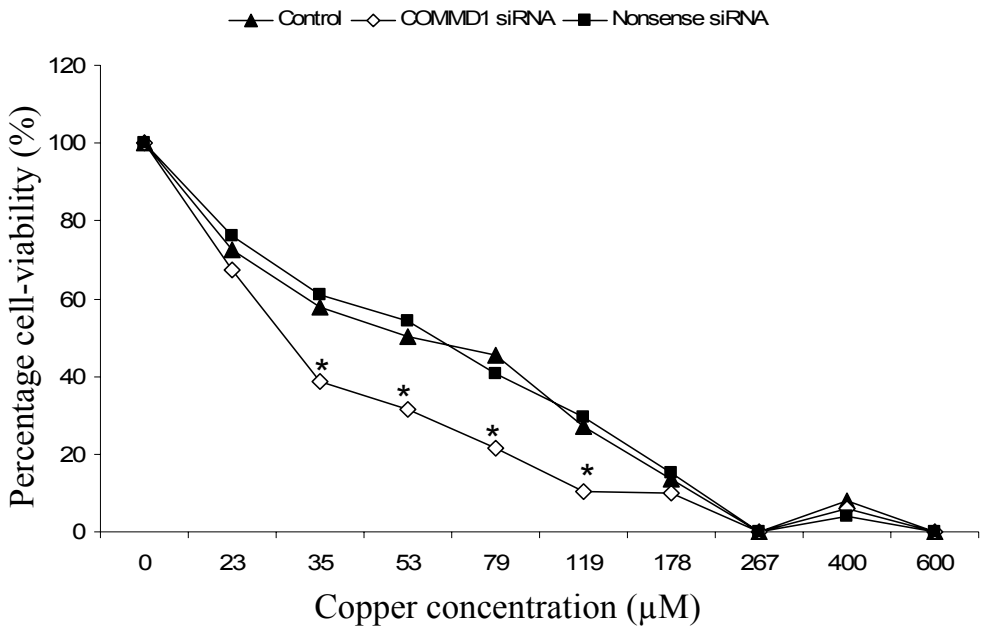

Figure 3. *Cell viability after two day copper treatment with a serial dilution of copper. Viability of mock transfected (control), COMMD1 siRNA treated, and nonsense treated BDE cells after a two-day treatment of a serial dilution of copper. Viability was assessed with an MTT assay and corrected to percentage viability. MTT measurements did not indicate a decrease in viability in the non-copper treated samples (data not shown) between control, COMMD1 treated, and nonsense treated. Statistical significance of differences in viability of the COMMD1 siRNA treated cell-lines at different copper concentrations compared to control cells was determined by a one-way ANOVA using the Dunnett multiple comparisons test. * = $p < 0.05$ was considered to indicate statistical significance.*

Measurements on radioactive labeled copper in COMMD1 depleted cells

BDE cells were treated with different copper concentrations (0, 25, 50, 100 μM) for two days, control remained untreated. A MTT assay was run in parallel to correct for cellular-death. Results (Figure 4) showed the average amount of gamma-counts corrected for the percentage viable cells. After 2 days in the presence of 25 μM copper retention was not statistically different between COMMD1 depleted and mock- and nonsense-treated control cells. With increasing extracellular copper concentrations a significant difference between COMMD1 depleted and control cells occurred. Copper retention was increased 1.5-fold in the 100 μM copper treated COMMD1 siRNA treated group.

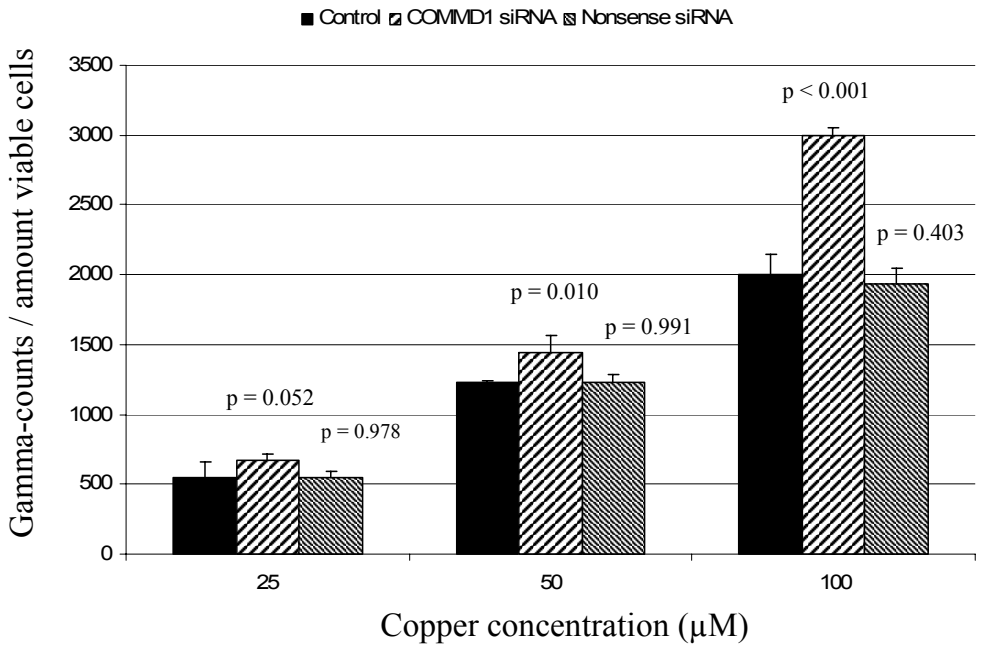

Figure 4. *Copper isotope measurements in COMMD1 depleted cells. Copper isotope (^{64}Cu) measurements in mock transfected (control), COMMD1 siRNA treated, and nonsense treated BDE cells after a two-day treatment of a 25 μM, 50 μM, and 100 μM ^{64}Cu. Gamma-counts were corrected for cellular death by means of an MTT assay which ran in parallel. Statistical significance of differences in gamma-counts of the COMMD1 depleted cell-lines compared to control and mock treated cells were determined by a one-way ANOVA using the Dunnett multiple comparisons test. A p-value < 0.05 was considered statistically significant.*

Copper effects on Metallothionein gene-expression in COMMD1 depleted cells

Metallothionein (MT1A) is known to be regulated by intracellular copper levels [17]. In order to show copper effects on MT1A gene-expression, cells were exposed to the same copper concentration range as in the survival and copper accumulation experiment. As depicted in Figure 5, MT1A mRNA expression is upregulated two-fold after 50 μM copper, and seven-fold after 100 μM copper treatments in COMMD1 expressing cells. Interestingly COMMD1 depleted cells showed a 15-fold increase in MT1A expression after 100 μM copper treatment. Statistical analysis showed a significant change in the 100 μM treated group between non-depleted and COMMD1 depleted cells.

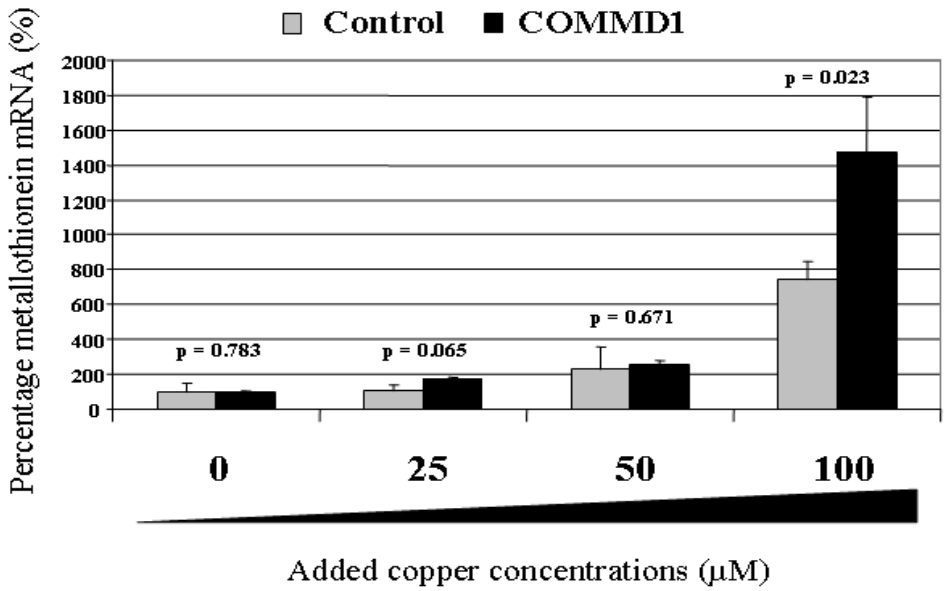

Figure 5. *Gene-expression analysis of metallothionein after copper treatment. Gene-expression of copper metallothionein (MT1A) two days after copper treatment. Data depicts mean + SD. Statistical significance of differences between treated and control samples were determined by using the Mann-Whitney U-test. A p-value < 0.05 was considered statistically significant.*

Discussion

COMMD1 was discovered after positional cloning and is responsible for an autosomal recessive form of hepatic copper toxicosis that affects Bedlington terriers [6]. Although an interaction with ATP7B was already described [18], the mechanism by which COMMD1 affects copper metabolism remains elusive. Here we report the characterization of COMMD1 depleted hepatic epithelial cells in order to describe the functions of the COMMD1 protein.

Recently some exceptions of mutated *COMMD1* were found in different breeds not resulting in increased hepatic copper [19]. It could be hypothesed in these cases yet another copper chaperone was responsible for the excretion (or storage) of excess copper. First choice of such compensatory proteins is ceruloplasmin or metallothionein. In our studies we examined possible compensatory effects of these proteins. Although ceruloplasmin seemed to be reduced in COMMD1 depleted cells, metallothionein did show an increase after copper treatment (Figure 2). The underlying

mechanisms leading to the changed mRNA levels of copper related gene products, other then COMMD1, needs further exploration. The observation that 25 μM copper treatment only slightly reduced cell-viability (Figure 3) indicated the cells ability to overcome the toxic effects when copper is presented in moderate amounts.

The reduction in XIAP mRNA levels as seen in the COMMD1 depleted cells (Figure 2) could decrease the cell-viability because XIAP is a major apoptosis inhibitory protein [20, 21]. The MTT measurements between mock transfected, nonsense siRNA-treated, and COMMD1 depleted cells were equal in standard media indicating a similar cellular homeostasis. In the presence of high extra-cellular copper concentrations, COMMD1 depleted cells are indeed much more vulnerable for excessive extra-cellular copper than the nonsense and mock-controls. Studies in dogs showed that D-penicillamin improved liver pathology Dobermann dogs with subclinical hepatitis [22]. This is indicative for a primary role of copper in toxicity rather than a secondary effect or an epiphenomenon.

At present no human copper storage diseases are associated with COMMD1 mutations and no *COMMD1*$^{-/-}$ mice are available. In view of the relevance of the BDE cell line and the species used in this study, these *in vitro* data can be extrapolated to the only known clinical cases associated with COMMD1 mutations; hepatic copper accumulation in Bedlington terriers [23]. To facilitate future research, we have an in-house dog breed (mixed Bedlington with Beagle) that is homozygous for the exon-2 deletion in *COMMD1*. This allows us to study longitudinally and in great detail how copper toxicosis develops *in vivo*. More general, these dogs are potential animal models for chronic liver diseases, since at the genetic, clinical, and physical parameters, dogs resemble the human clinical situation much closer than mice [24].

COMMD1 is localized within the cytoplasma within perinuclear compartments that do not represent mitochondria or lysozomes [7]. This observation together with the observed copper accumulation in COMMD1 depleted cells indicates the excretory function of COMMD1. Copper accumulation has previously been detected in COMMD1 depleted Human Embryonic Kidney (HEK) 293 Cells [8]. As copper is transferred to blood in the intestine, the liver is the first organ involved in the detoxification of high amounts of copper. In our measurements we show copper metabolism in a mammalian hepatic epithelial cell line with several biochemical techniques.

We have shown that siRNA directed against canine COMMD1 strongly down regulate both COMMD1 mRNA and protein levels. This effect cannot be reverted by

high concentrations of extra-cellular copper (Figure 1). A reduction of COMMD1 levels resulted in a higher sensitivity of these cells for extra-cellular copper concentrations (Figure 3). Clearly copper accumulation is higher in COMMD1 depleted cells than in the mock and nonsense siRNA treated cells (Figure 4). Finally, MT1A, which is strongly inducible by copper, is twice as much increased in COMMD1 depleted cells. Taken together, in this study we showed the importance of COMMD1 in copper metabolism with its excretory function in hepatic epithelial cells.

Acknowledgements

The authors would like to acknowledge Prof. Cisca Wijmenga, Dr. Leo Klomp, and Patricia Muller for the use of the COMMD1 antibody.

References

[1] Burstein E, Hoberg JE, Wilkinson AS, et al. COMMD proteins, a novel family of structural and functional homologs of MURR1. J Biol Chem 2005, 280:22222-22232.

[2] de Bie P, van de Sluis B, Klomp L, et al. The Many Faces of the Copper Metabolism Protein MURR1/COMMD1. J Hered 2005, 96:803-811.

[3] Biasio W, Chang T, McIntosh CJ, et al. Identification of Murr1 as a regulator of the human delta epithelial sodium channel. J Biol Chem 2004, 279:5429-5434.

[4] Forman OP, Boursnell ME, Dunmore BJ, et al. Characterization of the COMMD1 (MURR1) mutation causing copper toxicosis in Bedlington terriers. Anim Genet 2005, 36:497-501.

[5] Ganesh L, Burstein E, Guha-Niyogi A, et al. The gene product Murr1 restricts HIV-1 replication in resting CD4+ lymphocytes. Nature 2003, 426:853-857.

[6] van de Sluijs B, Rothuizen J, Pearson PL, et al. Identification of a new copper metabolism gene by positional cloning in a purebred dog population. Hum Mol Genet 2002, 11:165-173.

[7] Klomp AE, van de Sluijs B, Klomp LW, et al. The ubiquitously expressed MURR1 protein is absent in canine copper toxicosis. J Hepatol 2003, 39:703-709.

[8] Burstein E, Ganesh L, Dick RD, et al. A novel role for XIAP in copper homeostasis through regulation of MURR1. EMBO J 2004, 1:244-254.

[9] Dorsett Y, Tuschl T. siRNAs: applications in functional genomics and potential as therapeutics. Nat Rev Drug Discov 2004, 3:318-329.

[10] Dykxhoorn DM, Novina CD, Sharp PA. Killing the messenger: short RNAs that silence gene expression. Nat Rev Mol Cell Biol 2003, 4:457-467.

[11] Scherr M, Morgan MA, Eder M. Gene silencing mediated by small interfering RNAs in mammalian cells. Curr Med Chem 2003, 10:245-256.
[12] Sorensen DR, Leirdal M, Sioud M. Gene silencing by systemic delivery of synthetic siRNAs in adult mice. J Mol Biol 2003, 327:761-766.
[13] Oda D, Savard CE, Nguyen TD, et al. Dog pancreatic duct epithelial cells: long-term culture and characterization. Am J Pathol 1996, 148:977-985.
[14] Spee B, Mandigers PJ, Arends B, et al. Differential expression of copper-associated and oxidative stress related proteins in a new variant of copper toxicosis in Doberman pinschers. Comp Hepatol 2005, 4:3.
[15] Vandesompele J, de Preter K, Pattyn F, et al. Accurate normalization of real-time quantitative RT-PCR data by geometric averaging of multiple internal control genes. Genome Biol 2002, 3:RESEARCH0034.
[16] Coyle P, Philcox JC, Carey LC, et al. Metallothionein: the multipurpose protein. Cell Mol Life Sci 2002, 59:627-647.
[17] Sternlieb I. Copper toxicosis of the Bedlington terrier. J Rheumatol Suppl 1981, 7:94-95.
[18] Tao TY, Liu F, Klomp L, et al. The copper toxicosis gene product Murr1 directly interacts with the Wilson disease protein. J Biol Chem 2003, 278:41593-41596.
[19] Hyun C, Lavulo LT, Filippich LJ. Evaluation of haplotypes associated with copper toxicosis in Bedlington Terriers in Australia. Am J Vet Res 2004, 65:1573-1579.
[20] Nachmias B, Ashhab Y, Ben-Yehuda D. The inhibitor of apoptosis protein family (IAPs): an emerging therapeutic target in cancer. Semin Cancer Biol 2004, 14:231-243.
[21] Yang YL, Li XM. The IAP family: endogenous caspase inhibitors with multiple biological activities. Cell Res 2000, 10:169-177.
[22] Fuentealba IC, Aburto EM. Animal models of copper-associated liver disease. Comp Hepatol 2003, 2:5.
[23] Mack GS. Cancer researchers usher in dog days of medicine. Nat Med 2005, 11:1018.

Chapter 10

Specific down-regulation of XIAP with RNA interference enhances the sensitivity of canine tumor cell-lines to TRAIL and doxorubicin

Bart Spee, Martijn D.B. Jonkers, Brigitte Arends, Gerard R. Rutteman, Jan Rothuizen and Louis C. Penning.

From the Department of Clinical Sciences of Companion Animals, Faculty of Veterinary Medicine, Utrecht University, the Netherlands.

Submitted

Abstract

Apoptosis resistance occurs in various tumors. The anti-apoptotic XIAP protein is responsible for inhibiting apoptosis by reducing caspase-3 activation. Our aim is to evaluate whether RNA inhibition against XIAP increases the sensitivity of canine cell-lines for chemotherapeutics such as TRAIL and doxorubicin. We used small inhibiting RNA's (siRNA) directed against XIAP in three cell-lines derived from bile-duct epithelia (BDE), mammary carcinoma (P114), and osteosarcoma (D17). These cell-lines represent frequently occurring canine cancers and are highly comparable to their human counterparts. XIAP knock-down was measured by means of quantitative PCR (Q-PCR) and Western blotting. The XIAP depleted cells were treated with a serial dilution of TRAIL or doxorubicin and compared to mock- and nonsense-treated controls. Viability was measured with a MTT assay. All XIAP siRNA treated cell-lines showed a mRNA knock-down over 80 percent. Western blot analysis confirmed mRNA measurements. No compensatory effect of IAP family members was seen in XIAP depleted cells. The sensitivity of XIAP depleted cells for TRAIL was highest in BDE cells with an increase in the ED_{50} of 14-fold, compared to mock- and nonsense-treated controls. The sensitivity of P114 and D17 cell-lines increased six- and five-fold, respectively. Doxorubicin treatment in XIAP depleted cells increased sensitivity in BDE cells more than eight-fold, whereas P114 and D17 cell-lines showed an increase in sensitivity of three- and five-fold, respectively. XIAP directed siRNA's have a strong sensitizing effect on TRAIL-induced apoptosis and a smaller but significant effect with the DNA damaging drug doxorubicin. The increase in efficacy of chemotherapeutics with XIAP depletion provides the rationale for the use of XIAP siRNA's in insensitive canine tumors. In view of the comparable chemotherapeutic approach to canine and human mammary tumors as well as osteosarcoma, *in vivo* studies are mutually beneficial for both man and dog.

Introduction

The inhibitor of apoptosis proteins (IAPs) are a family of structurally related proteins with anti-apoptotic functions. To date, eight family members have been identified all carrying a functional baculovirus IAP repeat (BIR) domain. Members of the IAP family include Survivin, c-IAP1, c-IAP2, and X-linked inhibitor of apoptosis (XIAP) which directly bind and inhibit caspases 3, 7, and 9 [1]. XIAP (hILP/MIHA/BIRC4) is the most potent caspase inhibitor of all family members [2,3]. XAF1 and Smac-/DIABLO regulate XIAP activity, which indicates an important function of this protein in maintaining proper apoptotic functions within the cell.

Apoptosis can be initiated via the intrinsic and/or the extrinsic pathway [4]. The intrinsic pathway is activated by intracellular stress such as growth factor withdrawal, hypoxia, and DNA damage. In this pathway the caspase cascade is triggered by cytochrome c release from the mitochondria. On the other hand the extrinsic apoptotic pathway is triggered by death receptors such as Fas/CD95, TNF receptor, and the TRAIL receptor. Activation of these death receptors usually involves caspase 8 activation which in turn activates effector caspases-3 and -7 [5,6]. Overall, activation of these two pathways is not distinctly separated as activation of one usually involves the other. Resistance to apoptosis is a hallmark of various (canine) cancers [6]. Indeed in various (chemoresitant) tumors the XIAP protein has been shown to be induced when compared to normal tissue [7-9]. XIAP knockout mice have shown that the absence of XIAP does not have a negative effect on the development of normal tissues [10]. On the other hand, knockdown of XIAP with antisense techniques provides antitumor activity in non-small-cell lung cancer (NSCLC) xenografts [11]. Furthermore studies with stable expression of short-hairpin RNAs (shRNA) against XIAP dramatically increased sensitivity of cell-lines to chemotherapies [12]. Thus, XIAP may represent a novel and tumor-selective therapeutic target for anti-cancer drug design [13].

In this study we describe the use of siRNA's directed against XIAP for sensitizing canine cell-lines to TRAIL and doxorubicin induced apoptosis. Whereas TRAIL treatment will provide proof of principle, sensitizing tumor cells to doxorubicin will greatly benefit the use of this chemotherapeutical in canine tumors. We chose three cell-lines derived from bile duct-, mammary-, and bone tumor-tissue which could provide the basis for the therapeutic use of siRNA's. *Taken together*, in order to develop anti-neoplastic therapeutic protocols in dog tumors, which represent good clinical models [14], we investigated the effect of XIAP siRNA on different apoptotic agents in canine tumor cell-lines.

Materials and Methods

Cell-lines

Canine bile duct epithelial (BDE) cells were acquired from the Amsterdam Medical Center, Experimental Liver cell bank (Amsterdam, The Netherlands) [15]. BDE cells were grown in DMEM (Life Technologies, Inc., Invitrogen, Breda, The Netherlands) supplemented with 580 mg/l glutamine, 10 μg/ml gentamicin, and 10% heat-inactivated fetal bovine serum (FBS; Harlan Sera-Lab, Loughborough, United Kingdom) at 37°C in a humidified atmosphere of 5% CO_2 in air. P114 canine mammary tumor cells were grown in DMEM:F12 medium (Invitrogen, Breda, The Netherlands) containing 580 mg/l glutamine, 10 μg/ml gentamicin, and 10% FBS at 37°C in a humidified atmosphere of 5% CO_2 in air [16]. The canine osteosarcoma cells (D17) were acquired from the American Type Culture Collection (ATCC, Cat.no. CRL-6248) and were maintained in DMEM medium (Invitrogen) supplemented with 580 mg/l glutamine, 10 μg/ml gentamicin, and 10% FBS at 37°C in a humidified atmosphere of 5% CO_2 in air. For all experiments cells were seeded in a concentration of 4 X 10^3 cells per well in a 96-well plate 24 hours before transfection.

Establishment of XIAP knock-down in canine tumor cell-lines

For silencing experiments, Stealth™ dsRNA molecules were obtained from Invitrogen. A specific sequence for canine XIAP silencing (5'-CCAUGUGCUAUACAGUCAUUACUUU-3') was selected after general recommendations (Invitrogen) and was designed from the canine XIAP gene sequence (Genbank accession no. AY603038). A nonsense sequence was used as a negative control (5'-GCAGGUGCUAGUACAAGUCCGACAA-3'). Transfection was performed with the Magnet Assisted Transfection (MATra) technique (IBA BioTAGnology/Westburg b.v., Leusden, The Netherlands), in combination with Lipofectamine2000™ (Invitrogen), according to the manufacturer's instructions. In short, 50 nM siRNA molecules were transfected into the cell-lines in the presence of an optimized concentration Lipofectamin2000™ (1.2 μl/ml), for 20 minutes on the plate magnet under cell-culture conditions. After transfection, growth media including antibiotics replaced the transfection media. Control samples were mock transfected with Lipofectamine2000™ and magnetic beads from the MATra technique.

Treatments

For TRAIL treatment, a serial dilution of 400 to 0 ng/ml recombinant TRAIL (R&D Systems Europe Ltd., Abingdon, United Kingdom) was used in DMEM media (Invitrogen) including 10 % FCS, glutamine (580 mg/l), and gentamycin (10 µg/ml). Treatment started 48 hours after transfection. After a 24 hour treatment proliferation and viability was measured with a MTT assay (5 mg/ml). For doxorubicin treatment, a serial dilution of 100 to 0 µg/ml doxorubicin hydrochloride (Pharmachemie b.v., Haarlem, The Netherlands) was used diluted in growth medium. Treatment started 48 hours after transfection. After 24 hour treatment proliferation and viability was measured with a MTT assay (5 mg/ml). Statistical significance of differences in viability of the XIAP siRNA treated cell-lines at different drug concentrations compared to control cells were determined by an one-way ANOVA using the Dunnett multiple comparisons test. $P< 0.05$ was considered to indicate statistical significance. Analysis was performed using SPSS software (SPSS Benelux, Gorinchem, the Netherlands).

RNA isolation and Reverse-transcription polymerase chain reaction

For total cellular RNA isolation we used the Qiagen RNeasy Mini Kit (Qiagen, Leusden, The Netherlands) according to the manufacturer's instructions. In short, RNA was isolated from each sample by adding 100 µl lysis buffer (RLT containing 1 % (v/v) β-mercaptoethanol) directly after decanting the media. The RNA samples were treated with DNase-I (Qiagen RNase-free DNase kit). In total 3 µg of RNA were incubated with poly(dT) primers at 42°C for 45 min, in a 60 µl reaction volume, using the Reverse Transcription System from Promega (Promega Benelux, Leiden, The Netherlands).

Table 1. *Nucleotide Sequences of Canine Specific Primers for Real-Time Quantitative PCR.*

Gene	F/R	Sequence (5'-3')	Tm (^{o}C)	Size (bp)	Accession number
GAPDH	F	TGT CCC CAC CCC CAA TGT ATC	58	100	AB038240
	R	CTC CGA TGC CTG CTT CAC TAC CTT			
HPRT	F	AGC TTG CTG GTG AAA AGG AC	56	100	L77488 /
	R	TTA TAG TCA AGG GCA TAT CC			L77489
XIAP	F	ACT ATG TAT CAC TTG AGG CTC TGG TTT C	54	80	AY603038
	R	AGT CTG GCT TGA TTC ATC TTG TGT ATG			
c-IAP1	F	AGG CGT CCC CGT GTC CGA GAG	68	96	XM_858260
	R	TAG CAT CAG GCC GCA GCA GAA GC			
c-IAP2	F	AGG CCA ATG TAA TTA ATA AAC AGG A	62	94	DQ223014
	R	AAC TAA GAC AGT ATC AAT CAG TTC TCT C			
Smac	F	AGC AGA AGC TGC ATA TCA AAC TGG AG	62	90	XM_534661
	R	ACT TCC TGC ACC TGC GAC TTC AC			
p53	F	GCC CCT CCT CAG CAT CTC ATC	67	100	NM_001003210
	R	GGC TCA TAA GGC ACC ACC ACA C			
Caspase 3	F	ATC ACT GAA GAT GGA TGG GTT GGT	58	140	AB085580
	R	GAA AGG AGC ATG TTC TGA AGT AGC ACT			
p27KIP	F	CGG AGG GAC GCC AAA CAG G	60	90	AY455798
	R	GTC CCG GGT CAA CTC TTC GTG			
CCND1	F	ACT ACC TGA ACC GCT	56	151	AY620434
	R	CGG ATG GAG TTG TCA			

F: Forward primer; R: reversed primer

Quantitative measurements of the mRNA levels

Quantitative real-time PCR was performed on a total of 10 gene products; GAPDH, HPRT, XIAP, c-IAP1, c-IAP2, Smac/Diablo, p53, caspase-3, p27kip, and CCND1. The abundance of mRNA was measured by real-time quantitative PCR using appropriate primers (Table 1) as previously described [17]. In short, Q-PCR was based on the high affinity double-stranded DNA-binding dye SYBR® green I. For each experimental sample, the amount of the gene of interest and of the two independent endogenous references (glyceraldehyde-3-phosphate dehydrogenase (GAPDH) and hypoxanthine phosphoribosyl transferase (HPRT)) was determined from the appropriate standard curve in autonomous experiments. If relative amounts of GAPDH and

HPRT were constant for a sample, data were considered valid and the average amount was included in the study (data not shown). Results were normalized according to the average amount of the endogenous references. The normalized values were divided by the normalized values of the calibrator (healthy group) to generate relative expression levels [18]. A Kolmogorov-Smirnov test was performed to establish a normal distribution and a Levene's test for the homogeneity of variances. If samples were normally distributed, the statistical significance of differences between diseased and control animals was determined by using the Student's *t*-test. A p-value < 0.05 was considered statistically significant. Analysis was performed using SPSS software (SPSS Benelux, Gorinchem, the Netherlands).

Western blot analysis

Samples were homogenized in 350 µl RIPA buffer containing 1 % Igepal, 0.6 mM Phenylmethylsulfonyl fluoride, 17 µg/ml aprotinine and 1 mM sodium orthovanadate (Sigma chemical Co., Zwijndrecht, The Netherlands) for 30 minutes on ice. Protein concentrations were obtained using a Lowry-based assay (DC Protein Assay, Bio-Rad, Veenendaal, The Netherlands). Fifteen µg of protein of the supernatant were denatured for 3 min at 95^{o}C and electroferesed on 15 % Tris-HCl polyacrylamide gels (BioRad) and the proteins were transferred onto Hybond-C Extra Nitrocellulose membranes (Amersham Biosciences Europe, Roosendaal, The Netherlands) using a Mini Trans-Blot® Cell blot-apparatus (BioRad). The procedure for immunodetection was based on an ECL Western blot analysis system, performed according to the manufacturer's instructions (Amersham Biosciences Europe). The membranes were incubated with 4 % ECL blocking solution and 0.1 % Tween 20 (Boom B.V., Meppel, The Netherlands) in TBS for 1 hour under gentle shaking. Primary antibodies were incubated at 4^{o}C overnight. For XIAP a mouse anti-dog XIAP (BD Biosciences, Alphen aan den Rijn, The Netherlands) was used in a dilution of 1:1,000 in TBST with 4% BSA. As a loading control a mouse anti-dog Beta-Actin antibody was used in a 1:2,000 dilution in TBST with 4% BSA. After washing, the membranes were incubated with a goat anti-mouse (R&D Systems/Westburg b.v.) in TBST with 4% BSA for 1 hour at room temperature. Exposures were made with Kodak BioMax Light-1 films (Sigma chemical Co.).

Results

Establishing a XIAP knock-down

Using the Lipofectamine reagent in combination with magnetic assisted transfection (MATra), we transfected the cell-lines with siRNA designed from the canine XIAP gene sequence. The cellular uptake of oligoribonucleotides was initially determined using fluorescent labeled dsRNA (Invitrogen). The transfection-efficiency was optimized and proved to be greater than 95% of the cells as displayed by green fluorescence FITC labeled siRNA (data not shown). When treated with the optimal amount of siRNA (50 nM), the XIAP expression was markedly reduced in all cell-lines with the highest decrease at 72 hours (Figure 1). At this time point the mRNA-levels were decreased to fifteen percent in BDE cells, ten percent in D17 cell-lines, and thirteen percent in P114 cell-lines lines, compared to the different controls used. At 72 hours Western blotting (Figure 1B) yielded a 57 kDa immunoreactive band of XIAP in the control and scrambled siRNA transfected samples. Specificity was proven in controls without first antibody, which was deemed negative (not shown). Densitometric analysis indicated a strong reduction of XIAP protein in the XIAP siRNA treated samples. Cells treated with nonsense siRNA exhibited a similar expression pattern as the control cells (Figure 1).

Treatments

We have measured the effect of XIAP depletion by siRNA-mediated gene silencing on TRAIL and doxorubicin induced cell death. As shown in Figure 2, siRNA transfection increased the sensitivity for TRAIL of all three cell-lines used. This effect was highest in BDE cells, whereas P114 cells and D17 were less sensitized by siRNA treatment. XIAP-depleted BDE cells (Figure 2A) showed the strongest increase in TRAIL-sensitivity; a 14-fold reduction of the ED_{50}. The P114 and D17 cell-lines showed an increase in sensitivity of six and five-fold, respectively (Figures 2B and C). For doxorubicin treatment (Figure 3), again the largest increase in sensitivity was seen in the BDE cells showing a more than eight-fold reduction in the ED_{50}. The P114 and D17 cell-lines showed an increase in sensitivity of three and five-fold, respectively (Figures 3B, C).

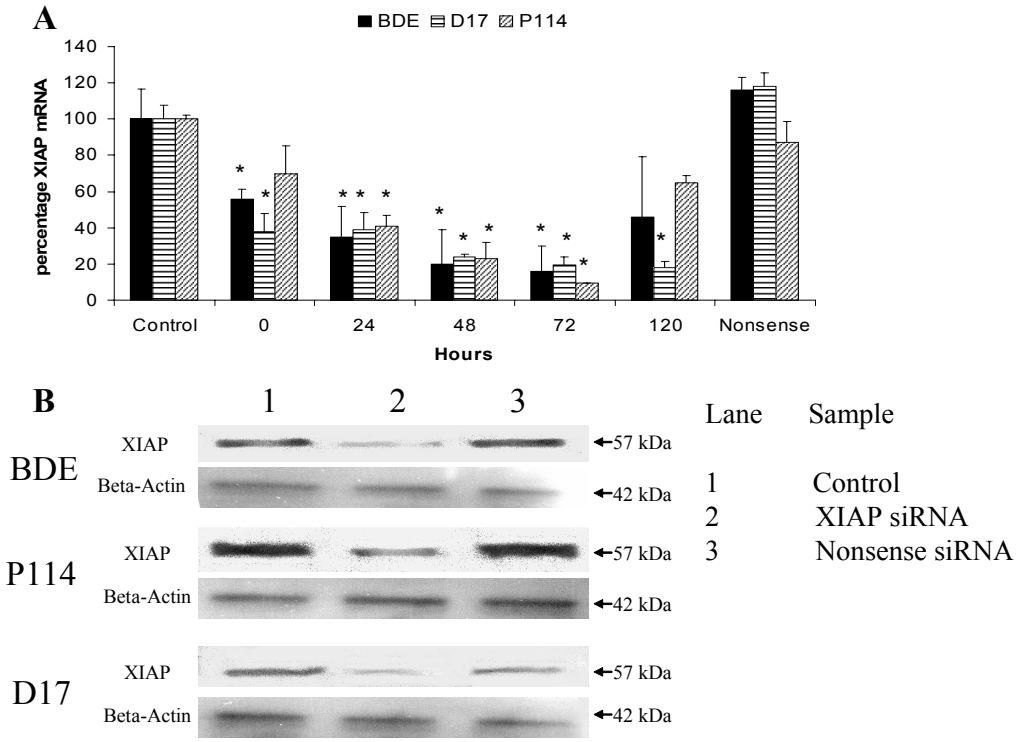

Figure 1. *Knock-Down XIAP levels compared to control. Relative mRNA levels from different time points just after transfection up to 5 days set towards control is shown in (A). Data represent mean + SD of six independent samples (n = 6). Western blot analysis of immunoreactive bands of 57 kDa large XIAP protein levels after 72 hours is shown in (B). Statistically significant differences in knock-down of XIAP mRNA at different time-points towards control were determined by a student t-test (*P<0.05).*

Gene expression of IAP family members and cellular homeostasis

In Figure 4, the effect of XIAP siRNA on XIAP and family members such as cIAP-1 and cIAP-2 mRNA levels is depicted. Results showed that none of these IAP-family members were affected. Nonsense siRNA did induce c-IAP1 levels (165 percent) and Smac/Diablo levels (142 percent) in D17 cells. Measurement of parameters for cellular homeostasis revealed an increase in p53 levels in BDE cells and D17 cells in the nonsense siRNA treated cells. The introduction of siRNA's in P114 cells seemed to induce cell-cycle and increase viability through inductions in CCND1, decreases in p27kip, and decreases in caspase-3 mRNA levels in XIAP and nonsense siRNA treated cells.

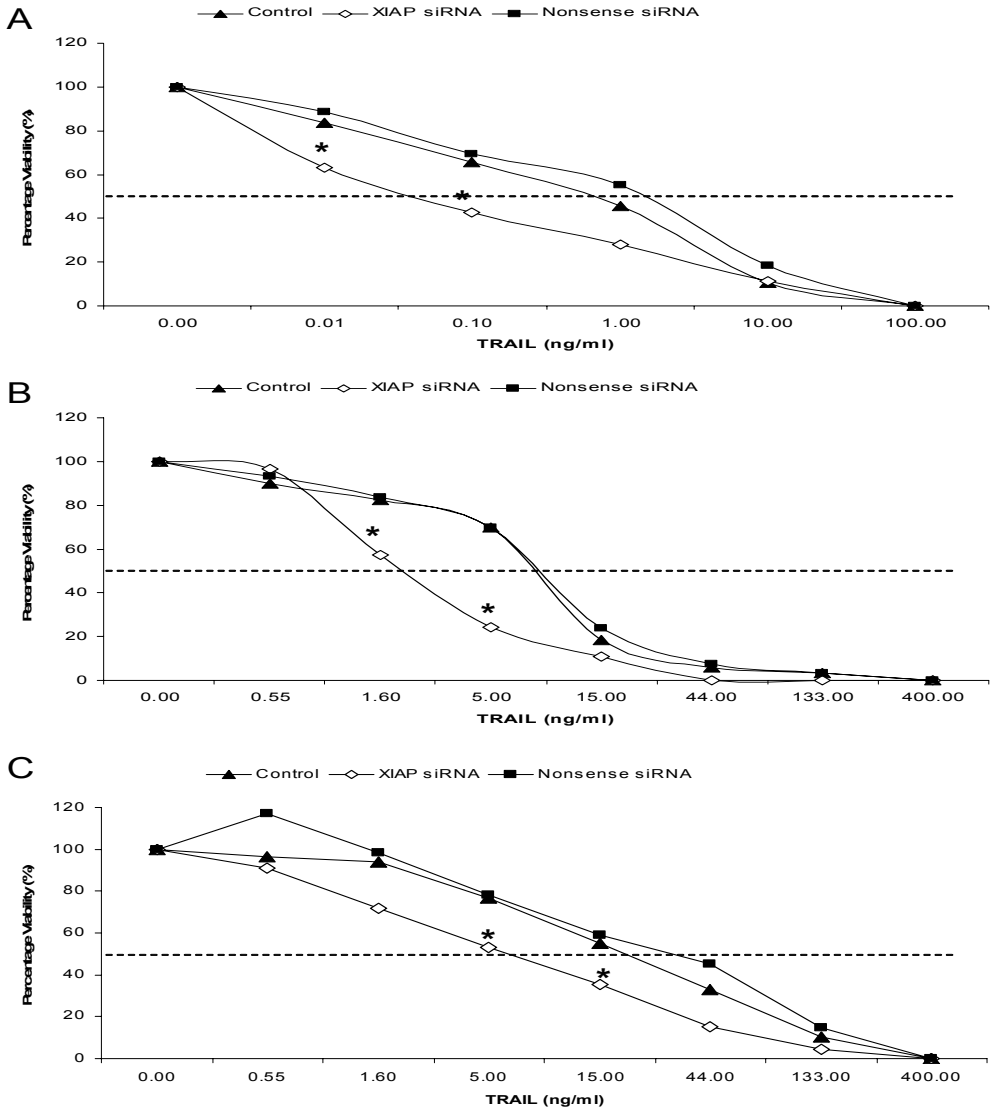

Figure 2. *Effect of XIAP loss on TRAIL sensitivity in canine cell-lines. The effect on viability is shown for BDE cells in (A), for P114 cells in (B), and for D17 cells in (C). Control (▲); 50 nM XIAP siRNA (■); 50 nM Nonsense siRNA (◊). Points represent average of four independent samples (n = 4). Statistical significance of differences in viability of the XIAP siRNA treated cell-lines at different drug concentrations compared to control and nonsense were determined by an one-way ANOVA using the Dunnett multiple comparisons test (*P<0.05).*

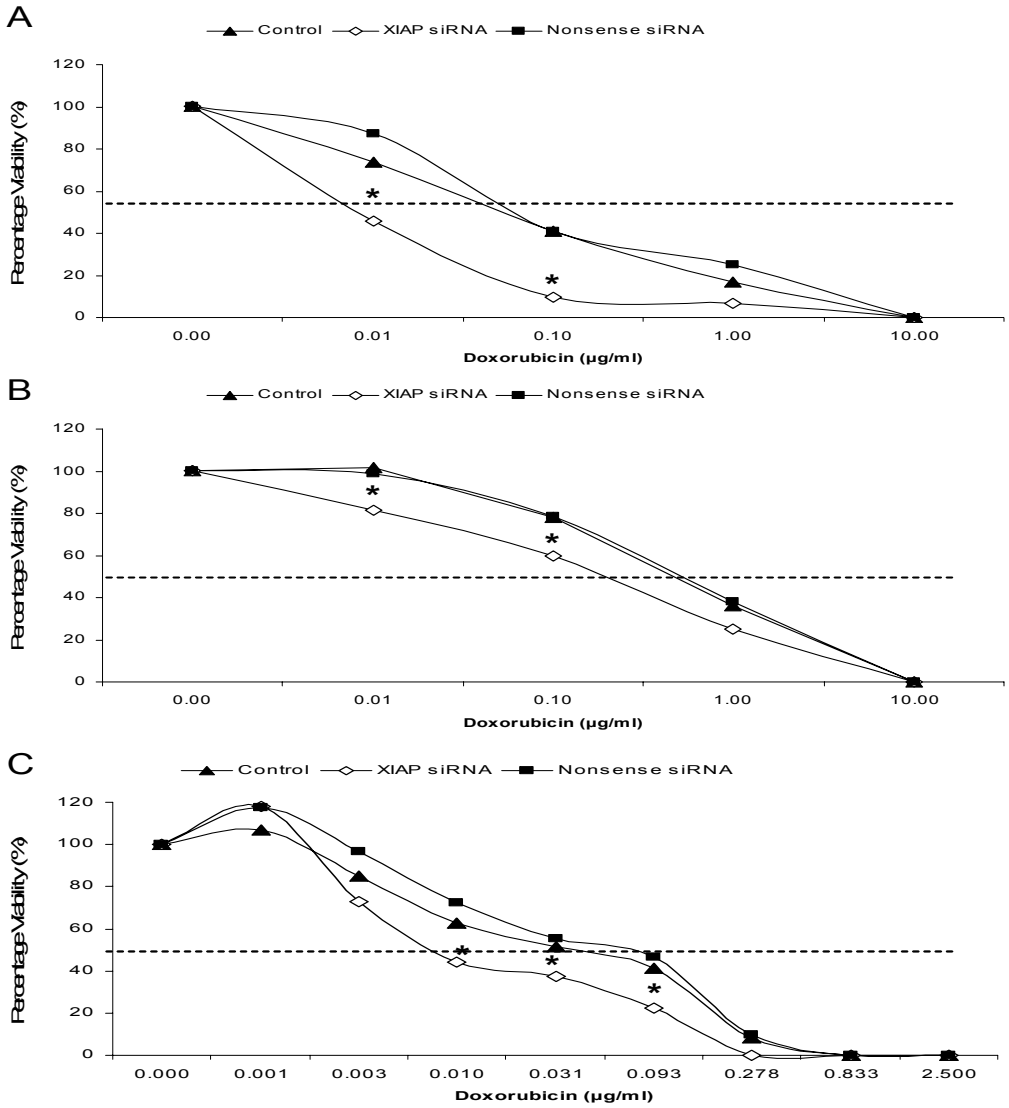

Figure 3. *Effect of XIAP loss on doxorubicin sensitivity in canine cell-lines. The effect on viability is shown for BDE cells in (A), for P114 cells in (B), and for D17 cells in (C). Control (▲); 50 nM XIAP siRNA (■); 50 nM Nonsense siRNA (◊). Points represent average of four independent samples (n = 4). Statistical significance of differences in viability of the XIAP siRNA treated cell-lines at different drug concentrations compared to control and nonsense were determined by an one-way ANOVA using the Dunnett multiple comparisons test (*P<0.05).*

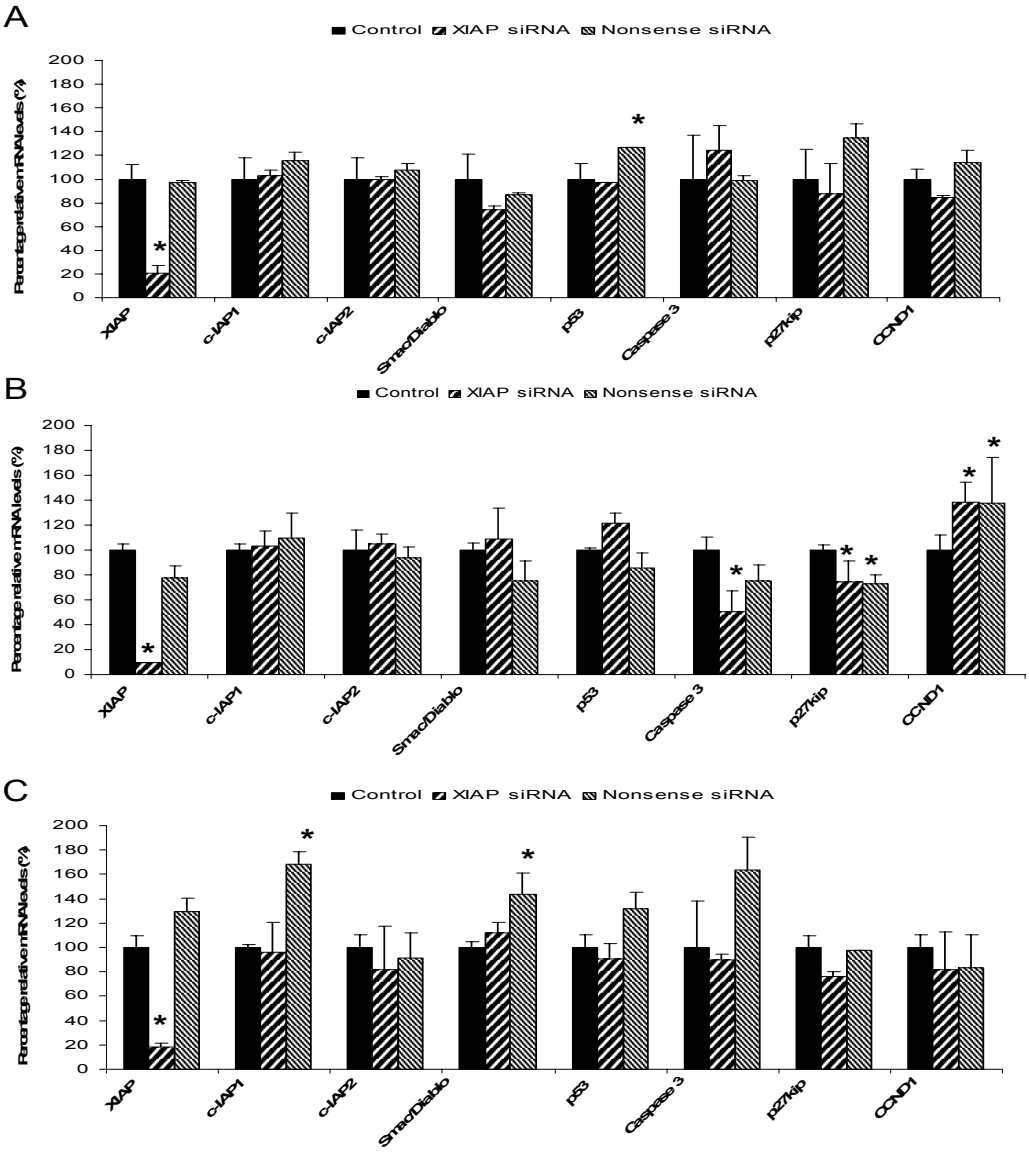

Figure 4. *Gene-expression profiles canine cell-lines. Quantitative mRNA measurement of IAP family members and gene-products involved in cellular homeostasis. Gene-expression profile of BDE-cells is shown in (A), P114-cells is shown in (B), and D17-cells is shown in (C). Data represent mean + SD of six independent samples (n = 6). Statistically significant differences in gene-expression of different treatments towards control were determined by a student t-test (*P<0.05).*

Discussion

In the present study we observed a strong enhancement of TRAIL- and doxorubicin-induced apoptosis with XIAP siRNA in canine cell-lines. We have used three different tumor cell-lines in order to be able to conclude about the general applicability of the outcomes of this study. The first cell-line studied, a canine liver epithelial cell-line of biliary origin (BDE) can be considered as an *in vitro* counterpart of cholangiocarcinoma. The P114 cell-line was derived from a mammary tumor [16], and the third cell-line was derived from a canine osteosarcoma (D17). In order to show the proof of principle that XIAP depletion in canine cell-lines increases the sensitivity to apoptosis inducing anti-neoplastic drugs, a treatment with TRAIL was used. As TRAIL solely induces apoptosis through the extrinsic pathway, an increase in sensitivity will show a decreased capacity of inhibiting caspase-3 and -7. Second doxorubicin, a DNA damaging drug which type is frequently being used for treatment of canine tumors, was used.

Although we did not measure an induction of apoptosis in our cell-lines when XIAP was knocked-down (data not shown), as described by several papers [19,20], we could demonstrate an increase in the sensitivity for different chemotherapeutic treatments. The fact that the introduction of XIAP siRNA's alone does not seem to induce apoptosis indicates a need for triggering the cells by chemotherapy. XIAP has been proposed as a possible treatment of various cancers [21]. Our results showed a strong increase in sensitivity of all three tumor cell-lines to TRAIL treatment up to fourteen fold in XIAP siRNA treated BDE cells. This indicates that the measured results represent a general effect. The fact that all canine cell-lines were increasingly sensitized through XIAP depletion holds promises that therapeutic low concentrations TRAIL may be effectively used without effecting somatic cells.

Doxorubicin hydrochloride, a cytotoxic anthracycline antibiotic, is commonly used in veterinary clinical treatments for various cancers [22]. However, many dog tumors appear to be resistant to doxorubicin. In the *in vitro* experiments of Macy et al. [23], five out of twenty-one carcinomas were deemed sensitive (24 %), whereas three out of thirteen (23 %) sarcomas showed sensitivity to a 14 day treatment with 1 µg/ml doxorubicin. Because of this insensitivity to high amounts of doxorubicin, a pretreatment with XIAP siRNA could be beneficial for many canine tumors, lowering the concentrations needed for a beneficial effect in sensitive tumors and could even make insensitive tumors treatable. Although this added effect remains to be proven *in vivo*, the application of siRNA's against XIAP in combination with a chemotherapeutic agent such as doxorubicin seems a realistic option based on the present results. *In vivo* experiments with siRNA's already have been used in various models [24-27]. In

these experiments results show that injected siRNA's are stable and can be found in the blood for long periods, even knocking-down long half-life proteins over several days [28]. However, the use of targeted drug-delivery systems should still be considered for siRNA delivery [29] or chemotherapy [30], which further enhances specificity and potentially reduces drug-associated side-effects.

Measurements on gene expression of IAP family members and cellular homeostasis genes did not reveal major differences in cell-cycle progression. In the P114 cell-line, however, the introduction of siRNA's in general seemed to induce the cell-cycle and cellular viability. Although this may imply an adverse effect *in vivo* the MTT measurements did not reveal differences in viability of the groups (data not shown). The IAP family members under study (besides XIAP) did not show many significant differences in gene-expression. In P114 cells however, a significant increase in c-IAP1 and Smac/Diablo was seen in the nonsense-treated cells. The effect of these differences remains elusive, but the antagonistic properties of these proteins could explain why little if any effect was observed in cell viability. Taken together, no large differences were seen in cellular homeostasis or IAP family members indicating an absence of non-specific target knock-down effects. However, unpublished results on TRAIL-treated cells did show differences in gene-expression in c-IAP1. When treated for 5 hours with 50 ng/ml TRAIL, c-IAP1 induced two to three-fold in the D17 cell-line and six to seven-fold in the P114 cell-line, whereas no effect was seen in the BDE cells. This indicates that the reduction in XIAP mRNA when treated with TRAIL, could be counteracted with an increase in c-IAP1. Furthermore, the cell-line with the highest induction in c-IAP1 (seven-fold increase in P114) has the least sensitivity for TRAIL treatment. This result corroborates the hypothesis as described by Harlin et al. where XIAP knock-out mice did not show any negative side effects during development [10]. In this paper compensation due to increased gene-expression of other family members such as c-IAP1 was seen which could counteract the negative side effects in the absence of XIAP.

The use of spontaneously occurring tumors in companion animals as models for human cancer has already been described previously [14]. In this study several tumor types have been suggested as models that offer the best comparative interest, including canine osteosarcoma and mammary tumors. Important factors contributing to the advantages of companion animals referred to our veterinary clinic as human models are high incidence of tumors in both species, a similar biological behavior, genetic diversity, variations in age, comparable body weight, and similar drinking- and feeding behavior. All together this suggests a comparable etiology and molecular basis of tumors in both man and dog.

In conclusion, the use of XIAP siRNA to increase the sensitivity of canine tumors for chemotherapy holds great potential. In this study we showed an increase in sensitivity in canine cell-lines derived from osteosarcoma, mammary carcinoma, and cholangiocarcinoma for TRAIL and doxorubicin induced apoptosis. These *in vitro* results provide a rational for the use of XIAP siRNA in *in vivo* therapeutical use. Furthermore dogs, which represent good clinical models to man, could be considered as a large mammalian model for the use of siRNA therapy.

References

[1] Nachmias B, Ashhab Y, Ben-Yehuda D. The inhibitor of apoptosis protein family (IAPs): an emerging therapeutic target in cancer. Semin Cancer Biol 2004, 14:231-243.
[2] Deveraux QL, Takahashi R, Salvesen GS, et al. X-linked IAP is a direct inhibitor of cell-death proteases. Nature 1997, 388:300-304.
[3] Stennicke HR, Ryan CA, Salvesen GS. Reprieval from execution: the molecular basis of caspase inhibition. Trends Biochem Sci 2002, 27:94-101.
[4] Kim R. Recent advances in understanding the cell death pathways activated by anticancer therapy. Cancer 2005, 103:551-560.
[5] Boatright KM, Salvesen GS. Mechanisms of caspase activation. Curr Opin Cell Biol 2003, 15:725-731.
[6] Bergman PJ. Mechanisms of anticancer drug resistance. Vet Clin North Am Small Anim Pract 2003, 33:651-667.
[7] Hofmann HS, Simm A, Hammer A, et al. Expression of inhibitors of apoptosis (IAP) proteins in non-small cell human lung cancer. J Cancer Res Clin Oncol 2002, 128:554-560.
[8] Krajewska M, Krajewski S, Banares S, et al. Elevated expression of inhibitor of apoptosis proteins in prostate cancer. Clin Cancer Res 2003, 9:4914-4925.
[9] Shiraki K, Sugimoto K, Yamanaka Y, et al. Overexpression of X-linked inhibitor of apoptosis in human hepatocellular carcinoma. Int J Mol Med 2003, 12:705-708.
[10] Harlin H, Reffey SB, Duckett CS, et al. Characterization of XIAP-deficient mice. Mol Cell Biol 2001, 21:3604-3608.
[11] Hu Y, Cherton-Horvat G, Dragowska V, et al. Antisense oligonucleotides targeting XIAP induce apoptosis and enhance chemotherapeutic activity against human lung cancer cells in vitro and in vivo. Clin Cancer Res 2003, 9:2826-2836.
[12] McManus DC, Lefebvre CA, Cherton-Horvat G, et al. Loss of XIAP protein expression by RNAi and antisense approaches sensitizes cancer cells to functionally diverse chemotherapeutics. Oncogene 2004, 23:8105-8117.
[13] Huang Y, Lu M, Wu H. Antagonizing XIAP-mediated caspase-3 inhibition. Achilles' heel of cancers? Cancer Cell 2004, 5:1-2.
[14] Vail DM, MacEwen EG. Spontaneously occurring tumors of companion animals as models for human cancer. Cancer Invest 2000, 18:781-792.
[15] Oda D, Savard CE, Nguyen TD, et al. Dog pancreatic duct epithelial cells: long-term culture and characterization. Am J Pathol 1996, 148:977-985.

[16] van Leeuwen I, Hellmen E, Cornelisse CJ, et al. P53 mutations in mammary tumor cell lines and corresponding tumor tissues in the dog. Anticancer Res 1996, 16:3737-3744.
[17] Spee B, Mandigers PJ, Arends B, et al. Differential expression of copper-associated and oxidative stress related proteins in a new variant of copper toxicosis in Doberman pinschers. Comp Hepatol 20005, 4:3.
[18] Vandesompele J, De Preter PK, Pattyn F, et al. Accurate normalization of real-time quantitative RT-PCR data by geometric averaging of multiple internal control genes. Genome Biol 2002, 3:RESEARCH0034.
[19] Amantana A, London CA, Iversen PL, et al. X-linked inhibitor of apoptosis protein inhibition induces apoptosis and enhances chemotherapy sensitivity in human prostate cancer cells. Mol Cancer Ther 2004, 3:699-707.
[20] Schimmer AD, Welsh K, Pinilla C, et al. Small-molecule antagonists of apoptosis suppressor XIAP exhibit broad antitumor activity. Cancer Cell 2004, 5:25-35.
[21] Wang S, El-Deiry WS. TRAIL and apoptosis induction by TNF-family death receptors, Oncogene 2003, 22:8628-8633.
[22] Cagliero E, Ferracini R, Morello E, et al. Reversal of multidrug-resistance using Valspodar (PSC 833) and doxorubicin in osteosarcoma. Oncol Rep 2004, 12:1023-1031.
[23] Macy DW, Ensley BA, Gillette EL. In vitro susceptibility of canine tumor stem cells to doxorubicin. Am J Vet Res 1988, 49:1903-1905.
[24] Scherr M, Morgan MA, Eder M. Gene silencing mediated by small interfering RNAs in mammalian cells. Curr Med Chem 2003, 10:245-256.
[25] Sorensen DR, Leirdal M, Sioud M. Gene silencing by systemic delivery of synthetic siRNAs in adult mice. J Mol Biol 2003, 327:761-766.
[26] Takei Y, Kadomatsu K, Yuzawa Y, et al. A small interfering RNA targeting vascular endothelial growth factor as cancer therapeutics. Cancer Res 2004, 64:3365-3370.
[27] Zender L, Hutker S, Liedtke C, et al. Caspase 8 small interfering RNA prevents acute liver failure in mice. Proc Natl Acad Sci U S A 2003, 100:7797-7802.
[28] Dykxhoorn DM, Novina CD, Sharp PA. Killing the messenger: short RNAs that silence gene expression. Nat Rev Mol Cell Biol 2003, 4:457-467.
[29] Gilmore IR, Fox SP, Hollins AJ, et al. The design and exogenous delivery of siRNA for post-transcriptional gene silencing. J Drug Target 2004, 12:315-340.
[30] Ma Y, Manolache S, Denes FS, et al. Plasma synthesis of carbon magnetic nanoparticles and immobilization of doxorubicin for targeted drug delivery. J Biomater Sci Polym 2004, Ed 15:1033-1049.

Chapter 11

Summarizing Discussion

The research described in this thesis was largely accommodated in the research program Tissue Repair. Tissue Repair has a mission statement committed to the investigation of the pathophysiology of tissue dysfunction and potential mechanisms of repair. The strategic goal of the program is to develop new methods for stimulating regeneration by delivery of essential cells and/or signals and to develop preventive strategies against cellular degeneration, cell death, and scar formation / fibrosis. This thesis describes the biochemical analysis of pathophysiological mechanisms in dogs with liver tissue dysfunction and provides the basis for several therapeutic approaches with a high relevance to human clinical medicine.

Translational studies

In chapters 2 to 4 we have evaluated the role of growth factors, especially of hepatocyte growth factor and transforming growth factor-β1 and their signal transduction pathways, in dogs with different liver diseases. These diseases were characterized by inadequate growth due to inherited vascular disorders, or by chronic hepatitis, fibrosis, and cirrhosis. With respect to etiology, the best characterized disease was copper toxicosis due to a deletion in the *COMMD1* gene. We propose the use of the dogs presented at our clinics as possible models for hepatic (and other) diseases in man. The increased interest in the dog as a model would speed up the laborious process of designing new therapies which will ultimately benefit both man and dog. Although ethical restrictions still apply, the restrictions would be considered lower in the dog models compared to human clinical practice. Several publications already propose the use of the canine spontaneous diseases as large mammalian models for man [1-4]. Therefore we attempted to enforce these assumptions by indicating the high similarity of canine diseases at a biochemical level with respect to their human counterparts. Already many therapies for hepatic diseases have been evaluated in toxin-induced or surgical rodent models [5-9]. Although in many cases successful, the translation to human clinical practice proved very difficult. Several rodent models such as the toxin induced rodent model only depict a small part of the very complex pathophysiology in human hepatic diseases. Also the mode of application and possible toxicity of drugs cannot be translated to human clinical practice without encountering various problems. In this thesis the biochemical study of canine hepatic diseases indicated a high similarity with their human counterparts. In some cases this was deduced from the already available literature; in other cases we had the opportunity to directly apply our methods on human clinical samples indicating the high homology between species (chapter 3 and 4). In addition to the description of canine hepatic diseases we have analyzed several tumors as translational models and provided the basis for novel therapeutic strategies against these tumors. Spontaneous occurring cancers have already been proposed as possible models for humans [1,10].

Spontaneous tumors in dogs offer a unique opportunity as models due to the relatively high incidence of some cancers and similar biological behavior. Moreover, their large body size, comparable responses to cytotoxic agents, and shorter overall lifespan all contribute to the advantages of the companion animal model. Overall the companion animal model could provide useful populations to test the efficiency and toxicity of new therapeutic strategies. Taken together, as canine (hepatic) diseases are highly comparable to their human counterparts, dogs could function to bridge the gap between fundamental rodent research and human clinical practice.

Biochemical molecular analysis and technical approach

- *Quantitative real-time PCR*.

In this study we have set up quantitative real-time PCR (Q-PCR) using a separate reverse polymerase step followed by the SYBR Green I Real-Time PCR (two-step Real-Time PCR). This greatly enhances the specificity of the Q-PCR and reduces the artifacts, such as primer-dimers and a-specific products, normally associated with a one-step PCR [11]. Because of the sensitivity of Q-PCR, canine specific sequences must be obtained for accurate analysis. Therefore, in the pre-canine genome era, we have successfully cloned and sequenced 25 canine cDNAs on which canine specific primers were designed. Overall we have setup a panel of 68 target genes in various fields of interest such as regeneration/growth, fibrosis, copper-metabolism, and oxidative stress. The sensitivity of gene-expression measurements by means of Q-PCR is prone to several variables that affect the general outcome; therefore internal controls are needed [12]. These internal controls are known as reference genes (RG) or housekeeping genes. With these RG's target gene expression can be normalized as the expression of the reference genes should be equal in all cells or tissues, healthy or diseased. However, the use of one reference gene should be avoided as controls are needed to indicate if the chosen RG is indeed equally expressed between different groups of interest. Although many journals still accept this normalization with one single RG the data in these manuscripts could potentially be false. In this thesis we have used two widely used reference genes namely glyceraldehyde-3-phosphate dehydrogenase (GAPDH) and hypoxanthine phosphoribosyl transferase (HPRT). These endogenous references showed no variation in any of the here described studies and showed to be good internal controls. More recently we have setup a new panel of nine canine specific RG's which can be used in various forms of veterinary research (Brinkhof et al, submitted). It also describes the proper use of internal controls and variables which have to be controlled in gene expression analysis, such as the amount of starting material, enzymatic efficiencies, and differences between tis-

sues or cells in overall transcriptional activity. The outcome of the study not only indicated the need of two or more RG's, but also showed a new panel of reference genes which were stable in a wide variety of cell-lines and healthy and diseased tissues. In most of the chapters of this thesis GAPDH and HPRT were used as RG's. Results in the survey of nine RG's showed that GAPDH and HPRT were fairly stable internal controls with the latter always in the top four of the highest ranking RG's. Target gene products depicted in this thesis have been scrutinized under various controls such as product size, GC-levels, specificity, and efficiency over a wide dynamic concentration range. The efficiency was controlled in all plates with a standard line containing known concentrations of cDNA. Also each run was ended with a melt-curve analysis indicating the production of single products eliminating the probability of primer-dimers or a-specific products.

- *Western blot analysis for (active) proteins*.

The Western blot analysis was used to confirm measured mRNA levels at the protein level. In addition Western blot analysis was used to show activated forms of proteins caused by proteolytic cleavage or phosphorylation. The direct comparison of our Western blot data in canine hepatic diseases with human clinical samples greatly enhanced our translational description of these canine diseases. In chapter 3 and 4 human clinical samples obtained form human explant samples of alcoholic cirrhosis and cirrhosis due to hepatitis c virus (HCV) infection were used. Of course it is difficult to obtain healthy human samples as comparison to the diseases but homology within groups and between (in)activated proteins can still be shown. Moreover, the absence of healthy human samples showed the importance of the canine model where healthy samples (control biopsies) are routinely obtained.

- *Gene silencing with small inhibitory RNA (siRNA) molecules*.

RNAi indicated to be a fast and reliable method for knocking down target genes of interest elucidating their fundamental functions and were used as possible therapeutic applications. In the past the use of siRNA's showed to induce interferon pathways leading to apoptosis [13-15]. To overcome this, siRNA's can be chemically modified to minimize these effects [16]. In the chapters 3, 9, and 10 we used chemically modified siRNA's called stealth siRNA from Invitrogen (www.invitrogen.com). Although in some cases negative side effects were found, the majority did indeed not induce cellular apoptosis. When presented to a cell, siRNA's will be automatically be taken up by into the cytoplasm. For *in vitro* analysis we increased this amount by adding a cationic lipid formulation called Lipofectamine2000™. In our studies we found that the combination with a Magnetic Assisted Transfection (MATra™) enhanced our

knock-down with an average of 15 percent-points. This technique uses magnetic beads which bind to the oligo-Lipofectamin complex which in a magnetic field can easily get transfected into the cells without any added negative side-effects. In fact, because of the decreased transfection time (6 hours to 20 minutes) overall cell viability was better than with Lipofectamine alone. *In vivo* experiments with siRNA's already have been used in various rodent models showing that injected siRNA's are stable and can be found in the blood over prolonged periods. Overall the use of siRNA's in fundamental research and applied therapeutics holds great potential.

General pathways studied

- *Regeneration*.

The regenerative capacity of the liver has been described in several canine hepatic diseases. In chapter 2 we describe regenerative pathways in two relative simple diseases without cholestasis or inflammation; e.g. congenital portosystemic shunt (CPSS) and primary portal vein hypoplasia (PPVH) which are both characterized by insufficient hepatic growth (hypoplasia). The results showed that regenerative pathways could still be activated by growth factor therapy. This was deduced from the observation that phosphorylated c-MET, PKB, STAT3, and ERK1/2 in both diseases were still present. This indicated that these regenerative pathways could be used as possible therapeutic targets. Comparing these diseases without inflammation or cholestasis to more complex hepatic diseases such as chronic hepatitis (CH), lobular dissecting hepatitis (LDH), and cirrhosis (CIRR) showed a high similarity in regenerative pathways. In contrast the absence of phosphorylated c-MET and downstream PKB in acute hepatitis (AH) indicated that in this disease regeneration was affected (chapter 3). The effect of HGF as possible therapy in this disease could be questioned and requires further research. As indicated by our RNAi experiments against c-MET (chapter 3), low c-MET levels can be phosphorylated after treatment with HGF increasing the proliferative response of canine hepatic cells *in vitro*. Besides c-MET in AH, the phosphorylated (thus activated) form of the receptor was equally expressed in controls compared to CPSS and PPVH, and even induced in some cases. This could be contributed to regenerative pockets which is a hallmark of several hepatic diseases. Measurements on activated ERK1/2, p38MAPK, and STAT3 (Ser) confirmed these results. In contrast to CPSS and PPVH, HGF mRNA and protein levels were shown to be induced in CH, LDH, and CIRR. In these cases the source of HGF is by all probability due to an increase in activated stellate cells called myofibroblasts, which are the only cells expressing HGF in the liver. In CPSS and PPVH described in chapter 2, the HGF levels were shown to be equally present towards

healthy tissue which was in contrast to the mRNA levels. In this chapter we described the possible source of HGF which can be sought in the intestinal tract or pancreas. The question remains if this systemic HGF is also being formed during hepatic diseases as an increase of HGF protein was found. Interestingly preliminary results on measurements of p38MAPK in PPVH indicated a complete lack of the phosphorylated form of the protein whereas total p38MAPK is still present. This could indicate a possible defect of this disease which remains to be proven. Overall, no indications (other than a lack of p38MAPK in PPVH and non-phosphorylated c-MET in AH) of affected regenerative pathways were found in our hepatic diseases. As hepatic diseases could be seen as disturbed balance between growth/regeneration on one side and apoptosis/fibrosis on the other, the stimulation of the regenerative pathways would be considered a good option for therapy. Moreover as the etiology in the majority of chronic hepatic diseases is largely unknown, the use of growth factors would benefit all hepatic diseases as regeneration is the common faulty denominator.

- *Fibrosis*.

As described in chapter 4 the pathogenesis of human hepatic fibrosis has been investigated extensively and many publications describe the process of excessive extracellular matrix (ECM) formation [17,18]. In dogs however the biochemical pathways of fibrosis had not been studied. Due to the high similarity between these two species a similar process would be anticipated. As we propose the dog as a possible model for man, these pathological processes have to be confirmed in canine samples. Again in our relative simplistic hypoplastic diseases (CPSS and PPVH) the presence of an activated fibrotic pathway through TGF-β1 was found in PPVH, often associated with fibrosis (chapter 2). In CPSS, liver hypoplasia without apparent fibrosis, the TGF-β1 signaling cascade was not increased. The more complex liver diseases (CH, LDH, and CIRR) indicate a similar activation of the TGF-β1 pathway with mRNA and protein levels of TGF-β1 induced and downstream transcription factors (Smad2/3) activated (chapter 4). The comparison of TGF-β1 and Smad2/3 activation with human samples from human explant samples (alcoholic cirrhosis and cirrhosis due to HCV infection) not only showed the high homology between these diseases, the inter-species differences were also minimal. Taken together, the current paradigm of the pathophysiology of human hepatic fibrosis is highly comparable to the canine counterparts. As excess fibrosis is not restricted to the liver alone, studies will be conducted on other diseases were fibrosis is a part of the pathophysiological process, such as kidney diseases [19]. With regard to fibrous tissue formation, fundamental research in privately owned dogs can be mutually beneficial for canine and human biomedical research.

- *Copper metabolism*.

Copper metabolism was analyzed in various breeds predisposed with hepatic copper accumulation. In dogs several breeds have been shown to have congenital defects resulting in copper accumulation in the liver, a few examples are Bedlington terriers, Doberman pinschers, Sky terriers, West-Highland white terriers, Dalmatians, Anatolian shepherds, and Labrador retrievers. In chapter 4 we have analyzed the copper metabolism in Bedlington terriers with copper toxicosis (CT) towards healthy animals and dogs with chronic extra-hepatic cholestasis. As the main excretory route of copper is through bile these results would show if cholestasis would induce copper accumulation [20,21]. Another control, idiopathic chronic hepatitis, would show if inflammation or differences in liver function would increase copper. Results clearly showed that cholestasis and inflammation cause no or only limited copper accumulation. This implies that high increases of copper in the liver (histochemical staining of copper above 3+) and/or changes in the expression of copper metabolic genes, other than ATP7B, indicate the presence of a primary disease of copper metabolism. These findings may help to determine the (inherited) nature of potential primary copper storage diseases in different dog breeds. Two other predisposed breeds were analyzed for copper metabolism; Doberman pinchers and Labradors of which the Doberman is described in this thesis (chapter 7). Results in the Doberman indicated significant decreases in gene-expression of copper efflux proteins (ATP7A and ceruloplasmin), this observation in the Doberman is very specific as non-copper associated hepatitis will not reduce ATP7A, as proven in the N-CASH group and CH group, and could indicate a possible defect in this breed. Overall, the results in Doberman pinchers (chapter 7) describe a new variant of primary copper toxicosis. In the Bedlington terriers with copper toxicosis due to a mutation in *COMMD1*, a specific gene-expression profile was found. Probably due to the lack of functional COMMD1 an increase in ATP7A (responsible for exocytose of copper) was seen, probably to compensate the reduced excretion (chapter 6). Unpublished results from the Labrador gene-expression also showed an increase in ATP7A which could indicate a reduced excretion to bile or storage proteins (G. Hoffmann). The human Wilson's disease protein ATP7B was seen to be reduced in all canine inflammatory liver diseases, whereas subclinical hepatitis cases did not have reduced expression of ATP7B. Overall the gene-expression profiles of these three copper toxicosis disease groups are different suggesting separate possible defects.
The only proven hereditary form of copper toxicosis can be found in the Bedlington terriers due to a mutation in *COMMD1* [22]. However the complete function of COMMD1 has not been fully elucidated. Although a role in copper metabolism of COMMD1 has been suggested, evidence of copper retention in COMMD1 depleted hepatic epithelial cells has not been shown. We used dog hepatic epithelial cells and

analysed the copper metabolic function after siRNA mediated COMMD1 knock-down. Results (chapter 9) confirmed that COMMD1 has an essential role in copper metabolism in hepatic epithelial cells and showed that COMMD1 depletion sensitizes canine hepatic cells to high extracellular copper levels. Furthermore the knock-down of COMMD1 gave no indications for general compensatory mechanisms.

It is well known that free copper in the cell can induce the Haber-Weiss reaction resulting in increased reactive oxygen species (ROS) [23]. All copper related diseases were also investigated for increases in ROS. In all copper toxicosis diseases we saw a decrease in defenses against oxidative stress (SOD and CAT), accompanied by a decrease in total glutathione. As the reductions of these protective enzymes are also reduced by inflammation, it is not a specific copper effect. This said, the decreases as seen in the copper toxicosis cases are far greater than in non-copper associated hepatitis.

Copper toxicosis is a chronic process which is subclinical over a prolonged period of time [24]. During this period histochemical staining of copper already showed a massive increase in hepatic copper without any clinical effects. It has not been established which process and/or signal converts these basically healthy dogs towards clinical cases. In our department studies are being performed with a mixed breed of Bedlington terriers and Beagles who carry the *COMMD1* deletion and are being followed in time; hopefully these dogs will show the effect what leads them to get hepatitis. A few ideas can be deduced from our observations. It could be that metallothionein, which is upregulated at a transcriptional level in acute copper loading is down-regulated in chronic copper loading leading to an insufficient storage and sequestration of intracellular copper. Furthermore, proliferation of hepatocytes has been suggested by us (chapter 7), potentially leading to an overall reduced presence of copper due to regeneration. Because the proliferation of hepatocytes is limited due to (for instance) telomere length, it could be concluded that after several years of chronic damage the liver looses its ability to regenerate.

- *Apoptosis*.

Apoptosis is a tightly regulated process leading to the removal of affected cells [25]. To dissect the molecular regulation of apoptosis in different forms of hepatitis, we have analyzed the expression of pro- and anti-apoptotic gene products in dogs with liver diseases referred to the university clinic. To correlate expression profiles with pathophysiology we compared four different forms of hepatitis; Acute Hepatitis (AH), Chronic Hepatitis (CH), Cirrhosis (CIRR), and a specialized form of cirrhosis, Lobular Dissecting Hepatitis (LDH). Quantitative real-time polymerase chain reaction (Q-PCR) was used to analyze the canine specific mRNA expression of anti-apoptotic Bcl-2 and the recently discovered Pim-2 [26-28] as well as the pro-apoptotic gene products caspase-3 and FasL (Fas ligand, also known as CD95L, TNFSF6, APT1LG1, CD178). Furthermore, we have analyzed the proteolytic activation of caspase-3 with Western blotting. Preliminary results indicated an increase in gene-expression of anti-apoptotic Bcl-2 and a decrease of pro-apoptotic FasL and caspase-3. However Western blotting on the activation of caspase-3 showed a strong increase in apoptosis in all four diseases. Immuno-histochemistry confirmed Western blot results indicating an increase in apoptosis in AH, CH, and CIRR. The striking observation of a reduced Pim-2 (28- and 47-fold reduction in AH and CIRR respectively) would strongly affect (induce) apoptosis and requires further research.

HGF therapy versus anti-TGF-β1 strategies

The counteracting activities of HGF and TGF-β1 have already been shown in dogs treated with TGF-β administered through a disconnected central portal vein branch after creation of an Eck fistula (porto-caval shunt) [29]. Our first emphasis was on the systemic application of recombinant growth factors such as HGF during liver pathologies. The first positive results were seen with a possible major treatment group, the hypoplastic diseases. These diseases, congenital portosystemic shunt (CPSS) and primary portal vein hypoplasia (PPVH), occur frequently in dogs [30,31]. Results showed that regenerative pathways were unaffected in CPSS and PPVH providing the rationale for HGF treatment (chapter 2). Similar results were found in chronic hepatitis (CH), lobular dissecting hepatitis (LDH), and cirrhosis (CIRR), although PKB/Akt showed no phosphorylation in acute hepatitis (chapter 3). However there were no other indications that the protein could not be activated after HGF treatment. An important step in devising therapeutics is the production, purification, and application of the product. Therefore, in parallel to analyzing biochemical pathways, HGF was produced and tested for its biological activity (chapter 5). As mentioned previously, the found increase of HGF (mRNA and protein) in chronic liver diseases do not indicate an application of recombinant HGF as HGF is still

present systemically. This said it has not been shown if the systemic HGF was indeed a mature, thus active, protein. In addition the effect of HGF has already been established in various models of hepatic damage including acetaminophen intoxications, CCL_4, thioacetamide, and partial hepatectomy (PHx) [5-8,32,33]. Moreover, the use of this growth factor in hypoplastic diseases such as CPSS and PPVH could be of great interest as surgery of the diseases is expensive and especially for intrahepatic portosystemic shunts and primary portal vein hypoplasia often fatal. Current research is investigating prognostic factors for effective surgery (A. Kummeling). Chapter 5 describes the successful production and isolation of canine HGF with a high proliferative capacity *in vitro*.

In chapter 2 and 4, we showed that fibrotic diseases (PPVH, CH, CIRR, LDH) all had induced TGF-β1 pathways resulting in increased ECM deposition. Although HGF treatment will effect TGF-β1 pathways by inducing anti-fibrotic (anti-TGF-β1) gene-products (e.g. TGIF and Ski/Sno), direct treatments against the TGF-β1 pathway have been proven very effective [34,35]. TGF-β1 intervention can be implied in several ways. Some of these techniques act on cell-type specific intervention inhibiting stellate cell transition to myofibroblasts [36-38] whereas others halt TGF-β1 signaling through the use of antibodies or RNAi directed against TGF-β1, its receptors, or Smads [39]. TGF-β1 intervention is still an effective way for treating liver diseases. However these techniques, in contrast to HGF treatment, have only been applied successfully in small animal models [34-39].

Besides HGF therapy and anti-TGF-β1 strategies measurements on other biochemical pathways indicated possible other forms of therapy. As described in chapter 6 and 7, the increased presence of reactive oxygen species (ROS) during copper toxicosis indicated a possible therapeutic approach. In these diseases gene-expression profiles of major enzymatic defenses against ROS and GSH/GSSG ratios (indicative of oxidative damage) all indicated a high increase in ROS. Therefore many therapies with anti-oxidants or GSH esters may be effective in treating these liver pathologies. In chapter 6 we propose the use of the GSH precursor S-adenosylmethionine (SAM-e or AdoMet), which already was shown to reduce oxidative stress levels in cultured primary hepatocytes [40]. Another therapy we suggested for treating canine tumors was the use of RNA interference (RNAi) [41-44]. In chapter 10 we induced apoptosis in various canine cell-lines (derived from tumors) by depleting the cells of XIAP with RNAi. Although this was previously described the use of small inhibitory RNA's (siRNA) in the veterinary field had not been done before. The therapies suggested in chapter 10 combined siRNA's with conventional chemotherapies. To show proof of principle, TRAIL, a protein known for its direct activation of caspases-3 and -7, was used. Doxorubicin was the DNA damaging drug of choice because of the already described use in the veterinary field and the relative insensitivity of different

tumors for this drug [45]. Taken together, although the clinical use of recombinant HGF holds great promise, other therapies should be considered against the cause of a disease and/or negative effects associated with the disease, and could enhance the use of HGF if used in parallel.

Remaining questions

Measurements on regenerative and fibrotic pathways in various forms and stages of canine hepatitis raised several questions. Measurements on biochemical pathways were performed in biopsies or necropsy material. However these measurements will only indicate a general trend in that particular part of tissue. Ultrasonic sonography of canine liver diseases showed that our investigated diseases can be defined as homogenous, diffuse diseases. Furthermore the use of different biopsies per individual should indicate non-homogenous distribution of the disease by showing a high degree of variation in gene-expression; our duplicates, however, all had small standard deviations. This said, the presented analysis of liver diseases does not depict the difference between the various cell-types that are present in the liver as well as any infiltrate seen during inflammation. Therefore we propose the use of (immuno)-histochemistry and laser micro-dissection as tools for analyzing the regenerative and fibrotic pathways of different cells. Currently we have initiated close collaborations to isolate the different canine liver cell types either by FACS (Prof A. Geerts, VU-Brussel) or by micro-dissection (Prof T. Roskams, KU-Leuven). Immunohistochemistry will provide vital information on protein content and location whereas laser micro-dissection will enable us to quantify mRNA levels of specific isolated cells. It is already known that mesenchymal cells such as the stellate cells have important functions during fibrosis [18]. During pathophysiological processes these cells are stimulated to become myofibroblasts [46,47]. The analysis of these processes of transition and involved signals could greatly enhance our current knowledge of fibrosis. Taken together the analysis of specific cells/compartments during liver disease would greatly enhance the current knowledge on liver regeneration in both man and dog, providing new rationales for therapeutic approaches suggested in this thesis and others.

Another remaining question is the role of yet another cell-type which can be found in the liver; the hepatic progenitor cells (HPC), also known as oval cells [48-55]. Although the role of bone-marrow derived stem cells in liver regeneration was deemed unlikely [56], HPCs could function as committed cells to differentiate into hepatic epithelial cells during regeneration. Dormant HPCs have been detected in healthy tissue in both man and dog (J. IJzer, unpublished results). In this thesis the possible role of these cells has only been examined in moderate amounts. Recent

results did show a decrease in BMI-1 during (all) hepatic diseases, a transcription factor involved in stem cell renewal of neuronal and (leukemic) bone marrow stem cells. To investigate the role of HPCs in liver regeneration specific immunohistochemical analysis such as cytokeratin 7 (CK7) could provide insight into the importance of HPCs in liver regeneration. As recent reports already showed the activation and differentiation of HPCs in rat models and virtually all human liver diseases, we would like to investigate the involvement of the HPC-compartment (also known as the stem cell 'niche') which depends largely on the severity and stage of the disease. In this part the dog could play a major role as materials from different diseases (and stages of diseases) are more easily obtained.

Our *in vitro* results showed active HGF and molecular studies on biopsies indicated a possibility to apply HGF in a clinical situation. However negative side effects must be investigated. Evaluation of the safety of HGF should be performed in a risk-assessment study before any clinical trials will start. In this risk-assessment study the doses should be given in higher amounts than estimated to get a biological response and over a prolonged period. This said, many publications have indicated that HGF is only present in the blood for a short period of time and the binding to its receptor is transient [57,58]. Also many hepatocellular carcinomas are insensitive for HGF due to mutations in the proto-oncogene c-MET indicating the relative unimportance of HGF in oncogenesis [59]. Moreover, HGF does not induce growth in dormant tissues such as hepatocytes, in which an injury has to occur before cells become sensitive for the tumorigenic action of growth factors [60].

Another question raised by HGF treatment concerns the timing of application. For instance, fulminate or severe acute hepatitis is a lethal acute disease. In such cases, the immediate availability of the HGF protein for a relatively short period (a few days) may be life-saving, as previously shown in rodents [5,61]. Chronic diseases like chronic hepatitis and especially cirrhosis a long-term administration should be foreseen to reach sufficient effect (several weeks). Congenital portosystemic shunts form a group in between. As re-growth of the liver after successful surgery occurs within three weeks, HGF administration possibly requires a similar time-frame. From the many above described animal model studies it has recently become clear that HGF administration is potentially very promising. This is well summarized in a recent article in Nature Medicine [62] and in several editorials [63-66]. The next step is to study the effects in clinical cases. For veterinary medicine it is feasible to start studies into the clinical effects of administration of HGF in dogs with relevant liver diseases in the near future. There is no doubt that such therapies will take over many of the classical therapies or make medication possible in cases where patients will die at present. HGF is a very attractive candidate, because it has potential use not only in

hepatic diseases, but it has been shown to be a promoter of regeneration and a protector against epithelial cell damage for many other organs, such as the kidney [67-70] and the heart [71]. However, by far most of the experimental work has been done on the effects in the main target, the liver, and it is logical to start with liver diseases, as described in chapter 2.

Conclusions

In the field of canine hepatic diseases we have made great advances in understanding the biological mechanisms underlying different diseases such as hepatitis, copper-toxicosis of the liver, hepatic hypoplasia, and tumor formation. Furthermore, we provided the basis for new forms of therapy such as HGF treatment in hepatic diseases and the use of innovative techniques in canine oncology. Overall, we have achieved our aims in this thesis which was to prevent/cure canine liver diseases through a rational approach of molecular analysis of specific pathways. More specifically, we have maid great progress in understanding these diseases and have provided a basis for various novel therapies.

References

[1] Mack GS. Cancer researchers usher in dog days of medicine. Nat Med 2005, 11:1018.

[2] Luvoni GC, Chigioni S, Allievi E, et al. Factors involved in vivo and in vitro maturation of canine oocytes. Theriogenology 2005, 63:41-59.

[3] Spee B, Penning LC, van den Ingh TS, et al. Regenerative and fibrotic pathways in canine hepatic portosystemic shunt and portal vein hypoplasia, new models for clinical hepatocyte growth factor treatment. Comp Hepatol 2005, 4:7.

[4] De Vico G, Maiolino P, Restucci B, et al. Spontaneous tumours of pet dog as models for human cancers: searching for adequate guidelines. Riv Biol 2005, 98:279-296.

[5] Kosai K-I, Matsumoto K, Funasoshi H, et al. Hepatocyte growth factor prevents endotoxin-induced lethal hepatic failure in mice. Hepatology 1999, 30:151-159.

[6] Gupta S, Rajvanshi P, Aragona E, et al. Transplanted hepatocytes proliferate differently after CCl_4 treatment and hepatocyte growth factor infusion. Am J Physiol 1999, 276:G629-638.

[7] Kaibori M, Kwon AH, Nakagawa M, et al. Stimulation of liver regeneration and function after partial hepatectomy in cirrhotic rats by continuous infusion of recombinant human hepatocyte growth factor. J Hepatol 1997, 27:381-390.

[8] Matsuda Y, Matsumoto K, Yamada A, et al. Preventive and therapeutic effects in rats of hepatocyte growth factor infusion on liver fibrosis/cirrhosis. Hepatology 1997, 26:81-89.

[9] Ueno S, Aikou T, Tanabe G, et al. Exogenous hepatocyte growth factor markedly stimulates liver regeneration following portal branch ligation in dogs. Cancer Chemother Pharmacol 1996, 38:233-237.

[10] Vail DM, MacEwen EG. Spontaneously occurring tumors of companion animals as models for human cancer. Cancer Invest 2000, 18:781-792.

[11] Vandesompele J, De Paepe A, Speleman F. Elimination of primer-dimer artifacts and genomic coamplification using a two-step SYBR green I real-time RT-PCR. Anal Biochem 2002, 303:95-98.

[12] Vandesompele J, De Preter K, Pattyn F, et al. Accurate normalization of real-time quantitative RT-PCR data by geometric averaging of multiple internal control genes. Genome Biol 2002, 3:RESEARCH0034.

[13] Sledz CA, Holko M, de Veer MJ, et al. Activation of the interferon system by short-interfering RNAs. Nat Cell Biol 2003, 5:834-839.

[14] Moss EG, Taylor JM. Small-interfering RNAs in the radar of the interferon system. Nat Cell Biol 2003, 5:771-772.

[15] Wall NR, Shi Y. Small RNA: can RNA interference be exploited for therapy? Lancet 2003, 362:1401-1403.

[16] Eckstein F. Small non-coding RNAs as magic bullets. Trends Biochem Sci 2005, 30:445-452.

[17] Schuppan D, Ruehl M, Somasundaram R, et al. Matrix as a modulator of hepatic fibrogenesis. Semin Liver Dis 2001,21:351-372.
[18] Bataller R, Brenner DA. Liver fibrosis. J Clin Invest 2005, 115:209-218.
[19] Schnaper HW. Renal fibrosis. Methods Mol Med 2005, 117:45-68.
[20] Sternlieb I. Copper and the liver. Gastroenterology 1980, 78:1615-1628.
[21] Dijkstra M, Vonk RJ, Kuipers F. How does copper get into bile? New insights into the mechanism(s) of hepatobiliary copper transport. J Hepatol 1996, 24:109-120.
[22] Klomp AE, van de Sluis B, Klomp LW, et al. The ubiquitously expressed MURR1 protein is absent in canine copper toxicosis. J Hepatol 2003, 39:703-709.
[23] Klotz LO, Kroncke KD, Buchczyk DP, et al. Role of copper, zinc, selenium and tellurium in the cellular defense against oxidative and nitrosative stress. J Nutr 2003, 133:1448-1451.
[24] Thornburg LP. A perspective on copper and liver disease in the dog. J Vet Diagn Invest 2000, 12:101-110.
[25] de Graaf AO, de Witte T, Jansen JH. Inhibitor of apoptosis proteins: new therapeutic targets in hematological cancer? Leukemia 2004, 18:1751-1759.
[26] White E. The pims and outs of survival signaling: role for the Pim-2 protein kinase in the suppression of apoptosis by cytokines. Genes Dev 2003, 17:1813-1816.
[27] Fox CJ, Hammerman PS, Cinalli RM, et al. The serine/threonine kinase Pim-2 is a transcriptionally regulated apoptotic inhibitor. Genes Dev 2003, 17:1841-1854.
[28] Allen JD, Verhoeven E, Domen J, et al. Pim-2 transgene induces lymphoid tumors, exhibiting potent synergy with c-myc. Oncogene 1997, 15:1133-1141.
[29] Francavilla A, Azzarone A, Carrieri G, et al. Effect on the canine Eck fistula liver of intraportal TGF-beta alone or with hepatic growth factors. Hepatology 1992, 16:1267-1270.
[30] Hunt GB. Effect of breed on anatomy of portosystemic shunts resulting from congenital diseases in dogs and cats: a review of 242 cases. Aust Vet J 2004, 82:746-749.
[31] Van den Ingh TS, Rothuizen J, Meyer HP. Portal hypertension associated with primary hypoplasia of the hepatic portal vein in dogs. Vet Rec 1995, 137:424-427.
[32] Oe H, Kaido T, Mori A, et al. Hepatocyte growth factor as well as vascular endothelial growth factor gene induction effectively promotes liver regeneration after hepatectomy in Solt-Farber rats. Hepatogastroenterology 2005, 52:1393-1397.
[33] Hasuike S, Ido A, Uto H, et al. Hepatocyte growth factor accelerates the proliferation of hepatic oval cells and possibly promotes the differentiation in a 2-acetylaminofluorene/partial hepatectomy model in rats. J Gastroenterol Hepatol 2005, 20:1753-1761.
[34] Liu Y. Hepatocyte growth factor in kidney fibrosis: therapeutic potential and mechanisms of action. Am J Physiol Renal Physiol 2004, 287:F7-16.

[35] Dai C, Liu Y. Hepatocyte growth factor antagonizes the profibrotic action of TGF-beta1 in mesangial cells by stabilizing Smad transcriptional corepressor TGIF. J Am Soc Nephrol 2004, 15:1402-1412.

[36] Qi Z, Atsuchi N, Ooshima A, et al. Blockade of type β transforming growth factor signaling prevents liver fibrosis and dysfunction in the rat. Proc Natl Acad Sci USA 1999, 96:2345-2349.

[37] Nakamura T, Sakata R, Ueno T, et al. Inhibition of transforming growth factor β prevents progression of liver fibrosis and enhances hepatocyte regeneration in dimethylnitrosamine-treated rats. Hepatology 2000; 32:247-255.

[38] Yang J, Dai C, Liu Y. A novel mechanism by which hepatocyte growth factor blocks tubular epithelial to mesenchymal transition. J Am Soc Nephrol 2005, 16:68-78.

[39] Laping NJ. Therapeutic uses of smad protein inhibitors: Selective inhibition of specific TGF-beta activities. IDrugs 1999, 2:907-914.

[40] Lotkova H, Cervinkova Z, Kucera O, et al. Protective effect of S-adenosylmethionine on cellular and mitochondrial membranes of rat hepatocytes against tert-butylhydroperoxide-induced injury in primary culture. Chem Biol Interact 2005, 156:13-23.

[41] Takei Y, Kadomatsu K, Yuzawa Y, et al. A small interfering RNA targeting vascular endothelial growth factor as cancer therapeutics. Cancer Res 2004, 64:3365-3370.

[42] Scherr M, Battmer K, Dallmann I, et al. Inhibition of GM-CSF receptor function by stable RNA interference in a NOD/SCID mouse hematopoietic stem cell transplantation model. Oligonucleotides 2003, 13:353-363.

[43] Zender L, Hutker S, Liedtke C, et al. Caspase 8 small interfering RNA prevents acute liver failure in mice. Proc Natl Acad Sci U S A 2003, 100:7797-7802.

[44] Sorensen DR, Leirdal M, Sioud M. Gene silencing by systemic delivery of synthetic siRNAs in adult mice. J Mol Biol 2003, 327:761-766.

[45] Macy DW, Ensley BA, Gillette EL. In vitro susceptibility of canine tumor stem cells to doxorubicin. Am J Vet Res 1988, 49:1903-1905.

[46] Sato M, Suzuki S, Senoo H. Hepatic stellate cells: unique characteristics in cell biology and phenotype. Cell Struct Funct 2003, 28:105-112.

[47] Gressner AM, Weiskirchen R, Breitkopf K, et al. Roles of TGF-beta in hepatic fibrosis. Front Biosci 2002, 7:d793-807.

[48] Roskams T, De Vos R, Desmet V. "Undifferentiated progenitor cells" in focal nodular hyperplasia of the liver. Histopathol 1996;28:291-299.

[49] Roskams T, De Vos R, Van Eyken P, et al. Hepatic OV-6 expression in human liver disease and rat experiments: evidence for hepatic progenitor cells in man. J Hepatol 1998, 29:455-463.

[50] Libbrecht L, Desmet V, Van Damme B, et al. The immunohistochemical phenotype of dysplastic foci in human liver: correlation with putative progenitor cells. J Hepatol 2000, 33:76-84.

[51] Libbrecht L, Desmet V, Van Damme B, et al. Deep intralobular extension of human hepatic 'progenitor cells' correlates with parenchymal inflammation in chronic viral hepatitis: can 'progenitor cells' migrate? J Pathol 2000, 192:373-378.
[52] Libbrecht L, Roskams T. Hepatic progenitor cells in human liver diseases. Semin Cell Dev Biol 2002, 13:389-396.
[53] Roskams T. Progenitor cell involvement in cirrhotic human liver diseases: from controversy to consensus. J Hepatol 2003, 39:431-434.
[54] Reeves HL, Friedman SL. Activation of hepatic stellate cells--a key issue in liver fibrosis. Front Biosci 2002, 7:d808-826.
[55] Safadi R, Friedman SL. Hepatic fibrosis--role of hepatic stellate cell activation. MedGenMed 2002, 4:27.
[56] Cantz T, Sharma AD, Jochheim-Richter A, et al. Reevaluation of bone marrow-derived cells as a source for hepatocyte regeneration. Cell Transplant 2004, 13:659-666.
[57] Appasamy R, Tanabe M, Murase N, et al. Hepatocyte growth factor, blood clearance, organ uptake, and biliary excretion in normal and partially hepatectomized rats. Lab Invest 1993, 68:270-276.
[58] Liu KX, Kato Y, Narukawa M, et al. Importance of the liver in plasma clearance of hepatocyte growth factors in rats. Am J Physiol 1992, 263:G642-649.
[59] Corso S, Comoglio PM, Giordano S. Cancer therapy: can the challenge be MET? Trends Mol Med 2005, 11:284-292.
[60] Taub R. Liver regeneration 4: transcriptional control of liver regeneration. FASEB J 1996, 10:413-427.
[61] Nakamura T, Akiyoshi H, Shiota G, et al. Hepatoprotective action of adenovirus-transferred HNF-3gamma gene in acute liver injury caused by CCl(4). FEBS Lett 1999, 459:1-4.
[62] Ueki T, Kaneda Y, Tsutsui H, et al. Hepatocyte growth factor gene therapy of liver cirrhosis in rats. Nat Med 1999, 5:226-230.
[63] Wrana JL. (editorial) Transforming growth factor-β signaling and cirrhosis. Hepatology
[64] Michalopoulos GK, DeFrancis MC. Liver regeneration. Science 1997, 276:60-66.
[65] Maher J. Gene therapy for hepatic fibrosis - bringing treatment into the new millennium. Hepatology 1999, 30:816-818.
[66] Wrana JL. Transforming growth factor-β signaling and cirrhosis. Hepatology 1999, 29:1909-1910.
[67] Matsumoto K, Morishita R, Morguchi A, et al. Prevention of renal damage by angiotensin II blockade, accompanied by increased renal hepatocyte growth factor in experimental hypertensive rats. Hypertension 1999, 34:279-284.
[68] Azuma H, Takahara S, Kitamura M, et al. Effect of hepatocyte growth factor on chronic rejection in rat renal allografts. Transplant Proc 1999, 31:854-855.

[69] Liu Y, Tolbert EM, Lin L, et al. Up-regulation of hepatocyte growth factor receptor: amplification and targeting mechanism for hepatocyte growth factor action in acute renal failure. Kidney Int 1999, 55:442-453.

[70] Takada, S, Takahara S, Nishimura K, et al. Effect of hepatocyte growth factor on tacrolimus-induced nephrotoxicity in spontaneously hypertensive rats. Transplant Int 1999, 12:27-32.

[71] Ueda H, Sawa Y, Kitagawa-Sakakida S, et al. Gene transfection of hepatocyte growth factor attenuates reperfusion injury in the heart. Ann Thorac Surg 1999, 76:1726-1731.

Chapter 12

Nederlandse samenvatting
voor niet-ingewijden

Achtergrond

Leverziekten komen bij de hond frequent voor; van alle zieke honden die naar de faculteit diergeneeskunde doorverwezen worden heeft 1-2% een leverziekte. Zoals bij mensen zijn leverziekten in de meeste gevallen chronisch en worden ze veroorzaakt door een aanhoudende ontsteking vanwege celschade door verschillende ziekteverwekkers en/of gifstoffen. In alle gevallen leidt de doorlopende levercelschade tot een verlaging in het aantal functionele levercellen, vaak gecombineerd met een verhoogde aanmaak van bindweefsel (fibrose). Deze twee observaties: verlies van (lever)regeneratie en toegenomen fibrose, zijn de belangrijkste factoren die bijdragen aan een slechte leverfunctie wat uiteindelijk kan leiden tot de dood.

De lever is een orgaan dat een grote rol speelt bij het opruimen van schadelijke stoffen in het bloed. De lever zelf is in grote mate dan ook goed bestand tegen bepaalde (gif)stoffen. Bij celschade zal de lever snel het verlies van functionele cellen herstellen door nieuwe cellen te laten groeien. Deze hoge mate van regeneratie of groei na celschade is al langere tijd bekend, maar het verlies van deze regeneratiecapaciteit tijdens chronische leverziekten blijft een bron van onderzoek.

Er is groeiend bewijs dat twee elkaar tegenwerkende factoren: Hepatocyte Growth Factor (HGF) en Transforming Growth Factor-β1 (TGF-β1), de uitkomst van leverziekten bepalen. Waar HGF een groeifactor is die levergroei stimuleert en fibrose onderdrukt, verhoogt TGF-β1 de aanmaak van bindweefsel en het ontstaan van celdood. Deze observaties hebben geleid tot het experimentele gebruik van HGF als behandeling bij diermodellen waarbij leverschade is veroorzaakt door gifstoffen. De toevoeging van HGF bij deze modellen leidde tot een volledige regeneratie van de lever, terwijl onbehandelde dieren stierven. Het omzetten van een dergelijke therapie naar een functionele toepassing bij de mens is nog niet gelukt. Het gebruik van nieuwe therapieën bij honden met natuurlijke voorkomende leverziekten zou een veel relevanter diermodel zijn voor het vertalen van een therapie naar een humane klinische toepassing. HGF therapie zou dan ook een enorme impact kunnen hebben in het behandelen van leverziekten bij mens en hond.

Samengenomen behandelt dit proefschrift verschillende doelen. Het eerste doel is om de regulerende werking van HGF en TGF-β1 en hun processen tijdens leverziekten in de hond te beschrijven. Het tweede doel is het ontwerpen van therapieën op de hierboven beschreven inzichten welke gebruikt kunnen worden bij het verlies van levercellen of fibrose, door de biochemische werking van HGF en TGF-β1 te beïnvloeden. Uiteindelijk zou dat leiden tot een evaluatie van zulke therapieën bij de hond.

Indeling

De indeling van dit proefschrift is gebaseerd op de verschillende vragen die van te voren gesteld zijn of tijdens het onderzoek naar boven kwamen. Opeenvolgend beschrijven we hier de specifieke vragen en resultaten van dit proefschrift.

Leverziekten zoals hepatitis zijn biochemisch gezien complex, vele factoren en processen bepalen de uiteindelijke uitkomst van hepatitis. Om de verschillende processen zoals regeneratie te bekijken en beschrijven, is eerst gekozen voor relatief simpele ziekten waarbij maar enkele processen veranderd zijn. In **hoofdstuk 2** beschrijven wij de biochemische analyse van regeneratie in aangeboren afwijkingen waarbij de levermassa niet volledig uitgroeit. De eerste, aangeboren portosystemische shunt, is een veelvoorkomende erfelijke ziekte waarbij de toevoer van bloed aan de lever wordt omgeleid en niet, of in veel mindere mate, naar de lever gaat. Hierdoor blijft groei uit maar is er geen sprake van ontsteking of fibrose (bindweefselvorming). Bij de tweede ziekte, primaire vena porta hypoplasie, zijn de laatste kleine vaten in de lever niet aangelegd waardoor de lever ook hier geen goede bloedtoevoer heeft. Bij deze ziekte blijft de groei ook uit, maar er is vaak wel fibrose. De resultaten laten zien dat de biochemische celreacties voor regeneratie in deze ziekten nog steeds functioneel waren en dus gebruikt kunnen worden voor groeifactor therapie zoals HGF behandeling. Analyse van fibrose laat zien dat de eiwitten verantwoordelijk voor de aanmaak van (te veel) bindweefsel (o.a. TGF-β1) erg sterk geactiveerd zijn.

De volgende stap is het beschrijven van dezelfde biochemische processen in complexere ziekten zoals hepatitis. In **hoofdstuk 3** is gekozen voor verschillende vormen van hepatitis zoals acute hepatitis en chronische hepatitis. Bij deze analyse zijn ook cirrose en lobular dissecting hepatitis (LDH) meegenomen. Cirrose beschrijft het eindstadium van chronische hepatitis waarbij de leverarchitectuur volledig is omgebouwd door bindweefsel. LDH beschrijft een speciale vorm van cirrose die een snelle (ziekte) verloop heeft, en waarbij een excessieve mate van fibrosering en verstoring van de normale lobulaire architectuur optreedt. Vergelijkbaar met aangeboren portosystemische shunts en vena porta hypoplasie, is ook bij deze complexere leverziekten geen defecte regeneratie gevonden. De belangrijkste biochemische paden die bij regeneratie actief zijn, worden zelfs geactiveerd tijdens hepatitis. Humane monsters van leverziekten laten bovendien zien dat bij de mens een zeer vergelijkbaar beeld bestaat, wat het potentiële belang van natuurlijk voorkomende leverziekten bij de hond als model voor de mens alleen maar groter maakt. Concluderend, een over-stimulatie van deze regeneratie biochemische paden, bijvoorbeeld door HGF,

zou een goede manier kunnen zijn om de balans door te laten slaan van afbraak (fibrosering) naar regeneratie.

In dezelfde ziekten als beschreven in hoofdstuk 3 hebben wij ook gekeken naar de (mate van) fibrosering. Fibrosering wordt omschreven als de aanmaak van te veel bindweefsel dat de werking van de lever remt. In chronische hepatitis is dit nog gering maar het zal geleidelijk voortschrijden tot het eindstadium waarbij niet alleen abnormaal veel bindweefsel is gevormd, maar ook cirrose waarbij een totaal verstoorde weefselopbouw ontstaat. In **hoofdstuk 4** laten wij zien dat de bekende veroorzaker van fibrose bij de mens, TGF-β1, in alle leverziekten van de hond waar te veel fibrose gevonden wordt, is verhoogd. Ook hierin vertoonden humane monsters van leverziekten een reactiepatroon dat volkomen overeenkomt met de bevindingen bij de hond. Concluderend kunnen we stellen dat het biochemische proces van fibrose bij honden identiek is aan dat bij de mens. Vanwege het belang van een goed model voor fibrose in (grote) zoogdieren, is dit van grote waarde.

Samenvattend over de eerste hoofdstukken kunnen we concluderen dat HGF therapie een mogelijke toepassing is om leverziekten bij de hond te behandelen, zowel wat betreft de regeneratie als de fibrosering. Hierop anticiperend is een synthetisch (recombinant) honden HGF eiwit gemaakt en getest op zijn regenererend vermogen (**hoofdstuk 5**). Resultaten laten zien dat honden-HGF levercellen in kweek sterk laat vermenigvuldigen. Bovendien activeert het honden-HGF alle benodigde eiwitten voor regeneratie en de afbraak van fibrose.

Koperstapeling komt vaak voor bij verschillende hondenrassen en leidt in de meeste gevallen tot chronische hepatitis. Koper zelf is een essentieel metaal en is nodig in veel belangrijke processen in het lichaam. Echter een teveel aan koper kan leiden tot oxidatieve schade en celdood. Een overmaat wordt daarom via de gal uitgescheiden. Om te bepalen of de koperstapeling bij de hondenrassen met een predispositie voor koperstapeling wordt veroorzaakt door een celdefect of als gevolg van een leverziekte met verminderde galafvoer is het kopermetabolisme van de lever onderzocht (**hoofdstuk 6**). Resultaten laten zien dat in honden met chronische hepatitis door onbekende oorzaak en met extra-hepatische totale cholestase (galstuwing) geen koperstapeling plaatsvindt. Concluderend kunnen we stellen dat, als er opeenstapeling plaatsvindt, er gesproken kan worden van een primaire genetische aandoening en niet een secundaire verandering door o.a. galstuwing of ontsteking. Onderzoek naar de effecten van koperstapeling laat in de koper gerelateerde hepatitis zien dat de afweer tegen oxidatieve stress sterk afneemt bij een stapeling van koper.

Vanwege de grote onbekendheid van de rol van koper bij hepatitis hebben we ook naar een specifiek hondenras gekeken met een predispositie voor koperstapeling in de lever, de Doberman (**hoofdstuk 7**). Omdat koperstapeling over een langere tijd op kan treden zonder dat er negatieve effecten zijn hebben we hier ook gekeken naar monsters met subklinische hepatitis. In deze groep is er al wel koperstapeling maar is de hond nog steeds 'gezond'. Hoewel het gendefect van de Doberman niet is gevonden, waren specifieke koper uitscheidingseiwitten verlaagd bij de koperstapelingsziekte. Bij de subklinische groep is één eiwit verlaagd, te weten ATP7A, een eiwit dat in de humane ziekte van Menkes defect is. Behalve bij klinische hepatitis, was in de Doberman ook bij subklinische hepatitis al een verlaging in de afweer tegen oxidatieve stress te zien.

Analyse van koper toxcicose van de lever bij Bedlington terriërs heeft er toe geleid dat er een nieuw eiwit is ontdekt met een belangrijke rol bij het transporteren van koper door de levercellen naar de gal. Het defect bij deze honden bleek een mutatie te zijn in het *COMMD1* gen (ook bekend als *MURR1*). De genetische analyse van deze mutatie, en specifiek de detectie van dragers, is erg omslachtig. Hiervoor hebben wij in **hoofdstuk 8** een eenvoudige test ontwikkeld om dragers, lijders en gezonde Bedlington terriërs te onderscheiden. Met het gebruik van een kwantitatieve PCR methode hebben wij laten zien dat DNA analyse van monsters (bloed of wangslijmvlies) met een hoge nauwkeurigheid dragers van gezond en lijders kan onderscheiden.

Vanwege de relatieve onbekendheid hebben we in **hoofdstuk 9** gekeken naar de specifieke werking van het COMMD1 eiwit bij kopermetabolisme. In dit hoofdstuk hebben we gebruik gemaakt van een nieuwe techniek, genaamd RNAi of RNA interferentie, om heel specifiek één eiwit uit te schakelen. Hierbij wordt gebruik gemaakt van zeer kleine moleculen die specifiek op het RNA van een eiwit binden en dit afbreken voordat een eiwit wordt gemaakt. Als we deze moleculen gebruiken om COMMD1 uit te schakelen kan het effect op het kopermetabolisme bekeken worden en krijgen we inzicht in de werking van dit eiwit. De kweekresultaten laten zien dat als het COMMD1 eiwit uitgeschakeld is, koper zich opstapelt in de levercellen. Bovendien worden ze hierdoor veel gevoeliger voor koper en gaan ze sneller dood. Hiermee is vastgesteld dat COMMD1 een belangrijke rol speelt in de uitscheiding van koper uit levercellen en is de oorzakelijke rol van dit eiwit in de ontwikkeling van deze vorm van hepatitis, onomstotelijk vastgesteld.

Het gebruik van de siRNA techniek in het vorige hoofdstuk, leidde tot het idee om siRNA moleculen te gebruiken als therapie om tumoren gevoeliger te maken voor bestaande chemotherapieën. Onze aandacht ging uit naar x-linked inhibitor of apop-

tosis (XIAP), een eiwit dat we al eerder hadden bestudeerd bij kopergerelateerde toxcicose van de lever. Een verlies van dit eiwit leidt tot een verhoging in gereguleerde celdood, ook wel apoptose genoemd. In **hoofdstuk 10** laten we zien dat een specifieke remming in de productie van XIAP leidt tot een verhoogde gevoeligheid van tumoren (prostaat, galgang en melkklier) voor experimentele (TRAIL) en bestaande chemotherapieën (doxorubicine).

Conclusies

In het onderzoeksveld van leverziekten bij de hond hebben we grote vooruitgang geboekt in het begrijpen van biologische mechanismen in leverziekten zoals hepatitis, koper toxcicose van de lever, lever hypoplasie en tumor vorming. In dit proefschrift leggen we de basis voor nieuwe therapieën zoals HGF behandeling. Mogelijk dat een analyse aan individuele cellen kan leiden tot gedetailleerdere beschrijving van hepatitis bij honden en daarmee ook bij mensen. Samenwerking met humane hepatologie (Prof. Roskams, Leuven, België) is de afgelopen jaren sterk geïntensiveerd en zal hopelijk nog vele wetenschappelijke vruchten afwerpen.

List of Publications

Peer reviewed articles in this thesis

- **Spee B**, Mandigers PJ, Arends B, Bode P, van den Ingh TS, Hoffmann G, Penning LC, Rothuizen J. Differential expression of copper associated and oxidative stress related proteins in a new variant of copper-toxicosis in Doberman pinschers. Comp Hepatol 2005, 4:3.
- **Spee B**, Favier RP, Penning LC, Rothuizen J. Quantitative PCR method to detect a 13-kb deletion in the MURR1 gene associated with copper toxicosis and HIV-1 replication. Mamm Genome 2005, 16:460-463.
- **Spee B**, Penning LC, van den Ingh TS, Arends B, IJzer J, van Sluijs FJ, Rothuizen J. Regenerative and fibrotic pathways in canine hepatic portosystemic shunt and portal vein hypoplasia, new models for clinical hepatocyte growth factor (HGF) treatment. Comp Hepatol 2005, 4:7.
- **Spee B**, Arends B, van den Ingh TS, Brinkhof B, IJzer J, Nederbragt H, Penning LC, Rothuizen J. TGFβ-1 signaling in canine hepatic diseases, new models for human fibrotic liver pathologies. Submitted
- **Spee B**, Arends B, van den Ingh TS, Penning LC, IJzer J, Rothuizen J. Major regenerative pathways in dog models of hepatitis and cirrhosis, in comparison with man. Submitted
- **Spee B**, Arends B, Favier RP, van den Ingh TS, Hoffmann G, Penning LC, Rothuizen J. Copper Metabolism and Oxidative Stress in Chronic Inflammatory and Cholestatic Liver Diseases in the Dog. Submitted
- **Spee B**, Jonkers MD, Arends B, Rutteman GR, Rothuizen J, Penning LC. Specific down-regulation of XIAP with siRNA enhances the sensitivity of canine tumor cell-lines to TRAIL and doxorubicin. Submitted
- **Spee B**, Arends B, Penning LC, Rothuizen J. Impaired copper metabolism in hepatic epithelial cells after RNA interference targeting COMMD1. Submitted
- Arends B, **Spee B**, Penning LC, Rothuizen J. Functional *in vitro* studies on purified recombinant canine Hepatocyte Growth Factor. Ms in preparation

Peer reviewed articles not in thesis

- Boomkens SY, **Spee B**, IJzer J, Kisjes R, Egberink HF, van den Ingh TS, Rothuizen J, Penning LC. The establishment and characterization of cHCC, a hepatocyte tumor cell line of canine origin. Comp Hepatol 2004, 3:9.
- Schipper L, **Spee B**, Rothuizen J, Woutersen-van Nijnanten F, Fink-Gremmels J. Characterisation of 11beta-hydroxysteroid dehydrogenases in feline kidney and liver. Biochim Biophys Acta 2004, 1688:68-77.
- Mandigers PJ, van den Ingh TS, **Spee B**, Penning LC, Bode P, Rothuizen J. Chronic hepatitis in Doberman pinschers. A review. Vet Q 2004, 26:98-106.
- Boomkens SY, Kusters JG, Hoffmann G, Pot RG, **Spee B**, Penning LC, Egberink HF, van den Ingh TS, Rothuizen J. Detection of Helicobacter pylori in bile of cats. FEMS Immunol Med Microbiol 2004, 42:307-311.
- Laan TT, Bull S, Pirie RS, de Vrieze G, **Spee B**, Brons S, Fink-Gremmels J. Macrophages in the pathogenesis of current airway obstruction in horses. Submitted
- **Bart Spee**, Jooske IJzer, Jan Rothuizen, Ted S.G.A.M. van den Ingh, Louis C. Penning. A severe reduction in anti-apoptotic Pim-2 is correlated with increased apoptosis in canine liver diseases, despite reduced levels of caspase-3, FasL, p27KIP and an increase in bcl-2. Ms in preparation
- Fieten H, **Spee B**, IJzer J, Penning LC, Kik M, Kirpensteijn J. Expression of Hepatocyte Growth Factor (HGF) and it's receptor c-MET in canine osteosarcoma. Ms in preparation
- Bull S, Laan TT, deVrieze G, **Spee B**, vandenHoven R, Fink-Gremmels J. Modulation of LPS-induced cytokine production by clenbuterol in equine alveolar macrophages. Journal of veterinary pharmacology and therapeutics 2003, 3:234-235.
- Brinkhof B, **Spee B**, Rothuizen J, Penning LC. A new panel of validated canine reference genes for measurements of gene expression. Submitted

Meetings and proceedings

- **Spee B**, Penning L.C, van den Ingh T.S.G.A.M, IJzer J, Rothuizen J. Differential gene expression in canine liver diseases. Poster presentation and abstract at the FEBS Advanced study Institute on "From Transcription to Physiology: Regulation of Gene Expression and Protein Function in an Integrated Context". Spetses, Greece, September 8-September 14, 2003; page 231.
- **Spee B**, Penning L.C, van den Ingh T.S.G.A.M, IJzer J, Rothuizen J. Differential gene expression in canine liver diseases. Abstract at the Special

FEBS 2003 Meeting on Signal Transduction, Brussel, Belgium, July 3-July 8, 2003.

- **Spee B**, Rothuizen J, van den Ingh T.S.G.A.M, Arends B, IJzer J, van Sluijs F.J, Penning L.C. Differential gene expression of regenerative and fibrotic pathways in canine hepatic portosystemic shunt and portal vein hypoplasia. Poster presentation and abstract at the Signal Transduction 2004, Kirchberg, Luxemburg, January 25-January 28, 2004; page 261.
- **Spee B**, Rothuizen J, van den Ingh T.S.G.A.M, Arends B, IJzer J, van Sluijs F.J, Penning L.C. Gene expression of regenerative and fibrotic pathways in canine models of hepatitis and cirrhosis. Oral presentation and abstract at the Science day 2004, Zeist, The Netherlands, November 17, 2004; page 21.
- **Spee B**, Penning L.C, Rothuizen J, Rutteman G.R. Use of regeneration pathways by tumors? Oral presentation and abstract at the Seventh International Conference on Anticancer Research, Corfu, Greece, October 25-October 30, 2004; page 3597-3598.
- Mandigers P.J, van den Ingh T.S.G.A.M, **Spee B**, Penning L.C, Rothuizen J. The pathogenisis of Doberman hepatitis. Oral presentation and abstract at the ECVIM conference, Barcelona, Spain, September 9-September 11, 2004; page 120-123.
- Penning L.C, **Spee B**, Arends B, IJzer J, Boomkens S.Y, Favier R.P, van den Ingh T.S.G.A.M, Rothuizen J. Regulation of genes involved in liver regeneration and fibrosis in dogs with acute and chronic hepatitis. Oral presentation and abstract at the ECVIM conference, Barcelona, Spain, September 9-September 11, 2004; page 124-126.
- Penning L.C, **Spee B**, Rothuizen J, Rutteman G.R. Use of regeneration pathways by tumors? Oral presentation and abstract at the FECAVA-FEEVA-Voorjaarsdagen Congress 2005, Amsterdam, The Netherlands, April 14-April 17, 2005; page 5-6.
- Fieten H, **Spee B**, IJzer J, Penning L.C, Kirpesteijn J. Protein expression of HGF and c-MET in canine osteosarcoma. Poster presentation and abstract at the FECAVA-FEEVA-Voorjaarsdagen Congress 2005, Amsterdam, The Netherlands, April 14-April 17, 2005; page 337.
- **Spee B**, Arends B, van den Ingh T.S.G.A.M, Brinkhof B, Nederbragt H, IJzer J, Penning L.C , Rothuizen J. Pathways of liver fibrosis and Regeneration in the dog as a basis for new therapies. Oral presentation and abstract at the ECVIM conference, Glasgow, Scotland, September 1-September 3, 2005; page 179-181.

Acknowledgements (Dankwoord)

Mijn promotieonderzoek zit erop. Met plezier, een voldaan gevoel en trots kijk ik terug op de afgelopen vier jaar. Nu er nog maar twee pagina's over zijn voor mijn dankwoord, realiseer ik me dat dit eigenlijk veel te weinig is.

Allereerst Prof. Dr. Jan Rothuizen, Dr. Louis Penning, Dr. Ted van den Ingh; alledrie hart voor de wetenschap, inzet voor onderzoek en een inspirerend enthousiasme. Jan, wat mij bij blijft is je geloof in mij als wetenschapper, al vanaf het begin, toen je mij in de levergroep wilde hebben. Ik was daar echter nooit terecht gekomen als iemand anders mij niet had aangemoedigd om uit te vinden waar mijn hart lag. Vandaar hierbij ook een speciaal dankwoord naar Prof. Dr. Johanna Fink-Gremmels. Jan, de begeleiding, stimulans en vrijheid die jij me gaf, hebben veel bijgedragen aan mijn ontwikkeling als onderzoeker. Louis, je enthousiasme was enorm, zelfs zo groot dat ik sommige van je ideeën ('wilde ideeën') helaas in de map moest laten zitten. Van begin tot eind heb je je enorm ingezet voor mijn onderzoek. Eerst samen in het lab, werken aan nieuwe methoden, eindeloos pipetteren. De laatste maanden e-mail in de weekenden of midden in de nacht. Ik was tenminste niet alleen als ik op zondag nog aan een artikel aan het schrijven was. Ted, een onuitputtelijke bron van kennis, altijd tijd om mee te denken, een stayer in het onderzoek. De stukken tekst die je aan mijn artikelen toevoegde, waren geregeld onmetelijk in lengte, maar ook in waarde.

Brigitte, samen hebben wij bergen werk verzet, het onderzoek op gang gebracht en nieuwe technieken ontwikkeld. Je idealen in onderzoek en je kritische blik op methoden ('datamassage'), hebben me scherp gehouden. Naast de steun en praktisch werk, waren daar ook de etentjes, alcoholische versnaperingen en goede gesprekken. Bedankt voor alles, wat mij betreft gaan we hiermee door. Gaby, je uitleg over koper gerelateerde onderwerpen was voor mij heel waardevol, net als je kwaliteiten als gastvrouw, je etentjes waren onvergetelijk. Nagesha, I have enjoyed your company very much. Although we didn't share research topics, we had a common interest in dogs. Ies, je digitale bijdrage was erg belangrijk, maar de vermakelijke filmpjes misschien nog wel belangrijker. Jullie zijn voor mij allen 'medewerker van de maand'.

Mijn co-auteurs Bert Nederbragt, Peter Bode, Tania Roskams, Louis Libbrecht, Freek van Sluijs, Jooske IJzer, Gerard Rutteman, Ank van Wees, Paul Mandigers en Robert Favier. Bedankt voor jullie steun, advies en vitale materialen! Estel en Bas, hoewel pas kort betrokken bij mijn onderzoek, hebben jullie zeker een bijdrage kunnen leveren. Een speciaal bedankje aan 'mijn' analisten.

Mijn student Martijn, bedankt voor je inzet en gezelligheid. Hoewel ik veel tranen heb zin vloeien op de afdeling, heb jij het als één van de weinigen droog gehouden en ook nog bijgedragen aan een mooi artikel! Ik wens je voor de toekomst als analist veel succes.

Labgenoten, ondanks mijn constante afwezigheid bij de lablunch (je kunt maar zoveel in een week vergaderen) heb ik altijd meegeleefd met ontbrekende pipetpuntjes e.d. Ik dank Sandra, Frank van S, Frank R, Elpetra, Monique, Adri en Manon voor hun gezelschap tijdens koffiepauzes, lunches en labuitjes en natuurlijk hun bereidheid mij te helpen in de kleinere (maar vitale) lab beslommeringen. Een extra bedankje voor Jeanette, mijn eerste leermeester, die altijd op het laatste moment mijn bestellingen door wilde voeren. Mede-lotgenoten Jeanette H, Palona, Evelien, Linda en Yvette, heel veel succes bij de afronding van jullie promotie. Bedankt voor jullie gezelligheid, het allerbeste. Lieve Sacha, dr. Boomkens, bedankt dat ik jou 'nimf' mocht zijn, bedankt dat ik mocht 'afkijken'. Na je vertrek, was het stiller dan ooit.

Het samenwerken tussen de afdelingen (departementen) is naar mijn mening vitaal voor onderzoek, daarom wil ik graag de volgende personen bedanken. Pathobiologie: Ronald en Anne Marie. VFFT: Louska, Geert, Jan, Lilian, Marjolein, Felice en Roel. Landbouwhuisdieren: Bernard. Voor zijn hulp aan dit prachtige boek(je): Anton, hartelijk dank.

A special thanks to the sponsors of this research, from Intervet Boxmeer; Paul and Karin. From Intervet Angiers (France); Sophie and Paul-Olivier. Your questions during our meetings kept me sharp, your funding made it happen, I thank you all.

Ik eindig met een dank naar het thuisfront, en in het speciaal Jasper, Lucas, Maaike, Marike, Tim, Hiske, Hannie, Dick, Frank, Tony, Monique en Joost. De avondjes in de kroeg, potjes squash, etentjes, rondjes bier en goede gesprekken, maakte dat ik iedere maandag (soms niet geheel) fris kon beginnen. Lieve Eefje, een eervolle vermelding heb je meer dan verdiend! Bedankt dat je er voor me was en hopelijk nog heel lang zult zijn! Voor mijn ouders: dit proefschrift was niet tot stand gekomen als ik geen goede basis had gehad. De in mij verenigde nauwkeurigheid van mijn vader en doorzettingsvermogen van mijn moeder, hebben geleid tot dit product, daarvoor mijn dank…

Bart

Appendix

Chapter 2, Figure 1, page 38.

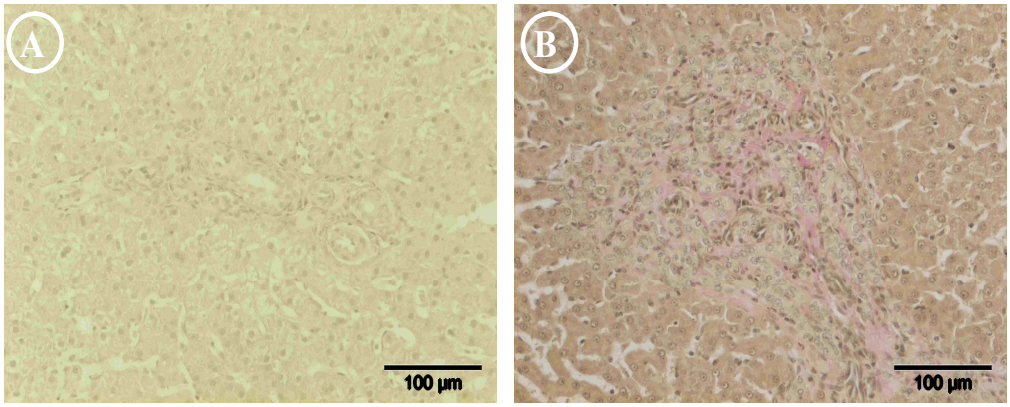

Appendix 1. Histological grading of fibrosis.
(A) CPSS, Portal area without recognizable portal vein and arteriolar proliferation. Van Gieson stain. (B) PPVH, Markedly enlarged portal area with fibrosis and extensive arteriolar and ductular proliferation. Van Gieson stain.

Chapter 4, Figure 5, page 85.

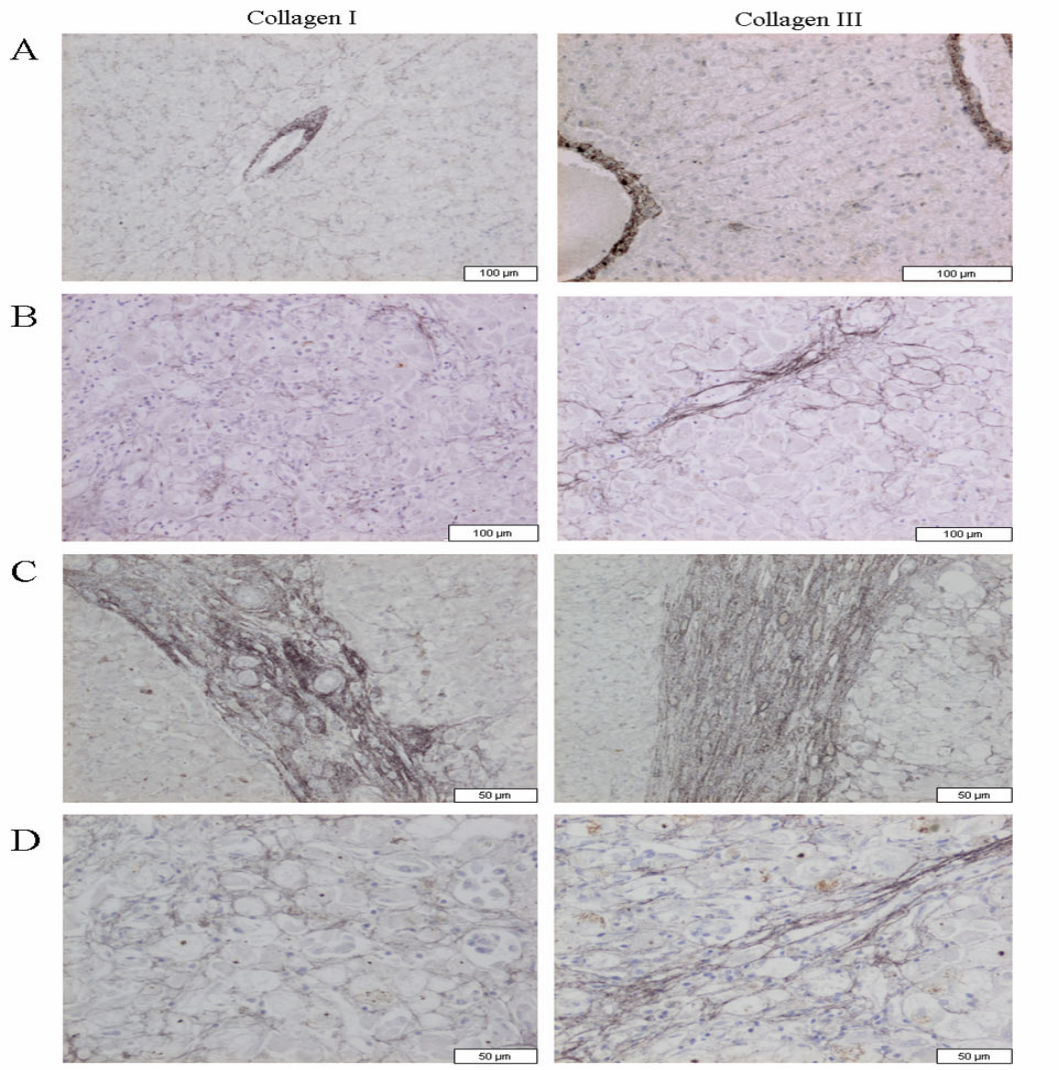

Appendix 2. Immunohistochemistry on collagen-I and -III in liver samples.
Collagen-I and-III in healthy liver tissue is shown in (A). Collagen-I and -III in Chronic Hepatitis is shown in (B). Collagen-I and -III in cirrhotic liver tissue is hown in (C). Collagen-I and -III in Lobular Dissecting Hepatitis is shown in (D). Size bar indicated in figures.

Curriculum Vitae

The author of this thesis was born on May 4, 1978 in Gouda, The Netherlands. He was educated in biochemistry (MLO, Rotterdam), molecular biology (HLO, Utrecht), before he worked as a student at the VFFT department on the PhD-project of Dr. L. Schipper, under guidance of Prof. Dr. J. Fink-Gremmels. Here he analyzed feline and canine 11beta-hydroxysteroid dehydrogenases in kidney and liver tissues. In February 2002, he started his graduate program at the Department of Clinical Sciences of Companion Animals (CSCA), a project supervised by Prof. Dr. Jan Rothuizen, Dr. Louis Penning (CSCA), and Dr. Ted van den Ingh (Pathobiology), in an Intervet sponsored programme called "Hepatocyte Growth Factor in canine liver diseases". The graduate project focused on the analysis of regenerative- and fibrotic- biochemical pathways during canine liver diseases. The results are described in this thesis, which will be defended publicly on April 6, 2006. In May 2006, we will start a research project, in cooperation with Prof. Dr. T. Roskams (Leuven & Utrecht), on the "stem-cell niche" in both man and dog.

Curriculum Vitae

De auteur van dit proefschrift werd op 4 mei 1978 geboren in Gouda, Nederland. Hij studeerde biochemie op het Zadkine college in Rotterdam (MLO), en moleculaire biologie bij de Hogeschool Utrecht (HLO). Hij deed zijn stage bij de afdeling Veterinaire Farmacie, Farmacologie en Toxicologie aan het project van Dr. L. Schipper, onder begeleiding van Prof. Dr. J. Fink-Gremmels. Hier analyseerde hij het 11beta-hydroxysteroid dehydrogenase enzym in nier- en lever weefsel van honden en katten. In februari 2002 startte hij zijn promotie-onderzoek bij de afdeling Geneeskunde van Gezelschapsdieren (GD), onder supervisie van Prof. Dr. J. Rothuizen, Dr. L.C. Penning (GD) en Dr. T.S.G.A.M. van den Ingh (Pathobiologie), in een door Intervet gesponsord programma genaamd "Hepatocyte Growth Factor in canine liver diseases". Dit promotie-onderzoek focuste zich op de analyse van regeneratieve en fibrotische biochemische paden tijdens leverziekten bij de hond. De resultaten zijn beschreven in dit proefschrift, openbaar te verdedigen op 6 april 2006. In samenwerking met Prof. Dr. T. Roskams (Leuven & Utrecht) zal vanaf mei 2006 onderzoek verricht gaan worden naar de lever "stam-cel niche" bij mens en hond.

Chapter 6, Figure 1, page 114.

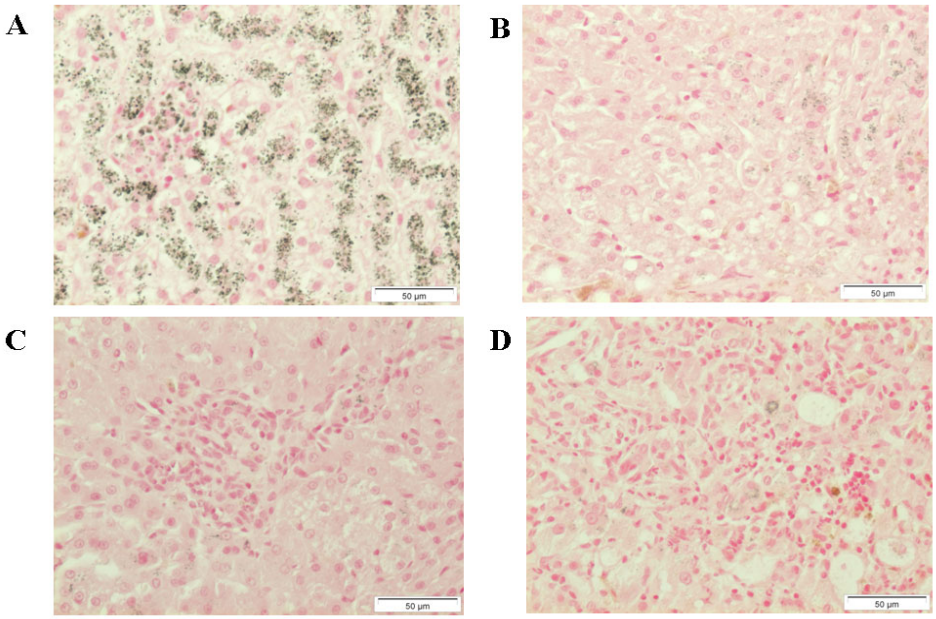

Appendix 3. Examples of Rubeanic acid staining on Copper Toxicosis with 5+ copper shown in (A), Extrahepatic cholestasis with 1-2+ centrolobular staining (B), Extrahepatic cholestasis with staining in periportal hepatocytes in (C), and Chronic hepatitis with 1-2+ copper shown in (D).

Chapter 7, Figure 1, page 131.

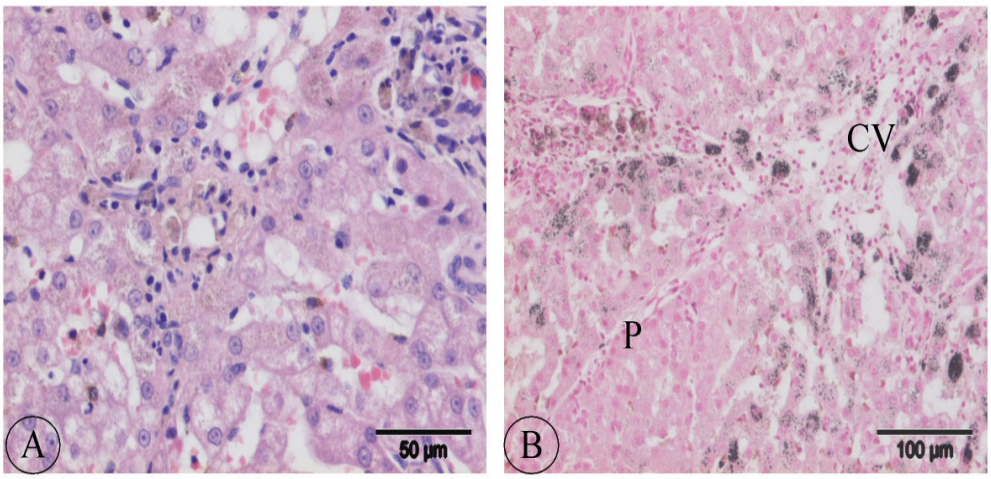

Appendix 4. Histological evaluation of Doberman hepatitis**.**
Hepatitis characterized by accumulation of pigmented granules (probably Cu) in hepatocytes (A), and inflammation with lymphocytes and pigmented (probably Cu) macrophages. HE staining. (B) Centrolobular accumulation of copper in hepatocytes and band of fibrous tissue with inflammatory cells and Cu-laden macrophages. Rubeanic acid staining. P = Portal area, CV = Central Vein area.

List of abbreviations

- AH, acute hepatitis
- ATOX1, anti-oxidant protein 1
- ATP7B, ATPase Cu(2+)-transporting beta polpeptide
- BDE, canine bile-duct epithelial cells
- CASH, copper associated subclinical hepatitis group
- CAT, catalase
- CAV-1, canine adenovirus-1
- CCS, copper chaperone for superoxide dismutase
- CH, idiopathic chronic hepatitis
- CIRR, cirrhosis
- COMMD1, copper metabolism MURR1 domain-containing protein 1
- COX17, cytochrome c oxidase assembly protein
- CP, ceruloplasmin
- CPSS, congenital portosystemic shunts;
- CT, copper toxicosis in Bedlington terriers
- DH, Doberman hepatitis group
- DTNB, 5,5′dithiobis-2-nitrobenzoic acid
- EC, chronic extrahepatic cholestasis
- ECM, extracellular matrix
- FOXO, forkhead box, sub-group "O" transcription factors
- GAPDH, glyceraldehyde-3-phosphate dehydrogenase
- GPX1, gluthathione peroxidase 1
- GSH, reduced gluthathione
- GSS, gluthathione synthetase
- GSSG, oxidized gluthathione
- hALC, human liver samples from cirrhotic stages of alcoholic liver disease
- HGF, hepatocyte growth factor
- hHC, human liver samples from cirrhotic stages of chronic hepatitis C infection
- HIF-1α, hypoxia induced factor-1α
- HPRT, hypoxanthine phosphoribosyl transferase
- LDH, lobular dissecting hepatitis
- MAP kinase, mitogen-activated protein kinase
- MT1A, metallothionein 1A
- MTT, 3-[4,5-dimethylthiazole-2-yl] 2,5,-diphenyl tetrazolium bromide
- N-CASH, non-copper associated subclinical hepatitis group
- PI3K, phosphoinositide 3-kinase
- Phx, partial hepatectomy
- PKB, protein kinase B (Akt)
- PPVH, primary portal vein hypoplasia;
- Q-PCR, quantitative real-time polymerase chain reaction
- RNAi, RNA interference
- ROS, reactive oxygen species
- siRNA, small inhibitory RNA molecules
- SOCS3, suppressor of cytokine signaling
- SOD1, Cu/Zn superoxide dismutase
- STAT, signal transducer and activator of transcription
- TGF-β1, transforming growth factor β1
- TNB, 2-nitro-5-thiobenzoic acid
- TGFα, transforming growth factor α
- XIAP, X-linked inhibitor of apoptosis